**Province of British Columbia**
Ministry of Energy, Mines and
Petroleum Resources
**Hon. Anne Edwards, Minister**

MINERAL RESOURCES DIVISION
Geological Survey Branch

# GEOLOGY AND MINERAL DEPOSITS OF THE GALORE CREEK AREA (104G/3, 4)

**By J.M. Logan, P. Geo. and V.M. Koyanagi, P. Geo.**

**BULLETIN 92**

Canadian Cataloguing in Publication Data
Logan, James Metcalfe, 1954-
Geology and mineral deposits of the Galore Creek area (104G/3,4 )
(Bulletin, ISSN 0226-7497 ; 92)

Issued by Geological Survey Branch.
Includes bibliographical references: p.
ISBN 0-7726-2148-9

1. Geology - British Columbia - Galore Creek Region. 2. Geochemistry - British Columbia - Galore Creek Region. 3. Geology, Economic - British Columbia - Galore Creek Region. 4. Mines and mineral resources - British Columbia - Galore Creek Region. I. Koyanagi, V.M. II. British Columbia. Ministry of Energy, Mines and Petroleum Resources. III. British Columbia. Geological Survey Branch. IV. Title. V. Series: Bulletin (British Columbia. Ministry of Energy, Mines and Petroleum Resources) ; 92.

QE187.L63 1994 557.11'85 C94-960195-0

VICTORIA
BRITISH COLUMBIA
CANADA

JUNE 1994

*Geological fieldwork for this project carried out during the period 1988 to 1990.*

# SUMMARY


The Galore Creek area, in northwestern British Columbia, straddles the western boundary of the Intermontane Belt and Coast Belt and is underlain by rocks of the Stikine Terrane. Northwestern Stikinia is a composite allochthonous terrane made up of an amalgamation of volcanic island arcs ranging in age from mid-Paleozoic through Middle Jurassic, and intruded along its western margin by Jurassic to Paleocene plutons of the Coast Plutonic Complex.

At this latitude basement to Stikinia is an Upper Paleozoic primitive island arc assemblage, known as the Stikine assemblage. It consists of Permian, Carboniferous and Devonian calcalkaline and bimodal flows and volcaniclastics, silicic intrusions, interbedded carbonate, minor shale and chert. Macro- and microfossil ages and isotopic dating indicate a composite stratigraphic sequence which includes: Devono-Carboniferous island arc volcanic and plutonic complex; middle Carboniferous carbonate and Late Carboniferous basaltic and dacitic volcanic and volcaniclastic apron; and the hallmark of the Stikine assemblage, a regionally extensive Early Permian carbonate slope deposit.

A Permo-Triassic (Tahltanian) period of uplift and erosion of Late Permian rocks is recorded by Early and Middle Triassic starved-basin sedimentary rocks or Late Triassic Stuhini Group volcaniclastic rocks nonconformably overlying Early Permian limestone of the Stikine assemblage.

The Upper Triassic marked renewed volcanism and a cessation of pelagic sedimentation. The Upper Triassic volcano-plutonic complex at Galore Creek consists of a lower (Carnian to Norian) assemblage of plagioclase and clinopyroxene-phyric calcalkaline basaltic and andesite breccias and lesser volcaniclastic sedimentary rocks, Orthoclase porphyry syenites, shoshonitic basalts and alkali-enriched pyroclastic rocks (208 Ma) overlie these and indicate a late stage alkalic magmatic event. Stuhini Group volcanic rocks are chemically similiar to rocks of the Takla Group. Plutonic rocks are coeval calcalkaline, ultramafic and intermediate plutons, and alkaline, shoshonitic intrusives. Early Jurassic Hazelton Group sediments and felsic tuffs overlie Upper Triassic volcanic conglomerates in apparent conformity.

Structural style at Galore Creek is dominated by brittle deformation and faulting and controlled by competency contrasts between volcanic and sedimentary rocks of the arc assemblage. Three or possibly four episodes of deformation have been recognized, but ages are poorly constrained. The earliest structures are synmetamorphic, pre-Triassic, possibly Carboniferous(?) age. These structures, and related northeast-striking penetrative foliations, are deformed by west-trending post-Triassic(?) folds. Two post-Early Jurassic events are recognized, one is characterized by north-trending southwest-verging folds and reverse faults; and the younger is characterized by northeast-verging kink folds.

Similarities between Stikinia and the northern Sierra-Eastern Klamath terranes of northern California include close faunal affinities of Permian corals and fusulinids, Devono-Carboniferous plutonism, Carboniferous and Permo-Triassic deformation and uplift events. These are all components of an Upper Paleozoic paleo-Pacific fringing arc system developed outboard of the cratonic shelf and now preserved as a disrupted, faulted belt of rocks extending the length of the North American Cordillera.

Metallogeny in the Galore area is related to plate boundary subduction processes and two separate mineralizing events, one in the latest Late Triassic and one in the Eocene. Each is characterized by a different base and precious metal suite. A Late Triassic to Early Jurassic alkalic volcanic centre at Galore Creek hosts ten synvolcanic copper-gold deposits. The largest, the Stikine Copper Limited central zone contains 125 000 000 tonnes of material with an estimated grade of 1.06% copper, 0.4 gram per tonne gold and 7.7 grams per tonne silver. A similiar deposit occurs at Copper Canyon. Pervasive potash metasomatism and retrograde calcsilicate alteration characterize the mineralized zones. Smaller tonnage, Eocene silver-rich base metal veins are associated with calcalkaline intrusions and hosted in northeasterly-striking faults at the Trek property and breccia-pipes at the Ptarmigan zone. Alteration and gangue minerals are quartz, sericite and iron carbonate assemblages. Volcanogenic massive sulphide deposits (*e.g.,* Tulsequah Chief) are an untested but viable exploration target in the Paleozoic Stikine assemblage rocks.

# TABLE OF CONTENTS

FIGURES



PLATES

# CHAPTER 1 INTRODUCTION

## LOCATION AND ACCESS

The Sphaler Creek and Flood Glacier map areas comprise the Galore Creek area, which is located within the Coast Mountains, between the Stikine River and Mess Creek, approximately 80 kilometres due south of Telegraph Creek in northwestern British Columbia (Figure 1). The large tonnage Galore Creek alkaline porphyry copper-gold-silver deposit is located within the area mapped. The two map sheets, 104G/3 and 104G/4, lie between latitudes 57°00′ and 57°15′ north, and longitudes 131°00′ and 132° 00′ west. Results of regional mapping and sampling in 1988 and one week in 1990 are summarized here. This report and accompanying maps incorporates new data and revisions to the 1:50 000 geology and mineral occurrence map, Open File 1989-8. The focus of the project was to produce detailed geological maps and a database to better understand the geological setting of the mineral deposits in the Galore Creek area and aid in making new discoveries.

The area mapped is located along the western margin of the Intermontane Belt. It is centred on Galore Creek and occupied by high-relief mountains of the Boundary Ranges. Topography is rugged, typical of mountainous and glaciated terrain with numerous snowfields and radiating glaciers. Elevations range from 30 metres on the Stikine River flood plain to over 2250 metres on peaks in the Hickman pluton. Permanent icefields and alpine glaciers cover approximately one-third of the map area, principally in the east. West of the Stikine River, the Coast Mountains are covered by large icefields, remnants of the Quaternary ice sheet, which feed two glaciers descending eastward into the Stikine valley. The Flood Glacier is the largest, approximately 2 kilometres wide and terminates at an elevation of less than 150 metres. It carries both medial and lateral moraines which merge over the last several kilometres to cover the ice completely. Dawson (1898) reported that the ice-dammed Flood Lake would discharge catastrophically almost annually in late summer, raising the level of the Stikine River from low stage to half flood. The last reported event took place in 1918 (Kerr, 1948a). Mud Glacier is somewhat smaller than Flood Glacier; it is is so named because its lower end is covered by rock debris.

The Galore Creek area is wholly contained within the drainage basin of the Stikine River. Physiography of the Stikine valley varies from mature, broad steep-walled to youthful canyons over its length from its source on the Stikine Plateau to where it discharges into Frederick Strait near Wrangell, Alaska. Northeast of Telegraph Creek the steep-walled "Grand Canyon" is a post-Tertiary drainage feature. Pre-Quaternary, the river may have flowed southwesterly from the head of this canyon, rejoining the present lower Stikine valley near the mouth of Mess Creek, or have been diverted into the Iskut valley (Kerr, 1948a, Mathews, 1991). In the Flood Glacier area the river occupies a broad, mature valley 3 to 4 kilometres wide. During high water, material carried into the Stikine from tributary streams exceeds the river budget and the river aggrades its channel. The result is a sinuous braided river of constantly shifting bars and channels (Souther, 1972). The Sphaler Creek area drains northward through the valleys of Galore Creek and the South Scud River into the west-flowing Scud River, a tributary of the Stikine River and westward down Sphaler Creek into the Porcupine River which joins the Stikine 9 kilometres west of Mount Scotsimpson. The north-trending drainages occupy fault-controlled valleys. Similiar structures control the Mess and Iskut valleys farther east.

Historically the Stikine River and its tributaries provided access through the Coast Mountains into the interior of the province. One of the main routes to the Klondike and Atlin Lake discoveries of 1896 and 1898 was up the Stikine to Telegraph Creek, then overland to Teslin or Atlin Lake (Kerr, 1948a). Paddle-wheel riverboats navigated between tidewater at Wrangell, Alaska as far upstream as the Stikine Canyon at Telegraph Creek until the late 1960s. The Stikine River provides riverboat and floatplane access to the western half of the map. Fixed-wing aircraft fly charters from Smithers, Dease Lake and Telegraph Creek to the Scud strip located on the river. A second, though shorter gravel air strip is located on the Galore Creek property. Access to the remaining areas is by helicopter. During summer field seasons in the past, helicopters have been stationed at Galore Creek, Scud strip, Forrest Kerr strip and Bronson strip. A permanent helicopter base is located 80 kilometres to the southwest at Bob Quinn Lake and 150 kilometres north at Dease Lake.

Wrangell, Alaska located on tidewater 90 kilometres to the southwest, provides commercial air connections to Anchorage, Alaska or Seattle, Washington. Cominco Ltd. is presently operating a hovercraft between Wrangell and the Bronson air strip on the Iskut River, 30 kilometres south of the map area.

## HISTORY OF EXPLORATION

The first recorded mineral assessment of the area was conducted by a group of Russian geologists who explored along the Stikine River in 1863 (Alaska Geographic Society, 1979). Placer gold was mined from bars on the Stikine River a short distance south of Telegraph Creek and later production is recorded from the Barrington River, during the late 1800s and early 1900s. Exploration for lode deposits began in the 1900s along access corridors provided by the Stikine River and its tributaries. Hudson Bay Mining and Smelting Company Limited initiated prospecting in the more remote parts of the map area in 1955, using helicopter-supported field parties. Discovery of the Galore Creek porphyry copper deposit in 1955 was a direct result of this program and focused porphyry exploration activity on the area. The

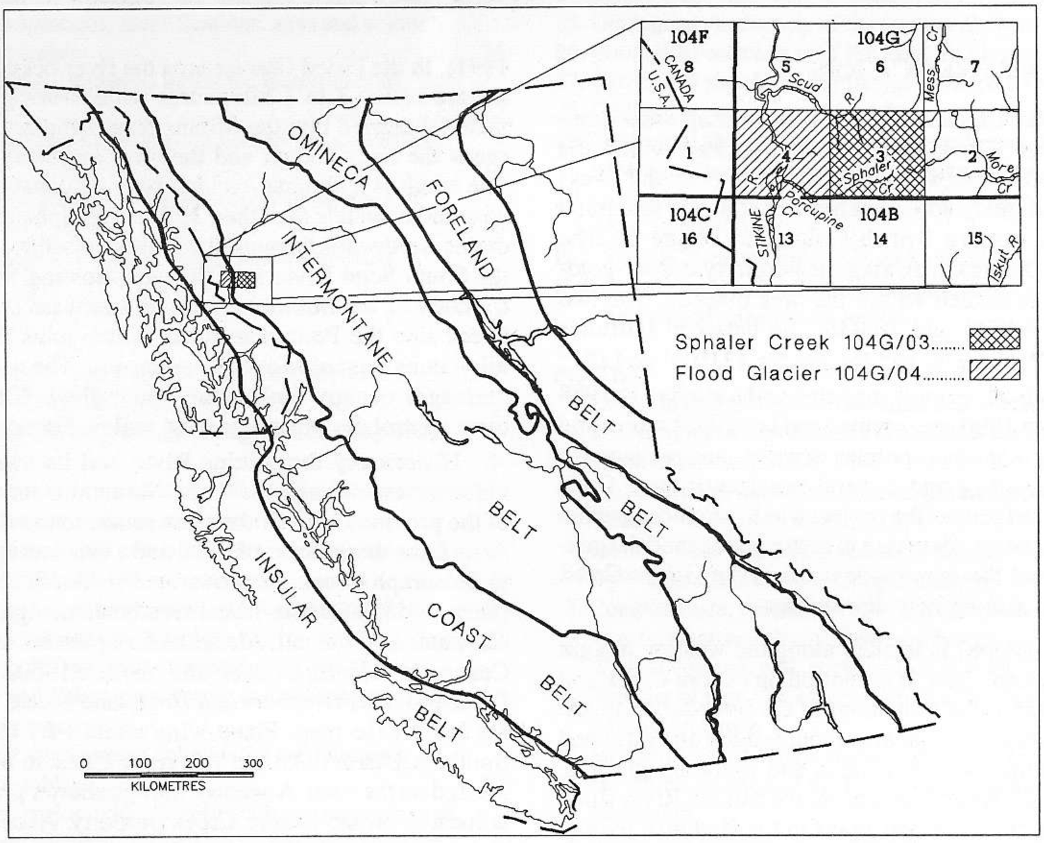


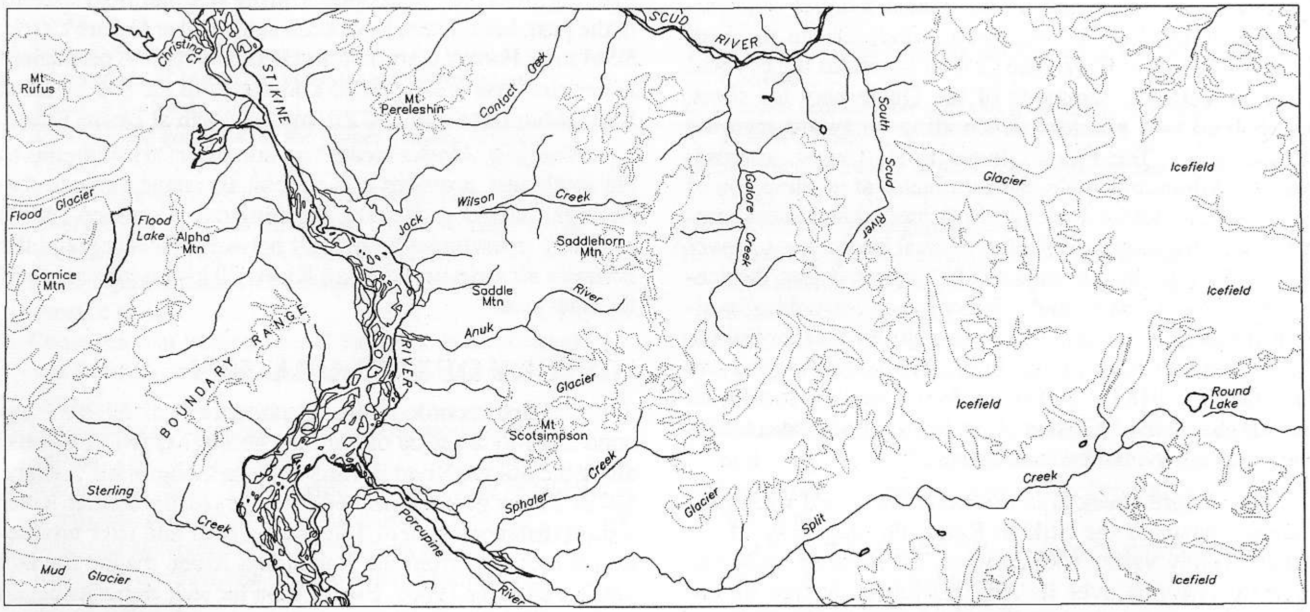


Figure 1. Location map and physiography of the study area.

Schaft Creek (Liard Copper) deposits were staked in 1957. The recent resurgence of mineral exploration has been in response to its geological similarities with the Sulphurets, Iskut and Golden Bear gold camps. Mining and exploration companies active in the map area during the fieldwork included Continental Gold Corporation (Trophy claims), Cominco Ltd., Mingold Resources Inc. and Kennecott Canada Inc. (Galore Creek), Equity Engineering Ltd. (JW and Trek/Sphal claims), Canamax Resources Inc. and Prime Equities International Corporation (Copper Canyon) and International Corona Corporation (now Homestake Mining Company; Sphaler Creek claims).

## PREVIOUS GEOLOGICAL WORK

Forrest Kerr carried out geological mapping along the Stikine and Iskut rivers from 1924 to 1929, but it was not until 1948 that his data were published (Kerr, 1948a, b). From his work in the Taku River valley of the Tulsequah map area, he defined the Late Triassic Stuhini Group, much of which underlies the current study area. In 1956, a helicopter-supported reconnaisance of the Telegraph Creek map area was conducted by the Geological Survey of Canada (1957, Operation Stikine). Other work by the Geological Survey of Canada (Figure 2) includes that of Souther (1971, 1972, 1988, 1992), Monger (1970, 1977a) and Anderson (1984, 1989). Jack Souther masterminded Operation Stikine and produced 1:250 000-scale geological maps of the Telegraph Creek sheet (104G), Tulsequah sheet (104K) and 1:50 000-scale detailed studies of Mount Edziza (1988, 1992). James Monger (1977a) further subdivided the late Paleozoic rocks and informally named them the Stikine assemblage. Robert Anderson's work includes studies to the north on the Hotailuh (1983) and Stikine batholiths (1984) and, more recently, a 1:250 000-scale geological map of the Iskut River area (Anderson, 1983). Peter Read has conducted regional mapping for the Geological Survey of Canada in the Stikine Canyon area (Read, 1983) and feasibility studies for B.C. Hydro in the Forrest Kerr Creek area (Read *et al.*, 1989).

Regional metallogeny studies and mapping by D.J. Alldrick, J.M. Britton and others of the British Columbia Geological Survey Branch have covered the Sulphurets, Unuk River and Snippaker areas to the south. A. Panteleyev

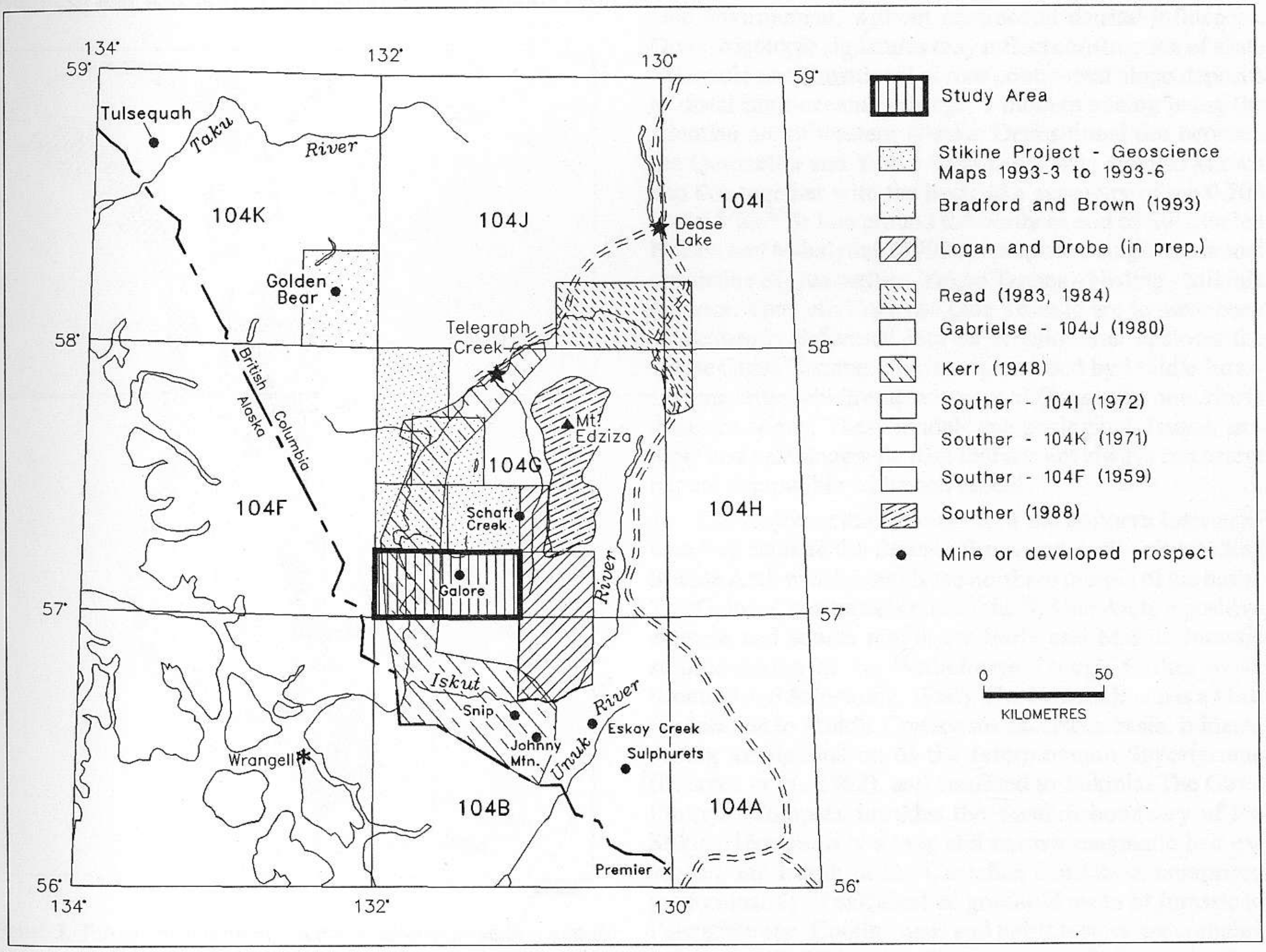


Figure 2. Compilation sources and previous work.

carried out mapping in the immediate area of Galore Creek, in conjunction with a study of the deposit between 1973 and 1975 (Panteleyev, 1973, 1974, 1975, 1976, 1983). All of his field maps and data were available to the authors. The distribution of syenite and some of the geology of the Galore Creek watershed has been compiled directly from these sources.

Further descriptions of the geology and mineral prospects within the area can be found in various Annual Reports of the British Columbia Minister of Mines dating from the early 1900s and assessment reports on file with the Ministry of Energy, Mines and Petroleum Resources .

## ACKNOWLEDGMENTS

We wish to acknowledge discussions with many people regarding various aspects of this study. In particular, Derek Brown, Andre Panteleyev and John Drobe of the British Columbia Geological Survey, Mike Gunning of the University of Western Ontario and Bob Anderson of the Geological Survey of Canada are much appreciated. Capable and enthusiastic assistance throughout the 1988 field season was provided by David Rhys and Darren Bahrey. The cooperation, logistical support and free disscussion of geological ideas by various mineral exploration companies made this study possible from its earliest stage. These people and companies include: Doug Forster and Greg Dawson of Continental Gold Corporation; Edward Yarrow of Hudson Bay Exploration & Development Company Limited; Henry Awmack and David Caulfield of Equity Engineering Ltd.; David Blann of Coast Mountain Geological Ltd. and Ian Paterson of Cominco Ltd.

We are indebted to W.E. Bamber, E.T. Tozer and B.L. Mamet, who provided important and timely fossil identifications, L. Rui and Silvia Pinard for fusulinacean identifications and M.J. Orchard of the Geological Survey of Canada for conodont identifications and colour alteration indices. J.E. Harakal and D. Runkle of the University of British Columbia carried out the radiometric dating.

W.J. McMillan reviewed an earlier version of this manuscript and suggested improvements. P. Chicorelli and J.R. Drobe of the Geological Survey Branch drafted the figures. Critical review by J.M. Newell and B. Grant improved the final version.

# CHAPTER 2 REGIONAL GEOLOGY

## TECTONIC SETTING

The study area (Figure 3) straddles the boundary between the Intermontane Belt and the Coast Belt and is underlain by rocks of the Stikine Terrane (Stikinia), the westernmost terrane of the Intermontane Superterrane. Stikinia is the largest of the allochthonous terranes. Like other terranes of the North American Cordillera, its geological history, paleontological and paleomagnetic signatures are unique. They indicate that it originated far removed from the margin of ancestral North America (Gabrielse *et al.*, 1991) and was amalgamated with the Cache Creek, Quesnel and Slide Mountain terranes prior to accretion to the craton (Figure 3).

Stikinia's outboard (western) position relative to the Cache Creek Terrane (Tethyan subduction complex) in British Columbia has always been an enigma (Monger, 1977b). Wernicke and Klepacki (1988) proposed that Stikinia and

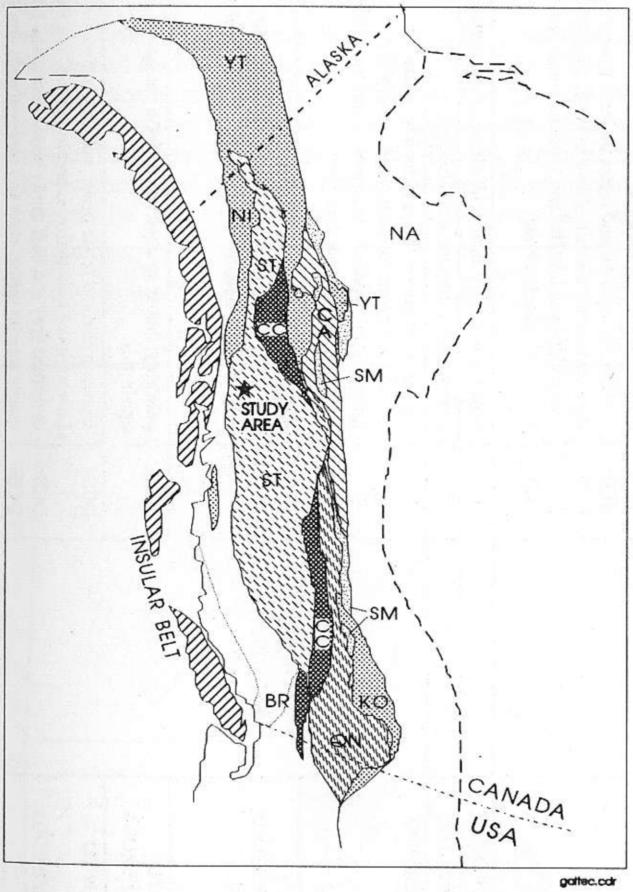


Figure 3. Terrane map showing tectonostratigraphic setting of the map area. NA=Ancestral North America, CA=Cassiar, NS=Nisling, KO=Kootenay, SM=Slide Mountain, SN=Quesnellia, CC=Cache Creek, ST=Stikinia, BR=Bridge River (modified from Wheeler and McFeely, 1991).

Quesnellia comprised a single arc generated by Mesozoic subduction of the Cache Creek Terrane, which through subsequent collision with Wrangellia and complex dextral movement, produced the present configuration. The result is a doubling up of the arc terranes, Stikinia and Quesnellia, with Cache Creek Terrane between the two. Recent geological studies in southeastern Alaska (Gehrels *et al.*, 1990; Rubin and Saleeby, 1991) and northwestern British Columbia (Gareau, 1991; McClelland 1992) correlate metamorphic rocks west of and within the Coast Belt with rocks of the Yukon-Tanana Terrane. McClelland and Mattinson (1991) and McClelland (1992) suggest that parts of the Paleozoic Stikine asemblage are correlative with and depositionally tied to Paleozoic rocks of the Yukon-Tanana Terrane. Neodymium isotope studies in the Iskut River area (Samson *et al.*, 1989) suggest the Stikine Terrane comprises juvenile (Phanerozoic) crustal material that evolved in an intra-oceanic environment, without continental detrital influences. Diverse isotopic signatures may reflect construction of a late Paleozoic arc transitional across continental slope deposits to distal intra-oceanic settings, a modern analog being the Aleutian arc of western Alaska. Depositional ties between the Quesnellia and Yukon-Tanana terranes are also known and this together with the hook-like geometry of the 0.706 initial $^{87}Sr/^{86}Sr$ line around the northern end of Stikinia led Nelson and Mihalynuk (1993) to propose a single arc model consisting of Quesnellia - Yukon Tanana - Nisling - Stikinia terranes. They envisage the Late Triassic arc to have been subsequently deformed into an orocline that encloses the Cache Creek Terrane. The orocline closed by Middle Jurassic time, after which emplacement of Quesnellia onto North America began. These models use geological, faunal, isotopic and paleomagnetic data that are not always consistent but are compatible with each model.

The major tectonic elements of the northern Intermontane Belt include the Bowser Basin and northeast-trending Stikine Arch which bounds the northern margin of the basin. The Galore Creek area is part of the Stikine Arch, a positive element and source region for Early and Middle Jurassic sedimentation in the Whitehorse Trough farther north (Souther and Armstrong, 1966). The Bowser Basin is a Middle Jurassic to Middle Cretaceous successor basin, initiated during amalgamation of the Intermontane Superterrane (Ricketts *et al.*, 1992), and confined to Stikinia. The Coast Plutonic Complex intrudes the western boundary of the Stikine Terrane. It is a long and narrow magmatic belt extending the length of the Canadian Cordillera, comprised predominantly of calcalkaline granitoid rocks of Jurassic to Paleogene age. Cooling ages and uplift history are complex across the belt. Plutonic rocks of the Coast Belt are mid-Cretaceous and older on the west side of the belt and mainly Late Cretaceous and Tertiary on the east where, in the study area, voluminous postorogenic Tertiary bodies obscure the

TABLE 1
TABLE OF FORMATIONS

| ERA | PERIOD | GROUP OR FORMATION | MAP UNIT | LITHOLOGY | THICKNESS (METRES) | INTRUSIVE SUITES |
|---|---|---|---|---|---|---|
| TERTIARY | QUATERNARY | | Qal | hotspring tufa deposit<br>unconsolidated glacial till, fluvial gravels | <5<br>10-20 | |
| | EOCENE | | | | | pink granite and quartz monzonite (**Eg**); grey medium-grained hornblende granodiorite (**Egd**) |
| MESOZOIC | LOWER JURASSIC | HAZELTON GROUP | lJHr<br>lJHs | felsite, tuffite<br>polymictic, maroon volcanic conglomerate, limy siltstone, shale and air-fall tuff | 500 | plagioclase quartz porphyritic diorite (**qp**) medium-grained quartz diorite, granodiorite (**eJgd**) potassium feldspar megacrystic hornblende granite to monzonite (**eJm**) |
| | UPPER TRIASSIC-LOWER JURASSIC | GALORE CREEK SUITE | TJv<br>TJt | potassium feldspar and pseudoleucite-bearing tuffs and flows,<br>well bedded maroon potassium feldspar crystal tuff, epiclastics and volcanic conglomerate | 200-300 | Galore Creek Intrusions: syenite, orthoclase porphyry monzonite (**TJs**) |
| | UPPER TRIASSIC | STUHINI GROUP | uTSp<br>uTSs<br><br>uTSt<br>uTSb<br>uTSv<br><br>uTSw | maroon pyroxene porphyry breccia flows and fragmentals,<br>fine-grained black clastics and bedded tuff; well bedded siltstone, sandstone, pyroxene crystal tuff, minor limestone<br>aphyric andesite lapilli tuffs<br>breccias, flows, lahar and intermediate fragmentals<br>massive basaltic andesite flows and tuff, plagioclase and hornblende-phyric<br>well bedded siliciclastics and volcanic wacke, minor andesite flows and basal polymictic conglomerate | 1000-2000 | **Hickman pluton:**<br>biotite hornblende granodiorite (**lTgd**), augite monzonite (lTm), plagioclase megacrystic diorite (**lTd**), gabbro (**g**), pyroxenite (**p**) |
| | MIDDLE TRIASSIC | | mTs | carbonaceous silty shale with elliptical concretions | <200 | |
| | LOWER TRIASSIC | | lTs | carbonaceous siltstone and limestone | <100 | |
| PALEOZOIC | LOWER PERMIAN | STIKINE ASSEMBLAGE | lPSc | Upper: light grey massive to thickly bedded, buff, bioclastic grainstone; foliated maroon and green epiclastics and tuff (**PSmv**)<br>Lower: thinly bedded, dark grey to buff bioclastic carbonate, common chert interbeds, argillaceous near base | <1000 | |
| | UPPER CARBONIFEROUS TO LOWER PERMIAN | | uCSv<br>uCSt<br>uCScg | maroon and green intermediate volcanics<br>green and buff siliceous siltstones and felsic tuffs<br>thick-bedded, boulder to pebble conglomerate, thinly bedded siltstone and sandstone | <2000 | |
| | LOWER-MID CARBONIFEROUS | | lCSc | pale grey, coarse-grained echinoderm packstone, interbedded maroon tuffs and epiclastics | <200 | |
| | DEVONIAN TO LOWER CARBONIFEROUS | | DCSv<br><br>DCSc<br>DCSs | Upper: mafic and felsic flows, volcaniclastics<br>Lower: intermediate flows, purple ash tuff, chlorite and sericite schist,<br>deformed grey and buff thinly bedded coralline limestone,<br>quartz sericite schist, slate and carbonaceous argillite | 500-1000 | Hornblende diorite (**lDd**) |

western margin of Stikinia. At this latitude, Stikinia consists of well stratified middle Paleozoic to Mesozoic sedimentary rocks and volcanic and comagmatic plutonic rocks of probable island arc affinity which include: the Paleozoic Stikine assemblage, the Late Triassic Stuhini Group and the Early Jurassic Hazelton Group (Figure 4).

## REGIONAL STRATIGRAPHY

Basement to Stikinia in the Galore Creek area is rocks of the Stikine assemblage, informally named by Monger (1977b) to include all upper Paleozoic rocks (within Stikinia) around the periphery of the Bowser Basin. The assemblage consists of Permian, Mississippian and Devonian age (using the geological time scale of, Harland *et al.*, 1989) calcalkaline and bimodal flows and volcaniclastics, interbedded carbonate, minor shale and chert (Table 1). The Permian carbonates and volcanics are a distinctive part of the Stikine assemblage, traceable for over 500 kilometres from north of the Stikine River to south of Terrace. Correlative Permian strata east of the Bowser Basin are assigned to the Asitka Group, a name applied to all Paleozoic strata in Stikinia (Wheeler and McFeely 1987). Unconformably overlying the Stikine assemblage is a succession of Lower to Middle Triassic sedimentary and Upper Triassic volcanic rocks. Upper Triassic volcanic rocks are exposed the length of the Canadian Cordillera. In the south, in Quesnellia, the Nicola and Takla groups lie east of the Cache Creek Terrane. Farther north, in Stikinia, the Stuhini and Lewis River groups lie west of the Cache Creek. There is little difference in age, lithology or chemistry of the Triassic strata across the northern end of the Intermontane Belt from one tectonostratigraphic terrane to the next (*i.e.*, between Takla and Stuhini). Unconformities separate the Upper Triassic Stuhini Group, mainly submarine volcanic rocks, from the chiefly subaerial Jurassic Hazelton Group volcanic and sedimentary rocks in the map area. Rocks of the Hazelton Group encircle the northern Bowser Basin inboard (basinward) of the Upper Triassic Stuhini volcanic arc (Figure 4). The Hazelton Group consists of a lower sequence of intermediate flows and volcaniclastics, a felsic volcanic interval and an upper sedimentary and submarine mafic volcanic accumulation. North of the King Salmon fault, sedimentary rocks of the post-amalgamation Jurassic Inklin overlap assemblage overly the Cache Creek Terrane.

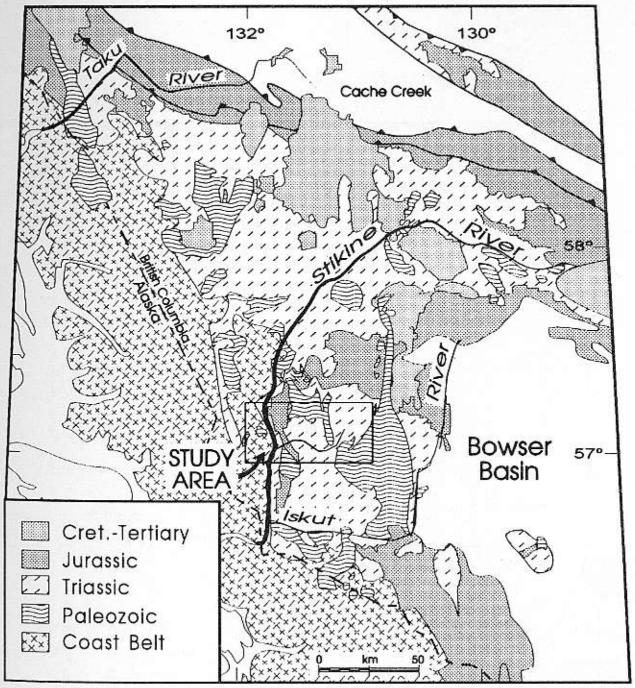


Figure 4. Location of study area relative to the major tectonstratigraphic features of the northwestern Cordillera and regional distribution of Paleozoic, Triassic, Jurassic and Cretaceous-Tertiary rocks of Stikinia (modified from Wheeler and McFeely 1987).

The pre-amalgamation Paleozoic and Mesozoic volcanic archipelagos, carbonate platforms and related clastics are overlapped by Middle Jurassic to Upper Cretaceous to Lower Tertiary successor basin sediments of the Bowser Lake and Sustut groups, north-trending Late Cretaceous to Tertiary continental volcanic rocks of the Sloko Group and Late Tertiary to Recent bimodal shield volcanic rocks of the Edziza and Spectrum ranges. Uplift and erosion, beginning in the Cretaceous and continuous through the Tertiary, has removed these latter elements from the study area (Figure 4).

## REGIONAL PLUTONISM

At least six discrete plutonic episodes: Late Devonian, Middle(?) to Late Triassic, Late Triassic to Early Jurassic, late Early Jurassic, Middle Jurassic and Paleogene are recognized in the Stewart-Iskut-Stikine area of northwestern Stikinia (Figure 5), through detailed work by Anderson (1989), Anderson and Bevier (1990), Brown and Gunning (1989a), Holbek (1988), Logan *et al.* (1992) and others. In a gross sense these episodes young westward from the Forrest Kerr pluton to the Coast Belt. Missing in this part of northwestern Stikinia are the three episodes of plutonism that span 100 million years of the late Jurassic (155 Ma) through Cretaceous (65 Ma). This report follows the informal terminology of Woodsworth *et al.* (1991) for the plutonic suites.

Late Devonian plutonism, unknown elsewhere in Stikinia, is represented by a composite body of tholeiitic hornblende diorite and younger calcalkaline granodiorite to tonalite phases of the Forrest Kerr pluton (Figure 5). Similar, though much smaller bodies that intrude Devonian rocks south of Round Lake, are not dated.

Middle(?) to Late Triassic plutonic rocks of the Polaris Ultramafic Suite and the Stikine suite intrude Stuhini Group volcanics and are considered to be comagmatic and coeval with them. The Polaris suite consists of numerous, small Alaskan-type ultramafic bodies; the Stikine suite, tholeiitic to calcalkaline granitoid plutons. The Hickman batholith comprising the Nightout and Hickman I-type plutons and the Hickman Ultramafic Complex contains both suites (Figure 5). In northwestern British Columbia, the Late Triassic to Early Jurassic Copper Mountain Plutonic Suite consists of numerous small alkaline and associated ultramafic bodies which occupy a north-northwest-trending belt along the east side of the Coast Range. They lie within Stikinia, are hosted by Upper Triassic Stuhini Group volcanics and include the

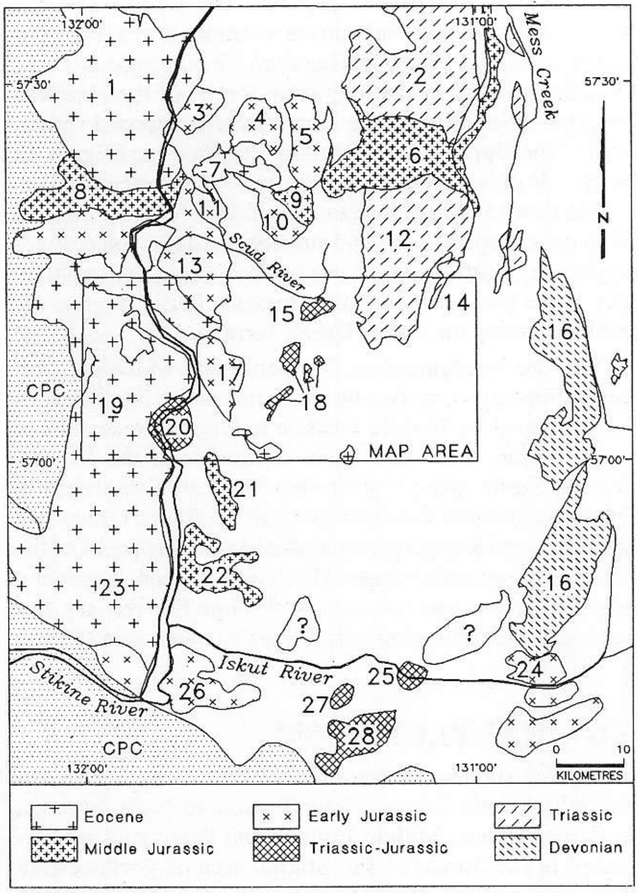


Figure 5. Location of map area relative to the six main plutonic suites in ithe Stikine-Iskut rivers area. Major intrusions are: 1=Sawback, 2=Nightout, 3=Devil's Elbow, 4=Dokdoan, 5=Strata Glacier, 6=Yehiniko, 7=Hamper, 8=Geology Ridge Diorite, 9=Niko, 10=Navo, 11=Cone, 12=Hickman, 13=Pereleshin, 14=Hickman Ultramafic, 15=Scud, 16=Forrest Kerr, 17=Saddle, 18=Galore, 19=Christina, 20=Stikine, 21=Middle Mountain, 22=Warm Springs, 23=Glacier, 24=McLymont, 25=Bronson, 26=Katete, 27=Zippa Mountain, 28=Seraphim. Compiled from Bevier and Anderson (1991), Brown and Gunning (1989), Holbek (1988), Logan and Koyanagi (1989), Logan *et al.* (1989), Macdonald *et al.* (1992) and McClelland (1992).

Bronson, Zippa Mountain and Galore Creek intrusions. These intrusives and their counterparts in Quesnellia host important alkaline porphyry copper mineralization.

The Early Jurassic Texas Creek Plutonic Suite consists of calcalkaline, I-type bodies that are slightly younger than the Copper Mountain suite. These plutons crop out discontinuously between the Coast and Intermontane belts as characteristically deformed and north-trending bodies metamorphosed to greenschist grade. They are cospatial and coeval with Hazelton Group volcanic rocks. Middle Jurassic plutons of the Three Sisters suite comprise calkalkaline, felsic intrusive phases of the Hotailuh batholith (Anderson, 1983) and Stikine batholith (Anderson, 1984) of the Stikine Arch. The Middle Jurassic Yehiniko pluton forms the central core of the Hickman batholith (Holbek, 1988) and two additional Middle Jurassic intrusions, the Warm Springs and Middle Mountain bodies (Bevier and Anderson, 1991) are exposed south of the map area (Figure 5).

Rocks of the Paleogene Hyder Plutonic Suite, representing the last major magmatic episode of the northern Cordillera, form the core of the Coast Plutonic Complex. This mainly Eocene event is characterized by plutons that are more siliceous, biotite rich and unaltered. They occupy a wide belt west of the Stikine River and are post-tectonic.

# CHAPTER 3 STRATIGRAPHY

## STIKINE ASSEMBLAGE

Initial work in the Stikine River area was by Kerr (1948a,b) who suggested a two-fold division for the Paleozoic strata; a deformed unit of pre-Permian metasedimentary and metavolcanic rocks; and an overlying less-deformed unit of Permian limestone (Figure 6). Souther (1972) and Monger (1970) recognized Lower Carboniferous limestone in the Telegraph Creek area and divided the Permian limestone succession into a lower, thinly bedded argillaceous or tuffaceous limestone and an upper massive, white grainstone. Kerr inferred Devonian ages, and recent work by Read *et al.* (1989) and Anderson (1989) identified a Lower to Middle Devonian unit near Forrest Kerr Creek, about 20 kilometres to the southeast. In the same area, Logan *et al.* (1990a, 1992) and Logan and Drobe (in preparation) have determined a Late Devonian (370 Ma) age for the Forrest Kerr pluton. Schematic Figure 6 illustrates the evolution and current geological understanding of the Stikine assemblage in the Stikine River area. The much simplified stratigraphic column is a compilation incorporating stratigraphy, radiometric dates and fossil identifications of Anderson (1989), Read *et al.* (1989), Logan *et al.* (1990a,b, 1992), Brown *et al.* (1991), Gunning (1990) and McClelland (1992) as well as ongoing work in the region by the authors.

Of particular significance is the recognition of Lower Triassic clastic sediments, a Lower Permian intermediate calcalkaline, and in part, subaerial volcanic sequence, Late Devonian felsic plutonism and a Devono-Carboniferous unconformity. A rapidly growing database and understanding of the Paleozoic history of Stikinia is emerging from current studies of the Stikine assemblage in the Iskut-Stikine-Tulsequah areas. It is from these areas that Early Devonian strata and Late Devonian plutons, the oldest dates for Stikinia are known and unconformities and deformational events are recorded in the Carboniferous and Permian stratigraphy. As such, the Stikine assemblage is retained for this discussion rather than the Asitka group of Wheeler and McFeeley (1987) and it is proposed that it be formalized to at least group status within the Stikine Terrane.

### DETAILED STRATIGRAPHY

The Stikine assemblage in the study area comprises five main subdivisions. The oldest consists of Devonian-Carboniferous(?) penetratively foliated limestone, phyllite, mafic and felsic flows and tuff overlain by a distinctive Lower to Middle Carboniferous limestone. Upper Carboniferous(?) to Permian thick-bedded conglomerate and siliceous siltstone overlie the limestone conformably to

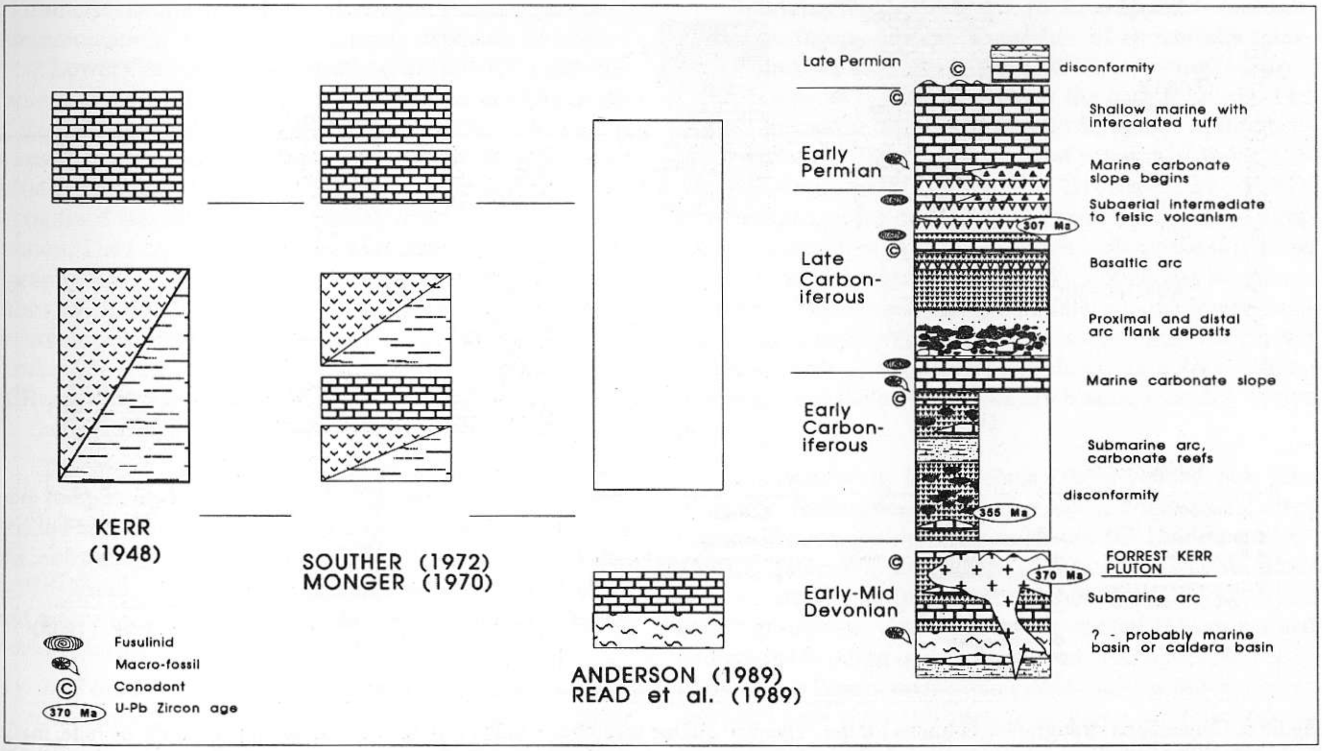


Figure 6. Evolution and current geological understanding of the Stikine assemblage stratigraphy, Stikine-Iskut area.

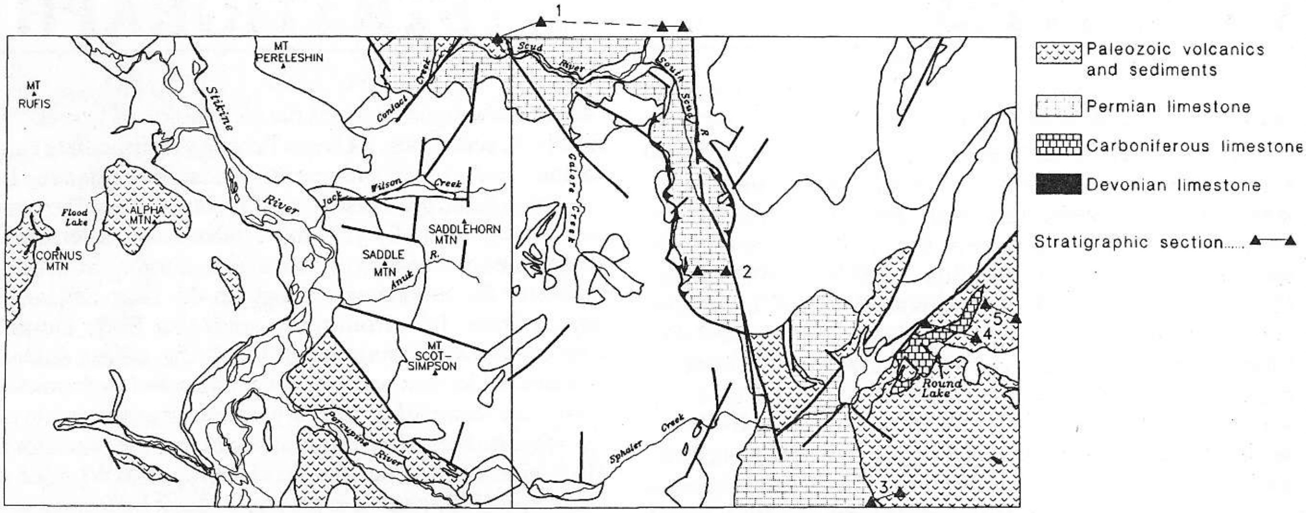


Figure 7. Distribution of Devonian, Carboniferous and Permian limestone and Paleozoic volcanic and sedimentary rocks in the study area. Lines show the locations of statigraphic sections in Figure 8.

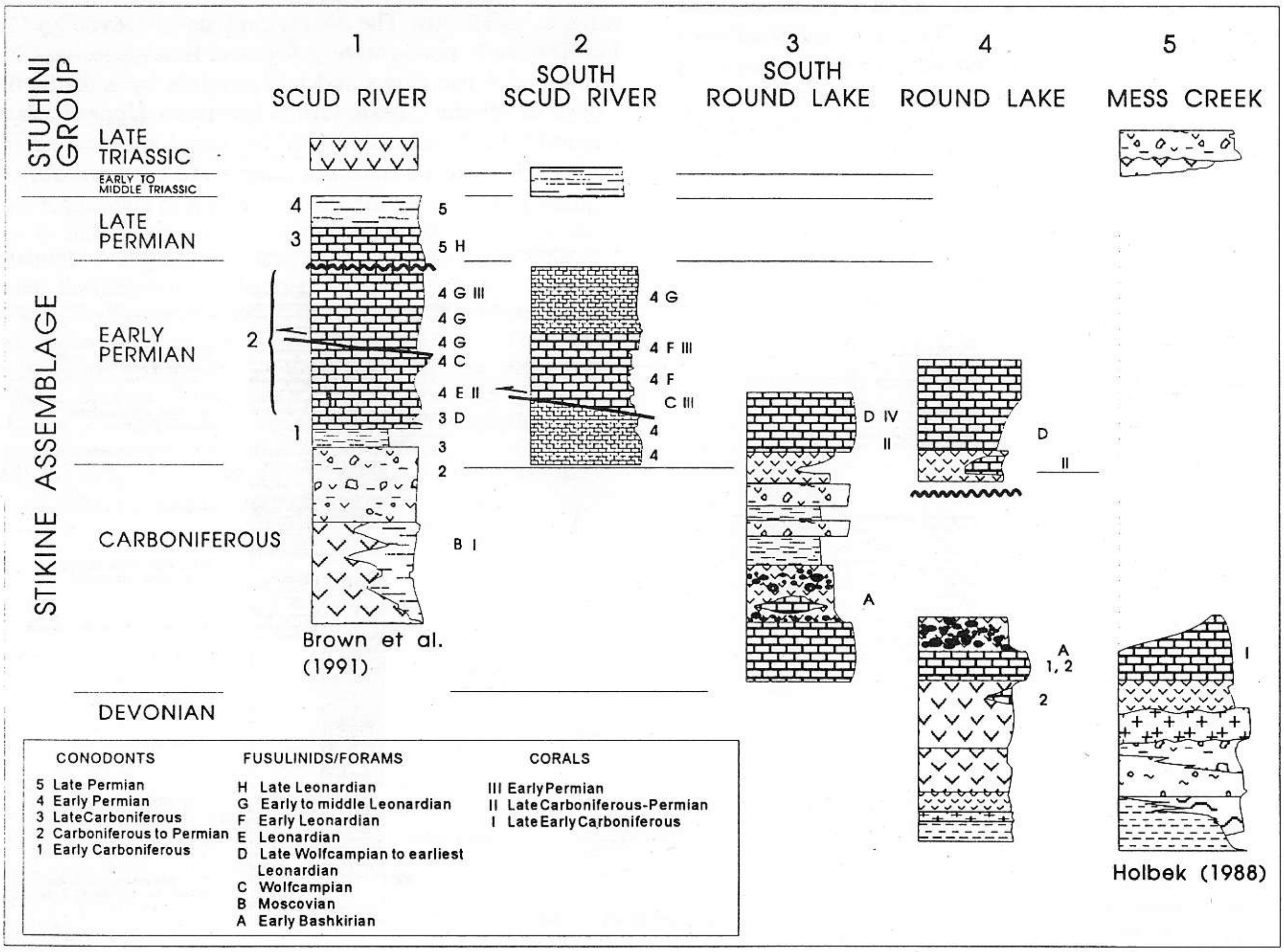


Figure 8. Generalized stratigraphic columns for the Paleozoic Stikine assemblage in the Galore Creek area. Volcanic units include: mafic flows (V), intermediate purple and green flows, tuff and felsic volcaniclastics (v). Sedimentary rocks include three main bioclastic limestone horizons, volcanic conglomerate, cherty siltstone and fine tuff. Numbers correspond to locations on Figure 7.

unconformably. Upper Carboniferous to Permian mafic and intermediate volcaniclastics overlie the siliceous siltstones and, in turn, are overlain in apparent conformity by a thick Lower Permian succession of fossiliferous limestone (Figure 6).

Paleozoic strata of the Galore Creek area occur as a northwesterly trending outcrop belt of predominantly Permian limestone extending from Sphaler Creek north to the Scud River. Farther west these rocks are exposed in the lower reaches of the Porcupine River, from where they extend northwestward into the Coast Belt as screens and roof pendants up to 4 kilometres across (Figure 7). Five generalized stratigraphic columns for the Stikine assemblage of the Galore Creek area, from northwest to southeast, are shown in Figure 8. Island arc deposition is characterized by stratigraphy and facies relationships which change rapidly and laterally from conformable in one place to nonconformable in another. Subdivision and correlation of volcanic assemblages, has therefore relied almost entirely on the presence of intercalated fossil-bearing carbonate units.

The most extensive and complete exposure of Devonian and Lower Carboniferous to Lower Permian strata is in the southeastern corner of the map area at Round Lake.

## DEVONIAN TO LOWER CARBONIFEROUS

A succession of variably foliated, Devonian to Lower Carboniferous metavolcanic and metasedimentary rocks underlies the southeast corner of the Sphaler Creek map. These rocks are the most penetratively deformed and metamorphosed rocks in the area mapped, with the exception of some pendant rocks in the Coast Belt. An isolated occurrence of Lower Devonian limestone crops out on a nanatack 7 kilometres southeast of Round Lake (M. Wescott, personal communication, 1991). A continuous exposure of uppermost Lower Carboniferous limestone and older(?) metavolcanic and metasedimentary rock is exposed in cliffs north of Round Lake (Figures 7 and 8). In general the rocks young westward. The southwest-dipping homoclinal section was initially estimated to be 2000 metres thick; subsequently we recognized isoclinal folding that structurally thickens the section. The Lower to middle Carboniferous carbonate stratigraphy has probably been thickened on the order of ten times. Without facing directions, thickness of the older metavolcanic and metasedimentary rocks is difficult to estimate. The stratigraphic sequence established for rocks east of Round Lake resembles that described by Holbek (1988) for the Mess Creek area.

The Mess Creek stratigraphic section (Figure 8) consists predominently of bimodal volcaniclastic rocks, interbedded sediments and minor flows. The lowest unit is a siliceous to graphitic argillite, gradationally overlain by mafic pyroclastic rocks. Felsic volcaniclastic rocks follow and are capped by subvolcanic diorite sills and undifferentiated volcanic flows (Holbek, 1988).

At Round Lake the lowest unit is graphitic argillite, siltstone and quartz-sericite schist at least 250 metres thick. The metasedimentary unit is characterized by abundant sigmoidal pressure-solution quartz veins and euhedral pyrite. The base is not exposed; its upper contact is conformable and the metasedimentary rocks are gradational with a structurally thickened succession (<750 metres) of metavolcanic rocks comprising three greenschist-grade, penetratively foliated purple and green units: intermediate volcanic rocks, mafic tuff and bimodal volcaniclastic rocks. All contacts are interfingering or gradational. The lowest volcanic unit comprises 100 metres of greenstone and chlorite schist derived from intermediate flows, sills and tuffs which, near the base, are interbedded with silver and green phyllite of the metasedimentary unit. The contact between metasedimentary and intermediate volcanic units is marked by a foliated medium to coarse-grained hornblende diorite sill, 20 metres thick. Stratigraphically equivalent intermediate volcanic rocks farther east (More Creek map sheet, 104G/2) contain numerous recrystallized limestone interbeds containing stromatoporoid *Favosites* sp. at least as old as late Early Devonian (Logan *et al.*, 1992). These same rocks are also intruded by Late Devonian dioritic to granitic intrusions. The intermediate volcanic rocks are followed by less than 200 metres of mottled and interbedded purple and green mafic lapilli and ash tuff overlain in turn by 450 metres of interbedded felsic tuff, plagioclase-porphyritic flows, tuff and conglomerate. The felsic pyroclastic rocks are altered to quartz-sericite-carbonate schists. Lower Carboniferous(?) limestone lenses containing rugose corals and large (2 to 5-centimetre diameter) echinoderm ossicles are present near the top of the volcanic sequence. Gnathodid conodonts from a limestone lens 50 metres below the top of the volcanic sequence are Carboniferous to Permian in age (C-159096, Table A-2).

## LOWER CARBONIFEROUS

Overlying the metavolcanic rocks in apparent conformity is a northwest-dipping homocline of structurally thickened carbonate 700 metres thick. Earlier mapping (Monger, 1970; Logan *et al.*, 1989) divided the carbonate into two distinct limestone units separated by 50 metres of interbedded foliated phyllite, tuff and intraformational limestone-pebble conglomerate (Figure 8; Brown *et al.*, 1991). Follow-up mapping outlined sections of tight folding, intrafolial isoclinal folds and faults which indicate the limestone is structurally thickened. The original thickness may have been only 175 metres, or the equivalent to the lower limestone unit of Brown *et al.* (1991). It is now clear that the two limestone units do not define a simple stratigraphy younging westward, but the subdivisions are retained for descriptive purposes.

The structurally lower unit is a thick-bedded, pale grey bioclastic limestone, 150 metres thick, containing Lower Carboniferous gnathodid conodonts (C-154498 and C-159078, Table A-2) and indeterminate colonial corals. Basal sections are locally ferruginous echinoderm packstone and coarse grainstone. Crinoid debris up-section is finer grained and graded bedding is well developed. The upper 50 metres of the lower limestone is intercalated with purple and green ash tuff. Less than 100 metres of green phyllitic, poorly sorted volcaniclastic rocks, cherty sediments and an intraformational limestone conglomerate (Plate 1) separates the two limestone units.

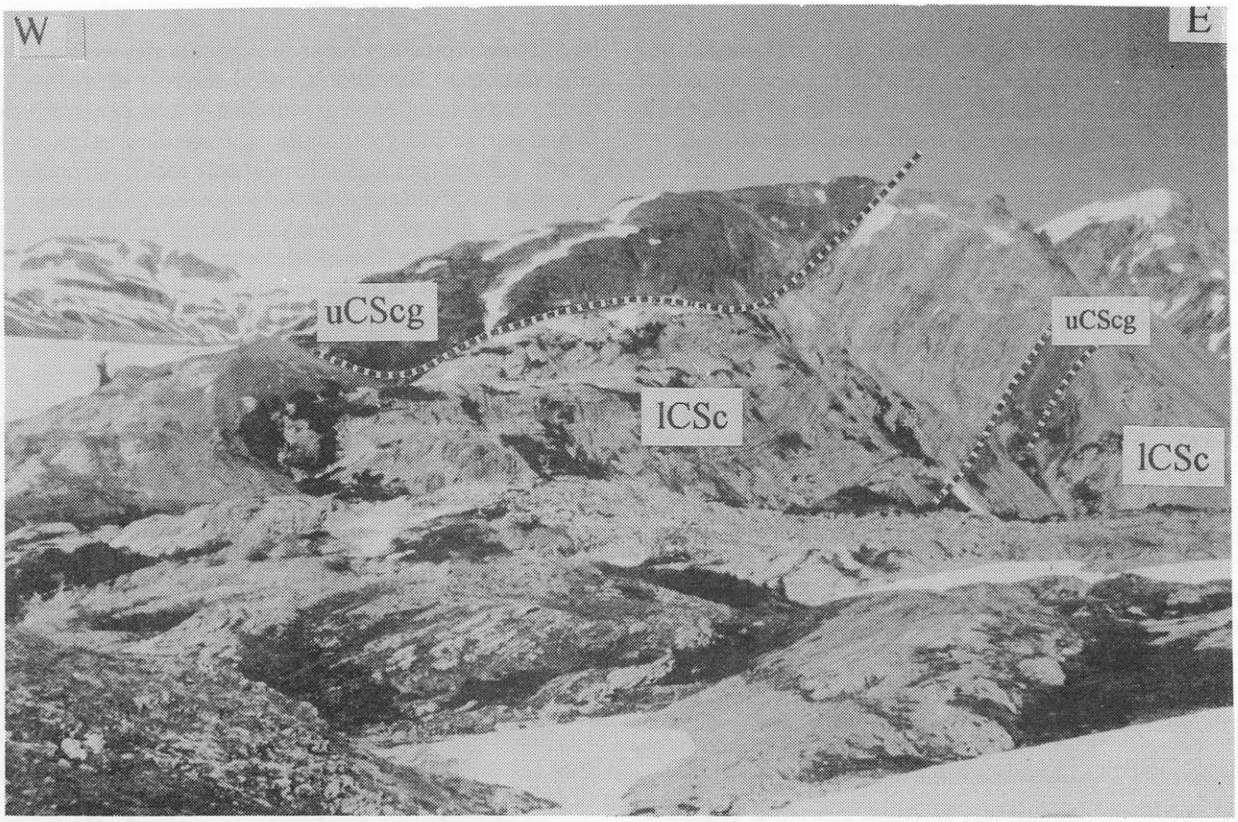


Plate 1. Lower to mid-Carboniferous limestone at Round Lake comprises a structurally thickened and imbricated succession of limestones, and a medial clastic wedge, overlain by an unconformity-bound Late Carboniferous to Permian volcanic conglomerate containing Carboniferous limestone clasts; view to the north.

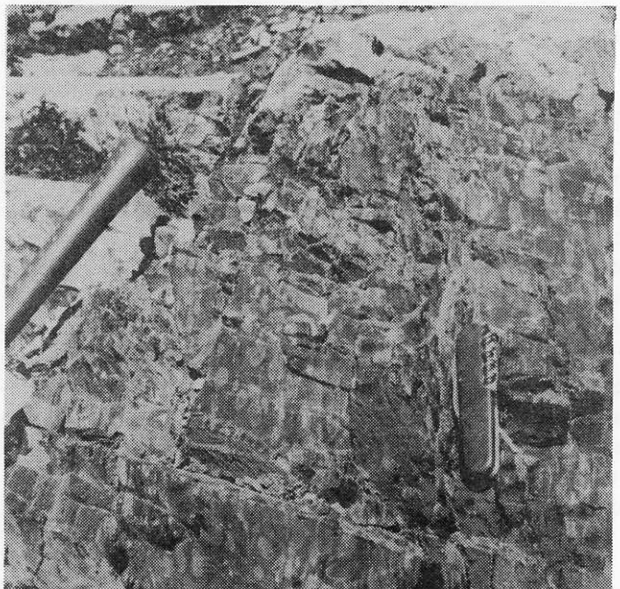

Plate 2. Lower to mid Carboniferous crinoidal wackestone from north of Round Lake contains variably strained *Acrocyathus* sp. corals of late Visean to Moscovian age (Table A-4).

The upper limestone member, 400 to 500 metres thick, is light grey, thick-bedded bioclastic grainstone. Yellow to black layers of amorphous silica, 10 to 40 centimetres thick, define bedding and constitute 15% of the outcrop. Rare lenses of green-purple tuff, 5 to 15 centimetres thick, occur throughout the limestone. Bryozoans and corals are abundant in the upper 50 metres. The presence of the coral *Solenodendrona* sp. cf. S. *furcatum* (Smith) indicates a late Early Carboniferous (?late Visean) age (C-159064, Table A-1).

The limestone stratigraphy was sampled systematically along three separate traverses in 1988, 15 conodont and 15 macrofossil samples were collected and subsequently identified (Tables A-1 and A-2). Strong deformation of the carbonate sequence was suspected, from recognition of deformed macrofossils (Plate 2) and elevated conodont C.A.I. values. A detailed stratigraphic and biostratigraphic sampling traverse was carried out in 1990 (Table A-2), in the hope that structural repetitions could be recognized biostratigraphically. Thin section studies of the carbonates were carried out by B.L. Mamet of the University of Montreal (Table A-4). The results of his study (Mamet, 1991a, b) follow. The carbonates are variably stressed; slightly to plastically sheared and recrystallized. The strain has been partitioned through the carbonate fold and thrust stack. Conodonts, foraminiferers and algae indicate a mid-Carboniferous, Bashkirian age across the width of the carbonates, but no biostratigraphic evidence for structural repetition. Corals indicate a broader range of late Visean to Moscovian age.

Bashkirian is lowermost Upper Carboniferous and as such these rocks might be better described under the next heading were it not for the seemingly continuous carbonate sequence including fauna ages of ?Visean to Bashkirian.

## UPPER CARBONIFEROUS TO PERMIAN

An arcuate, east-facing concave belt of Late Carboniferous to Permian sedimentary and volcanic rocks, 2 kilometres wide, crops out west of Round Lake (Figure 7). The section is complicated by normal faulting in the headwaters of Sphaler Creek, but repeated to the west. It is at least 300 metres thick and comprises three subdivisions: maroon and green polymictic volcanic conglomerate, a cherty siltstone, and mafic to intermediate tuffs and lava flows (Figure 8). These rocks crop out 8 kilometres south of Round Lake and extend as far as 10 kilometres southeast, onto the Forrest Kerr map sheet, 104B/15 (west of Newmont Lake).

At Round Lake, the upper limestone unit is overlain by more than 200 metres of fine-grained green to purple, calcareous lithic ash-tuff, wacke and volcanic conlomerate containing large blocks, boulders and clasts of upper Mississipian limestone (Monger 1977b). The conglomerate lies unconformably on deformed limestone. The top of the section is faulted.

South of Round Lake, at the southern edge of the map area, 200 metres of polymictic volcanic conglomerate, discontinuous limestone masses, well bedded siliceous epiclastics and intermediate volcanic rocks are exposed. They comprise a southwest-dipping homoclinal sequence which is overlain by Lower Permian limestone to the west. The conglomerate is medium bedded and locally fossiliferous. *Neospirifer* sp., *?Spiriferella* sp., and productoid brachiopods of probable Early Permian age (C-189355, Table A-1) are abundant in the conglomerate adjacent to limestone. Clasts of limestone in the conglomerate contain foraminifers of late Mississippian-Peratrovich facies and middle Carboniferous red algae facies (C-189355; Mamet, 1991a). An Early Permian to no older than middle Late Carboniferous age is indicated for the conglomerate. The middle Bashkirian age of the clasts indicates the age of the source rock. The succession in general fines upward and is comprised of volcanic sandstone, siltstone and siliceous argillite with plagioclase crystal tuff horizons and occasional conglomeratic beds. The fine-grained clastics display fining-upwards sequences, rip-up clasts and soft-sediment deformation features indicating a west-facing, right-way-up stratigraphic section. At this location, less than 100 metres of maroon plagioclase-porphyritic tuff caps the sequence and conformably underlies limestone containing Early Permian *Heritshiodes* sp. corals and *Pseudovidalena* sp. and *Clinacammina* sp. fusulinacean foraminifers (C-189356, Tables A-1 and A-3). The contact between Lower Permian limestone and maroon volcanics extends north to Sphaler Creek. Corals and fusulinacean foraminifers from lower sections of the limestone give age ranges from Late Carboniferous or Early Permian, Moscovian or younger (Clisiophyllid coral, C-159067, Table A-1) to late Asselian, Sakmarian (*Schubertella* spp., C-159067; *Schwagerina* sp. cf. S. *mccloudensis* Skinner and Wilde, *Pseudofusulinella* sp. indet., C-159066; fusulinacean foraminifers, Table A-3). Similar fauna are present in lower limestone sections west of Round Lake.

A similiar package of clastic rocks including light green, grey and black cherty siltstones, interbedded wacke and maroon conglomerates, overlies middle Carboniferous limestone in the northwest corner of Forrest Kerr map sheet (104B/15). Dark purple and green pyroxene-porphyritic and hornblende-plagioclase-porphyritic andesites, scoriaceous basalt and grey fossiliferous limestone clasts form up to 70% of the conglomerate. Angular blocks of limestone up to several metres across are common. In general the conglomerates are massive to thickly bedded.

West of Round lake, in the headwaters of Sphaler Creek, 300 metres of maroon and green volcanic flows, flow breccia, foliated tuff and well bedded, buff, siliceous tuff underly Lower Permian limestone (Figure 8). The contact is sheared. Thin limestone lenses, knots and boudins have been structurally interleaved with the volcanic rocks close to the contact, but others appear to be depositional. Limestones in this tectonized zone contain corals of Late Carboniferous or Permian age (*?Bothrophyllum* sp.; C-159077, Table A-1). Thin limestone lenses within a predominantly maroon volcanic and phyllitic siliciclastic sequence exposed 6 kilometres west and north of Sphaler Creek, contain the conodont *Neostreptognathodus* sp. of Early Permian, Artinskian age (C-154474, Table A-2). Over 500 metres of limestone conformably overlies the volcanic rocks.

The lower part of the Scud section (Brown *et al.*, 1991) comprises over 1500 metres of foliated greenschist-grade basaltic to andesitic flows and volcaniclastic rocks interfingering with phyllitic greywacke, siltstone, argillaceous chert and discontinuous limestone beds up to 200 metres thick. Early Carboniferous (Visean) corals and Late Carboniferous (Moscovian) foraminifers have been identified from the same locality (C-158927; Brown *et al.*, 1991). The age range is equivocal, but the section resembles the Moscovian volcanic and sedimentary rocks around the Tulsequah Chief volcanogenic massive sulphide deposit (Nelson and Payne, 1984; Figure 8). A felsic unit comprising 500 to 1000 metres of light coloured, well bedded aphanitic tuff, tuffaceous siltstone and chert gradationally overlies the volcanic and sedimentary rocks. South of the Scud River, a north-flowing creek exposes a panel of steep southwesterly dipping, light green siliceous siltstone and tuff (siliceous unit of Brown and Gunning, 1989a, b) overlain by thinly bedded Lower Permian limestones.

Monger (1970, 1977b) evoked a profound pre-Lower Permian unconformity to explain the disappearance of at least 1500 metres of Mississippian strata over a 5-kilometre strike distance at Round Lake. The section at Round Lake is now known to be structurally thickened and therefore reduces the erosional loss proposed by Monger. The distribution of Mississippian limestone also probably reflects paleotopography, with limestone representing accumulations on volcanic highs, rather than erosional remnants. The conglomerates and clastics of unit uCScg lie unconformably on Mississippian strata and represent post-Mississippian pre-Permian erosion. The strata are lithologically and biostratigraphically similar to the Baird Formation of the eastern Klamath Mountains as described by Watkins (1985).

## PERMIAN

Two regionally extensive Early Permian carbonate units characterize the Stikine assemblage of northwestern British Columbia. In the Scud River area the Permian limestone is areally extensive and locally thick. The carbonates are variably deformed, and have been structurally thickened by folds and thrust faults. The present map pattern reflects topography and the results of structural duplication (Figure 7). Within the map area, Permian limestones 800 to 1000(?) metres thick are exposed at the fork of the North Scud and South Scud rivers and can be traced south to the edge of the map area, west of Round Lake (Figure 7). Down-stream, to the east, the limestone forms the high, steep cliffs which flank the lower reaches of the Scud River.

The base of the Early Permian limestone crops out along the north and south sides of the Scud River valley at the northeast corner of the Flood Glacier map sheet (104G/03). The contact was examined where it is exposed in a north-flowing creek 10 kilometres north of Saddlehorn Mountain. The basal limestone is thinly bedded, contains the conodont *Streptognathodus* sp. of Late Carboniferous to Early Permian (Gzhelian-Asselian) age (C-189393, Table A-2) and conformably overlies light green siliceous siltstones and fine tuffs. The same stratigraphic relationships are described by Brown and Gunning (1989a, b) in the area to the north.

North of the Scud River, Brown and Gunning subdivide Permian strata into four lithologically and faunally distinct units (Figure 8). At the base is less than 85 metres of pyritic argillite and argillaceous micrite. Conformably overlying this section is over 1500 metres of thinly bedded bioclastic limestone further subdivided (Gunning, 1990) into a lower interbedded light and dark grey bioclastic micrite (550 metres), a middle thinly bedded light grey biomicarenite and varicoloured chert (700 metres) and an upper, thick-bedded grey to light biomicrite and biosparite (570 metres). This sequence contains an abundant Lower Permian macrofauna ranging from Wolfcampian to middle Leonardian, which includes solitary and colonial (fasciculate) rugose corals, fenestrate bryozoans, echinoderm ossicles, schwagerinid fusulinacean foraminifers, gastropods, and productoid and rhynchonellid brachiopods (Brown *et al.*, 1991). Fusulinid biostratigraphy from this unit suggests thrust faulting. The third unit is white-weathering sparry calcarenite with discontinuous beds of argillite and maroon crystal-lithic tuff to a minimum thickness of 180 metres. This is gradationally overlain by 210 metres of varicoloured siliceous sedimentary and volcanic rocks. The third and fourth units contain Upper Permian, Guadalupian conodonts (Brown *et al.*, 1991), the youngest age determinations for the Stikine assemblage in the area.

A belt of north-trending Permian limestone 3 kilometres wide crops out along both sides of the South Scud River valley. A section of limestone on the west side of the river between 1390 and 1970 metres elevation was measured and sampled for conodonts and fusulinids (South Scud River section, Figure 8). As well as can be established this section corresponds to the location of Pitcher's (1960) stratigraphic sections. He concluded the section was fault repeated higher on the slope. We recognized an older-over-younger repetition near the base of the section and limestones only as young as Artinskian. Studies of the fusulinids by Pitcher (1960) indicate a range in age from Wolfcampian to lower Guadulupian and similarities of these forms to faunas in the southwestern United States (*i.e.*, McCloud limestone).

The lower 350 metres of limestone are light grey, massive, mieritic calcarenites comprised predominently of echinoderm ossicles and lesser fusulinids, small horn corals, bryozoa and gastropods. This structurally lowest horizon contains the conodonts *Ellisonia* sp., *Hindeodus* sp., *Neogondella* sp., *Neostreptognathodus* sp. of Early Permian, Artinskian age (C-154484, Table A-2). These rocks are structurally overlain by 350 metres of older, grey medium-bedded grainstone interbedded with chert (Plate 3). The chert is both nodular and bedded and forms about 20% of the outcrop. Chert interlayers are 10 to 30 centimetres thick and discontinuous. The fauna includes abundant brachiopods (1-4% of the rock by volume), bryozoans, sparse gastropods and, near the base, solitary and colonial corals (form up to 2% of the rock by volume). Near the base are *Protolonsdaleiastraea* sp., ?*Bothrophyllum* sp., and *Petalaxis* sp., corals of Early Permian, Asselian or Sakmarian age (Bamber, 1988; C-154496). The corals in this collection form part of a widespread, Lower Permian, North American - Uralian coral fauna that occurs in the northern Ural Mountains, Spitzbergen, the Sverdrup Basin of the Canadian Arctic Archipelago, northern Yukon and Alaska, northern British Columbia, and at various localities in the western United States as far south as California. This fauna shows strong similiarities to the fauna reported from the McCloud limestone of northern California by Wilson (1982). Fusulinacean foraminifers of Sakmarian age (C-154496, Table A-3) occur near the base and are Artinskian age at the top (Rui Lin, written communication, 1991; C-154494). Overlying the calcarenite is 80 metres of light grey bryozoan-rich limestone characterized by 5 to 20-centimetre layers containing 30 to 60% fenestrate bryozoa in a micritic echinoderm-rich matrix (Figure 8). Overlying limestones (300+ metres) are light grey, massive-bedded bioclastic calcarenites with a fine-grained light grey micritic matrix containing variable percentages (5-40) of echinoderm ossicles, fusulinacean foraminifers, sparse fenestrate bryozoans and silicified productoid brachiopods. Lithologically these rocks correlate with the Lower Permian, Artinskian limestone of the lowest unit. A recessive section of poorly sorted, fine to medium-grained brown greywacke or tuff (5 metres thick), occurs near the top of the massive limestone section. This unit is correlative with the Lower to Middle Triassic sediments exposed at the top of the hill.

In the headwaters of Sphaler Creek, west of Round Lake, limestone overlies Upper Carboniferous to Permian, penetratively deformed, mafic volcaniclastics and pelites (Figure 8). The lower unit, 75 metres thick is dark grey, thin-bedded micrite and calcarenite interbedded with pyritic argillite. Fusulinaceans, small rugose corals, bryozoans,

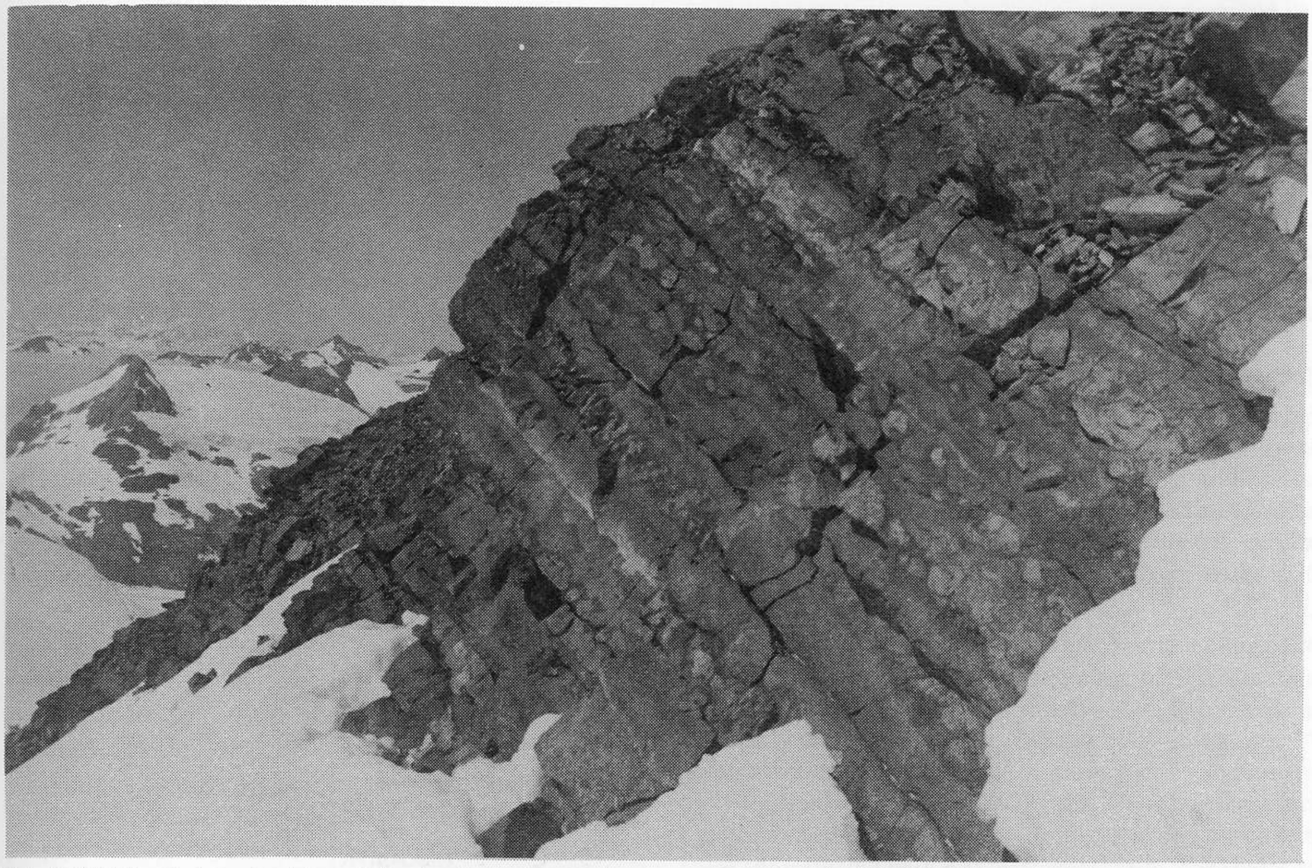

Plate 3. Well-bedded, moderately east-dipping Early Permian limestone exposed north of Sphaler Creek, viewed northwesterly. Limestone is a grey bioclastic grainstone containing bedded and nodular yellow or grey chert.

brachiopods and gastropods characterize this unit. ?*Bothrophyllum* sp. coral and *Pseudofusulinella* sp. and *Schubertella* spp. fusulinacean foraminifers indicate a late Asselian to Sakmarian age (C-159077, Table A-3). The rocks grade upward into pale grey to buff, thin to medium-bedded grainstone 450 metres thick, interbedded with discontinuous yellowish brown amorphous silica layers 10 to 30 centimetres thick that form about 20% of the outcrop. Bioclastic components consist predominantly of echinoderm ossicles, fusulinacean foraminifers, fenestrate bryozoans and indeterminate fossil fragments, within graded beds typical of low-energy (turbidity current) deposition. Fusulinacean foraminifers, associated with clisiophyllid corals indicate a middle Early Permian age (Artinskian; C-154491, Table A-2 and A-3). The upper 100 metres is tan to very light grey, bryozoan-rich and thin-bedded limestone with a micritic echinoderm-rich matrix.

## *GEOCHEMISTRY OF THE STIKINE ASSEMBLAGE*

Whole-rock major oxide and trace element analyses have been completed on twelve samples of Paleozoic Stikine assemblage volcanic rocks. Analyses were completed by the Ministry of Energy, Mines and Petroleum Resources analytical laboratory in Victoria. Results and sample locations are presented in Appendix B. The data were screened utilizing parameters discussed under "Geochemistry of the Stuhini Group", to identify and remove altered samples prior to plotting. Only five of the twelve samples were considered unaltered. Discrimination diagrams which utilize relatively immobile trace elements, are less affected by alteration and all twelve data points are plotted on these diagrams. Upper Carboniferous to Lower Permian tuffs and lava flows range in composition from basalt to dacite. On an alkalis versus silica diagram (Irvine and Baragar, 1971) the volcanics classify as subalkaline, and mainly as calcalkaline on the AFM diagram (Figure 9a, b). Basaltic andesite, andesite and dacite rocks classify as a medium-potassium suite on LeMaitre (1989) potash versus silica diagram (Figure 9c). The same nomenclature is evident on Figure 9e, the total alkalis versus silica plot of LeMaitre (1989). On the Ti-Zr-Y tectonic discrimination diagram of Pearce and Cann (1973), the single Devono-Mississippian basalt and Upper Carboniferous to Lower Permian volcanic rocks occupy fields characterized by calcalkaline basalts emplaced at plate boundaries (Figure 9d). Three basic lapilli tuff samples, collected from the same locality, structurally below Lower Permian(?) limestone, plot anomalously to the left of all other samples, outside the field boundaries of the diagram. The samples are altered; their position on the diagram results from an increased titanium content tied up with secondary magnetite.

## *CONTACT RELATIONSHIPS OF STIKINE ASSEMBLAGE TO EARLY MESOZOIC ROCKS*

Wheeler (1967) proposed the Tahltanian Orogeny to explain the Permian-Triassic disconformity in western Canada. With the exception of the Cache Creek Terrane (Or-

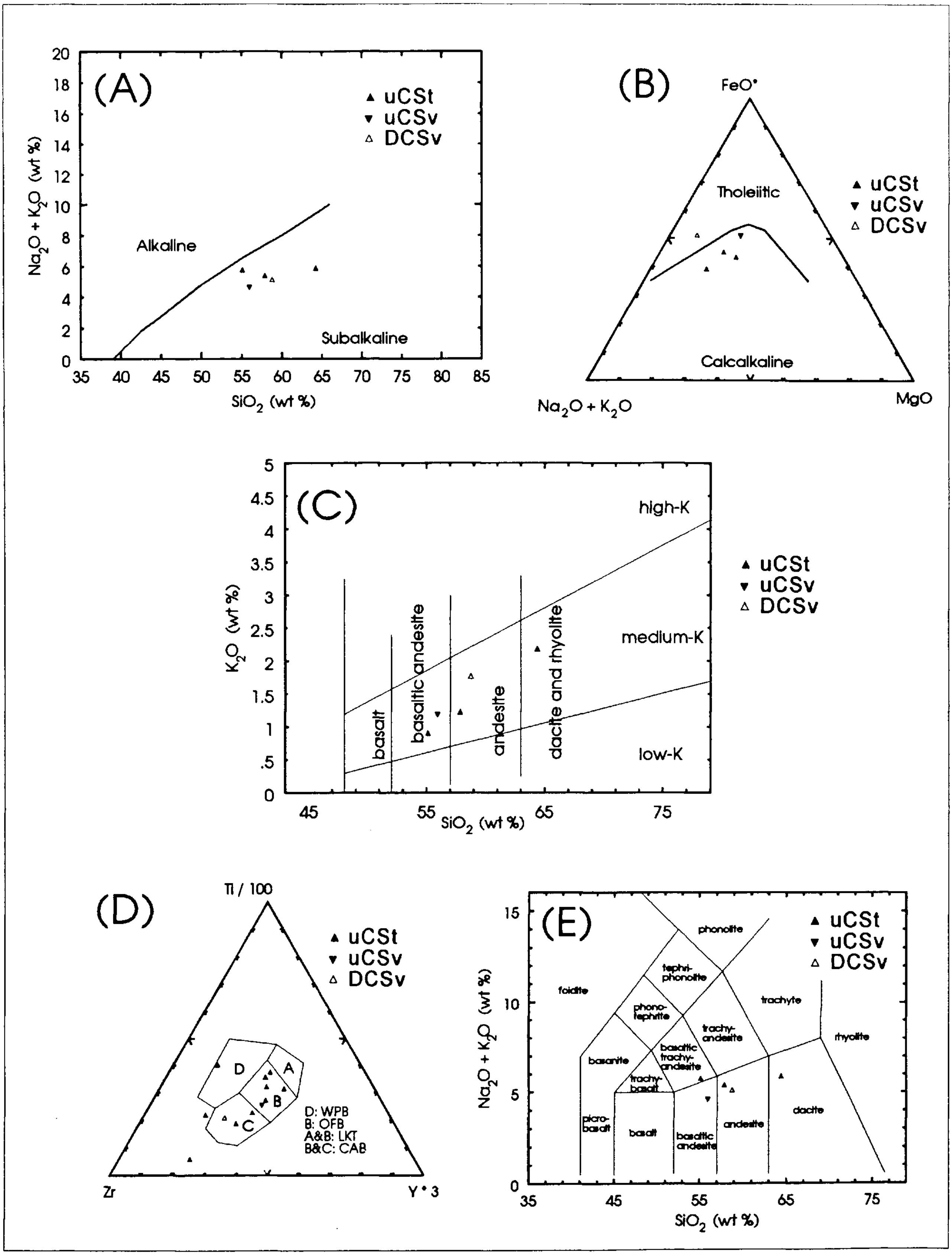


Figure 9. Whole-rock major oxide classification and trace element discriminant diagrams for Stikine assemblage volcanic rocks: A) and E) alkalis *vs* silica (after Irvine and Baragar, 1971 and LeMaitre, 1989), B) AFM (after Irvine and Baragar, 1971), C) potassium *vs* silica (LeMaitre, 1989), D) Ti-Zr-Y (after Pearce and Cann, 1973). WPB=Within-plate basalt, OFB=Ocean-floor basalt, LKT=Low-potassium tholeiite, CAB=Calcalkaline basalt.

chard, 1991a), this sedimentary and likely tectonic break has been recognized in Quesnellia, Stikinia, Taku and Wrangellia terranes at the Paleozoic-Mesozoic boundary. Souther (1972) suggested the deformation occurred between Middle and Late Triassic time in the Telegraph Creek area. To the north, in the Dease Lake area, Read (1983) recognized no metamorphic or structural disparity between Lower, Middle and Upper Triassic rocks and therefore concluded that the deformation occurred in the interval Late Permian to Early Triassic. South of Dease Lake, the Triassic rocks unconformably overlie the Permian and Carboniferous sequences (Read, 1984) and conodont colour alteration indices (CAI) show a significant thermal difference between the Triassic and older rocks. In the current study area, Lower Permian limestone is overlain paraconformably by unnamed Lower and Middle Triassic siliceous shale north of Copper Canyon, and elsewhere by Upper Triassic, Carnian conglomerate, wacke and volcaniclastic rocks. Due to the incompetent nature of the Lower to Middle Triassic sediments, they are generally very contorted and locally sheared in comparision with the more competent volcanic rocks of the Upper Triassic Stuhini Group. These fine clastics and cherts are infolded with Lower Permian limestones, but no basal unconformity has been recognized. Brown *et al.* (1991) identified a Late Permian, (Wordian) nonconformity north of the Scud River. In this locality, the Permian rocks consist of fine-grained clastics and ribbon chert, similiar to the lithologies of the Lower and Middle Triassic rocks to the south. These fine-grained, deep-water slope deposits suggest a similiar environment of deposition during the Late Permian to Middle Triassic, possibly a transgression and drowning of the carbonate platform.

## LOWER AND MIDDLE TRIASSIC

A narrow belt of Middle Triassic sediments extends 9 kilometres north from Copper Canyon (Souther, 1972). A second belt (about 5 kilometres long) of silty argillites containing the Middle Triassic fossil *Daonella* cf. *degeeri* Boehm (C-154459, Table A-1) and variegated cherts and siltstones has been recognized 3 kilometres to the east, above the South Scud River. In addition, small isolated exposures of Middle Triassic sediments crop out in faulted contact with either Upper Triassic Stuhini Group rocks or Lower Permian limestones along northwest-trending faults.

In the Stikine Canyon area to the north, Lower and Middle Triassic rocks of Read's (1983, 1984) informal Tsaybahe group consist of argillite, siltstone and chert with intercalated augite porphyry volcaniclastic rocks and an upper unit of augite-porphyritic volcanic rocks. No volcanic rocks are associated with the fine-grained sedimentary rocks in the Galore Creek area.

A preliminary stratigraphic interpretation suggests a two-fold division into a lower sequence of silty shales, argillites and limy dolomitic siltstones and an upper sequence of cherty siltstones and rare carbonaceous limestones. The entire section is tightly folded disharmonically and structurally thickened to at least 200 metres. The lowermost rocks are contorted rusty calcareous argillites which are structurally conformable with Permian limestones. The shales and silty slates of the lowermost sequence contain thin *Daonella*-bearing beds and distinctive silver-grey shale layers containing rusty, round to elliptical concretions. Overlying these shales is a thin-bedded package of black and dark grey siliceous and carbonaceous siltstones, in places limy and containing discontinuous carbonaceous limestones (Plate 4).

Plate 4. Lower to Middle Triassic thin-bedded shale and cherty siltstone, structurally overlain by Lower Permian limestone at Copper Canyon. Triassic clastic rocks are intruded by rusty weathering intermediate dikes, and disharmonically folded.

Biostratigraphic sampling was carried out in the Middle Triassic sediments and structurally overlying Lower Permian limestone above Copper Canyon in 1990. A large, diverse faunule of the conodonts *Ellisonia* sp(p)., *Neospathodus* ex gr. *conservtivus* (Muller 1956), *Neospathodus discreta* (Muller 1956) of Early Triassic, Smithian age was collected from thin limestone lenses in the sediments directly below the contact with the Permian limestones (C-189389, Table A-2). These are some of the oldest Triassic rocks recognized in Stikinia.

## UPPER TRIASSIC STUHINI GROUP

Kerr (1948b) first subdivided the Upper Triassic rocks of the Taku River area. He described lower clastic sedimentary rocks of the King Salmon Group, volcanic rocks of the Stuhini Group, and limestone of the Honakta (now Sinwa) Formation. Souther (1971) redefined the Stuhini Group to include all Upper Triassic volcanic and sedimentary rocks that lie above the mid-Triassic unconformity and below the Sinwa limestone. Monger (1980) followed this usage in the Tulsequah and Dease Lake map areas, where he interpreted the distribution of volcanic and sedimentary rocks in the southwest as proximal and in the northeast as distal facies equivalents. In characterizing the volcanic facies, Monger recognized a lower basic part and an upper intermediate to locally acid part. The lower sequence consists of augite porphyry volcaniclastics around the Hotaliuh batholith, however, these form only a minor component in the Tulsequah area, where aphanitic or fine-grained feldspar-porphyritic basalt flows dominate. The upper sequence of volcanic rocks around the Hotaliuh batholith and at the Taku River are intermediate fine-grained feldspar porphyries. At Kutcho Creek the upper sequence contains an acidic, quartz-phyric component (Monger and Thorstad, 1978). Upper Triassic volcano-sedimentary sequences elswhere have similiarities which correlate well with the general threefold subdivision established for the Stuhini Group at Galore Creek (Figure 10).

### *DETAILED STRATIGRAPHY*

Upper Triassic Stuhini Group flows, tuffs, volcanic breccias and sedimentary rocks define a volcanic edifice

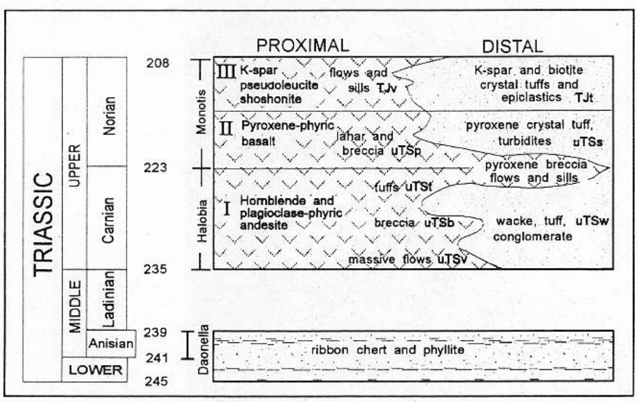


Figure 10. Generalized Triassic stratigraphy, illustrating the threefold subdivision of the upper Triassic volcanic and sedimentary facies rocks in the Galore Creek area.

centred on Galore Creek. Contemporaneous sedimentary rocks flank the volcanic centre and, east of the South Scud River fault, a sequence of metavolcanic breccias and massive volcanic rocks is intruded by the coeval Hickman pluton (Figure 11). Triassic arc rocks are floored by rocks of a Paleozoic arc, in particular Lower Permian calcalkaline volcanic rocks and areally extensive limestone of the Stikine assemblage. Stuhini stratigraphy ranges in age from early Carnian to late Norian, based on radiometric dates (Anderson, 1983) and fossil ages (Souther, 1972; Brown *et al.*, in preparation; this study).

Panteleyev (1976) subdivided the Galore Creek volcanic edific into a lower unit of submarine basaltic and andesitic breccias overlain by more differentiated, partially subaerial, alkali-enriched unit of flows and pyroclastics. In 1985 de Rosen-Spence, using unpublished geochemical data supplied by Panteleyev, interpreted the rocks to represent components of an emergent Upper Triassic island arc, characterized by shoshonitic and leucitic rocks. This study divides the Upper Triassic rocks into six sparsely fossiliferous, massive volcanic units and three well stratified sedimentary facies equivalent units; the latter contain diagnostic fossils. Volcanic rocks comprise the bulk of the Upper Triassic stratigraphy at Galore Creek and three different calcalkaline volcanic suites are recognized: a lower subalkaline hornblende-bearing basaltic andesite, a subalkaline to alkaline augite-porphyritic basalt and an uppermost alkaline orthoclase and pseudoleucite-bearing shoshonitic basalt.

The oldest, most voluminous and least distinctive units are aphyric and sparse hornblende and plagioclase-phyric flows, breccia and tuff of units uTSv, uTSb and uTSt. The rocks are fine to medium grained, massive and fragmental textures are common. Porphyries are trachytic, typically with 15% plagioclase phenocrysts and rarely up to 20% hornblende in a dense, green chloritic groundmass. Compositional similiarity of fragments and matrix in the fragmental units makes distinguishing them difficult. Fragmental rocks vary from block breccias to ash tuffs; lapilli tuffs are most abundant. The tuffs are brightly coloured; varieties include black, green and red. Where epidote or hematite preferentially replace fragments or matrix the rock colour is mottled. The size and density of fragments varies greatly over short distances and the monolithic nature of fragments and matrix make it difficult to trace these units. Black, lithic lapilli tuff is interbedded with Upper Triassic siltstones along Contact Creek and epidotized lapilli-block tuff underlies an extensive area between the Anuk River and Sphaler Creek near the eastern edge of the Coast intrusions (Figure 11).

Pyroxene-porphyritic breccia flows and fragmental rocks of unit uTSp typify the Stuhini Group. The flow rocks are predominantly basic augite and augite feldspar porphyries. They contain from 15 to 30% euhedral phenocrysts of pyroxene (up to 1 centimetre in size) set in a dense, dark green groundmass of feldspar and pyroxene. These medium to coarsely porphyritic basic flows are interlayered with aphanitic basalt, coarse-bladed feldspar porphyry and massive andesitic rocks. The lavas are pillowed, pillowed breccia flows or massive. Carbonate fills interstices between

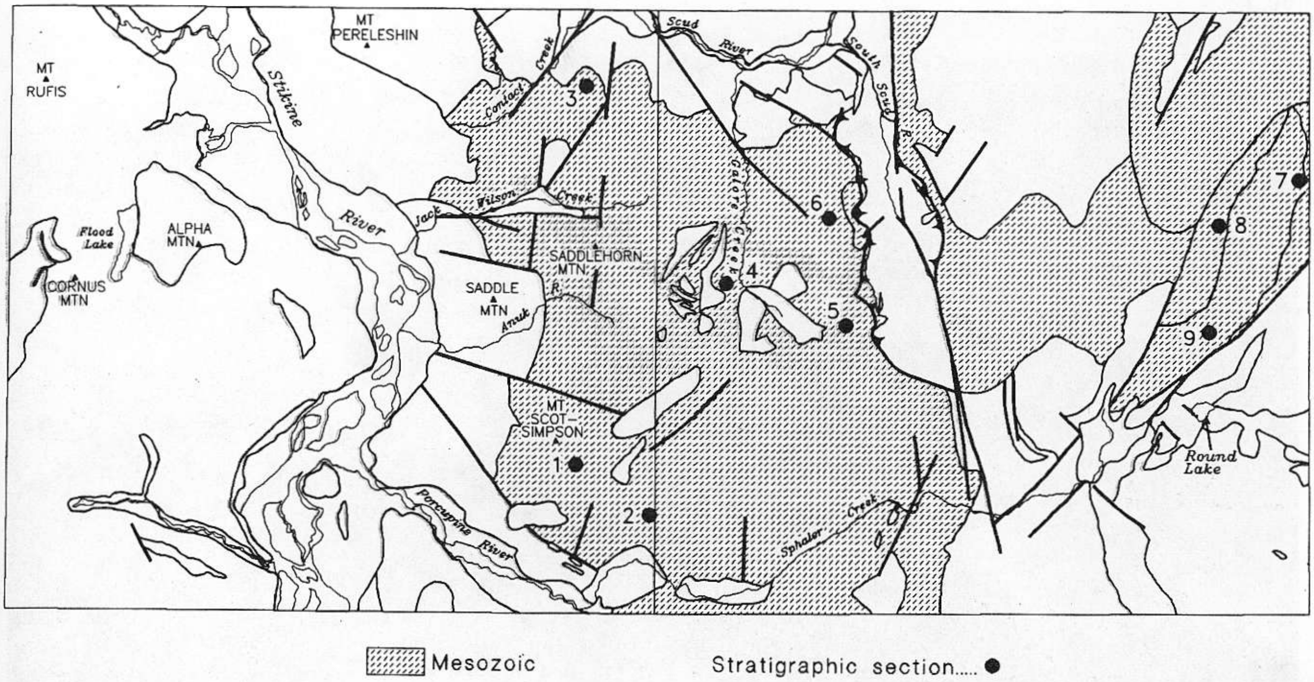


Figure 11. Distribution of Mesozoic volcanic and sedimentary rocks in the study area. Dots show the locations of statigraphic sections in Figure 12 and 14.

pillows and breccia fragments. Dikes and sills of pyroxene porphyry intrude upper Norian sediments and represent feeders to overlying flows (Plate 5). These porphyries cap several peaks and are some of the youngest Stuhini Group volcanics. Thick sections of green to purple augite basalt and andesite breccia form massive outcrops at the head of Hickman Creek and are overlain by purple amygdaloidal basalts. Rare, thin tuffaceous horizons and coarse-bladed plagioclase porphyry break the monotony of these thick piles of monolithic porphyry.

The upper volcanic unit (TJv) consists of an interbedded sequence of basic, coarse pyroxene feldspar flow breccias, orthoclase-feldspar crystal tuffs and coarse pseudoleucite flows and/or sills (Plate 6). Interlayered trachyte with coarse orthoclase porphyry flows and tuffs occupy the hangingwall of the Central zone at Galore Creek and are exposed on the ridge between the Anuk River and the head of Galore Creek. Purple to maroon, thin-bedded tuffs, epiclastics and siltstones of unit TJt crop out between Copper Canyon and Galore Creek (Figure 11). Red-purple thin-bedded ash tuff, siltstone and orthoclase crystal lithic tuff are interbedded with polymictic tuffaceous conglomerate and wackes. Maroon pyroxene basalt flows and ash tuff occur high in the section. Jeffery (1966) suggested that these distinctive maroon, well bedded rocks may be a separate suite of volcanics. They are interpreted to represent explosive extrusive equivalents of the syenite at Galore Creek, which accumulated in a subaqueous environment.

Stuhini stratigraphy is discontinuous and correlations of units between sections are obscured by facies changes and the lack of good age constraints on the volcanic strata. The most typical aspects of this Upper Triassic stratigraphy are best illustrated in the six columns on Figure 12. The stratigraphic sections include two predominately volcanic successions and four stratified sedimentary and volcaniclastic sequences. The distribution of Stuhini rocks is shown on Figure 11 and lithologies are described below, beginning with the volcanic facies.

## VOLCANIC FACIES

### *Mount Scotsimpson Section*

The rocks at Mount Scotsimpson comprise a thick mafic to intermediate volcanic pile, subdivideable into five stratigraphic units (Figure 12). Massive, undistinctive, even-grained hornblende plagioclase andesite flows make up the lowest unit. Massive flows are more abundant than flow breccias, and tuffs are only a minor component. Flow breccias are not scoraceous, but have lumpy weathered surfaces. Foliated sections are common. The volcanic rocks are massive, fine grained and plagioclase porphyritic; local areas with seriate textures are probably subvolcanic intrusions. The andesite contains millimetre-sized white to yellow plagioclase phenocrysts and dark chlorite clots after hornblende, in a grey-green, finely granular matrix.

A thick, fining-upwards volcaniclastic section overlies the lower division of massive flows. At the base are mafic block breccias and angular, coarse tuff breccias which grade upward into fine-grained feldspar crystal tuff and lithic ash tuff which cap the unit. The coarse fragmental rocks are scoraceous, epidote, chlorite and carbonate-altered basaltic andesite block tuff and flow breccias, with interbedded lapilli tuff and volcanic conglomerate. Up-section the matrix increases in proportion over fragments and finer fragmentals dominate; flows occur locally. The matrix and

Plate 5. Medium-bedded conglomerate, volcanic wacke and carbonaceous shale, overlie massive aphyric flows and breccias of the lowest Stuhini volcanic unit, north of Jack Wilson Creek. The sedimentary section has been thickened structurally and by intrusion of pyroxene-phyric sills and dikes.

Plate 6. Breccias of the upper alkalic volcanic facies, Unit TJv, exposed south of the headwaters of Contact Creek. Pseudoleucite porphyry clast in breccia suggests extrusion or explosive brecciation at the same time as syenite emplacement.

fragments are compositionally similiar and difficult to distinguish on unweathered surfaces. The uppermost fine volcaniclastic rocks are intermediate hornblende and plagioclase crystal lapilli and ash tuffs. Lapilli are flattened parallel to bedding. Tuff beds, 0.2 to 0.7 metre thick, are interbedded with lapilli and tuff breccias and the entire sequence fines upwards to the base of the overlying rusty weathering epiclastic unit.

Banded, slightly rusty weathering volcaniclastic and tuffaceous sedimentary rocks form a distinctive unit that is visible in cliff exposures below the peak of Mount Scotsimpson. The unit consists of thin-laminated grey siltstone, well bedded siltstone and sandstone with siliceous shale, interbedded with well sorted, fine to medium-grained feldspathic sandstone and tuffaceous grits. Several interbeds of well laminated, rusty weathering, pyritic black argillite occur. Fine-grained feldspar-phyric volcanic flows that cap the section and the mountain resemble the lavas of the lowest unit.

### *North Sphaler - Split Creek Section*

The northeast-trending ridge separating Sphaler and Split creeks is predominately volcaniclastic rocks and flows (Figure 12). A thin sedimentary unit of wacke and interbedded siltstone and shale crops out at the south end of the ridge. These sediments sit above the porphyritic andesite (at the top of the section), resembling the Mount Scotsimpson section. The lowest unit is a massive, very fine grained, indistinct pile of andesitic flows with lesser beds of lapilli tuff. Rare lavas exhibit good flow textures, such as aligned vesicules, breccia fragments and trachytic plagioclase. Most commonly the rock is a khaki green, finely granular to massive chloritic andesite; local areas have 5 to 10% millime-

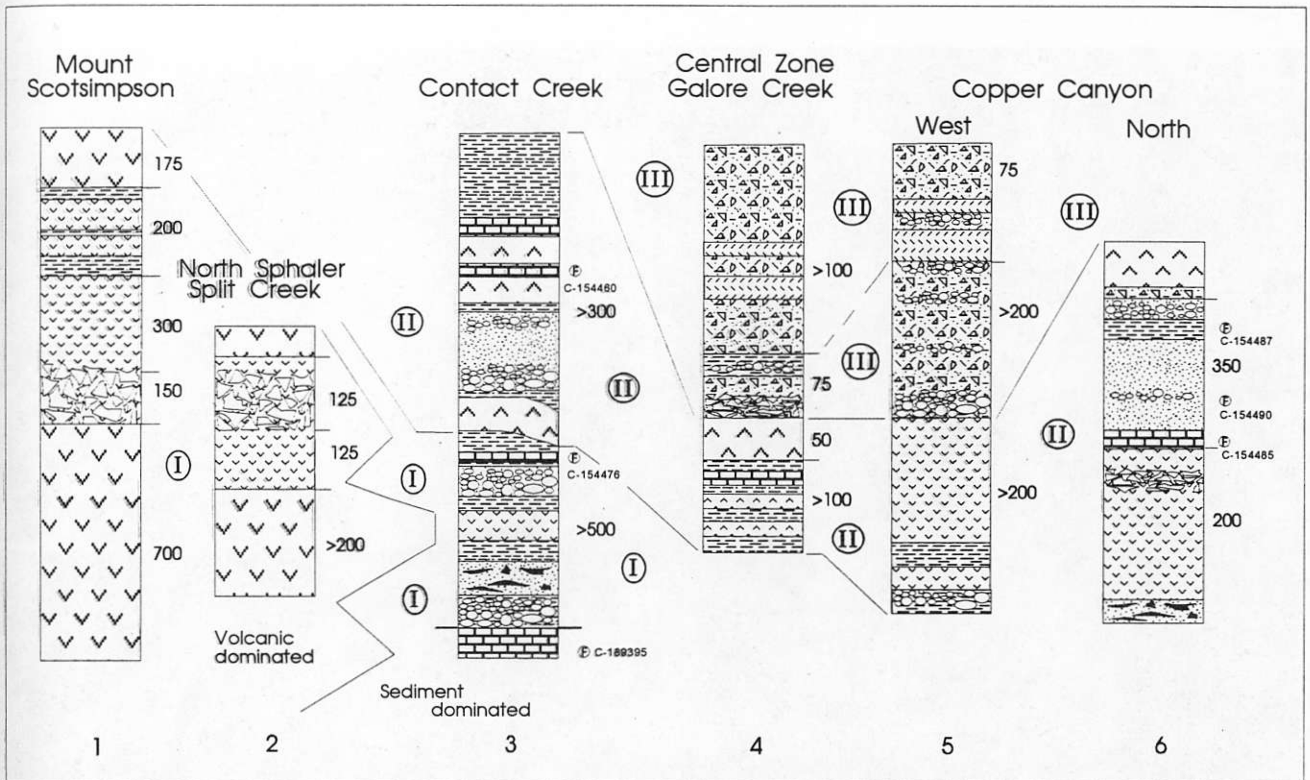


Figure 12. Generalized stratigraphic columns for the Upper Triassic Stuhini Group in the Galore Creek area. Volcanic units include: mafic green flows (V), intermediate maroon and green flows and tuffs (v), and pyroxene porphyritic volcanics (^). Alkaline lapilli and crystal tuffs and orthoclose-rich flows (herring bone pattern) comprise the uppermost subdivision. Sedimentary rocks include conglomerate, sandstone, siltstone and limestone. Numbers correspond to locations on Figure 11.

tre-size, chloritic hornblende and plagioclase phenocrysts. Fragmental rocks increase in abundance up section until, proportionally, they exceed the flow rocks. The top of the lower unit consists of well bedded lithic tuff and fine breccias.

The tuff unit comprises moderate to well bedded sections of lithic, lapilli tuff with a variety of porphyritic andesite, aphyric andesite and basaltic fragments. The tuffs coarsen up-section and grade into a very coarse and thick volcanic breccia. The matrix consists of scoriaceous ash and lithic clasts, not mud that might indicate a lahar. The unit is a coarse monolithic flow breccia containing 20 to 40% angular fragments that are indistinguishable from the matrix except in weathered outcrops. Clasts range to 50 centimetres and average 10 centimetres across; they include chiefly green aphyric andesite, scoraceous basalt and porphyritic andesite, as well as coarse boulders of flow breccia. Above these fragmentals are massive, very fine grained chloritic hornblende and plagioclase-phyric andesite of unit uTSv.

## SEDIMENTARY FACIES

Stratified, time-equivalent sedimentary and tuffaceous rocks that are distal facies equivalents of the lavas, were deposited on the flanks of the volcanic ediface. Their distance from the eruptive centres allowed the proliferation of Upper Triassic bivalves and periodically contributed material to engulf and preserve them. Carnian and Norian fossils characterize sediments in the area. An upper, partly subaerial alkali-enriched tuff and epiclastic sequence, with limited distribution close to the intrusive syenite complex of the eruptive centre, may have accumulated within a restricted basin or caldera on the volcanic edifice.

### *Contact Creek Section*

The best studied section of well bedded tuffaceous and argillaceous sediments and subordinate volcanic breccias crops out at high elevations between Jack Wilson Creek and Scud River (Figure 12). Lower Permian limestone underlies this package above the Scud River, and at Jack Wilson Creek, these sediments overlie Upper Triassic volcaniclastics and massive flows (Plate 5). West of Contact Creek the sedimentary succession begins with thin-bedded black calcareous and carbonaceous siltstone and ribboned chert of possible Early to Middle Triassic age. A pale green to yellow polymictic conglomerate forms the base of the succession from Contact Creek east to Galore Creek. Clast size ranges to 0.5 metre, but typical clasts are 5 to 10 centimetres in diameter. Clasts include well rounded drab-green and grey plagioclase-phyric andesite, buff-weathering subvolcanic intrusive rocks, angular chert and limestone, and siltstone and argillite rip-ups. The volcanic clasts differ from those in other Upper Triassic conglomerates we studied; there are no purple or maroon rocks, and no amphibole or pyroxene-phyric varieties. The conglomerates rest disconformably on limestone of probable Early Permian, Artinskian age (C-189395, Table A-1). Angular limestone clasts and chert fragments similiar to those interbedded with the Lower Permian limestone suggest a local erosional source. Carbonaceous siltstone beds are a minor component within the massive conglomerate.

Plate 7. Medium-bedded conglomerate, volcanic wacke and carbonaceous shale of the lower Stuhini sedimentary succession. The rocks are penetratively cleaved at a high angle to bedding, a rare occurrence in Stuhini Group rocks.

Plate 8. Orthoclase crystal-rich lapilli tuff horizon from a thick succession of alkaline flows and tuffs exposed on the ridge separating Galore Creek and Anuk River. Orthoclase crystals define a weak fabric; at centre of photo are syenite porphyry lapilli.

Above the conglomerate is a rusty brown weathering sedimentary succession comprised of volcanic wacke, carbonaceous fine clastic rocks, and interbedded black lithic and plagioclase crystal tuffs with rare limestone lenses. A distinctive unit from low in the section contains parallel-aligned siltstone and limy siltstone rip-up clasts. The siltstone rip-ups vary from 1 centimetre up to 0.5 metre in length and are elongate parallel to bedding in a fine to medium-grained calcite sand matrix. This lower sedimentary section contains the Late Triassic, (Carnian) conodont *Metapolygnathus* sp. (C-154476, Table A-2).

The lower package of chiefly brown-weathering fine wackes grades upward into thin variegated siltstone, well bedded ash and pyroxone crystal tuffs, reworked volcanic sandstone, minor limestone and polylithic conglomerate. The contact is gradational, but occasionally is marked by a pyroxene porphyry breccia flow or sill complex. The lower units are thin, repetitively graded AE-turbidites. They are characterized by soft-sediment slumping, faulting and scour-and-fill structures and crosscut by sedimentary dikes (Plate 7). Volcanic flow-breccia and coarse debris-flows erode and are interbedded with the turbidite sequence. Higher in the section thin-bedded and normal graded pyroxene crystal tuff, reworked volcanic sandstone containing vitreous pyroxene crystals, and pyroxene-porphyritic and bladed-plagioclase sills and lava flows are common. Thin silty sedimentary units within the uppermost package contain the upper Norian (Cordilleranus Zone) bivalve Monotis sp. (C-154460, Table A-1).

Correlative, well bedded, thinly laminated, tightly folded and contorted siltstone, sandstone and calcareous argillite outcrop on the slopes south of Sphaler Creek. These sediments are fissile, weather rusty and resemble the lower package of sediments exposed between Jack Wilson Creek and the Scud River.

### *Central Zone, Galore Creek*

Stratigraphy from drill holes (Figure 12) in the Central zone of the Galore Creek deposit is after Panteleyev (1976). Potassium enrichment and calcsilicate alteration has affected all rocks. The section is cut by relatively flat lying syenite sills and dikes, and steeply dipping basic and felsic dikes (not shown). Bedded rocks are divisible into four map units. The oldest are lithic and pyroxene crystal tuffs and epiclastic rocks, with minor breccia and rare trachyte flows, overlain by approximately 50 metres of massive pyroxene porphyry flows and breccias. Above the pyroxene flows is a thinly bedded unit of mainly tuff and breccia, containing orthoclase rather than pyroxene crystals, and rare flows. The uppermost unit comprises a sequence of layered and flow-banded orthoclase-rich flows, orthoclase crystal tuffs and crystal-lithic tuffs capped by, what might be, subaerial, variably welded ash flows.

Pseudoleucite trachyte flows crop out on the ridge between the Anuk River Valley and the head of Galore Creek. The tuffs are crystal rich in an ash matrix (Plate 8). The ridge is cut by a belt of very pronounced and strong penetrative deformation 0.5 kilometre wide and characterized by foliated and schistose rocks. A colourful, coarse polymictic boulder conglomerate is a conspicuous part of the Section. It contains clasts mostly of pale green sparsely porphyritic plagioclase andesite and some pyroxene basalt porphyry. Cobbles of pink potassium feldspar porphyritic syenite and granitic hornblende plagioclase porphyry occur near the top of the conglomerate unit.

### *Copper Canyon, West Section*

Alkaline volcaniclastic rocks dominate the section west of Copper Canyon. Volcanic rocks at the base of the section (Figure 12) are massive or flow brecciated porphyritic basalts. The rocks are pervasively potassium metasomatized, and in some places may be intrusive in origin. The lower unit is cut by coarse megacrystic syenite porphyry bodies and younger felsic and diabase dikes. Overlying the lower package are less altered tuff breccias, tuffaceous wackes and rare, interbedded orange-weathering grits containing shale rip-up clasts. The unit fines and becomes well bedded upward; the volcanic component also reflects a change to more alkaline magmatism.

Orthoclase and biotite crystal tuffs and fine epiclastics, lithic crystal tuffs, lapilli tuffs and polymictic volcanic conglomerates are interbedded with well laminated siltstone and fine-grained sandstone beds. The epiclastic and tuffaceous beds are characteristically feldspar rich, crossbedded and show both normal and reverse grading. Graded bedding, interpreted to be normal, indicates that the beds are overturned in places. To the northwest, the maroon lithic ash tuffs and lapilli tuffs interfinger with thin-bedded siltstone, conglomerate and clastic limestone pods. The finely laminated green cherty tuffs and limy sediments contain fossil fragments, unfortunately of indeterminate age.

Interbedded with the silts and tuffs are slump deposits of massive to chaotic maroon silt and sand containing crossbedded rip-up clasts and large angular breccia blocks of fine-grained tuff, some showing soft-sediment plastic deformation. The rocks are mainly purplish to violet coloured. Subhedral to euhedral clots and crystals of detrital biotite comprise from 2 up to 5% of a number of crystal lithic tuff beds (Plate 9). The euhedral crystals provide evidence for a pyroclastic origin for these rocks. Argon-argon step heating of biotite from this unit gives a plateau age of 212 Ma (Table 2). Among the sediments are polylithic conglomerates which contain syenite clasts typical of the Late Triassic to Early Jurassic Galore Creek intrusives. Orthoclase crystal tuffs contain large potassium feldspar crystals up to 1 by 2 centimetres in size. These purple tuffs and epiclastics are cut by numerous coarse to fine-grained pink syenite porphyry sills and plagioclase porphyry plugs. The top of the section consists of red and green augite basalt, basaltic andesite and breccias.

### *Copper Canyon, North Section*

A threefold subdivision of the Triassic stratigraphy is possible north of Copper Canyon (Figure 12). The lowest unit is a dark green sequence of medium to coarse volcaniclastics, massive amygdaloidal basaltic flows, and flow breccias. Poorly sorted, massive to thick-bedded wackes and pyroxene-crystal volcaniclastics predominate. Sections are calcareous and contain Triassic pentamerous echino-

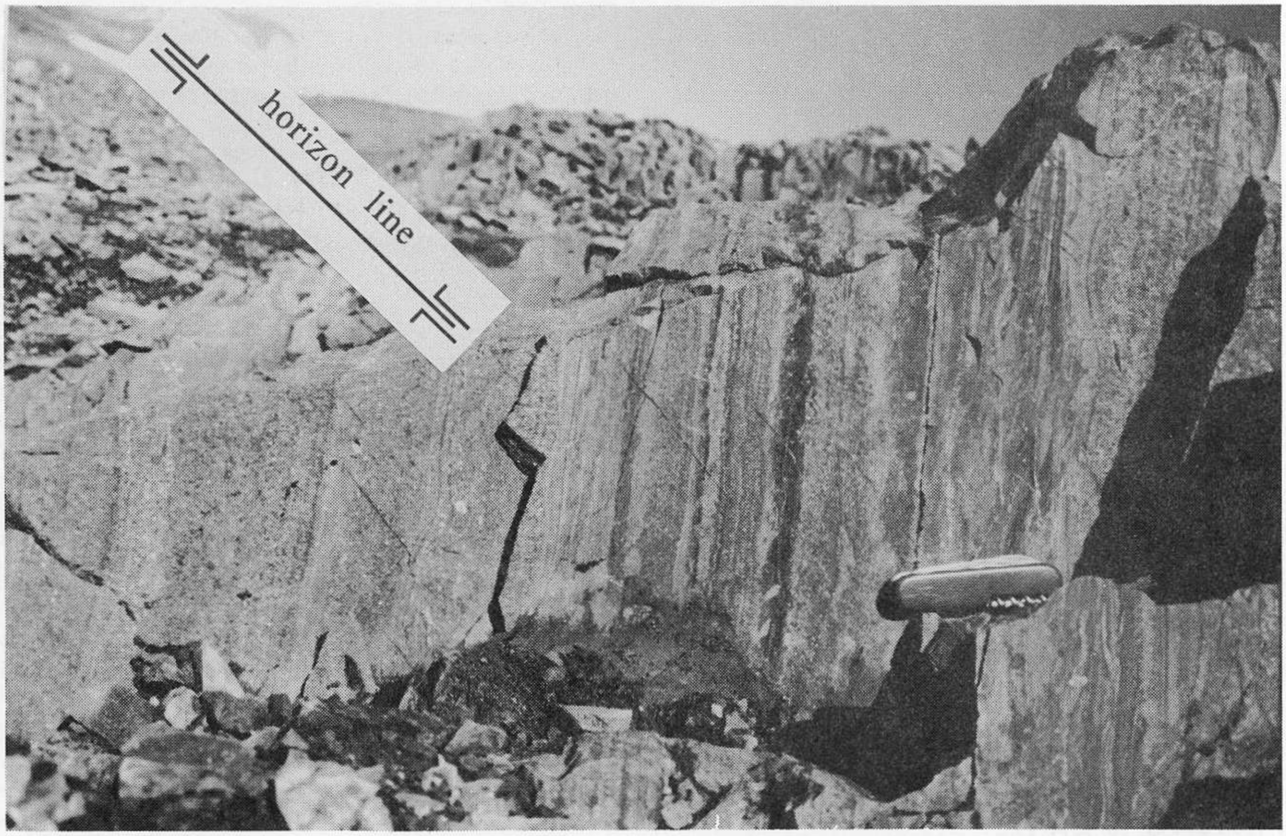


Plate 9. Overturned, tops to the left, thin and well bedded orthoclase and biotite crystal tuffs and epiclastic rocks west of Copper Canyon. Bedding dips 55° to north; photo is rotated, note horizon line.

TABLE 2
ISOTOPIC AGE DETERMINATIONS

| Map Number | Sample Number | NTS MAP | UTM East | Zone 09 North | Pluton or Locality | Map Unit | Method | Mineral | Age* | Interpret./ Reliability | Ref. |
|---|---|---|---|---|---|---|---|---|---|---|---|
| - | GC66-6 | 104G/05 | 330500 | 6351750 | Scud River | Egd | K-Ar | Bi | 45.1±2 | Good | 4 |
| 14 | 88VKO22-3 | 104G/03 | 358550 | 6321350 | Sphaler Creek | Egd | K/Ar | Bi | 47.3±1.7 | Good | 5 |
| 6 | 88VKO31-11 | 104G/04 | 346700 | 6328675 | Split Creek | eJm | K/Ar | $Bi^+$ | 48.2±1.7 | Good | 5 |
| 5 | 74AP-210 | 104G/04 | 346300 | 6327800 | Split Creek | Em | K/Ar | Bi | 48.5±1.7 | Good | 2 |
| 2 | 88VKO24-2 | 104G/04 | 333128 | 6335520 | Christina | Eg | K/Ar | Bi | 49.4±1.7 | Good | 5 |
| 1 | 88VKO24-1 | 104G/04 | 319774 | 6337895 | Felsite dike | Eg | K/Ar | Mu | 51.9±1.8 | Good | 5 |
| 4 | 73AP-73 | 104G/04 | 345500 | 6320800 | Sphaler | Egd | K/Ar | Bi | 53.5±1.6 | Good | 1 |
| 8 | GC66-1 | 104G/03 | 351200 | 6335400 | Galore Creek | eJs | K/Ar | $Bi^+$ | 177±9 | Reset/Poor | 4 |
| 13 | GC66-7 | 104G/03 | 358500 | 6332750 | Copper Canyon | eJs | K/Ar | Bi | 179.5±9 | Reset/Poor | 4 |
| 8 | GC66-2 | 104G/03 | 351200 | 6335400 | Galore Creek | eJs | K/Ar | $Bi^+$ | 192±9 | Reset/Poor | 4 |
| 10 | GC66-5 | 104G/03 | 353000 | 6342000 | Scud | eJgd | K/Ar | Bi | 185±9 | Stable/Fair | 4 |
| 11 | 75AP-107 | 104G/03 | 354000 | 6343500 | Scud | eJgd | K/Ar | Hb | 195±6 | Stable/Fair | 3 |
| 8 | A64-1 | 104G/03 | 351200 | 6335400 | Galore Creek | eJs | K/Ar | $Bi^+$ | 201±7 | Partial Reset | 4 |
| 7 | 75AP-142 | 104G/03 | 350000 | 6337000 | Junction | eJs | K/Ar | $Bi^+$ | 189±6 | Partial Reset | 3 |
| 7 | 75AP-142 | 104G/03 | 350000 | 6337000 | Junction | eJs | K/Ar | Hb | 251±7 | Partial Reset | 3 |
| 9 | 88JLO17-1 | 104G/03 | 351500 | 6334250 | Galore Creek | eJs | U/Pb | Zi | Insufficient Zi | .- | 5 |
| 3 | 73AP-75 | 104G/04 | 343250 | 6332800 | Anuk River | eJd | K/Ar | Bi | 120±5 | Reset/Poor | 1 |
| 3 | 73AP-75 | 104G/04 | 343250 | 6332800 | Anuk River | eJd | K/Ar | Hb | 197±5 | Stable/Fair | 2 |
| 7 | 75AP-751 | 104G/03 | 350000 | 6337000 | Junction | uTSv | Rb/Sr | WRx | 146±14** | Reset/Poor | 3 |
| 12 | 90JLO4-6 | 104G/03 | 356750 | 6334750 | Copper Canyon | TJt | Ar/Ar | Bi | 212*** | Stable/Fair | 5 |

Mineral abbreviations: Hb = Hornblende; Bi = Biotite; $Bi^+$ = alteration/secondary biotite; WRx = Whole rock; Mu = Muscovite; Zi = Zircon
Decay Constants after Steiger and Jäger (1977).
*Ages given with 2 sigma error
**Initial $^{87}Sr/^{86}Sr$ = 0.70449 ± 0.00014
*** 212 = mean of five plateaus, Total gas age = 204
References: 1,& 2 = Panteleyev (1975, 1976); 3 = Panteleyev, A. (unpublished); 4= White *et al.* (1968); 5= this study, 1990.

derms (star-shaped crinoids) and corals. Rare, thin interbeds of laminated siltstone and volcanic sandstone, grey-weathering clastic limestone (containing *Heterastridium* of Norian age, C-154485, Table A-1) and conglomerate are interbedded within the mostly massive volcaniclastic sequence.

The sequence fines upwards into an intermediate package of thin-bedded, fine-grained volcanic-derived sediments: black and grey siltstone and argillite, beige and grey shales and siltstones with numerous horizons containing the upper Norian bivalve *Monotis salinaria* Gabb (C-154490, Table A-1). Sedimentary structures are well preserved: flame and load structures, graded bedding and crossbedding. Distinctive coarse calcareous debris-flows are interbedded with these fine-grained sediments. They rarely exceed 2 to 3 metres in thickness and are comprised of granular carbonate and volcanic wacke matrix containing tabular rip-up clasts of fine shale, aligned parallel to bedding. Rarely, shale rip-up clasts have bivalve impressions. In general the section coarsens upwards, from fine shale and siltstone to sandstone, pebble and cobble conglomerate. Thin-laminated black argillite and pyroxene-crystal sandstone near the top of the middle unit contain the upper Norian bivalve *Monotis subcircularis* Gabb (C-154487, Table A-1).

The top of the unit is a well-bedded, green, clast-supported cobble conglomerate. The conglomerate is well sorted and beds are well layered. Clasts are rounded and mainly angite and plagioclase-phyric andesite; limestone clasts predominate in some beds. Less common clasts include hornblende diorite, orthoclase megacrystic porphyritic syenite and medium-grained granodiorite. The uppermost unit overlying this mature, waterlain beach-type conglomerate, is a coarse pyroxene-porphyritic breccia flow or lahar deposit. The pyroxene-rich volcanic rocks are mottled maroon and green and consist of coarse polylithic lapilli to block-sized volcanic fragments in a chaotic, massive pile of unknown thickness.

In summary, the three-unit stratigraphy (Figure 12) is evident from the fossil age constraints and lithologic and facies correlations. The lower unit is a volcanic package of basaltic, plagioclase and hornblende andesite flows and sedimentary equivalent wacke, turbidite and conglomerate. Above this unit are pyroxene-phyric volcanics and pyroxene-dominated sedimentary and epiclastic rocks of the second subdivision. The third and uppermost unit consists of alkali-rich tuff and epiclastic rocks and subaerial (?) flows. Between Jack Wilson Creek and the Scud River, well bedded Carnian wackes and conglomerates of unit I and Norian flows and pyroxene crystal tuffs of unit II disconformably overly Lower Permian limestone. North of Copper Canyon thin-bedded Norian argillite, limestone and volcaniclastics of unit II are overlain by green and maroon augite-bearing flows and breccias. Alkali-rich flows, tuffs and epiclastics of unit III overlie apparently correlative augite basalt at Galore Creek.

East of the South Scud River and south of the Hickman pluton is a thick succession of metavolcanic rocks. These mainly comprise a green, massive pile of mafic to intermediate flows, breccias and tuff deposits which host the Hickman pluton. The metavolocanics underlie the precipitous peaks south of the pluton in unknown contact relationships with Lower Permian limestone. Coarse granodiorite and locally 'pseudosyenite' (quartz diorite with megacrysts of anorthoclase not orthoclase) of the pluton intrude and metamorphose the volcanics. Lower greenschist grade assemblages of epidote, actinolite, chlorite and carbonate are seen in thin sections. Hornfelsed interbedded sedimentary layers are replaced by fine secondary biotite. Traverses were widely spaced and insufficient data are available to subdivide or correlnte the rocks in this area.

## *GEOCHEMISTRY OF THE STUHINI GROUP*

Whole-rock major oxide and trace element analyses have been completed on 15 samples of Stuhini Group volcanic rocks. These together with analyses of 45 samples collected by Panteleyev (c. 1974) are appended together with a sample location map (Appendix B). All analyses were completed by the analytical laboratory of the Ministry of Energy, Mines and Petroleum Resources in Victoria. The analysed suite includes thirteen samples from massive basaltic andesite flows, five flow-breccia samples and four tuff samples of the lower volcanic unit (I), six samples of pyroxene porphyry breccia flows, one of tuff and three from sills of the medial unit (II) and seven samples of alkaline trachyandesite flows and two of tuffs of the upper unit (III). The silica contents range from 46 to 60%, and indicate basalt and andesite compositions. On the total alkalis *versus* silica plot (Irvine and Baragar, 1971) the volcanics straddle the dividing line between the alkaline and subalkaline fields (Figure 13a). For reference, data for the comagmatic and coeval Hickman diorite and monzonite intrusions as well as the latest Late Triassic syenite samples are shown with the volcanic rocks on the major element plots. All samples plot in the calkalkaline field on the AFM diagram (Figure 13b).

Ratios of $K_2O/Na_2O$ vary widely from about 0.1 to over 20; ratios over 2 (the upper limit for unaltered rocks) are considered to be a result of potassium metasomatism. The high mobility of components such as $K_2O$, $Na_2O$, CaO, Rb, Sr and, to a lesser extent $SiO_2$ and $Fe_2O_3$, during metamorphism and weathering (Davies *et al.*, 1979) requires cautious interpretation of major element chemistry and favours utilization of relatively immobile trace elements such as Cr, Ti, Y, Zr, Co and Ni to discriminate magmatic affinities (Winchester and Floyd, 1977) and tectonic environments of volcanic emplacement (Pearce and Cann, 1973). Trace element chemistry was not completed on Panteleyev's sample suite and no sample pulps were retained for re-analysis. The result is a small and incomplete trace element data set. Thus, chemical characterization of the rocks relies, for the most part, on the major element chemistry and is subject to limitations imposed by alteration. To address this problem, both data sets were screened and the more altered samples removed prior to plotting the analyses on classification and discrimination diagrams. Samples were rejected based on two parameters: those with $K_2O/Na_2O$ ratios greater than 2 (eliminates hydrated and potassically altered samples), and those with loss on ignition (LOI) greater than 4% (eliminates oxidized and carbonate-altered samples). Where LOI

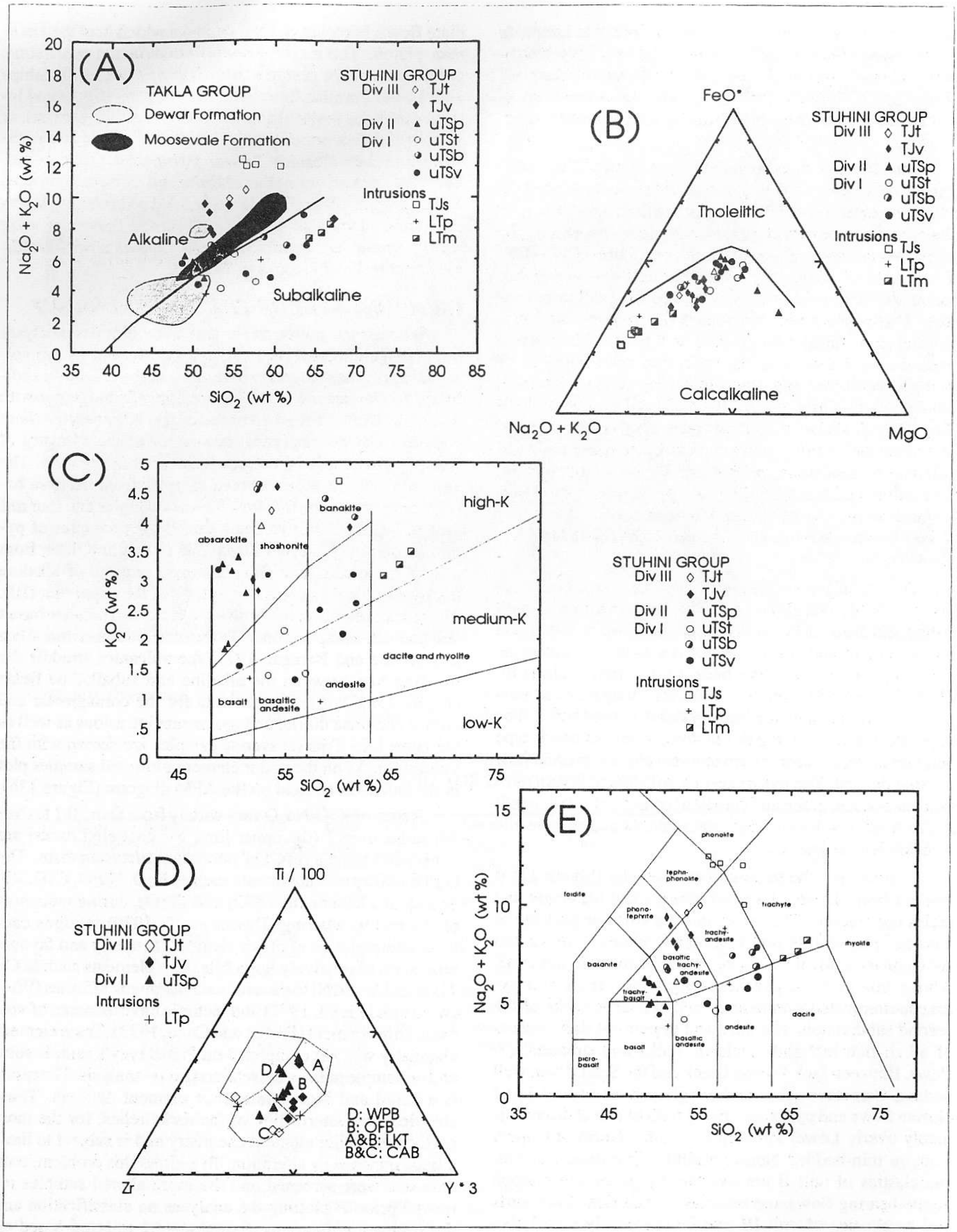


Figure 13. Whole-rock major oxide classification and trace element discriminant diagrams for Stuhini Group volcanic rocks, Hickman pluton and Galore Creek syenites: A) and E) alkalis *vs* silica (after Irvine and Baragar, 1971 and LeMaitre, 1989), B) AFM (after Irvine and Baragar, 1971), C) potassium vs silica (LeMaitre, 1989), D) Ti-Zr-Y (after Pearce and Cann, 1973). WPB=Within-plate basalt, OFB=Ocean-floor basalt, LKT=Low-potassium tholeiite, CAB=Calcalkaline basalt.

values were not available, samples with $CO_2$ contents greater than about 2% were rejected. Of the 60 samples, almost half (28) exceed these parameters and are not plotted on the diagrams.

The lower package of volcanics that underlies Mount Scotsimpson and Saddlehorn Mountain was well sampled by Panteleyev (1974) and corresponds with stratigraphic units of Figure 12. The rocks are chiefly basaltic andesite to andesite with silica contents that range from 52 to 60%. The alkalis *versus* silica plot shows the volcanics to be mainly subalkaline (Figure 13A). On the potassium *versus* silica plot (LeMaitre, 1989) the rocks are transitional medium to high-potassium basaltic andesite and andesite (Figure 13C). Two samples from high in the stratigraphy (unit I, Figure 12) plot as high-potassium shoshonites. Pyroxene-porphyritic flow breccias (unit II, Figure 12) are mainly potassic trachybasalt (*i.e.*, $Na_2O$ - 2.0 $K_2O$, LeMaitre, 1989). Silica values cluster around 48%; the two higher values, at 57%, represent a subvolcanic pyroxene plagioclase porphyry sill and a dike respectively. The rocks plot as high-potassium absarokite on the potassium *versus* silica diagram of LeMaitre (1989). The upper package of volcanics (unit III, Figure 12) occurs at generally high elevations and peripheral to the Galore Creek syenite intrusive complex, on the 'West Rim' between the Galore Creek and Anuk River watersheds, southeast of the Central zone deposit and west of the Copper Canyon deposit. These rocks were extensively sampled but due to their spatial and temporal association with mineralization are often strongly metasomatized. Silica contents range from 47 to 52%, although one more siliceous flow has 57% $SiO_2$. The alkalis *versus* silica plot shows these volcanics to be alkaline. On the potassium *versus* silica diagram (LeMaitre, 1989) the rocks plot as high-potassium shoshonites and banakite with three samples (75APA-126, 75APA-116 and 74APA-104) having greater than 5% $K_2O$. The Galore Creek syenites plot distinctively high in the alkaline field (Figure 13A). They are higher in potash content than typical alkaline rocks; unaltered samples have total alkali contents of 10 to 13%. The alkaline nature of the uppermost unit suggests a genetic association with the subvolcanic syenites.

The Ti-Zr-Y diagram (Pearce and Cann, 1973) in Figure 13D descriminates within-plate basalts from those extruded along plate margins. The Stuhini volcanics plot predominantly within the fields characterized by calcalkaline basalts emplaced at plate boundaries; samples plot outside the within-plate fields (WPB of field D). Distinguishing 'plate margin' basalts on the Ti-Zr plot of Pearce and Cann (1973) identifies the Stuhini volcanic rocks as calcalkaline basalts. This, together with their field relationships discounts an ocean floor basalt (OFB) setting.

The Late Triassic volcanic rocks are transitional from subalkaline to alkaline; by latest Triassic or possibly earliest Jurassic time volcanism was mainly alkaline in character. This same trend is evident for Late Triassic Takla Group rocks of the McConnell Creek area (Monger, 1977c). The Savage Mountain Formation rocks straddle the boundary between alkaline and subalkaline and the Moosevale Formation basalts, which are in part contemporaneous and partly younger are alkaline (Figure 13A). The overlap of fields suggests the alkali-rich younger rocks are differentiated end members of a magmatic-eruptive cycle. At Galore Creek, early volcanism is characterized by more differentiated andesitic compositions, potassium-rich trachybasalts are younger and may represent primitive precursors to the shoshonitic lavas of the upper volcanic unit.

## LOWER JURASSIC SEDIMENTS

Souther (1972) divided Jurassic rocks of the Telegraph Creek sheet into three units. The lowest consists of granitoid conglomerate, greywacke and mafic fragmentals containing Hettangian to upper Toarcian ammonites and pelecypods. Upper Toarcian to Bajocian shale and siltstone comprise the middle unit. The upper unit of mafic pillow lavas is equivalent to Anderson and Thorkelson's (1990) Eskay Creek facies. At Galore Creek, Lower Jurassic Hazelton Group equivalent rocks occupy a fault-bound wedge in the eastern part of the map area (Figure 11). The sequence is well bedded, not less than 1000 metres thick and characterized by brown to limonitic weathering sediments and subordinate volcanic rocks. The rocks are best exposed south of Hickman Creek in a tributary of Mess Creek, in a series of nunatacks in Scotch Glacier and farther to the south, above Round Lake (Figure 11).

### *Hickman Creek Section*

A 325-metre section of Lower Jurassic to possibly Middle Jurassic sedimentary rocks is exposed in a moderately west dipping homocline south of Hickman Creek in an east-flowing tributary to Mess Creek. The section includes a lower basal conglomerate unit, 150 metres thick, and an upper unit comprised of three fining-upward sequences of well bedded conglomerates and intercalated arkosic sandstones and siltstones (Figure 14). The basal conglomerate rests on Upper Triassic maroon augite andesite breccia flows. The basal unit is a hematized purple to red polymictic boulder and cobble conglomerate containing maroon plagioclase-hornblende-phyric volcanics, granodiorite (Hickman batholith) and distinctive potassium feldspar porphyry (Galore syenite equivalents?) clasts in a quartz-rich arkosic matrix. Clast lithologies indicate rapid uplift and erosion of the Hickman batholith, comagmatic Stuhini volcanics and high-level syenite bodies to the west.

The upper unit consists of thin to medium planar-bedded sandstone and siltstone turbidites with lesser cobble to granule conglomerate horizons. The fine clastic rocks contain appreciable proportions (increasing up-section) of quartz and potassium feldspar. The second fine carbonaceous shale horizon of the upper unit contains imprints of the conifer *Pityophyllum* sp. (G. Rouse, personal communication, 1988). This species existed throughout Middle Jurassic to Early Cretaceous time but was most abundant during the Late Jurassic, suggesting that the upper unit may be correlative with the Bowser Lake Group. The lower unit conglomerates are intruded by an areally extensive and continuous fine-grained basalt sill 5.5 metres thick. Continuity of this section is obscured by icefields. South and west of Hickman Creek, moderately west dipping sediments that

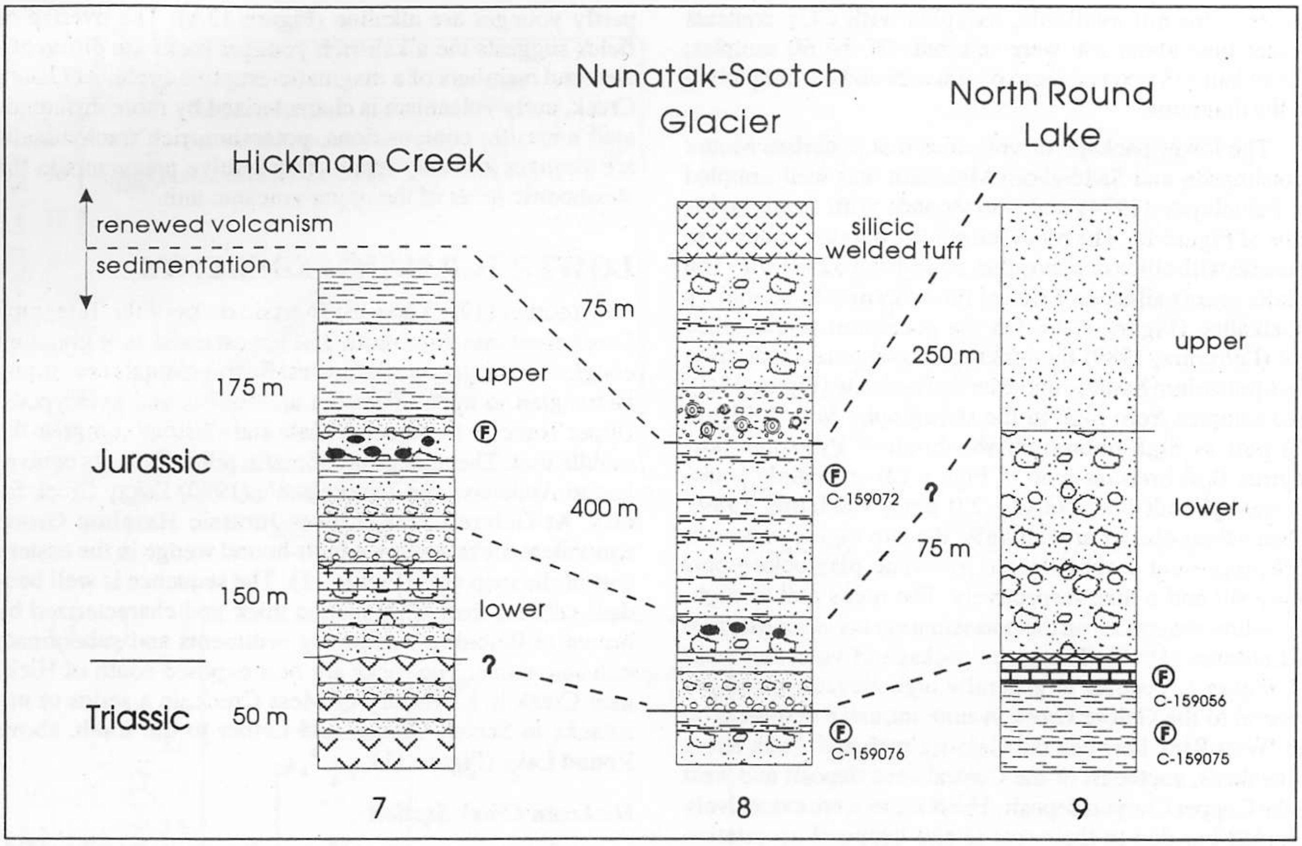


Figure 14. Generalized stratigraphic columns for Lower to Middle(?) Jurassic rocks in the Galore Creek area. Numbers correspond to locations on Figure 11.

crop out as nunataks in Scotch Glacier are interpreted to be correlative units.

### *Scotch Glacier Section*

At least 1000 metres of gently west dipping sediments, ranging in age from Triassic to Jurassic, are exposed in a series of nunataks in Scotch Glacier. The Triassic sequence is comprised of green to more commonly limonitic arkosic sandstone, locally with abundant carbonized plant material, interbedded argillite and maroon volcanic conglomerates.

The base of the sequence is not exposed; the top is a calcareous siltstone and interbedded argillite containing the upper Norian (Cordilleranus Zone) bivalve *Monotis subcircularis* Gabb (C-159076, Table A-1). Less than 50 metres of polymictic limonitic conglomerate overlies the Triassic rocks in apparent conformity. The basal conglomerate is overlain by approximately 400 metres of thinly bedded, friable black limy shale and argillite with subordinate calcareous sandstone and crystal tuff horizons. These rocks are thoroughly fractured and cleaved, weather recessively, and are exposed as rubble covered subcrop. Disjointed and discontinuous, coarse pyroxene gabbro sills and dikes cut the thin-bedded shale and argillite. Near the top of these fine-grained clastics, at the break in slope, a fauna of *Weyla*(?) (sp.) together with well preserved terebratulid and rhynchonellid brachiopods indicates a probable Early Jurassic age (C-159072, Table A-2).

Up-section are more resistant cliff-forming well bedded variegated accretionary lapilli tuffs and brown sandstones with abundant carbonized trees and plant material. These are overlain by 75 metres of polymictic cobble conglomerate with siltstone and sandstone interbeds. In general the section appears to coarsen upward and is capped by a white, silceous, welded lithic tuff (Plate 10). The accretionary lapilli tuffs and felsic welded tuff which overlie conglomerates at the top of the nunatak section (Figure 14) are probably correlative with the Mount Dilworth Formation (Alldrick, 1989).

### *Round Lake Section*

North of Round Lake the Jurassic section is less than 325 metres thick and consists of a lower polymictic conglomerate unit and an upper sequence of interbedded limy siltstones and arkosic sandstones (Figure 14). The lower 75 metres of pebble conglomerate, is correlative with conglomerates at Hickman Creek. The conglomerate is faulted against Upper Triassic, late Norian limestones containing the conodont *Epigondolella* ex gr. bidentata Mosher (C-159056, Table A-2) and siltstones with the pectenid bivalve, *Lima (Plagistoma)* sp. (C-159075, Table A-1) of Triassic to Jurassic age. The upper unit comprises at least 250 metres of orange and grey, well bedded marl, calcareous siltstone and sandstone containing conspicuous carbonized wood and plant fragments and lesser granule to pebble conglomerate. The section is moderate to steeply west dipping,

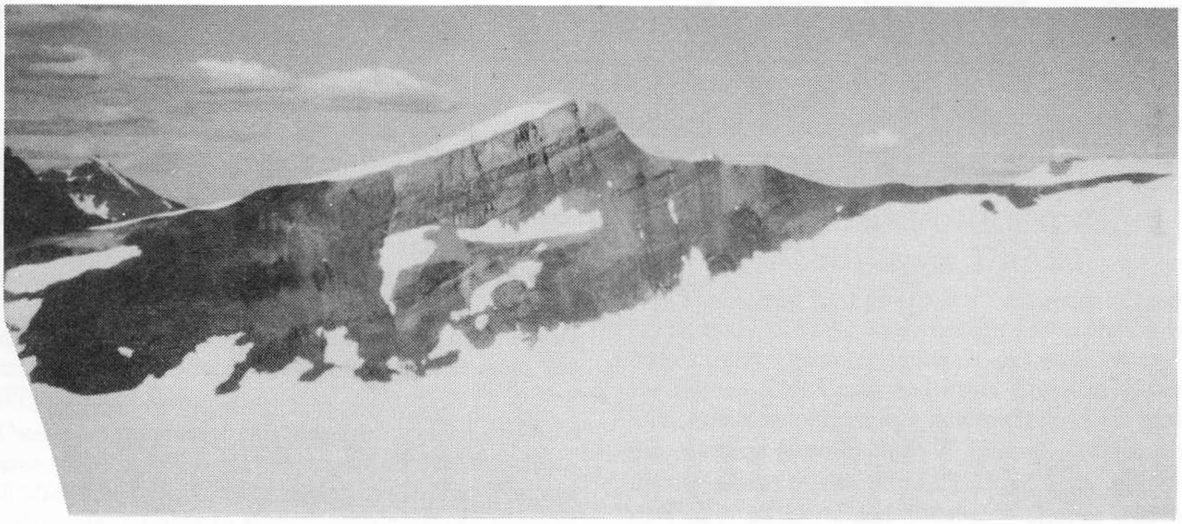

Plate 10. Jurassic sedimentary rocks dip and young westward at this nunatack exposure in Scotch Glacier (corresponds to section 8, Figure 14). From right to left are carbonaceous shale and siltstone, more resistive sandstones, accretionary lapilli tuff and conglomerate. A white weathering felsic welded tuff forms the top of the nunatak.

kinked about west to northwest-trending axes and intruded by a steep northwest-striking felsite dike.

Lower Jurassic rocks that are exposed in the eastern part of the map area are mainly sedimentary and indicate marine deposition. Local areas of subaerial deposition are apparent.

## QUATERNARY TUFA

A small warm-spring discharges into Sphaler Creek, approximately 11 kilometres southwest of Round Lake. It is located on the South Scud fault, a major north-striking structure which flanks the west side of the Hickman batholith. Deposits of calcareous tuffa up to a metre thick are present. These were sampled for geochemical analysis and returned low and below detection values for precious and base metals as well as for mercury, arsenic and antimony. The water smells of hydrogen sulphide.

# CHAPTER 4 INTRUSIVE ROCKS

Seven magmatic episodes are documented by Armstrong (1988) for the Mesozoic and Cenozoic epochs of the Canadian Cordillera; four of these are recognized in the study area. In addition, a pre-Mesozoic, late Paleozoic episode has also been recognized in the Forrest Kerr and More Creek areas (Logan *et al.*, 1992; Drobe *et al.*, 1992). Missing in this part of northwestern Stikinia are the three episodes of plutonism that span nearly 100 million years of time from the Late Jurassic (155 Ma) through to the Cretaceous (65 Ma) (Figure 15).

These five magmatic episodes are represented in the map area: the Late Devonian Forrest Kerr Plutonic Suite, the Middle(?) to Late Triassic Hickman (Stikine) Plutonic Suite, the Late Triassic to Early Jurassic Galore (Copper Mountain) Suite, the late Early Jurassic Texas Creek Plutonic Suite and the Paleogene Hyder Plutonic Suite (Figure 16). These are described in more detail following.

## LATE DEVONIAN FORREST KERR PLUTONIC SUITE (*ca* 370 Ma)

The Forrest Kerr pluton is a 590 square kilometre composite body of mafic and younger felsic phases which intrudes Early Devonian volcanic and sedimentary strata in the Forrest Kerr Creek and More Creek map areas to the east. Potassium-argon age determinations on biotite from the youngest granitic phase and hornblende from the older diorite phase of the pluton yielded ages of 346±10 Ma (Logan *et al.*,1992) and 330±9 Ma (Logan and Drobe, in preparation) respectively; the K-Ar ages are probably reset. Uranium-lead dating of zircons from the granitic phase pro-

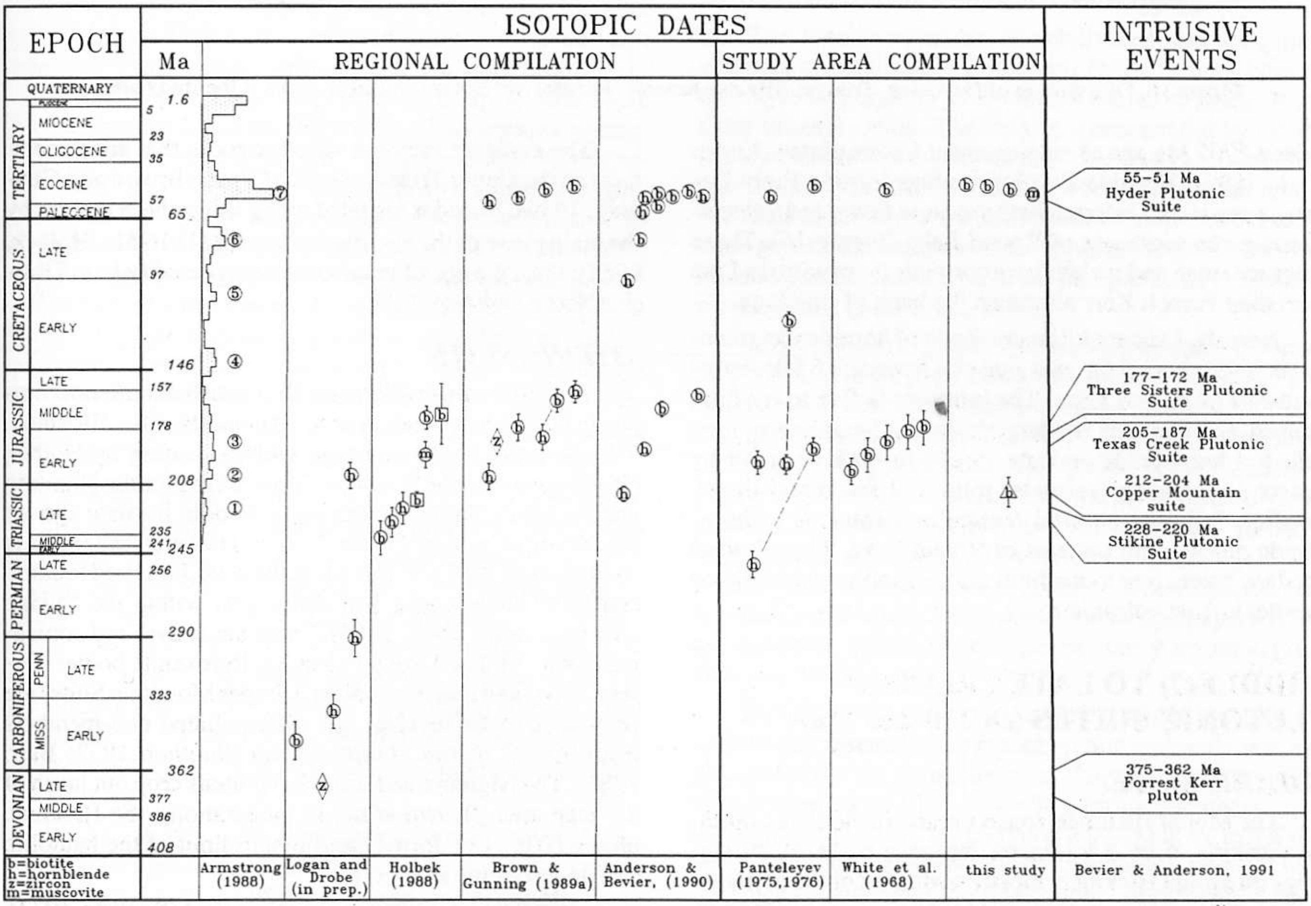


Figure 15. Regional and study area compilation of isotopic ages showing the main Mesozoic and Cenozoic magmatic events (Armstrong, 1988) and intrusive events (Anderson and Bevier, 1990) in northwestern British Columbia. Letters correspond to minerals; b=biotite, h=hornblende, m=muscovite, z-zircon. Shapes correspond to the dating technique; circle=K/Ar, triangle=Ar/Ar, diamond=U/Pb and rectangle=Rb/Sr. Vertical bars show 2 sigma errors.

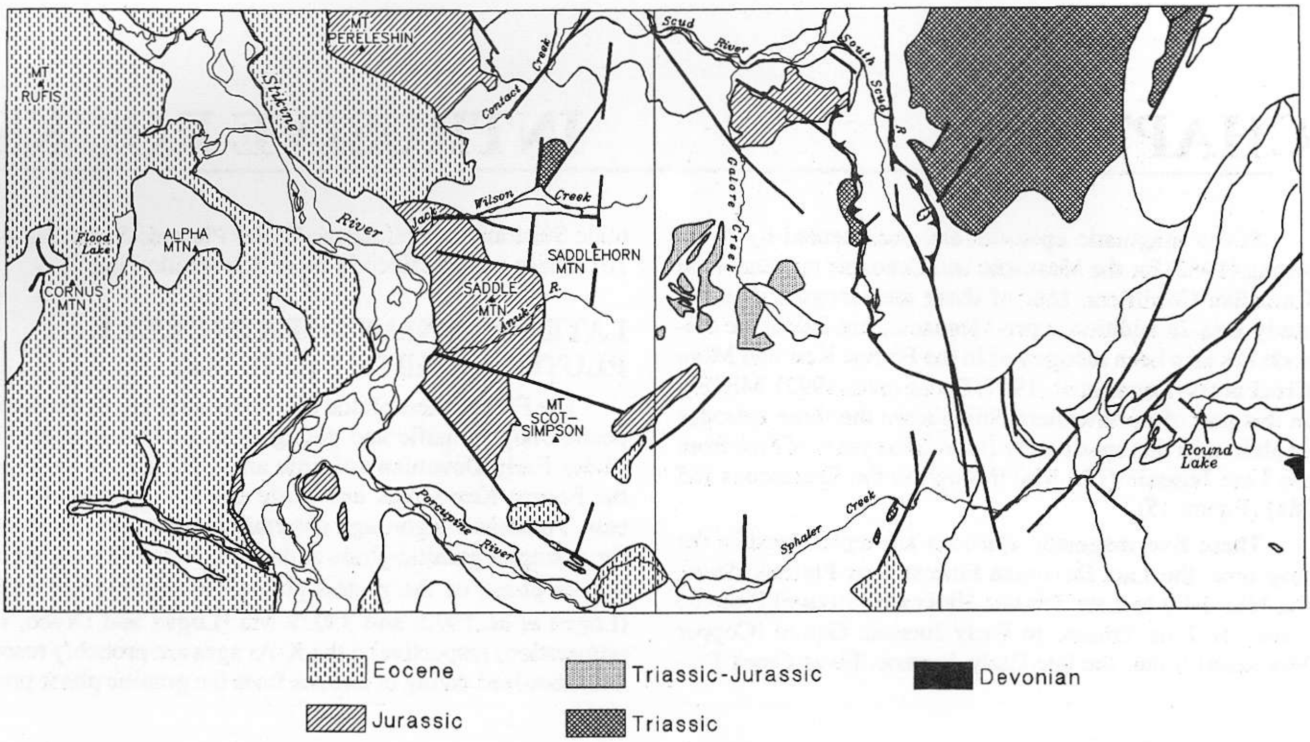


Figure 16. Distribution of Devonian, Triassic, Triassic-Jurassic, Jurassic and Eocene intrusive rocks in the study area.

vides a 3702 Ma age of emplacement for the pluton (Logan *et al.*, 1993). Hornblende diorite plugs intrude Early Devonian mafic and intermediate volcanic flows and volcaniclastic rocks southeast of Round Lake (Figure 16). These plugs are small and isolated; we correlate them with the Late Devonian Forrest Kerr pluton on the basis of lithology.

A small, 1 square kilometre body of hornblende granodiorite crops out on the east side of a nunatack 6 kilometres southeast of Round Lake. The intrusive is fine to medium grained and contains moderately fresh, 2-millimetre long euhedral hornblende crystals locally to 40%. It is cut by quartz and epidote veinlets, joint and fracture fillings. Smaller, foliation-parallel lenticular intrusions of hornblende diorite crop out east of Round Lake. These bodies are dark green, fine to medium grained and weakly foliated parallel to host volcanic rocks.

## MIDDLE(?) TO LATE TRIASSIC PLUTONIC SUITES (*ca* 230-226 Ma)

### *POLARIS SUITE*

The Mount Hickman zoned ultramafic body is a northeast-striking, 6 by 3 kilometre intrusive body which outcrops on Mount Hickman, mostly northwest of the northeast corner of the map area (Figure 16). The core is pyroxenite; plagioclase and hornblende abundances increase outward until the rock becomes a clinopyroxene gabbro to hornblende augite diorite (Souther, 1972). Its southern extremity, comprising pyroxenite and pyroxene gabbro, extends into the study area.

The complex intrudes volcanic rocks that are correlatives of the Upper Triassic Stuhini Group (Brown and Gunning, 1989a, b) and is intruded along its northern margin by the main phase of the Hickman pluton (221±16 Ma; Holbek, 1988); thus, the age of emplacement is probably Late Triassic (Nixon and Ash, 1989).

### *STIKINE SUITE*

The 1200 square kilometre Hickman batholith is a composite body. From south to north, it consists of the Hickman, Yehiniko, and Nightout I-type plutons. Dating by Holbek (1988) gave Middle(?) to Late Triassic ages for the Nightout and Hickman plutonic rocks and a Middle Jurassic age for the Yehiniko pluton (Table 2). The Hickman batholith is analogous to the Late Triassic to Middle Jurassic Hotailuh and Stikine composite batholiths, also within the Stikine arch (Anderson, 1983, 1984). These are coeval and comagmatic with Stuhini Group volcanics. Pyroxenite bodies (Polaris Suite) and alkalic syenites (Copper Mountain Suite) are postulated to be residual and differentiated end-members respectively, of the Stuhini Group (Souther, 1972; Barr, 1966). The Nightout and Yehiniko plutons crop out north of the map area (Brown *et al.*, in preparation); the Hickman pluton (lTd, lTm) forms the southern limit of the batholith and underlies the study area.

The Hickman pluton is crudely zoned (Souther, 1972), ranging in composition from pyroxene diorite in the core to biotite granodiorite near the margins. The main mass comprises biotite and hornblende pyroxene diorite to monzodiorite (lTd). Less mafic hornblende-biotite-pyroxene monzonite to quartz monzonite (lTm) predominates at the southern end of the pluton. Steeply dipping faults bound the pluton on both its western and eastern margins, but contacts between the pluton and Stuhini volcanics are intrusive. However, Holbek (1988), reports an unconformable relationship, citing Hickman intrusive clasts in basal Stuhini Group conglomerates as evidence. We interpret these conglomerates to be Lower Jurassic in age and to correlate with a thick succession to the east (Logan *et al.*, 1992; Logan and Drobe, 1993) where Lower Jurassic conglomerates lie in erosional contact on hornblende-plagioclase-porphyrytic diorite of probable Late Triassic age.

The biotite-hornblende-pyroxene diorite (lTd) is generally a medium to coarse-grained, equigranular rock, massive in outcrop and weakly jointed. Hornblende and augite are variably replaced by chlorite and carbonate, and together comprise 75 to 80% of the mafic minerals; biotite forms the remainder. In places, hornblende occurs as phenocrysts together with minor clinopyroxene in a fine-grained chlorite-carbonate-sericite-altered groundmass. Plagioclase (40%) crystals dominate: potassium feldspar (20%) and quartz (10-15%) are interstitial. Magnetite and rare honey-coloured euhedral titanite are accessories. Souther (1972) describes pegmatitic and porphyritic textures as common north of the map area, at the toe of the Scud Glacier.

Small bodies of coarse-grained, commonly trachytic, biotite augite diorite are distributed along the west and east margins of the pluton, north of Scotch Glacier (Figure 16). The rocks are coarsely porphyritic with up to 30% sodic plagioclase laths and tabular anorthoclase crystals averaging 1.5 centimetres in length. The groundmass comprises subhedral laths of albite with overgrown anhedral augite, biotite and an opaque oxide; potasium feldspar is less common. Mafic minerals are weakly to moderately altered to chlorite, epidote and actinolite. Actinolite makes up to 40% of the rock in some places. Accessories include as much as several percent magnetite (possibly secondary) as well as minor amounts of apatite and titanite. Contact relationships of the biotite augite diorite and Hickman granodiorite vary over relatively short distances, from intrusive to gradational to intruded suggesting a contemporaneous age for both.

The hornblende biotite monzonite to granodiorite (lTm) is a medium to coarse-grained, pink-weathering massive rock, texturally similiar to the mafic phase (unit lTd). The mafic minerals, hornblende, biotite and augite, form up to about 20% of the rock. They are generally chloritized. Plagioclase (35%) is euhedral, zoned and contains small inclusions of mafic minerals. Potassium feldspar (35%) is poikilitic to interstitial. Quartz (5-10%) is also interstial. The monzonite is intruded by north-striking felsic porphyritic monzonite to syenite and flow-banded mafic basaltic to andesitic dikes.

A 3 by 1 kilometre north-trending stock of medium-grained, equigranular biotite hornblende monzonite crops out 5 kilometres west of the southern end of the Hickman pluton (Figure 16). The stock intrudes Upper Triassic Stuhini Group strata; plagioclase-phyric tuffs and breccias at its north end, and green and maroon augite flow breccias, at the south end. At its southern end the body is a hornblende diorite (Read, 1988). Along its eastern edge, the stock is faulted against Middle Triassic shale and siltstone. The stock postdates the Upper Triassic volcanic rocks it intrudes and predates westerly directed thrusting of Middle Triassic sediments and Permian limestone. It may be as young as Early Jurassic but an absolute age is not known.

## LATE TRIASSIC TO EARLY JURASSIC COPPER MOUNTAIN PLUTONIC SUITE (*ca* 210 Ma)

Barr (1966) describes the the Galore Creek Syenite Complex as a series of ten orthoclase-porphyritic syenite intrusions hosted by and cutting coeval Upper Triassic Stuhini Group volcanics. This complex is characterized by syenite dike swarms, like those at the North Junction zone (Plate 11). This typical surface outcrop illustrates the flows, explosive volcanism, intrusion and metamorphism which accompanied episodes of mineralization. Allen *et al.* (1976) considered four intrusive pulses to be most closely associated with the copper-gold deposits: from oldest to youngest these are the dark syenite porphyry, the garnet syenite megaporhyry, the fine-grained porphyritic syenite, and the epidote syenite megaporphyry. They described these rocks in detail: the following observations of the intrusive phases are based on both their work and our mapping.

The syenite dikes can be subdivided into pre-, intra-, and post mineralization intrusives. In the Central zone the dark syenite porphyry is the oldest intrusive phase. It predates mineralization. The rock is characterized by tabular, white orthoclase phenocrysts in a matrix of potassium feldspar, biotite and plagioclase. Large remnant phenocrysts of pseudoleucite suggest a subvolcanic environment and a close genetic affiliation with the upper package of volcanics. Phenocrysts of pseudoleucite are interpreted as evidence of rapid cooling (Barr *et al.*, 1976)

The next pulse, garnet syenite megaporphyry, formed only dikes. It is grey and contains euhedral orthoclase phenocrysts and hornblende pseudomorphs, each to about 25%. The groundmass consists mainly of fine-grained trachytic potassium feldspar crystals. The garnet syenite megaporphyry is an intra-mineralization intrusive altered to endoskarn. It contains from 1 to 15% secondary garnet as disseminated aggregates and veinlets as well as up to 25% biotite replacing euhedral hornblende. Garnet compositions are mainly andradite. Those deposited as open-space filling are euhedral, titanium-rich, spectacularly zoned crystals (Watson, 1969).

During the third event, a fine-grained porphyritic syenite, that resembles the garnet syenite texturally, was emplaced; it cuts the garnet syenite. Fine-grained porphyritic syenite consists of 10 to 30% white orthoclase phenocrysts in a light grey to pink groundmass containing up to 5% disseminated fine-grained biotite or hornblende. Contact relationships indicate that the fine-grained porphyritic syenite postdates mineralization.

The fourth pulse was voluminous. Epidote syenite megaporphyry dikes form a large part of the intrusive complex and are the youngest porphyries in the Galore Creek area. Large phenocrysts of orthoclase, to 4 centimetres, form

Plate 11. Syenite dike swarm in altered and mineralized volcanic rocks at the North Junction zone, Galore Creek (photo by A. Panteleyev).

Plate 12. Epidote syenite megaporphyry. Sample has been etched and stained to distinguish potassium feldspars (large phenocrysts) from plagioclase (small light-coloured grains).

40 to 60% of the rock (Plate 12). Phenocrysts are zoned and partly replaced along rims by intermediate microcline. Phenocryst size indicates two generations of megaporphyry, an early phase with phenocrysts averaging 2.5 centimetres long, and a younger phase with much smaller phenocrysts (0.3 centimetres). Aggregates of epidote are dispersed through the rock giving it a greenish grey colour; epidote comprises up to 15% of the rock. Where garnet is abundant in the wallrock, the syenite also contains disseminated garnet as xenocrysts. Hornblende phenocrysts, replaced in part by biotite and chlorite, form up to 25% of the rock. The groundmass is fine-grained, grey potassium feldspar with accessory amounts of apatite and magnetite, each 1 to 2%. Epidote syenite megaporphyry also postdates mineralization.

In addition to the four main orthoclase porphyries of the Central zone, there are six additional syenite phases, all peripheral to it. Some are time-equivalent intrusions, others may be metasomatised volcanic rocks that are extrusive equivalents. These include epidote syenite porphyry, North 110 syenite porphyry, green syenite, buckshot syenite porphyry and Copper Canyon syenite porphyry (Barr, 1966; Panteleyev, 1976; Allen *et al.*, 1976).

Potassium-argon ages (recalculated to new decay constants) from porphyritic epidote syenite (North Junction syenite) gave discordant ages of 251±14 Ma (hornblende) and 189±12 Ma (biotite, Table 2). The hornblende age is unexpectedly old. This syenite, known colloquially as "wipe-out porphyry" (A. Panteleyev, personal communication, 1988), postdates mineralization. Drill-core samples of epidote syenite megaporphyry from the Central zone were collected for U-Pb zircon dating. After crushing and separation the samples contained insufficent material to date. Unfortunately this was a hindsight conclusion for these silica-deficient intrusions. Argon-argon step heating of an extrusive equivalent of the syenite was carried out by P. Reynolds at Dalhousie University. Biotite from this crystal tuff gave an age of 212 Ma (mean of five plateaus) and a total gas age of 204 Ma (Table 2).

## EARLY JURASSIC TEXAS CREEK PLUTONIC SUITE (*ca* 205-187 Ma)

The Texas Creek Plutonic Suite consists of calcalkaline (Saddle Mountain pluton, Scud pluton) and potassium megacrystic (not alkaline) bodies (Pereleshin pluton, Split Creek) in the study area.

Biotite hornblende diorite to granodiorite of the Saddle Mountain pluton (eJgd) is exposed on the eastern edge of the Coast Complex where it forms a belt 4 to 5 kilometres wide extending down the eastern side of the Stikine River from Saddle Mountain to the Porcupine River (Figure 16). At the confluence of the Porcupine and Stikine rivers the intrusive is roofed by pre-Permian(?) metasediments and metavolcanics. Numerous inclusions of partially assimilated pre-Permian(?) and/or Upper Triassic Stuhini Group(?) volcanics and sediments are exposed northward to Saddle Mountain. The xenoliths are fine grained and 1 to 4 metres and larger in size. They commonly are well rounded and altered to an assemblage of epidote, chlorite and calcite.

The diorite is medium grained but heterogeneous due to the abundance and assimilation of inclusions. It is commonly sheared and altered to a green-weathering massive rock. Megascopically the rock is generally equigranular, contains about 20% quartz, and has a plagioclase:potassium feldspar ratio of approximately 4:1. Prismatic, green pleochroic hornblende is more abundant than subhedral to anhedral, brown pleochroic biotite. The average composition of plagioclase in ten thin sections that Kerr studied (1948a) was andesine. It forms 60% of the rock; the balance is orthoclase, 13%; quartz, 17%; mafics, predominantly hornblende, 10%. Feldspar grains are moderately altered to sericite; clinopyroxene and hornblende crystals are altered to epidote and chlorite. Quartz grains are strongly rounded and embayed. Some pyroxene grains have been entirely replaced by chlorite. Zeolite is common in the groundmass. Accessory minerals include magnetite, titanite, apatite and zircon. Potassium-argon age determinations (Panteleyev, 1975, 1976; recalculated to new decay constants) from quartz diorite in the Anuk River area give discordant ages of 197±10 Ma (hornblende) and 120±10 Ma (biotite)(Figure 15).

The Scud River stock (eJgd) is a body 5 kilometres wide exposed south of the confluence of the Scud and South Scud rivers (Figure 16). The intrusive varies from medium-grained, equigranular biotite monzonite to hornblende-biotite quartz monzonite. Euhedral plagioclase and pink potassium feldspar are present in roughly equal amounts. Chloritized mafics form less than 10% of the rock with biotite more common than hornblende. The stock is crudely zoned, the margin is finer grained, hornblende and plagioclase are more abundant and garnets occur locally where endoskarn has developed. Andradite, wollastonite and calcite exoskarn developed in limestones at the intrusive contact. The outcrop pattern suggests that the stock is bisected by a group of northwest-striking faults. Hornfelsed pendants of well bedded variegated silicic siltstone, carbonaceous argillite and limy shale of probable Middle Triassic age crop out along the central fault trace. Potassium-argon dates (White *et al.*, 1968; Panteleyev, unpublished data; recalculated to new decay constants) are 185±18 Ma and 195±12 Ma on hornblende and biotite, giving an Early Jurassic apparent age of emplacement for the stock (Table 2).

The Mount Pereleshin stock (Brown and Gunning, 1989a,b) is a circular body, about 10 kilometres in diameter, that straddles the lower reaches of the Scud River (Figure 16). It is comprised of coarse-grained, equigranular to porphyritic hornblende biotite granite and quartz monzonite (eJm). A potassium feldspar megacrystic variety contains from 15 to 20% potassium feldspar laths 0.4 to 2.0 centimetres long. Fresh, euhedral hornblende and lesser biotite are interstitial to roughly equal proportions of equigranular plagioclase and potassium feldspar. Mafics, which constitute from 5 to 15% of the rock, are chloritic near the margins of the body. Quartz is interstitial, and varies from 10 to 20%. Accessories include titanite, magnetite and trace amounts of pyrite. Brown and Gunning (1989a) report a single K-Ar date of 204±7 Ma for hornblende, that is an Early Jurassic age. The authors argue that the apparent age may be low and partially reset.

A small potassium feldspar megacrystic granite plug outcrops south of Jack Wilson Creek on Saddle Mountain. The contact with Triassic volcanic rocks is knife sharp, undulose and dips west. No contact alteration zone affects the volcanic rocks. A weak east-west foliation and lineation fabric developed in the tuffs parallels post-intrusion faults. This contact is interpreted to be a fault. Contact relationships with the Early Jurassic Saddle Mountain granodiorite body were not seen.

A second potassium feldspar megacrystic body occupies the flats of the Stikine River at its confluence with the Porcupine River. Kerr (1948a) mapped this body as oligoclase granodiorite and grouped it with the Yehiniko pluton (Middle Jurassic, Holbek, 1988), though he inferred it to be slightly younger; and the Kahtate mass (Early Jurassic, Bevier and Anderson, 1991) which is exposed to the south on the Stikine and Iskut rivers (Figure 5). The intrusion is variably altered to greenschist assemblage minerals and iron carbonate.

The K-Ar data for Early Jurassic granitoid rocks in the area shows a large amount of scatter and discordant mineral pairs. Partial resetting of the Early Jurassic bodies is related to their position adjacent to the mainly Jurassic and younger intrusions which comprise the Coast Plutonic Complex.

## PALEOGENE HYDER SUITE (55-51 Ma)

A quarter of the map area is underlain by intrusive rocks of the Coast Plutonic Complex. Three texturally and compositionally distinct intrusive phases have been mapped. From inferred oldest to youngest these are: biotite hornblende diorite to granodiorite; hornblende biotite granodiorite; and biotite granite to biotite quartz monzonite.

The oldest phase, hornblende granodiorite (Egd), underlies the northwestern edge of the study area, west of the Stikine River and along the southwestern margin of the Pereleshin stock. The rock is medium to coarse grained, equigranular and composed of approximately equal proportions of plagioclase, potassium feldspar and acicular hornblende; quartz averages less than 20%, biotite 5%. The intrusive and specifically mafic minerals are pristine and unaltered. Contact relationships indicate more felsic, leucocratic rocks crosscut the diorite and granodiorite phases. Generally the phases are intermixed and merge across gradational contacts.

The youngest phase, biotite granite (Eg) of the Christina pluton (Plate 13) underlies a wide belt west of the Stikine River. The rock is a massive, mineralogically and texturally homogeneous, light grey rock that is commonly

Plate 13. Granitic apophyses intrude undivided metasedimentary and metavolcanic rocks of probable Paleozoic age at the upper contact of the Eocene Christina pluton.

well jointed. It is coarse to medium grained, equigranular and contains roughly equal proportions of plagioclase and potassium feldspar, each comprising about 30% of the rock. Quartz averages 25 to 30%. Biotite and lesser hornblende are interstitial to plagioclase and poikilitic feldspar and together comprise 5 to 10% of the rock. Honey-coloured titanite is conspicuous and up to several percent of the rock, magnetite and apatite occur in trace amounts. Quartz typically displays undulose extinction. Myrmekitic texture is common in some thin sections. These rocks are generally fresh, although sericite lightly dusts plagioclase and potassium feldspar. Minor chlorite and epidote partly replace otherwise unaltered biotire along eleavage planes. Local granite phases within the main body eontain two micas (biotite and muscovite) and disseminated garnets. Muscovite is present as subhedral, fresh grains to 2 millimetres in size, and honey-coloured, strongly resorbed garnets are up to 2 millimetres across.

Potassium-argon cooling dates from the Christina Lake pluton all cluster around the Paleocene-Eocene boundary (Table 2). Dates from sampling west of the Stikine River gave 49.4±3.5 Ma from a biotite separate and 51.9±3.6 Ma, for muscovite from a two-mica felsite dike. Hornblende from the older phase of the Christina Lake pluton, sampled east of the Stikine River, returned 56.1± 4 Ma (Brown *et al.*, in preparation), and 45.1±4 Ma from biotite from another locality (White *et al.*, 1968).

Small stocks and plugs of biotite quartz monzonite (Em) are scattered across the map. They form circular and elliptical bodies up to 3 kilometres in diameter, south of Sphaler Creek at its confluence with the Porcupine River and 10 kilometres farther east and at Split Creek. Read (1988) also identified a small plug south of the Hummingbird zonc, east of the sonth fork of the Scud River. The stocks generally are equigranular, medium grained and contain roughly equal proportions of plagioclase and potassium feldspar. Biotite averages 5 to 10% and quartz content varies to about 20%. Potassium-argon dates (Table 2) from these plugs are equivalent to those from the Christina pluton suggesting these are satellite bodies to the main Coast Plutonic Complex. Potassium-argon dates (recalculated to new decay constants) on biotite from the Sphaler Creek/Porcupine River stock gave 53.5±3.2 Ma (Panteleyev, 1974). Potassium-argon analyses on biotite from the Sphaler Creek stock gave 47.3±3.4 Ma.

## OTHER PLUTONIC ROCKS

Small plngs and dikes of plagioclase-porphyritic diorite (qp) intruded along north-trending faults within the South Scud River valley. The rocks are dense, green to grey coloured, with 20 to 25% phenocrysts of zoned plagioclase, rare chloritized hornblende and 5% quartz. Pyrite is ubiqnitous and outcrops are limonite stained. The age of these rocks is not constrained.

Narrow dikes of inferred Tertiary age (Tr, Tb) are found in north-striking, steep-dipping fault zones, east of South Scnd River and northeast-striking faults above Copper Canyon. Rhyolite and lamprophyre/basalt are prevalent, but felsite, hornblende andesite and amphibolite dikes have been identified. East-trending mafic dike swarms cut intrusive rocks as young as Early Jurassic in age.

### *ULTRAMAFIC ROCKS OF UNKNOWN AGE*

Several isolated outcrops of ultramafic rock occur adjacent to the Permian limestone - Middle Triassic and Upper Triassic contacts east of the South Scud River (Figure 16). Their distribution appears to be controlled by regional structures. Contact relationships suggest that these ultramafic rocks are intrusions and that they cut rocks that are Triassic or older in age. Similiar rocks in the Mess Lake area are extrusive ultramafic tuffs which occupy a lowest Upper Triassic stratigraphic position (Logan and Drobe, in preparation). Altered peridotites consist of serpentine pseudomorphs of olivine set in a groundmass that is largely altered to talc and chlorite. Pyroxenites comprise subhedral clinopyroxene that is moderately altered to chlorite, and interstitial plagioclase altered to sericite. One occurrence of troctolite consists of subequal amounts of very fresh olivine and calcic plagioclase, 5 to 10% magnetite, and minor amounts of brown pleochroic biotite. The tectonic significance of these ultramafic rocks is uncertain.

## GEOCHEMISTRY

Whole-rock major oxide and trace element analyses have been completed on 40 intrusive rock samples. Analyses were completed by the Ministry of Energy, Mines and Petroleum Resources analytical laboratory in Victoria. Results and sample locations are presented in Appendix B. The data were screened for alteration using $K_2O/Na_2O$ ratios and loss on ignition (LOI) values as discussed previously, under "Geochemistry of the Stuhini Group".

All intrusive rocks are classified according to modal mineral contents using the QAP diagram (Le Maitre, 1989), which uses the same classification nomenclature as Streckeisen (1976). Magmatic suites cluster consistently on Figure 17A, probably a function of the small data set, but also suggesting compositional homogeneity. The information in Figure 17A can be summarized as follows: Late Triassic Stikine intrusions (lTd, lTm) plot in the granodiorite field, Late Triassic - Early Jurassic Copper Mountain intrusions (TJs) plot in the syenite and foid-bearing syenite fields, Early Jurassic Texas Creek intrusions (eJgd, eJm) in the granodiorite, quartz monzonite and qnartz monzodiorite fields and Eocene intrusions in the granite and granodiorite fields.

All intrusions plotted on Figures 17B and 17C, have calcalkaline compositions on the alkalis *versus* silica and AFM diagrams (Irvine and Baragar, 1971) and are subalkaline, with the notable exception of the Galore Creek syenite suite. The Galore Creek syenites clearly plot in the alkaline field of Figure 17C. Unaltered samples have total alkali contents of 10 to 13% and higher potassium contents than typical alkaline rocks of island arcs (Gill and Whelan, 1989, Bloomer *et al.*, 1989). The syenite samples with greater than about 13% total alkalis have anomalously high $K_2O/Na_2O$ ratios and, in thin section, are seen to be strongly seritized. Total potassium versus $K_2O/Na_2O$ ratios of the four main

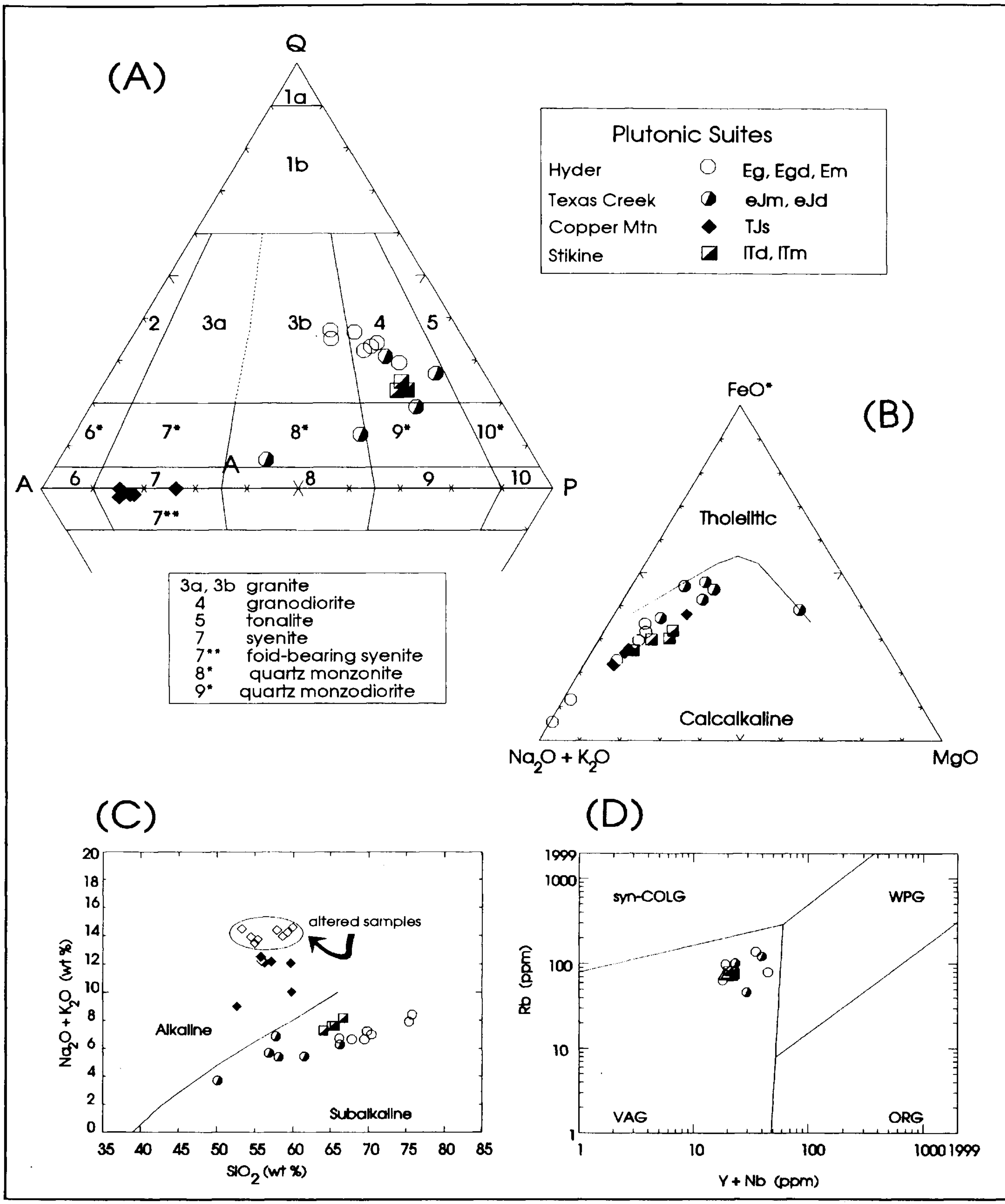


Figure 17. Whole-rock major oxide classification and trace element discriminant diagrams for intrusive rocks: A) QAP (after LeMaitre, 1989), B) AFM (after Irvine and Baragar, 1971), C) alkalis *vs* silica (after Irvine and Baragar, 1971), D) Y+Nb *vs* Rb (after Pearce *et al.*, 1984). VAG=Volcanic arc granites, syn-COLG=Collision granites, WPG=Within plate granites, ORG=Ocean ridge granites.

syenite phases (data from Table 1, Allen *et al.*, 1976) show that the oldest intrusions are relatively enriched in potassium. The higher potassium contents in the older phases may represent a cumulative potassium enrichment from metasomatism which accompanied successive intrusions. Barium and strontium enrichments are consistent with the basalt chemistry typical of shoshonitic island arc volcanism (*op. cit.*).

The Eocene, Early Jurassic and Late Triassic intrusive samples plot as volcanic arc granites (Figure 17D) on the Y+Nb *versus* Rb tectonic discrimination diagram (Pearce *et al.*, 1984). Trace element data are not available for the Late Triassic to Early Jurassic syenite intrusions (A. Panteleyev data). Tectonic environments postulated for alkaline arc magmatism include arc breakup, rifting and subduction reversals. Any or all of these scenarios may have occurred at the close of volcanism in the Galore Creek area; all are compatible with the geologic setting.

# CHAPTER 5 STRUCTURE

The dominant structures in the Galore Creek area are two approximately orthogonal fold trends, an earlier westerly trend and a later one trending northerly. These structures deform earlier synmetamorphic, pre-Permian(?) structures and related northeast-striking penetrative foliations. The youngest folds recognized are minor northwest-trending kink folds. East-dipping reverse faults which imbricate the Stikine assemblage and Middle Triassic rocks and offset Early Jurassic plutons are associated with north-trending folding. Northeast sinistral fault zones and younger north-striking extensional faults host Eocene stocks, mineralization and Miocene dikes respectively.

The deformational style is dominated by brittle deformation and faulting. The north-south and northeast-southwest distribution of lithologic units and intrusions is for the most part fault controlled (Figure 18). Ductile deformation is restricted to several discrete reverse and thrust fault zones. Complicated structures have resulted, in part, from polyform deformation, but also due to competency contrasts between the volcanic and sedimentary units. Penetrative planar fabrics are ubiquitous in Paleozoic strata. Ductile deformation of Paleozoic limestones often transposes bedding and more competent chert interbeds or dikes are broken and boudinaged. Penetrative deformation of Upper Triassic or younger rocks is rare and restricted to north-trending foliated zones. Triassic sedimentary rocks can be tightly folded and sheared while adjacent volcanic rocks did not fold but are faulted and fractured. The orientations of layered rocks around the Galore Creek intrusive complex outline a domal structure, possibly related to intrusion, but probably reflecting younger deformational events. North-northeasterly trending intrusive breccia zones, syenite intrusivions and faults occupy the centre of the Galore Creek basin. Structures in this subvolcanic setting are complex and in part related to volcanic and magmatic processes. They control a series of intrusions, contemporaneous mineralization, alteration and younger intrusions of a short-lived but probably continuous volcano-magmatic episode. The Galore Creek map area is a mosaic of fault-bounded blocks controlled by four main sets of faults.

At least two major folding events deform rocks of the Stikine Terrane in the Tatsamenie Lake area (Souther, 1971; Gabrielse *et al.*, 1991; Oliver and Gabites, 1993) and possibly as many as four (Bradford and Brown, 1993). Field relationships indicate the earlier folds are upright, tight and north trending and have been deformed by younger, broad, upright northeast-trending folds. Of note is the constraint recent geochronological data (Oliver and Gabites, 1993) places on timing of these deformational events. Pennsylvanian felsic rocks structurally overlie Lower Permian limestone on a thrust and together were deformed about north-trending early folds, presumably during Permo-Triassic time. An upper limit on second phase northeast-trending folds is Early Jurassic, based on sericite K-Ar dates from a fault which cuts the Sam Creek antiform (Oliver and Gabites, 1993). Paleozoic Stikine assemblage rocks are deformed by at least four phases of folding to the east in the More creek area (Holbek, 1988; Logan *et al.*, 1992) and

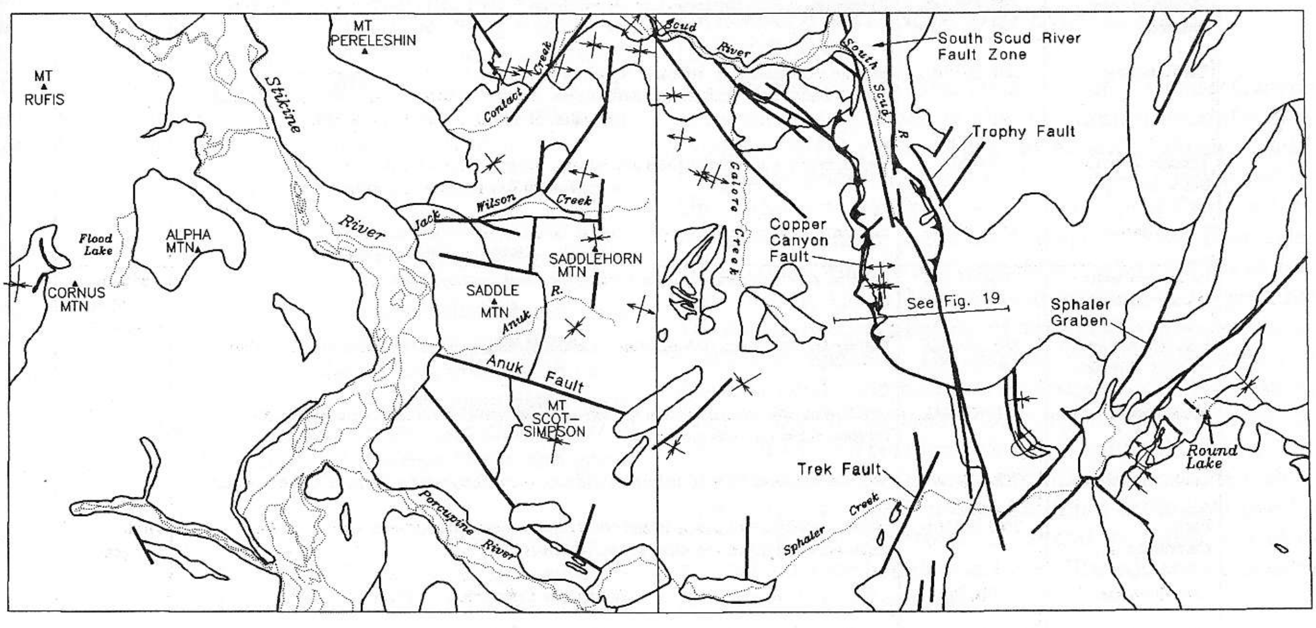


Figure 18. Structural elements of the Galore Creek area, faults, fold axes and lithological units.

south in the Forrest Kerr area (Elsby, 1992, Gunning, 1992). Panteleyev (1975) documented two generations of folding in the Triassic rocks at Galore Creek: an early set with west or northwesterly trending axes and a second generation of smaller, upright isoclinal to box folds with north-northwesterly trending axes which transect the larger west-trending structures.

Three, possibly four, regionally significant episodes of deformation have been recognized in the Galore Creek area. These correspond to well documented tectonic events known for northwestern British Columbia; Devono-Carboniferous Antler orogeny (Gabrielse, 1967, Gordey *et al.*, 1987, Smith *et al.*, 1993), Permo-Triassic Tahltanian orogeny (Souther, 1972, Read, 1983), Middle Jurassic obduction of Cache Creek Terrane onto Stikinia along the King Salmon fault (Thorstad and Gabrielse, 1986; Ricketts *et al.*, 1992) and the Late Jurassic to Cretaceous development of the Skeena fold belt (Evenchick, 1991). The north-trending distribution of lithologies, for the most part reflects the third phase of deformation. The earliest, phase 1, and a possible second coaxial phase (undesignated) are found only in the Carboniferous and older rocks. The second and third phases affect Permian and Triassic strata. The fourth phase affects rocks as young as Early to Middle(?) Jurassic.

Constraints on the timing of deformational events in the Galore Creek area are few. Pre-Permian, pre-Early Jurassic and possibly pre-Late Triassic regional angular unconformities provide some constraints, and it is in this context that folding is discussed. Timing of the varions deformation events is illustrated together with stratigraphic and intrusive episodes (Table 3).

# FOLDS

## *PRE-PERMIAN DEFORMATION*

Between Sphaler Creek and Round Lake (Figure 18) pre-Early Permian rocks are characterized by a moderate to steep, northwest-dipping compositional layer-parallel penetrative foliation. The foliation is axial planar to northeast-trending intrafolial isoclines and larger, tight to isoclinal recumbent folds (Plate 14). The folds have an overall east vergence. Ductile fabrics indicate layer-parallel shears with a top-to-the-northeast sense of shearing. Elongate fragments in volcaniclastic units and limestone conglomerate define a stretching lineation that lies within the plane of foliation and plunges gently to the southwest. Rarely, a second foliation, subparallel to the first, is developed in pre-Early Carboniferous volcanic rocks, suggestive of a second early phase of

TABLE 3
SUMMARYOF MAJOR GEOLOGICAL EVENTS, STIKINE RIVER AREA

| PERIOD | TIME | EVENT | OROGENY |
|---|---|---|---|
| Recent | 1340 years b.p. | Continued sporadic continental basaltic volcanism, hotspring activity and movement along Mess Creek fault | |
| Tertiary to Recent | 0.45±0.07 Ma to 50 Ma | Mt. Edziza Complex continental volcanism; high-angle faulting along Forrest Kerr and Mess Creeks<br>**Intrusion of Hyder Plutonic Suite** | |
| Late Cretaceous | 98-66 Ma | Deposition of Sustut Group continental sediments | |
| Post-Late Jurassic to Cretaceous | 150-130 Ma | Phase 3 and/or 4 folding, end of deposition, uplift | Skeena folding |
| Middle to Late Jurassic | 187-156 Ma | Extension, marine transgression, deposition of Salmon River and Bowser Lake Groups | |
| Early Jurassic | 208-187 Ma | Marine sedimentation , sporadic Hazelton Group volcanism, local deposition of conglomerate derived from uplifted Jurassic arc and underlying Triassic volcanic rocks<br>**Intrusion of Texas Creek Plutonic Suite** | ? |
| Triassic-Jurassic boundary | 208 Ma | Uplift, erosion of arc rocks and subsidence, Orogeny?, phase 2 or 3 folds<br>**Intrusion of Galore Plutonic Suite** | ? |
| Late Triassic | 235-208 Ma | Marine volcanism emerging to subaerial, arc-derived sedimentation<br>**Intrusion of Hickman Plutonic Suite** | |
| Late Permian to Middle Triassic | 250-235 Ma | Limited to non-deposition, then uplift and erosion; phase 1 folds (?) | Tahltanian Sonoman Orogeny |
| Late Carboniferous to Early Permian | 300-260 Ma | Mature arc volcanism (intermediate and felsic), ending with carbonate transgression | |
| Late Carboniferous | 320-300 Ma | Uplift, deposition of conglomerate derived from mid-Carboniferous carbonate and Devono-Carboniferous arc rocks | |
| mid-Carboniferous | 328-320 Ma | Subsidence, deposition of carbonate and arc-derived sediments; burial of Devonian arc | |
| Early Carboniferous | 362-328 Ma | Mafic and felsic volcanism, island arc sedimentation and carbonate accumulation, followed by uplift and erosion, phase 1 folds (?) | Antler Orogeny |
| Late Devonian | 370 Ma | **Intrusion of Forrest Kerr Plutonic Suite** | |
| Early to Middle Devonian | 408-362 Ma | Mafic and intermediate volcanism, fringing carbonate deposition<br>Oceanic arc initiation | |

Time= A geological time scale, 1989 (Harland *et al.*, 1989)

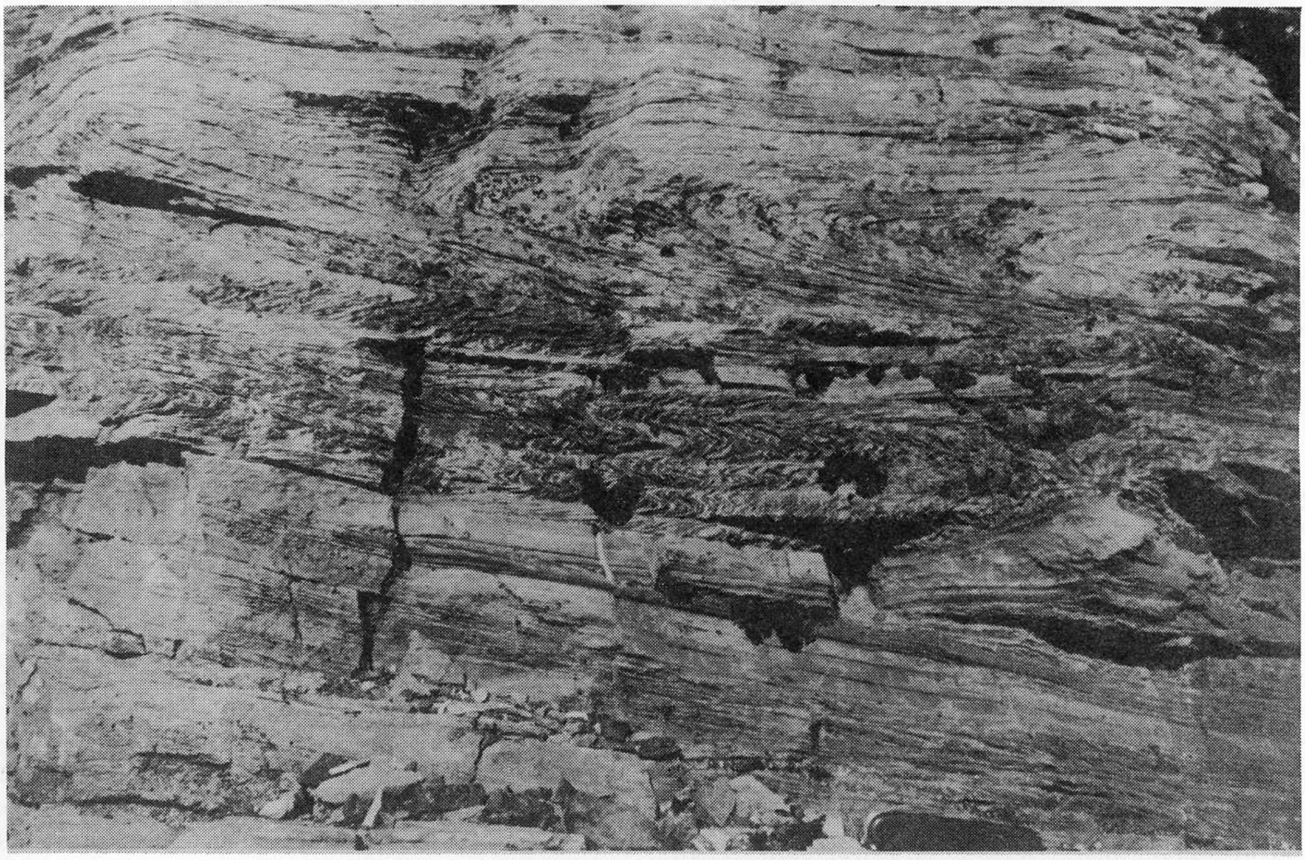

Plate 14. Tight first phase intrafolial isoclines and isoclinal recumbent folds in Lower to mid-Carboniferous limestones at Round Lake.

deformation. Superimposed on these foliations are gently west or northwest-plunging crenulations and kink folds of the youngest phase of deformation. Field mapping and thin section microfossil studies of the Lower Carboniferous limestone indicate heterogeneous strain partitioning within the section. Samples of limestone include strongly strained, ductily deformed, 'fluidal' echinid wackestone and packstone containing strongly deformed foraminiferal ghosts, interlayered with slightly stressed wackestones with pressure solution cleavage and deformed corals (Plate 2).

Sub-greenschist to greenschist-grade metamorphism is synchronous with earliest deformation. Phyllitic argillite west of Round Lake contains a muscovite-chlorite-albite-epidote metamorphic assemblage, mafic tuffs contain a chlorite-tremolite-albite-carbonate assemblage. Micaceous minerals define cleavage planes and are synkinematic. Metamorphism accompanied the earliest deformation and reached greenschist grade; metamorphism culminated prior to subsequent deformation. The crenulation cleavage is a brittle feature which crumples the earlier fabric and postdates metamorphism.

The gross map pattern of Lower Carboniferous limestone reflects a type 3 fold interference pattern. A sub-Permian unconformity is structurally conformable and folded together about the east-west axial trend. Mid-Carboniferous limestone clasts in a volcanic-dominated conglomerate comprise the basal unit of the Upper Carboniferous to Lower Permian volcanoclastic-sedimentary package. Lithic fragments are flattened in the foliation plane with length-to-width strain ratios commonly of 10 to 1.

## PRE-LATE TRIASSIC DEFORMATION (SONOMAN)

The Lower to Middle Triassic shale at Copper Canyon is assumed to lie below the Tahltanian unconformity (Souther, 1971) and has been folded and regionally metamorphosed prior to deposition of the Upper Triassic Stuhini Group (Souther, 1972; Figure 19). At Copper Canyon these fine-grained clastic rocks and Lower Permian limestones are paraconformable and have been tightly folded as one unit (Jeffery, 1966). Unequivocal evidence for a pre-Late Triassic contractional phase of deformation affecting these rocks is not apparent. The lack of appreciable difference in deformational style between Paleozoic and Triassic strata suggests that the Tahltanian Orogeny may have been an uplift event without compressive deformation. Post Early Permian to Late Permian strata are missing from the Galore Creek area. Lower Triassic, Smithian sediments overlie Lower Permian limestone in several locations, but elsewhere limestone boulders in Upper Triassic conglomerates indicate uplift and erosion.

Conodont colour alteration indices show no appreciable difference between Lower Permian and Lower, Middle

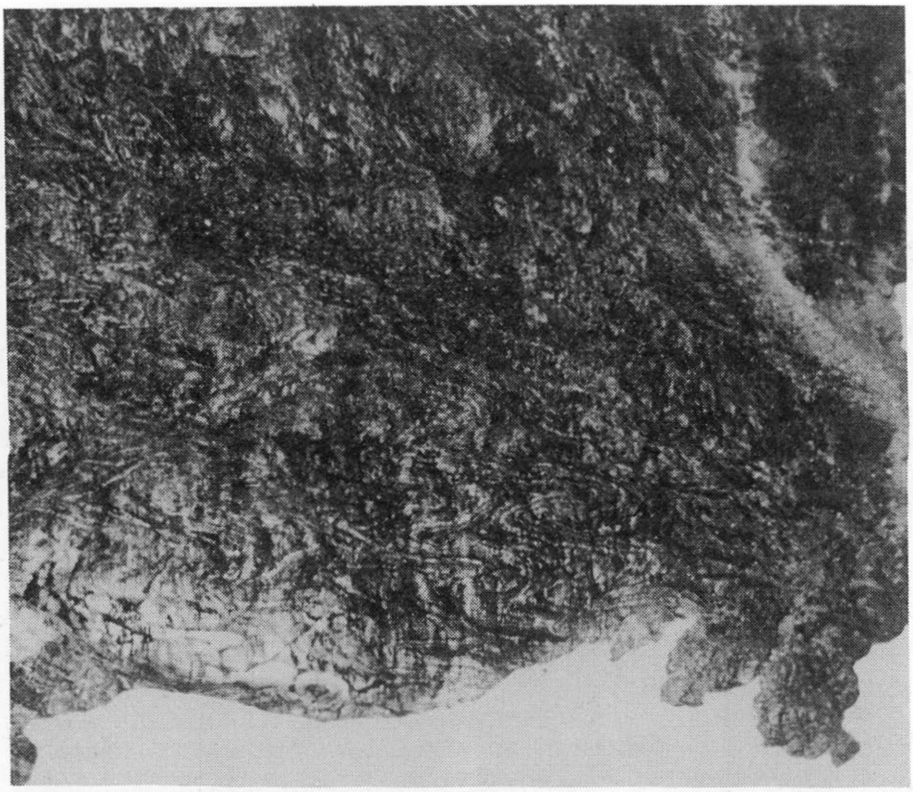

Plate 15. Recumbent isoclinal Z-folds on the overturned limb of a west-verging antiform in Permian limestone cliffs west of the confluence of Galore Creek and Scud River. View is southwesterly; width of photo is approximately 100 metres.

Plate 16. West-verging overturned synform, cored by Lower Permian limestone (pale grey) and outlined by boudinaged and thinned maroon volcaniclastic rocks (dark grey). Dark peaks in background are undivided Upper Triassic volcanic rocks, view is northward.

and Upper Triassic strata. Conodonts collected above Copper Canyon have colour alteration indices (CAI) of 5 for Middle Triassic sediments, 4.5 from Lower Triassic rocks and 4 from Lower Permian. Upper Triassic conodont CAI values from the area equal 5. In contrast, differing pre- and post-Upper Triassic conodont CAI values are noted elsewhere (Read *et al.*, 1983; Anderson, 1989) and define a period of deformation and metamorphism for this interval. However, in the Galore Creek area relatively high conodont CAI values are known for all ages (Brown *et al.*, 1991), suggesting elevated heat flow in the Scud River area. In addition, a Jura-Cretaceous or younger thermal event may overprint any earlier differences.

## *POST-LATE TRIASSIC AND PRE-LATE CRETACEOUS DEFORMATION*

Upper Triassic strata, for the most part sedimentary, and older rocks, are folded about two virtually orthogonal axes. The earlier is characterized by west-trending folds, the later by north to northwest axial trends. Although these are thought to represent two phases of folding, no folded cleavages or folded folds have been observed. Locally, north-trending folds progressively tighten westward into southwest-verging folds and thrust panels. In general, the Triassic volcanic rocks appear unfolded and are rarely foliated. Permian limestones, on the other hand, are weakly to pervasively foliated, generally parallel to bedding, and folding is characterized by thickened hinge areas and ductile flow of limestone around chert boudins in strongly attenuated fold limbs.

### SECOND PHASE

West-trending folds affect the form of later structures but for the most part, the fold pattern is dominated by the northerly trending folds and faults. West-trending antiformal-synformal warps suggest wavelengths on a scale of several kilometres are present in the southern part of the map area. Permian and older rocks at Round Lake are warped about a westerly trending antiformal axis and Upper Triassic volcanic and related rocks are folded about west and northwesterly trending axes into upright open to tight folds north of Sphaler Creek. At Copper Canyon, Permian limestone and Upper Triassic alkalic epiclastic rocks are folded about westerly trending fold axes; bedding in the latter is overturned to the south in places, but there is not a consistent overturned direction.

### THIRD PHASE

The distribution of Permian limestones reflects the regional northerly trend of third phase folding. It is characterized by upright and overturned to recumbent fold orientations. Folds are open to moderate to tight isoclinal. The axial traces trend north to north-northwest and assymetric folds are generally southwest verging. The map pattern of Upper Triassic and Permian rocks south of the Scud River and west of Galore Creek reflects this trend. Thrust faulting and fold interference from early west-trending structures complicate the pattern. In a general sense, the Permian limestone sections at higher elevations are characterized by upright, tight to open north-trending folds, while those exposed in cliff sections in the valley bottom are isoclinal, overturned to recumbent. This phenomenon is apparent east of Galore Creek in the limestone south of the Scud River and north of Sphaler Creek.

East of the confluence of Galore Creek and the Scud River are 1500 metres of structurally thickened limestone. The cliff exposure is stepped midway between creek and the top at 1000 metres elevation. Moderate to tight, overturned to recumbent isoclinal Z-folds are exposed above this break (Plate 15). Fold vergence and geometry suggest this is an overturned limb of a larger antiform verging westerly. At the top of the cliff, limestones are folded into tight, upright metre-scale folds about northerly trending, moderately southwest-plunging vertical axial planes. Mafic dikes intruded the limestone perpendicular to fold axes along west-trending AC-joints.

East of the South Scud River is a shallow to moderately east dipping homoclinal section of limestone more than 1000 metres thick. Lensoidal maroon volcanielastic boudins and detached fold limbs indicate structural complexities. Thickened and detached fold hinges in Permian limestones at the head of Sphaler Creek illustrate the geometries and complexities of carbonate deformation here, also noted by Souther (1972). Cliff exposures north of Sphaler Creek contain a large-scale west-verging overturned synform (Plate 16). To the east and structurally overlying this fold, along the top of the ridge, is a tight, upright antiform-synform pair. The overturned synform is cored by Permian carbonate rocks and outlined by boudinaged, tectonically thinned, maroon intermediate volcanic rocks which pinch out midway along the upper limb of the structure. Lensoidal boudins of older volcanic rock and segments of younger mafic augite-porphyritic dikes are suspended within plastically deformed limestone. It is this fold and thrust geometry which controls the outcrop pattern at Copper Canyon. The rocks at Copper Canyon comprise a structurally complex zone of imbricated thrust panels interleaving Lower Permian, Lower, Middle and Upper Triassic rocks. The rocks in general dip east and young west and therefore this is not a simple imbrication (Figure 19). Here, Lower to Middle Triassic sediments occupy the lower and upper limb of a southwest-overturned anticline that was thrust westerly. Thrusting has sheared out the lower synform and carried these older rocks westward over Norian volcanic rocks. Structural interleaving of Triassic sediments and Permian limestone along strike to the north reflects separate thrust splays. Stratigraphic repeats are recognized biostratigraphically in limestones to the east and structurally lower in the South Scud valley (*cf.* under

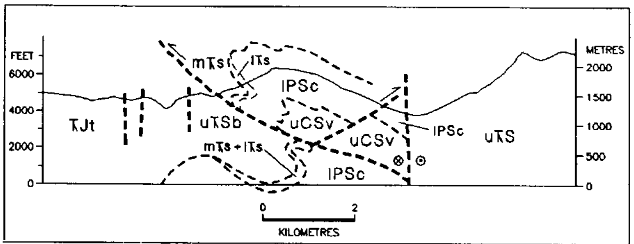


Figure 19. Schematic cross-section of the overturned strata at Copper Canyon. Section line is shown on Figure 18.

Stratigraphy, Chapter 3). Tight isoclinal folds wholly within limestone are visible in cliffs above the thrust fault.

Folds are sparse within the Stuhini Group; bedding commonly dips steeply but closures are rarely seen. Large-scale warps with kilometre-scale wavelengths are common. Small-scale folds are brittle features, typically upright box folds with chevron cores.

Late stage, third phase or fourth phase(?) deformation (Late Jurrasic to mid-Cretaceous) is manifest as chevron folds and kink bands north of Round Lake. Fold axes have generally west or west-northwesterly trends and plunges. The axial planes dip steeply southwest. Metre-scale north to northeast-verging, northwest-trending folds affect sedimentary rocks as young as Lower to Middle(?) Jurassic (Plate 17). The Jurassic sediments outcrop in a gentle westerly facing homocline. Northeast-trending faults rotate bedding into high-angle parallelism with fault structures.

### AGE CONSTRAINTS ON SECOND AND THIRD PHASE FOLDING

Placing age constraints on the post-Triassic folding is equivocal. Upright north-trending folds may be an early manifestation of progressive deformation which resulted in southwest-verging structures. Southwest-verging deformation involves the marginal phases of the Hickman pluton and so is, at least in part, no older than Late Triassic. North of the Scud River southwest-verging reverse faulting deforms a 185 Ma, Early Jurassic intrusion (Brown *et al.*, in preparation). Assuming the third phase structures are related to the Skeena fold and thrust belt, then post-185 Ma west-directed compression may be back thrusting related to the overall northeast directed compression recorded by northeasterly vergent chevron and kink folds in Lower to Middle(?) Jurassic rocks at Round Lake and in the northern Bowser Basin. The age of west-trending structures is more difficult to constrain, although they are older than northerly trending structures. Middle Jurassic deformation accompanying southward thrusting of Cache Creek Terrane onto Stikinia along the King Salmon fault may be reflected by phase 2 structures in the map area. Alternatively, a contractional event accompanied by uplift and erosion, represented by an angular unconformity, basal conglomerate and metamorphic disparity preceded Early Jurassic (Sinemurian) Hazelton arc volcanism and sedimentary rock accumulation in the Iskut River area (Henderson *et al.*, 1992) and Toarcian Hazelton volcanism in the Stikine river area (Brown and Greig, 1990). An angular unconformity separates tight upright folded Upper Triassic volcanic and sedimentary rocks from gently tilted Lower Jurassic sedimentary rocks in the Mess Lake area (Logan and Drobe, in prepation), but in the Galore Creek area truncated structures are not apparent and the Lower Jurassic conglomerate seems little deformed other than by moderate tilting. Relating the timing of structures to regional(?) unconformities developed in evolving volcanic arc environments is prone to error, but is a first attempt at synthesizing the structural history and, as such, suggests the older west-trending structures may have developed in post-Norian and pre-Sinemurian to sub-Toarcian time.

## FAULTS

Five sets of faults are recognized in the southern Telegraph map area. From oldest to youngest these include: north-trending vertical faults; east and west-dipping reverse faults; northwest-striking vertical faults in part coeval with, but also truncated by the north-trending structures; west-trending vertical shear zones and normal, generally north-side-down, extensional faults; and northeast-striking

Plate 17. Northeast-verging, late third or fourth phase kink folds in Lower to (?)Upper Jurassic calcareous siltstones and sandstones west of Round Lake. Section is cut by a north-trending, steeply east dipping felsic dike; view is to the east.

sinistral shear zones and vertical normal faults. These planar features have been related to deformational episodes which produced folding where possible. Cataclasite zones are associated with all but the youngest northeast-trending faults. These have channeled fluids and alteration has obliterated protolith rocks in zones up to tens of metres wide.

### *NORTH-TRENDING FAULTS*

The strongest and longest lived structures strike north. These include faults in the Iskut River, Forrest Kerr and Mess Creek valleys and parallel structures in the South Scud River valley between Sphaler Creek and the Scud Glacier. The Mess Creek structure has undergone repeated movement beginning at least as early as Late Jurassic and continuing into the Quaternary (Souther and Symons, 1974). More than one component of normal, strike-slip and reverse movement can be documented for these fault zones.

Northerly striking, vertical to steeply dipping faults occur in the South Scud River valley and south of Sphaler Creek. The most prominent of these, the South Scud River fault zone, follows the western flank of the Hickman pluton for approximately 7 kilometres south, from where it curves southeast and follows the South Scud River. It projects north to the Scud Glacier and south to the Twin Glaciers areas. The zone is approximately 2 kilometres wide and consists of an array of north-trending parallel and en echelon, subvertical normal and shallow reverse faults. Northwest-trending vertical faults merge into the South Scud River structure along its northern limits.

Adjacent to the Hickman pluton the fault juxtaposes Permian limestone with a narrow belt of Stuhini volcanic flows, tuffs and sediments intruded on the east by Hickman diorite. East of the confluence of the Scud and South Scud rivers the fault bifurcates into at least three parallel zones of sheared and brittle fractured rocks, for the most part, in the footwall Upper Triassic rocks. Faulting has rotated bedding in the Triassic rocks to subvertical, parallel to the faulted contact with Lower Permian limestones. Bedding in the limestones is complexly folded but generally moderately east dipping and truncated by the fault plane at a high angle. The main structure hosts lenticular bodies of sheared serpentinized peridotite and is characterized by a zone of listwanite alteration 15 to 20 metres wide. Northerly trending Tertiary or younger(?) rhyolite and basaltic dikes occupy the medial structure. Souther (1972) projected this fault south to Sphaler Creek where Upper Carboniferous to Lower Permian metasediments and metavolcanics are faulted against Upper Triassic volcanics. South of Sphaler Creek the fault zone is difficult to trace in the carbonate; at least two parallel structures are present and it is apparently truncated by the deeply incised northeast-trending faults along Sphaler Creek.

### *NORTHERLY TRENDING REVERSE FAULTS*

North-trending reverse faults with opposing vergence flank the northern section of the South Scud River fault zone. The Copper Canyon fault is exposed for 12 kilometres on the west side of the zone and marks the contact between Lower to Middle Triassic sedimentary rocks and Upper Triassic volcanic rocks. East of the South Scud River the same contact relationships are evident for 5 kilometres adjacent to the Hickman pluton. Both structures are convex in plan and merge with high-angle structures within the main South Scud River zone.

The north-striking, east-dipping thrust fault at Copper Canyon places overturned Permian limestones and Lower to Middle Triassic shale on Upper Triassic volcanics (Plate 18). The thrust fault is placed at the contact between Upper Triassic volcanic and Lower Triassic sedimentary rocks, although there is probably detachment and displacement along the contact with Permian limestone and possibly unrecognized west-directed reverse faulting within the Triassic sediments. The hangingwall limestones are characterized by tight, upright chevron folds, away from the thrust. Above the thrust and Lower-Middle Triassic contact, folds are overturned, tight, recumbent and verge to the west. The hangingwall strata have dips of 30° to 50° east. The Triassic sediments in the footwall of the thrust are strongly contorted, north and northeast-trending doubly plunging upright to recumbent folds. Competency contrasts between rusty weathering siltstones, graphitic shale and ribbon cherts have produced ptygmatically folded, boudinaged lenses and rootless folds of random orientation. Bedding plane detachments are common. A second, subparallel fault, defined by a footwall zone of limonite and ankerite alteration is mapped approximately 400 metres west of the thrust at Copper Canyon (Plate 18). It has been interpreted as a footwall splay from the main thrust fault (Leary, 1990), but the fault-bound panel consists of younger (bedded alkalic flows, lapilli tuff and breccia with minor shale and carbonate of the uppermost Stuhini Group stratigraphy) over older (andesite and trachyandesite breccias) rocks. Narrow, Eocene (?) felsic dikes cut the mineralized system, thrust fault and upper plate rocks. Dike offsets indicate latest movement was either normal or right-lateral strike-slip. The footwall of the 'footwall-splay' fault is intruded by latest Late Triassic to Early Jurassic syenite at Copper Canyon. Thrusting is believed to postdate these intrusions as their extrusive equivalents, alkaline flows, tuffs (*circa* 208 Ma) and epiclastic rocks were involved in the thrusting event. Alternatively, Leary (1990) interpreted movement on the thrust fault to have been largely younger than the alkalic intrusions.

The Early Jurassic Scud stock lies at the northern extension of the Copper Canyon fault. Read (1988) suggests the fault is sealed by the intrusion and therefore movement predates 185±9 Ma (K-Ar biotite date, White *et al.*, 1968). The outcrop pattern of the pluton is bisected by northwest-trending, subvertical linears along which thin-bedded siliceous Lower to Middle Triassic(?) sedimentary rocks crop out. The linears are interpreted to be faults. The medial structure, central to the pluton, was examined in 1991, but neither mylonite nor foliation zones cut the granodiorite. It is uncertain whether this structure offsets, truncates or merges with the thrust fault at the southeast corner of the intrusion, but any movement must predate the intrusion. The thrust is projected to continue northward along the intrusive contact (Figure 18).

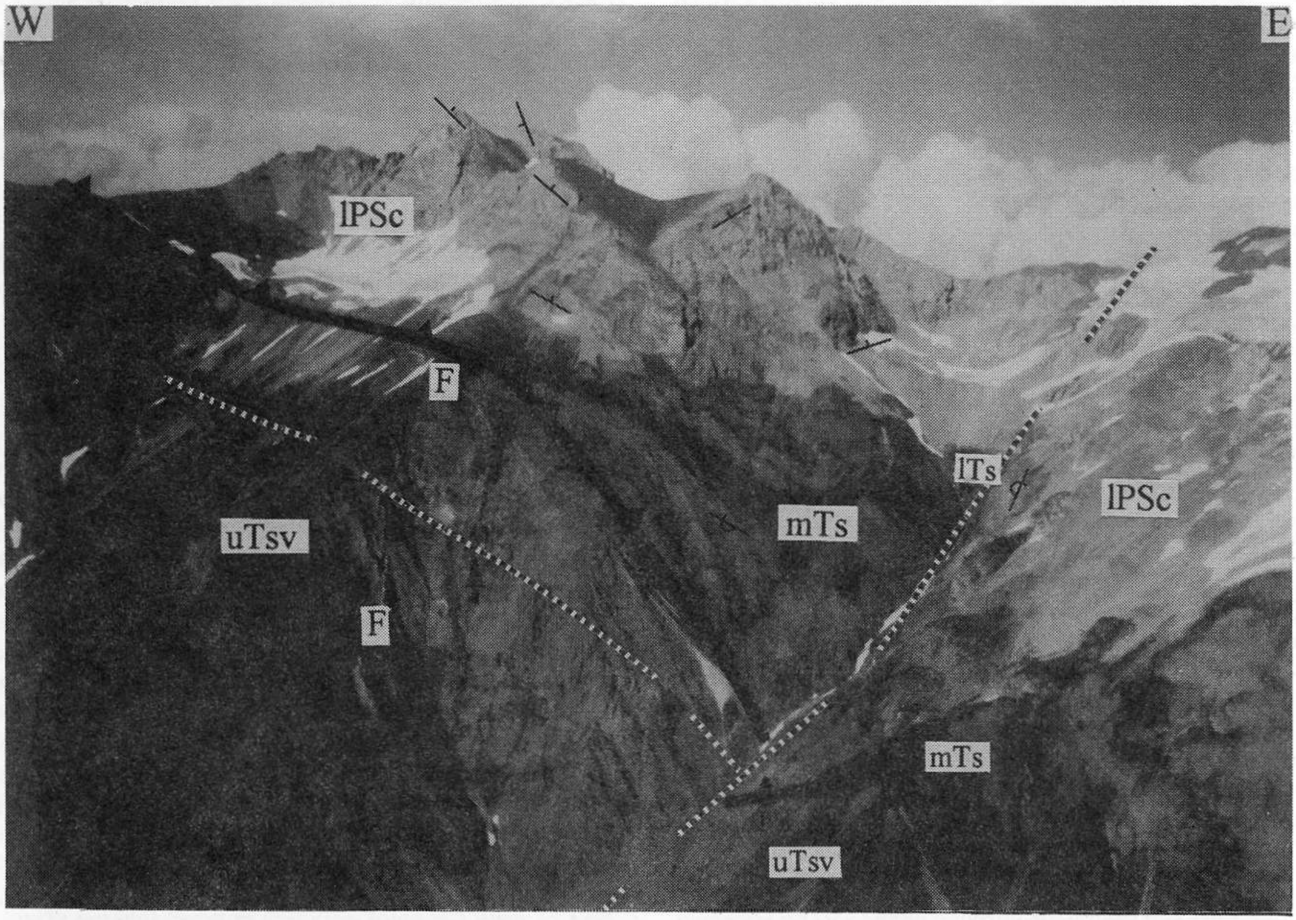


Plate 18. North-striking, east-dipping thrust fault at Copper Canyon places overturned Lower Permian limestone (lPSc) and Lower to Middle Triassic sediments (l-mTs) on uppermost Upper Triassic alkaline volcanics (uTSv). Normal or dextral offset along a parallel structure is indicated by a felsite dike (F). View is easterly.

East of the south fork of the Scud River, the Permian limestone, Middle Triassic siltstone and chert and Upper Triassic Stuhini Group volcanics are overturned to the east and young eastward. West of the South Scud River these units are overturned to the west and young westward. The opposing thrust vergence across the South Scud River fault zone and their geometries represent a positive flower structure (Wilcox *et al.,* 1973). The positive flower structure is a feature developed in strike-slip regimes. It is bounded by sinuous faults which, in cross-section, are nearly vertical at depth and flatten upwards and outwards (Sylvester, 1988). Strike-slip faults usually cut bedding at high angles and this accounts, in part, for the braided geometry of mature strike-slip zones. However, no Early Jurassic north-south strike-slip movement can be demonstrated from displacements of lithology or kinematic indicators. The low-angle faults which flank the South Scud River fault zone are within upper sections of Middle Triassic sediments, a relatively incompetent succession in the sequence of Permian carbonate and Upper Triassic volcanic rocks and, as such, might argue against a transpressive origin.

## *NORTHWEST-TRENDING FAULTS*

A group of parallel northwest-trending fault structures in the northern part of the map area has offset the drainage pattern of the Scud River and the outcrop pattern of the Early Jurassic Scud River pluton. The faults are subvertical and normal or strike-slip. The outcrop pattern of the intrusion suggests right-lateral displacement similiar to that on late faults at Copper Canyon. The faults merge southeasterly into the north-trending South Scud River fault. West of the Scud pluton, a prominent northwest-trending structure in the Permian carbonates separates mainly northerly trending folds in the structurally higher southwest panel from southeasterly trending folds in limestones to the northeast. It is pyritic and deeply weathered and can be traced 12 kilometres southward almost to Copper Canyon (Figure 18). Projection of this structure northwestward (onto 104G/5) coincides with the Cone Mountain thrust fault (Brown *et al.,* in preparation), a northeast-dipping reverse fault. It has carried a southwest-facing imbricate stack of Stikine assemblage rocks westward onto foliated granodiorite of the Cone Mountain pluton. The footwall is a mylonite zone, 500 metres wide, dipping 40° to 65° east, which coincides with the eastern margin of the pluton. Thrusting is synchronous or postdates emplacement of the intrusion (185 Ma) and provides a lower age limit for the Cone Mountain thrust (Brown *et al.*, in preparation). West of the Scud pluton (104G/3) the structure consists of a series of steep, stepped normal faults with unknown amounts of displacement. The variability of fold geometry across adjacent blocks suggests juxtaposition, probably by reverse faulting, which has structurally thickened the section.

Other northwest-trending faults, east of the South Scud River structure, include the Trophy fault, on the southwest end of the Hickman pluton. The faulted contact between Late Triassic Hickman monzonite and Triassic metavolcanic and metasedimentary rocks dips moderately west. The magnitude and direction of fault displacement is not known. Read (1988) attributed the absence of a fine-grained marginal phase and contact metamorphic effect in the wallrock to considerable displacement along the fault. These intrusive contact features are present north and south of the Trophy fault.

## *WESTERLY TRENDING FAULTS*

West and northwest-trending faults traverse the general north-south intrusive contact between the Coast Range intrusions and older layered rocks in the area east of the Stikine River (Figure 18). These are mostly vertical faults. They are discussed below, beginning in the south. A northwest-trending lineament separates the Upper Triassic volcanic package from an undivided Paleozoic assemblage of metasedimentary and metavolcanic rocks north of Sphaler Creek at the Stikine River. The structure is poorly exposed and the sense of motion is unknown. Timing is equivocal but the faulted contact with Early Jurassic granodiorite to the north suggests the structure postdates its intrusion. Southeast along strike the structure is cut by Eocene biotite granite plugs, placing an upper limit on the timing of movement.

To the north, above the Anuk River, is a west to northwest-trending vertical to steeply dipping mylonite zone, marked by a strong airphoto lineament for 3 kilometres of strike length. The fault offsets the intrusive contact between Upper Triassic Stuhini Group volcaniclastic rocks and Early Jurassic granodiorite, 1 kilometre in a dextral sense. Kinematic indicators are well developed in the iron carbonate, sericite, chlorite alteration which is pervasive across the 10 metre wide zone. Post-shear, fine-grained mafic dikes parallel the structure and occupy the zone.

Two steep, west to northwest-trending faults separate Upper Triassic volcanic and sedimentary rocks from younger Jurassic and Eocene intrusions between Saddle Mountain and Jack Wilson Creek. The northern fault is offset by a subvertical west-striking normal fault in Jack Wilson Creek. A north-side-down movement is assumed for the normal fault, but no sense of vertical displacement is obvious from the distribution of hydrothermal alteration assemblages. Those on the south side of Jack Wilson Creek, at 1200 to 1400 metres elevations, are high-level low-temperature assemblages, and those on the north side at elevations of less than 300 metres, characterize deeper levels.

## *NORTHEASTERLY TRENDING FAULTS*

Northeasterly striking faults offset the general north to northwesterly structural and stratigraphic grain. Apart from the northerly trending extensional structures controlling Miocene volcanism, these are the youngest faults in the map area. They control second and third order drainage patterns. Movement along these faults was mainly sinstral stike-slip in nature. Eocene intrusions and mineralization are often associated with these structures.

The upper reaches of Sphaler Creek follow steep to vertical structures trending 020° to 040°. One of these faults can be traced for 6 kilometres, trending northeasterly across the Sphal/Trek property (MINFILE 104G-022, 029). An apparent 1200 metres of sinstral offset is indicated where the fault crosses Sphaler Creek, assuming the northwest and northeast faults are not a contemporaneous conjugate set. The fault cuts Upper Triassic pyroxene flows and volcaniclastics for much of its length, but follows the contact with Eocene granodiorite at its southern end. The fault zone, where it is exposed in Sphaler Creek, is marked by a bleached, silicified and pyritic alteration zone more than 5 metres wide. Parallel shear structures host base and precious metal prospects of probable Eocene age.

A northeast-trending graben, 2 kilometres wide, occurs at the headwaters of Sphaler Creek (Figure 18). Bounding faults are subvertical to northwest dipping. Early Jurassic to possibly Middle Jurassic sedimentary rocks are preserved at the northeast end of the structure. At the southwest end strata generally trend north but are complexly folded and faulted. They consist of Permian limestones overlain by little deformed Triassic(?) to Jurassic conglomerates and fine-grained sediments. West of Round Lake northwest-trending kink folds affect both the graben and bounding rocks, suggesting graben formation postdates Late Jurassic to Cretaceous northeast-directed compression.

A set of northeasterly striking shears and fractures on the Trophy claims is mineralized by quartz-carbonate veins. Mineral assemblages and galena-lead model ages suggest an Eocene age for mineralization. These fracture fillings may represent dilational features related to latest movement on the northwest-trending Trophy fault. Other north-northeast-trending faults are found in the Galore Creek syenite complex. These faults postdate Triassic to Early Jurassic mineralization. The faults dip westerly at about 30° to 50°, and display up to 150 metres of normal displacement (Panteleyev, 1974).

# CHAPTER 6 ECONOMIC GEOLOGY

Stikinia is a composite allochthonous terrane made up of an amalgamation of volcanic island arcs ranging in age from late Paleozoic through Middle Jurassic. Modern anologs include the Pacific island arcs from Japan south through the Philippines, or New Guinea to New Zealand. Sillitoe (1989a) documented the western Pacific island arcs as a major gold province; it contains more than 5350 tonnes of gold in 56 deposits. These young, epithermal deposits are mainly related to intrusions; there is only a single volcanogenic massive sulphide deposit. Mineral deposits commonly found in island arc settings include porphyry, mesothermal vein, metasomatic skarn, epithermal vein and volcanogenic massive sulphide deposits of the Kuroko type. Regional examples of these deposit types are found in Stikinia (Figure 20). Tulsequah Chief is a Kuroko type volcanogenic gold-silver-zinc-copper-lead massive sulphide deposit located in the Tulsequah area of northwestern Stikinia. Porphyry copper deposits in the area include both the alkaline copper-gold-silver (Galore Creek) and calcalkaline copper-molybdenum-gold (Schaft Creek) types. Early Jurassic mesothermal gold-quartz veins at the Golden Bear gold mine are hosted by a regional north-trending fault. The largest epithermal silver-gold deposit in the province is the Premier mine, formerly the Silbak Premier mine in the Stewart area.

Several separate mineralizing epochs have been postulated for northwestern British Columbia (Alldrick *et al.*, 1987; Britten and Alldrick, 1990; Godwin *et al.*, 1991), based on deposit mineralogy, galena-lead isotope data, age, and the composition of associated intrusive rocks. Copper-zinc mineralization characterizes the Triassic; gold-silver-copper mineralization associated with alkaline and calcalkaline intrusions characterizes the Early Jurassic; and molybdenum and silver-rich base metal deposits characterize the Eocene event. Most precious metal mineralization is related to a latest Triassic and earliest Jurassic island arc, and to early accretion-related magmatic activity. Tertiary post-accretionary mineralization is related to continental volcanism and epizonal plutonism.

Mineral deposits in the Sphaler Creek - Scud River area comprise five groups: porphyry copper-silver-gold deposits associated with syenitic sills and monzonite plugs; mesothermal silver-gold and copper-zinc mineralization in quartz and carbonate veins; copper-iron skarns; breccia-hosted copper-silver-gold; and massive polymetallic sulphides carrying precious metals. The first four types can often be related to one hydrothermal system and represent only different sites and ore-forming environments within it. Precious metal porphyry and vein deposits related to alkaline rocks are well documented (Mutschler *et al.*, 1985; Barr *et al.*, 1976) and currently important exploration targets. Figure 20 shows the location and type of mineral occurrences recorded in MINFILE. Table 4 briefly summarizes occurrence name(s), location, hostrock, known and inferred age, and reserves or best assays, together with appropriate references. Major occurrences and those receiving recent exploration attention are described here.

## ALKALIC PORPHYRY DEPOSITS

Alkalic porphyry copper-gold deposits occur throughout the length of the Intermontane Belt in both Stikinia and Quesnellia. They are restricted to Late Triassic and Early Jurassic volcanic island arc assemblages of the Nicola, Takla and Stuhini groups and form a class distinct from the calcalkaline porphyry deposits (Barr *et al.*, 1976). Mineralization occurs in alkaline magmatic centres that are characterized by alkaline intrusions and comagmatic subalkaline to alkaline and shoshonitic volcanic rocks (de Rosen-Spence, 1985, Mortimer, 1986). Crowded feldspar porphyritic textures are characteristic of both the intrusives and the volcanics; pyroxene-phyric basalts are typical. The alkaline intrusions evolved from crystal-fractionated, volatile and metal-enriched magmas (Fox, 1989; Mutschler *et al.*, 1990) that were emplaced rapidly and often intrude their volcanic edifice. Multiple intrusions of crystal-rich magma produce porphyritic textured intrusives, intrusive breccias and hydrothermal breccias. These intrusive pulses predate, coincide and postdate alteration and mineralization related to the magmatic centres. The intrusive bodies are typically small (less than 2 to 3 kilometres across), spatially related to long-lived regional-scale faults (Preto 1989, Nelson, 1991) and commonly have spatial and temporal relationships with calcalkaline magmatism.

The deposits occupy brecciated and faulted zones related to extensively altered subvolcanic intrusions and their volcanic country rocks. Alteration patterns are distinctly different from those of classic calcalkaline deposits, characterized by concentric potassic-phyllic-argillic-propylitic zones. The alkalic deposits typically have a central potassic or sodic-plagioclase zone which passes outward into a propylitic zone; often these overlap and are overprinted by retrograde metasomatic alteration (Figure 21). Magnetite breccias and disseminations are associated with the potassic alteration, which hosts most of the copper and gold mineralization. Disseminated pyrite and minor copper mineralization mantle the propylitic alteration zone. Typical sulphide assemblages include pyrite, chalcopyrite, bornite, chalcocite and pyrrhotite in decreasing abundance. The deposits are characteristically enriched in silver and gold, and are particularly silver-rich in comparision with calcalkaline porphyry deposits (Sinclair *et al.*, 1982). However, both types may carry significant gold values (Sillitoe, 1989b).

In the Galore Creek camp, a latest Triassic alkaline magmatic centre comprising Stuhini Group volcanic rocks and comagmatic syenitic intrusives hosts more than ten synvolcanic fracture controlled copper-gold deposits.

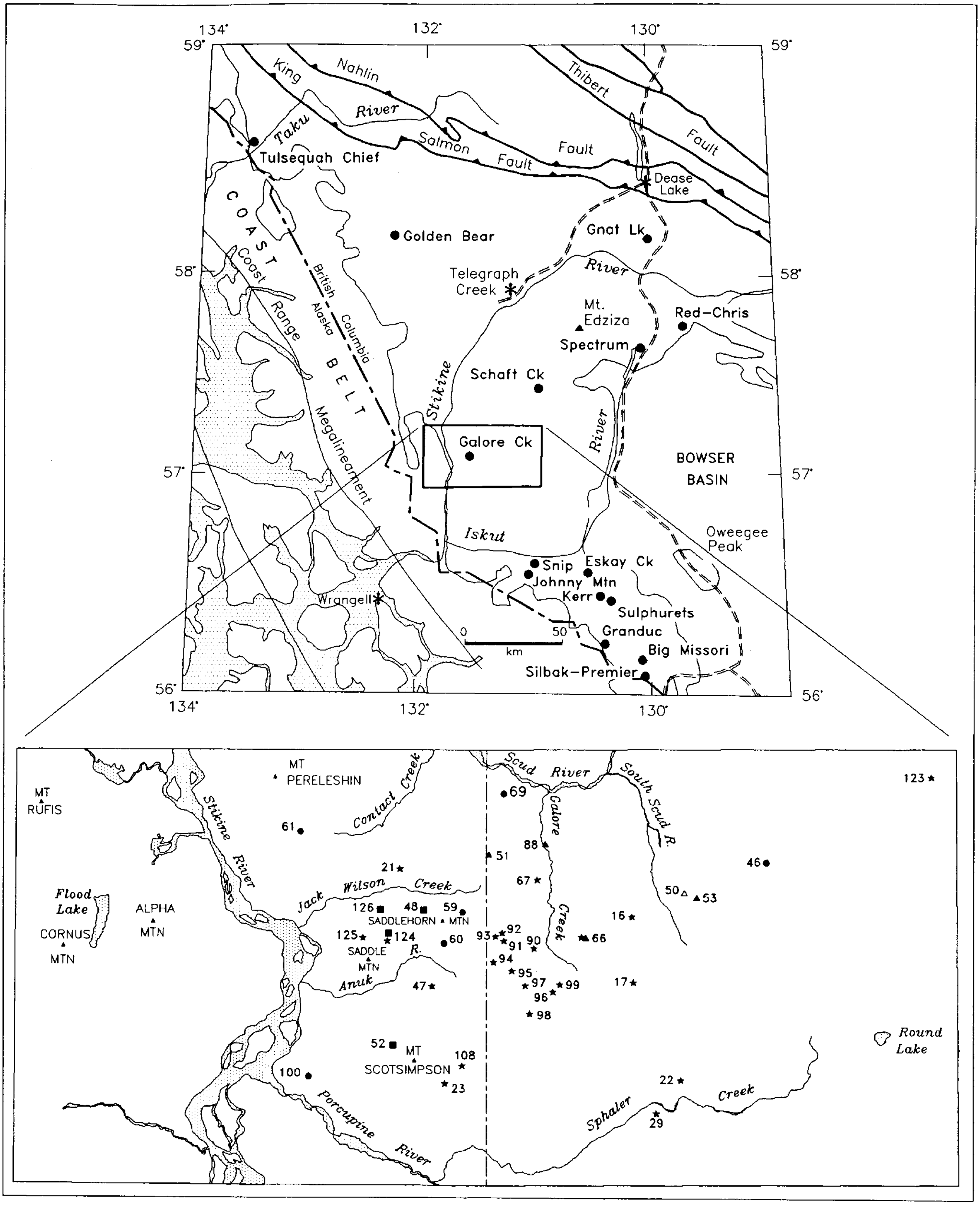


Figure 20. Location of map area relative to the major tectonostratigraphic features of the northwestern Cordillera (modified from Wheeler and McFeely 1987), showing regionally significant mineral deposits; and other deposits in the study area recorded in the MINFILE database. Numbers and symbols correspond to Table 4.

# TABLE 4
## MINERAL OCCURRENCES IN THE SPHALER CREEK AND FLOOD GLACIER MAP AREAS

| MINFILE No. 104G- | PROPERTY NAME | UTM East | Zone 09 North | COMMODITY | HOSTROCKS | RESERVES OR BEST ASSAY g/t = grams per tonne, Mt= million tonnes | REFERENCES |
|---|---|---|---|---|---|---|---|
| **Porphyry Cu, Au, Ag ; Breccia ★** | | | | | | | |
| 90 | Galore Ck, Central | 351500 | 6335000 | Cu,Au,Ag | uTSv, uTSs, TJv, TJs | 125 Mt 1.06% Cu, 0.4 g/t Au, 7.7 g/t Ag | Allen *et al.* (1976)* |
| 91 | Galore Ck, Junction | 349750 | 6335600 | Cu | uTSv, uTSs, TJv, TJs | - | Barr (1966), Allen *et al.* (1976) |
| 92 | Galore Ck, North Junction | 349700 | 6336000 | Cu,Au,Ag | uTSv, uTSs, TJv, TJs | 4.8 Mt 2.0% Cu, 0.75 g/t Au | Taylor (1989)*, Barr (1966), Allen *et al.* (1976) |
| 93 | Galore Ck, West Rim | 349250 | 6335750 | Cu | uTSv, uTSs, TJv, TJt, TJs | - | Barr (1966), Allen *et al.* (1976) |
| 94 | Galore Ck, Butte | 349150 | 6334200 | Cu,Fe | uTSv, uTSs, TJv, TJt, TJs | - | Barr (1966), Allen *et al.* (1976) |
| 95 | Galore Ck, Southwest | 350250 | 6333550 | Cu,Au,Ag | uTSv, uTSs, TJv, TJs | drill core: 61 m 5.14 g/t Au, 1.88% Cu | Yarrow and Taylor (1990)*, Barr (1966), Allen *et al.* (1976) |
| 96 | Galore Ck, Saddle | 352850 | 6332100 | Cu,Au,Ag | uTSv, uTSs, TJv, TJt, TJs | drill core: 12 m 3.98 g/t Au, 2.49% Cu | Yarrow and Taylor (1990)*, Barr (1966), Allen *et al.* (1976) |
| 97 | Galore Ck, West Fork Glacier | 350850 | 6332650 | Cu | uTSv, uTSs, TJv, TJs | - | Barr (1966), Allen *et al.* (1976) |
| 98 | Galore Ck, South Butte | 351250 | 6330750 | Cu | uTSv, uTSs, TJv, TJs | - | Barr (1966), Allen *et al.* (1976) |
| 99 | Galore Ck, South 110 | 353300 | 6332500 | Cu | uTSv, uTSs, TJv, TJt, TJs | - | Barr (1966), Allen *et al.* (1976) |
| 66 | Stikine East | 354800 | 6335500 | Cu,Au Ag | TJs | 11.9 m chip: 0.1% Cu | Gale (1964)* |
| 67 | Stikine North | 352200 | 6339400 | Cu | uTSp, uTSs, uTSb, TJv, TJs | Grab: over 18 m, 0.13 % Cu | Falconer (1964)* |
| 17 | Copper Canyon, Penny, CC | 358000 | 6333000 | Cu,Au,Ag | uTSb, TJs | 27 Mt 0.72% Cu, 0.43 g/t Au | Spencer and Dobell (1958)*, Leary (1990) |
| 21 | JW, Jack Wilson Creek | 343400 | 6340000 | Cu,Au.,Ag | uTSv, lTgd | chip; over 14 m, 0.98 % Cu, 0.51 g/t Au (Trench 3) | Blann and Vulimiri (1990)* |
| 124 | Ridge | 342650 | 6336560 | Cu,Au | uTSv, uTSb, TJs | 1m chip: >1.0% Cu, 0.48 g/t Au | Blann and Vulimiri (1990)* |
| 125 | Saddle Mountain | 341050 | 6336250 | Cu,Au | uTSv, uTSb, TJs | Grab; >1.0 % Cu, 0.07 g/t Au | Blann and Vulimiri (1990)* |
| 23 | Ann, Split Creek, Sue | 345500 | 6326700 | Cu, Au | uTSv, Eg | drill core: averages 0.02% Cu | Jeffery (1966)* |
| 108 | Paydirt, AC | 347100 | 6327650 | Au, Cu | uTSv, eJgd, Eg | 185,000 t 4.11g/t Au | Folk (1982), Holtby (1985)* |
| 22 | Kim, Sphal 17 | 360850 | 6326000 | Cu,Au,Ag | uTSv, uTSp, Eg | 18x20 m area chip: 2.45% Cu, 0.23 g/t Au, 10.63 g/t Ag | Rayner and Ney (1964), Folk (1981)* |
| 29 | Sphal 27 | 359000 | 6323000 | Cu,Au | uTSv, Egd, lTm | 30 m chip: 0.67% Cu, 1.82 g/t Au | Rayner and Ney (1964), Folk and Spilsbury (1980)* |
| - | Trek, Gully, Heel | 359500 | 6332900 | Ag,Au,Pb,Zn | uTSv, Egd, lTm | 3.6 m chip: 8.77g/t Au, 14.4 g/t Ag, 5.31% Cu (Gully zone) | Awmack and Yamamura (1988)*, Awmack (1991) |
| 47 | Joan and MB | 345000 | 6333000 | Cu | uTSv, uTSs, TJs | - | Asano (1965) |
| **Au, Ag, Base Metal Veins ●** | | | | | | | |
| 16 | Lot | 358000 | 6336250 | Cu,Au,Pb,Ag | uTSb, uTSp, lTgd | 5 m chip: 0.38% Cu; 1.37g/t Au; 10.29 g/t Ag. | Hill (1964)* |
| 46 | Jay | 369700 | 6340500 | Cu, Au, Ag | lTgd | grab: 8.9% Cu, 2.7g/t Au, 24.1g/t Ag | Heinrich *et al.* (1989)* |
| 59 | Horn | 347250 | 6337400 | Cu | uTSv, uTSb, uTSp, lTm Egd | - | |
| 60 | Devils Club | 346000 | 6335500 | Cu,Ag,Au | uTSv, uTSb, TJs | 8.2m chip: 3.57% Cu, 0.69 g/t Au, 96.0 g/t Ag | Northern Miner (Aug 3,1967) |
| 61 | Pereleshin | 336389 | 6324997 | Cu | eJm | - | Kerr (1948a) |
| 69 | OP | 350000 | 6345000 | Cu | lPSc, uTSw, uTSb | - | |
| 100 | Cam | 337150 | 6327300 | Cu | PSu, eJgd, Eg | - | |
| **Au, Ag Base Metal Quartz Veins ■** | | | | | | | |
| 48 | Jack | 344550 | 6337650 | Ag,Pb,Zn,Cu | uTSv, uTSs | grab: 49.4 g/t Ag, 1.0% Pb, 0.21% Zn | Folk (1987)* |
| 52 | Sal | 343000 | 6329000 | Cu | uTSv, uTSs | - | James (1965) |
| 123 | Glacier | 378450 | 6346500 | Cu, Zn, Ag | uTSp | grab: 9 g/t Ag, 0.14% Cu, 0.15% Zn, 0.11% As | Logan et al. (1989)* |
| 126 | JW-6 | 342300 | 6337850 | Au | uTSv | grab: 3.77 g/t Au | Blann and Vulimiri (1990)* |
| 124 | Ridge | 342650 | 6336560 | Cu,Au | uTSv, uTSb, TJs | grab: 67.9 g/t Au, 100.9 g/t Ag, 6.27% Cu | Blann and Vulimiri (1990)* |
| **Ag, Au Base Metal Quartz-Carbonate Veins** | | | | | | | |
| 53 | Trophy, Ptarmigan | 362350 | 6338000 | Ag,Au,Pb,Zn | lPSc, mTs, uTSv, lTm, Egd | drill core: 3.4 m 7.68 g/t Au, 56.2 g/t Ag, 1.27% Zn (TR88-4) | Heinrich et al. (1989)*, Caulfield and Archambault (1990) |
| - | Trek, Toe, East | 359500 | 6332900 | Ag,Au,Pb,Zn | uTSv, uTSp, uTSp, Egd, lTm | grab: 1.23 g/t Au, 267.8 g/t Ag, 5.22 % Cu, 1.06% Zn (Toe) | Awmack and Yamamura (1988)*, Awmack (1991) |
| 51 | CW, Pup | 349000 | 6341000 | Cu,Au | uTSv, uTSp, uTSb | 6.1m chip: 0.03% Cu | Grant (1964)* |
| 88 | CW-EAST | 352600 | 6341500 | Cu | lPSc, uTSv, uTSw, eJgd | grab: 2.57 % Cu, trace Au | Grant (1964)* |
| 66 | Stikine East | 354800 | 6335500 | Cu,Au,Ag | TJs | grab: 0.3 g/t Au, 109 g/t Ag, 8.04% Cu, 0.65% Pb, 3.3%Zn | Logan *et al.* (1989)* |
| **Cu, Au, Ag Skarns Δ** | | | | | | | |
| 50 | Trophy, Hummingbird | 361750 | 6338000 | Cu,Au,Ag | lPSc, mTs, uTSv, lTm, Egd | 1.0 m chip: 1.7 g/t Au, 65.5 g/t Ag, 0.81% Cu | Heinrich *et al.* (1989)*, Caulfield and Archambault (1990) |

* source of reserves or best assay

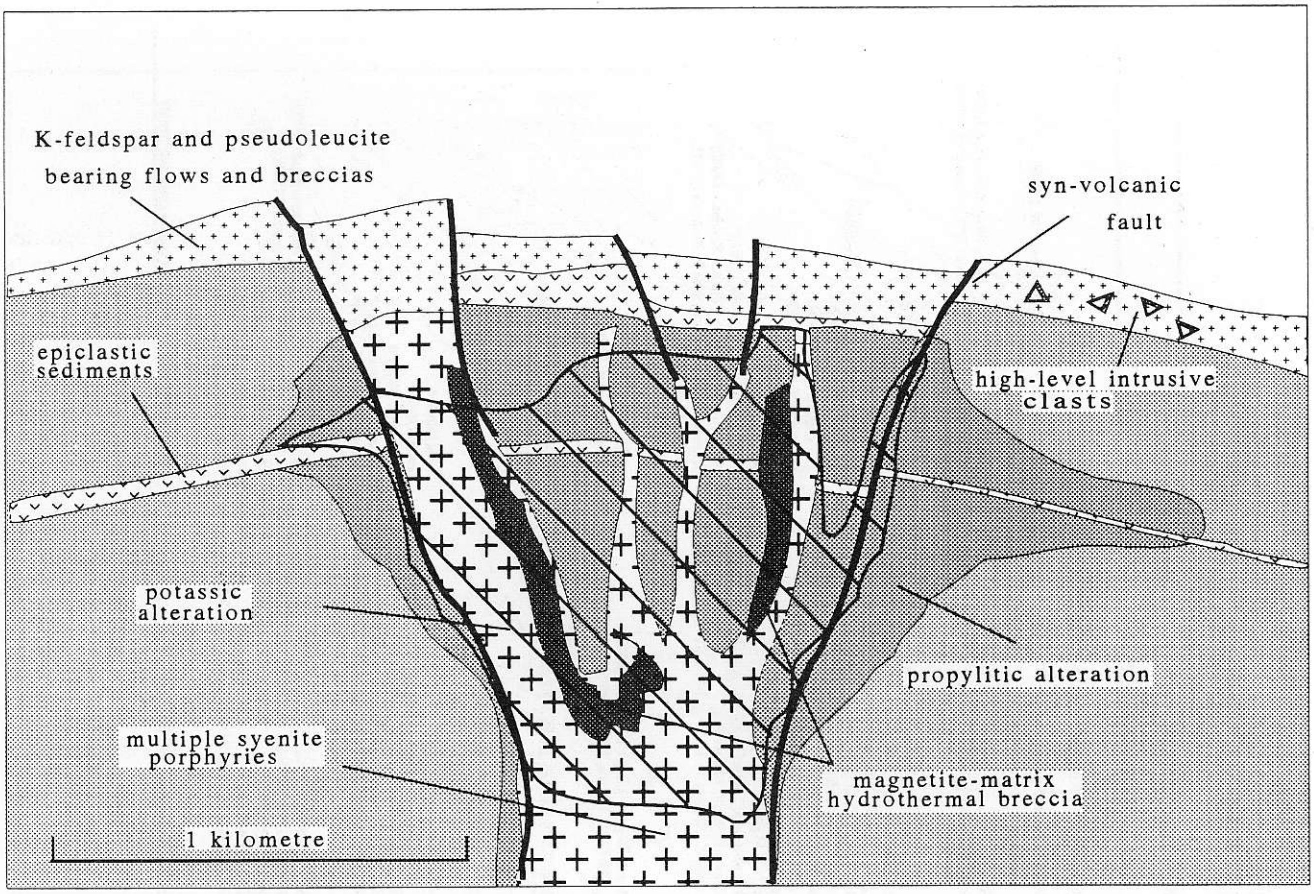


Figure 21. Alkaline porphyry copper-gold deposit model (modified from Sutherland Brown, 1976).

## *GALORE CREEK (MINFILE 104G 090 to 104G 099)*

The Galore Creek deposits are located in the headwaters of Galore Creek in the centre of the map area (Figure 20). The first claims were staked in 1955. In 1963 Kennco Explorations, (Western) Limited (59%), Hudson Bay Mining and Smelting Company Limited (34%) and Consolidated Mining and Smelting Company of Canada, Limited (5%) incorporated their respective interests to form Stikine Copper Limited. Between 1960 and 1969, 53 164 metres of diamond drilling and 807 metres of tunnelling in two adits were completed, with Kennco as operator. During this time, a road was built from the airstrip at the confluence of the Stikine and Scud rivers along the Scud River and up Galore Creek to the camp. An additional 25 352 metres of diamond drilling was completed in 111 holes between 1972 and 1973 under the direction of Hudson Bay Mining and Smelting Company.

In 1987, Mingold (Hudson Bay Exploration) began to assess the potential of copper-gold and gold mineralization outside the Central zone. Existing assay pulps were re-analyzed for gold. In 1989, geochemical soil sampling, a VLF-EM survey, trenching and sampling of the North Rim, Southwest and Saddle zones was completed. Diamond drilling in 1990 outlined good gold grades in the Southwest zone. This zone and others outside the Central zone, such as the Junction and North Junction zones, were the focus of drilling (49 holes, 13 830 metres) in 1991. Recent interest in the property stems from its importance as a regional exploration model and its future development possibilities (reserves are calculated to contain 50 million grams of gold).

## GEOLOGY

Ten porphyry copper-gold deposits are known on the Galore Creek property, the Central and North Junction zones have drill-indicated reserves, the remaining deposits are considerably smaller and less well tested (Figure 22). The deposits are interpreted to be high-level, synvolcanic mantos related to alkaline plutonic rocks that intrude and breach the volcanic edifice (Allen *et al.*, 1976). The Galore Creek Syenite Complex comprises a series of orthoclase-porphyritic syenite intrusions that intrude coeval Upper Triassic Stuhini Group volcanic rocks and related sediments. A threefold subdivision has been established for the Upper Triassic stratigraphy: a lower unit of plagioclase and hornblende-phyric volcaniclastics and flows; a medial package of stratified tuffs, intercalated pyroxene-phyric flows and lesser siltstones; and an upper unit of maroon, subaerial in part, potassium feldspar and pseudoleucite-bearing flows, tuffs and epiclastics. Close to the syenite complex these sedimentary and volcanic rocks are severely folded, sheared, faulted, brecciated and metasomatized. Copper deposits are associated with four distinct intrusive pulses of

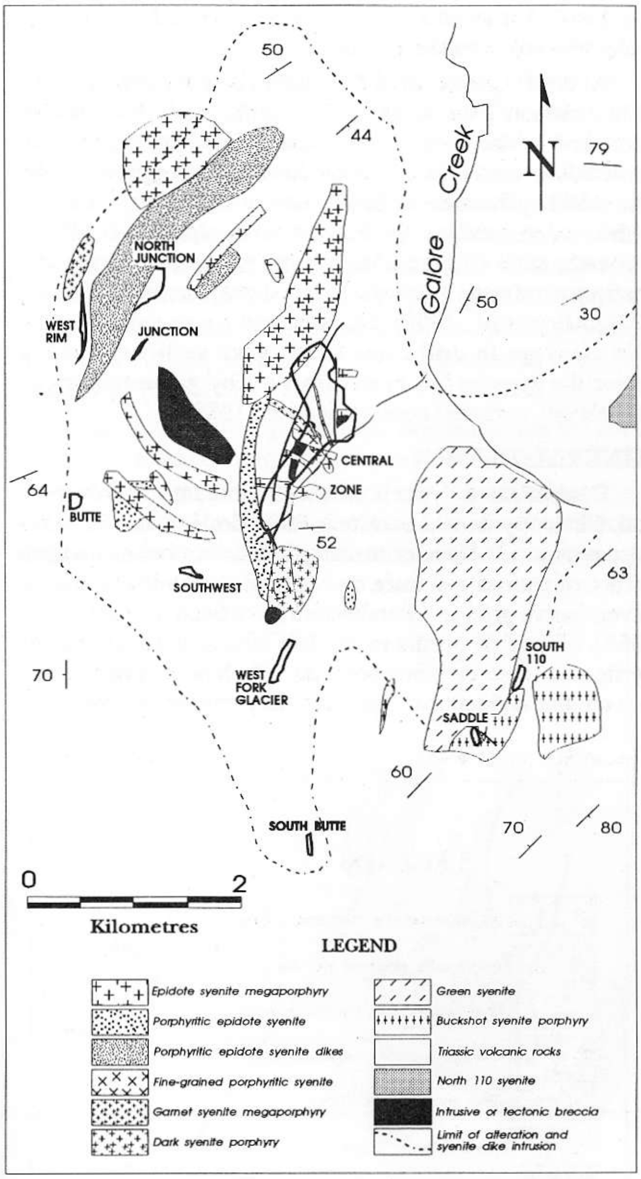


Figure 22. Generalized geology of Galore Creek, showing mineral occurrences and extent of alteration and syenite dike emplacement (after Allen *et al.*, 1976).

syenite: dark syenite porphyry, garnet syenite megaporphyry, fine-grained porphyritic syenite and epidote syenite megaporphyry. The first phase is premineralization, the second intramineralization and the last two phases postmineralization.

The deposits are hosted by potassium-enriched volcanic rocks and pipe-like breccias adjacent to syenite dikes and stocks. They are manto-shaped and trend north to northeast (Figure 22); following syenite contacts and structural breaks (Allen *et al.*, 1976).

## ALTERATION

Alteration and mineralization are contemporaneous and spatially overlap. The hydrothermal system was extensive; resultant alteration led to the formation of large gossans that extend around the west wall of the Galore basin as far north as the North Junction deposit (Figure 22). Malachite and azurite stain the cliffs on the Butte showing.

Alteration has converted the volcanic rocks to skarns and fenitic porphyroids, consequently, original rock types are uncertain. Potassium feldspar, biotite, garnet and anhydrite are ubiquitous and locally replace hostrocks completely. Consistent logging of early drill core was maintained by classifying these rocks as hornfels and describing them in terms of relative proportions of orthoclase, biotite and garnet (Panteleyev, 1973). Mineral zoning (Allen, 1966) is related in part to proximity to syenite bodies and breccia pipes but also reflects hostrock composition.

Prograde and retrograde alteration mineral assemblages characterize the hydrothermal system that was centred on the Central zone. Early, hot, dominantly magmatic fluids caused the potassic alteration. Cooling and collapse of the hydrothermal system downward produced patchy propylitic alteration, and a late-stage more fluid-rich(?), oxidized system overprinted the earlier assemblages with calcsilicate minerals and later anhydrite (Table 5).

Potassic alteration converted syenites and volcanic rocks (some probably orthoclase-rich phonolites) to pink, white and orange rocks composed almost entirely of orthoclase (Allen *et al.*, 1976). Orthoclase also occurs with biotite as vein and fracture fillings. Hydrothermal biotite occurs as fine-grained replacements of volcanic rocks and the early, dark syenite. Coarse euhedral titanium-biotite occupies veins and forms the matrix to breccias, together with magnetite, anhydrite, garnet and chalcopyrite. Preliminary microprobe analyses of Galore Creek biotites suggests that annite contents have remained high during potassium metasomatism (J. Hassanzadeh, personal communication, 1990). This assumes that the 3% $TiO_2$ contained in cores of large secondary biotite books from the north end of the Central zone (drill hole 189A) reflects primary biotite compositions.

The alteration of pyroxene, hornblende and biotite to assemblages of chlorite and calcite characterizes the

TABLE 5
ALTERATION ZONES AND CHARACTERISTIC MINERAL ASSEMBLAGES, CENTRAL ZONE, GALORE CREEK DEPOSIT

| Alteration Type | Mineral Assemblage | Associated Sulphide/Sulphate |
|---|---|---|
| Potassic | K-feldspar + Ti-biotite + magnetite | bornite + chalcopyrite > pyrite |
| Propylitic | chlorite + calcite ± albite ± epidote | pyrite + chalcopyrite |
| Calcsilicate | Ti-andradite + epidote + albite ± diopside | anhydrite |

propylitic zone. These assemblages are best developed in the syenite intrusives. Calcite and siderite veinlets are associated with the margins of the intrusive complex in volcanic rocks.

Epidotization is more widespread in the syenites than in the volcanic rocks (*i.e.*, epidote syenite megaporphyry, porphyritic epidote syenite and green syenite). It occurs as disseminated grains and subhedral aggregates replacing chlorite.

Garnet occurs throughout much of the Central zone, but is absent from other deposits in the area. It replaces up to 50% of metavolcanic rocks and infills breccias near the northern end of the Central zone breccia pipe (Figure 23). Diopside is also restricted to the area northeast of the Central zone, where it occurs as a coarse skarn assemblage together with biotite and garnet. Watson (1969) recognized two types of andradite garnet in the Central zone; euhedral zoned crystals in veins and breccias, and massive to ragged, isotropic aggregates in intrusives and wallrock volcanics. Oscillatory growth zoning, marked by increasing anisotropy from core to edge, is related to the titanium content of the garnets. Titanium oxide contents range from 0.58% in the darkest zones to 0.04% in the lightest, most birefringent zones (Watson, 1969). Unzoned garnets average 0.25% titanium oxide. Anhydrite replaces the garnet.

At depths greater than 150 metres below surface, anhydrite commonly forms up to 10% of the rock. It occurs as veins and replacements, and cements breccias. Nearer the surface, the anhydrite has been converted to gypsum. The line marking the base of the gypsum and the top of the anhydrite zone parallels the current topography and reflects the water table (Figure 23). Volume expansion during hydration produced subhorizontal sheet fractures (Allen, 1971; Allen *et al.*, 1976). These produce a so called poker-chip cleavage in drill cores from upper sections of holes where the gypsum has been dissolved by groundwater (A. Panteleyev, personal communication, 1989).

## MINERALIZATION

Disseminated pyrite is the most abundant sulphide mineral. Chalcopyrite and bornite in the ratio 10:1, are the main copper minerals. Sphalerite and galena are associated within garnet-rich areas and trace amounts of molybdenite, native silver, native gold and tetrahedrite have been noted, (Allen, 1966). Magnetite occurs in veinlets with or without chalcopyrite and often cements breccias. Chalcocite, cuprite, native copper and tenorite are secondary copper minerals.

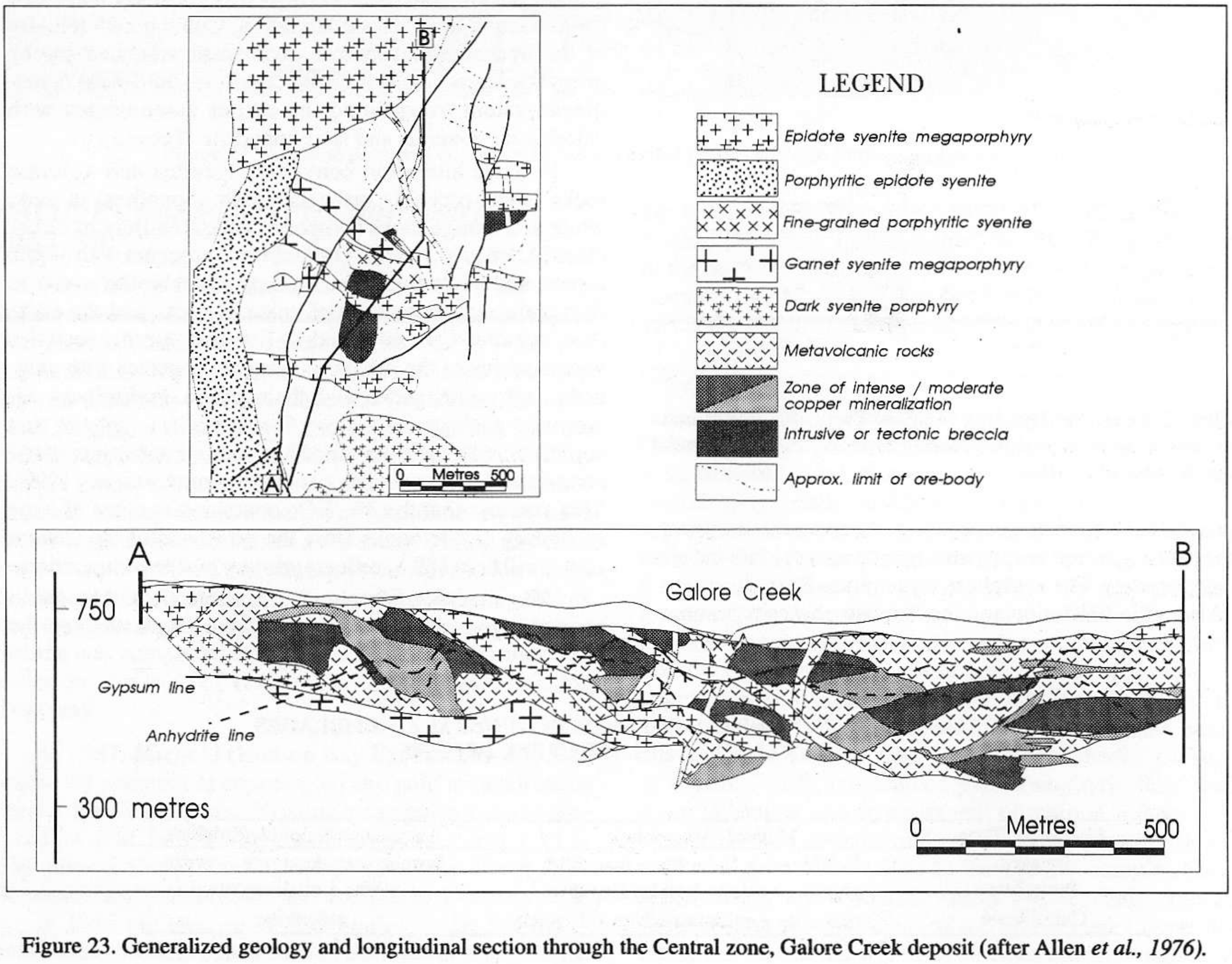


Figure 23. Generalized geology and longitudinal section through the Central zone, Galore Creek deposit (after Allen *et al., 1976).*

Although the metasomatic overprint (calcsilicate mineral assemblage) at Galore Creek is unusual, the distribution of sulphides, precious metals and magnetite (Figure 24) is consistent with the expected zoning pattern for alkalic porphyry deposits (Jones and Leveille, 1989, McMillan, 1991). Bornite and generally higher grade gold occur in the zone of intense potassic alteration in the core; associated minerals are magnetite and sparse pyrite. Peripheral to this, but inside the propylitic zone, chalcopyrite and pyrite mineralization coincides with a moderately developed potassic alteration zone. Replacement lodes of gold, silver and base metals formed in the propylitic alteration zones external to the potassic zone (Table 5).

Panteleyev (1983, p. 124) has suggested that the composition of hostrock might have been a dominant factor controlling redox reactions and ultimately the ore mineralogy. Using the chlorite buffer (controlled by biotite-chlorite-magnetite-pyrite stability relations), he interpreted the observed discrete mineral assemblages pyrite and chalcopyrite, chalcopyrite alone, chalcopyrite and bornite with erratic magnetite and bornite-magnetite-chlorite decreasing sulphur availability.

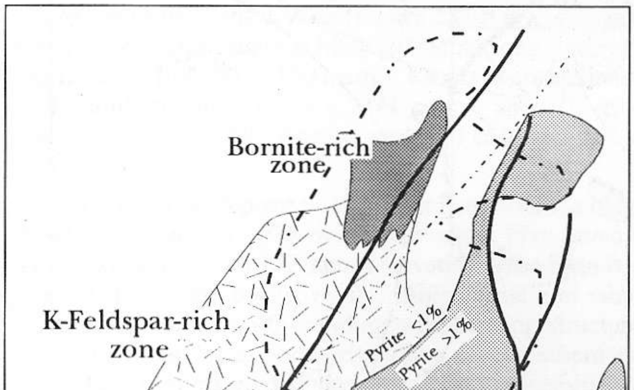


Figure 24. Mineral zonation, 610-metre level plan, Galore Creek deposit (modified from Allen *et al.*, 1976). Solid triangles indicate breccia zones, lines show faults.

Gold is generally associated with higher grades of copper mineralization. There is not always a strong correlation; many areas of high copper lack appreciable gold. However, higher gold grades are associated with bornite in the north and south parts of the Central zone. Re-assayed drill core from four holes located along an east-trending fence at approximately 24+600 N in the Central zone returned values as listed in Table 6. (E.W. Yarrow, personal communication, 1991).These are an order of magnitude greater than the deposit average, which is typically 0.5 gram per tonne gold, and represent attractive exploration targets.

Delta 34S values for sulphides and sulphates in the Central zone are low in comparision with other alkaline and calcalkaline porphyry deposits (Ohmoto and Rye, 1979; J. Hassanzadeh, personal communication, 1990). At Galore Creek, this may mean the oxidation state of the fluids was high or that the sulphides incorporated some sedimentary sulphur (Ohmoto and Rye, 1979). Assuming there was equilibrium between $SO_4^{2-}$ and $H_2S$, a temperature range of 300 to 400°C is indicated by sulphur isotope thermometry on chalcopyritepyrite-anhydrite-gypsum mineral assemblages (J. Hassanzadeh, personal communication, 1990).

## DEPOSITS

The descriptions of the Galore deposits presented here rely heavily on published works by Panteleyev (1973, 1974, 1975, 1976, 1983), Barr (1966) and Allen *et al.* (1967).

The largest deposit is the Central zone. It extends 1950 metres north-northeasterly and varies in width from 200 to 500 metres (Figure 23). The deposit plunges gently to the north and at its maximum thickeness is 335 metres. It is composed of several parallel, en echelon copper zones centred on a steeply dipping breccia pipe. Mineral zoning consists of an intense potassic core zone, which hosts the mineralization, and spotty propylitic alteration zones which occur mainly along the eastern edge of the deposit.

The plan and south to north longitudinal section (Figure 23, from Allen *et al.*, 1976) show the intrusive relationships between the syenites and the outline of the potential orebody. The dark syenite at the south end of the deposit is mineralized and cut by garnet syenite porphyry that is locally mineralized along its margins.

TABLE 6
SELECTED DRILL-CORE ASSAY RESULTS, NORTH CENTRAL ZONE, GALORE CREEK DEPOSIT

| Hole | Intercept (m) | Au (g/t) | Cu (%) |
|---|---|---|---|
| DDH189 | 48.75 | 3.48 | 1.20 |
| DDH137 | 85.34 | 2.77 | 1.19 |
| DDH120 | 176.78 | 3.48 | 1.77 |
| DDH200 | 39.62 | 1.90 | 1.00 |

(E.W. Yarrow, personal communication, 1991)

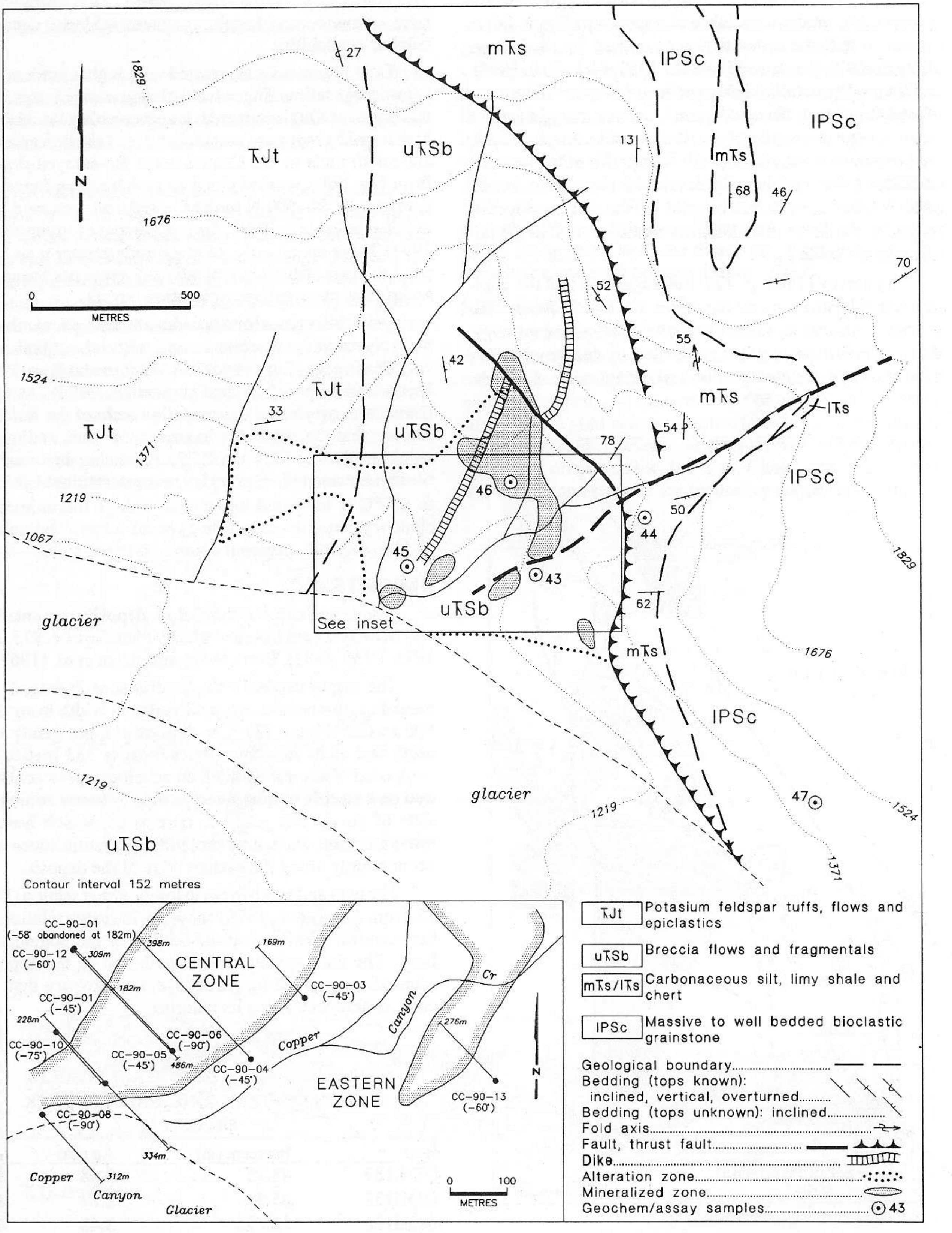


Figure 25. Geological sketch map of the Copper Canyon area; inset shows location of 1990 diamond-drill holes and mineralized zones (after Consolidated Rhodes Resources Ltd. news release, 1990).

On longitudinal section A-B, the breccia pipe is located south of the creek. It is cut by flat-lying dikes of garnet and epidote syenite megaporphyry. The breccia is composed mainly of metavolcanic rocks but also contains fragments of dark syenite. Coarse euhedral garnet, biotite, unhydrite, pyrite and chalcopyrite comprise the matrix. Garnet abundance decreases outwards from the breccia pipe, suggesting that it was the main conduit for hydrothermal fluids (Allen *et al.*, 1976). Magnetite breccias occur south of the Central zone and at the Saddle zone, but to date, the garnet-rich matrix in the Central zone breccia pipe is unique.

The Central zone has sharp assay boundaries, changing from 0.3% copper to background over very short distances. Reserves are estimated at 125 million tonnes grading 1.06% copper, 0.40 gram per tonne gold and 7.7 grams per tonne silver (Allen *et al.*, 1976). Oxide mineralization (chiefly malachite and azurite) is restricted to the southern half of the deposit where it reaches depths of 15 to 30 metres (Barr, 1966).

The North Junction deposit lies about 2 kilometres northwest of the Central zone (Figure 22). It is a northeast-trending irregular manto, at least 370 metres long, and varying in width from 50 to 150 metres. Reserves are estimated at 4.8 million tonnes grading 2.0% copper and 0.75 gram per tonne gold (E.W. Yarrow, personal communication, 1991).

The Junction deposit is 350 metres south of the North Junction deposit, at 1075 metres elevation. Five hundred metres to the east, at 1275 metres elevation is the West Rim deposit. In both deposits, pyrite, chalcopyrite and minor bornite mineralize north-trending west-dipping structures parallel to contacts of porphyritic dikes. The southern end of the Junction deposit contains supergene copper minerals, including native copper, cuprite, covellite, chalcocite and malachite.

The Butte deposit crops out on the west edge of the syenite complex, 2 kilometres west of the Central zone. It is localized along a west-dipping faulted contact between altered volcanic rocks and syenite intrusions.

The Southwest deposit crops out 750 metres southwest of the south end of the Central zone in altered, brecciated syenite porphyry. The main zone of mineralization strikes east to southeast and dips steeply south. Sulphides and magnetite occur as disseminations, fracture fillings and replacements.

The West Fork Glacier deposit lies below the West Fork glacier, 1250 metres south of the Central zone. Drilling suggests it strikes northeasterly and dips steeply, in an area of complex, multiple syenite intrusions and breccias. Mineralization includes disseminated and massive replacements of the intrusive rocks.

The South Butte deposit crops out on a nunatak in the West Fork Glacier, 4000 metres south of the Central zone. North-trending dikes and mineralized shear zones cut the altered host volcanics, but most of the chalcopyrite and pyrite mineralization is fracture controlled.

The Saddle deposit crops out on a steep slope 3 kilometres southeast of the Central zone. It trends easterly and dips northerly at 50°, along the contact between buckshot syenite and green syenite porphyry (Figure 22). Primary mineralization is contained within a magnetite-cemented breccia body; secondary copper minerals extend beyond the breccia. The breccia contains angular fragments of buckshot syenite and green syenite porphyry and metavolcanic rocks. Graded beds and flow textures suggest that some of the green syenite represents potassium-metasomatized volcanic extrusives rather than intrusives.

The South 110 Creek deposit is exposed between 1220 and 1300 metres elevation on the west slope of 110 Creek, some 500 metres north of the Saddle deposit. Disseminated mineralization trends north, along the fractured contact between buckshot syenite, green syenite porphyry and metavolcanic rocks. Magnetite and sulphides are intimately associated as at the Saddle deposit (Figure 22).

Most deposits have an average trend of 020°, parallel to the contacts of dikes and sills, northerly trending fold axes and normal faults. The easterly strike of the Southwest and the Saddle deposits are at variance with the general northeasterly strikes of the other eight deposits.

In summary, a Late Triassic volcanic centre is preserved at Galore Creek. Sulphide deposition within it was related to a dynamic system of synvolcanic faults, syenite intrusions, explosive breccias and comagmatic extrusive volcanics. Because dikes, sills and explosive breccias dominate, together with pseudoleucite-bearing intrusives, this is envisioned to have taken place in a high-level setting, possibly within the throat of a volcano. Intense potassium metasomatism and copper-gold mineralization is synvolcanic and latest Triassic in age.

## *COPPER CANYON (104G-017)*

The Copper Canyon showing is located approximately 8 kilometres due east of the Galore Creek deposit (Figure 25). It was tested by seven diamond-drill holes (1010 metres) drilled in 1957 by the American Metal Company Limited. At that time, geological reserves of 27 million tonnes with an average grade of 0.72% copper and 0.43 gram per tonne gold were inferred (Spencer and Dobell, 1958). In 1990, Consolidated Rhodes Resources Ltd. conducted contour-line soil geochemistry, mapping and 3784 metres of diamond drilling in thirteen holes. Copper mineralization is associated with a syenite porphyry and a hydrothermal system that is similiar to, but smaller than that at Galore Creek.

The deposit is hosted by Late Triassic to Early Jurassic alkaline flows, tuffs, epiclastics and syenite intrusives. To the east, Middle Triassic sediments and Lower Permian limestones are thrust westward over these volcanics at the head of Copper Canyon Creek. Two northwesterly trending dikes of syenite porphyry crop out in the lower part of the creek. The porphyry is similiar to the dark syenite porphyry at Galore Creek. It contains potassium feldspar megacrysts up to 4 centimetres in length, abundant biotite and disseminated pyrite. Pseudoleucite phenocrysts form 10% of the syenite along Doghouse Creek. An intrusive breccia phase or brecciated intrusive is developed locally.

Oxidization of pyrite and bleached halos have produced an extensive gossan around the intrusions. Potassic altera-

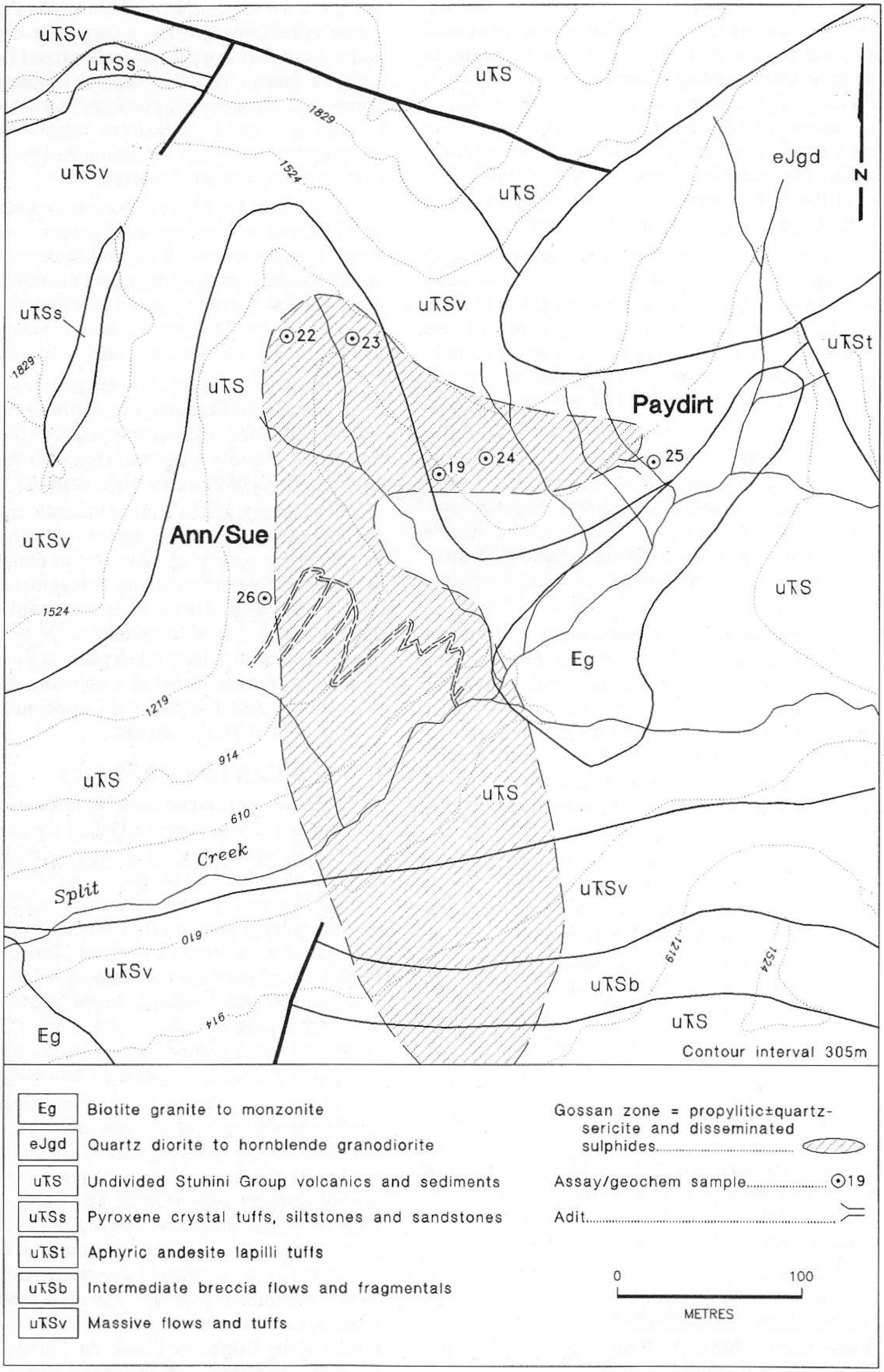


Figure 26. Geological sketch map of the Split Creek area, showing the locations of Ann/Sue and Paydirt prospects.

tion is widespread and pervasive. Abundant potassium feldspar, biotite, garnet and magnetite are developed. Gypsum has been reported (Jeffrey, 1966). Malachite and azurite stain cliffs in the canyon.

Three zones of copper mineralization have been identified; the North, Central (Western Copper) and Eastern (news release, Consolodated Rhodes Resources Ltd., Dec. 20, 1990). The Central zone was tested along 450 metres of strike length by the 1990 drilling. Copper mineralization occurs as disseminations of chalcopyrite and trace amounts of bornite. Gold and silver values accompany the sulphides. Associated minerals include pyrite, magnetite, specularite, hematite, molybdenite and fluorite.

Assay and geochemical values of samples from the Copper Canyon deposit and surrounding area are shown in Table 7. Elevated gold values coincide with higher copper grades, althongh surface weathering and leaching of these mineralized and pervasively altered rocks may have enhanced gold relative to copper.

A K-Ar date (White *et al.*, 1968; recalculated to new decay constants) on alteration biotite yielded an apparent age of 179.5±18 Ma. This gives an Early Jurassic apparent age of mineralization and possible emplacement for the stock (Table 2). An Ar-Ar date from biotite crystal lithic tuff above Copper Canyon and distal from the pervasive potassium alteration has a plateau age of 212 Ma. This unit is believed to be the eruptive equivalent of one of the syenites and better constrains the age of the alkaline magmatism and related mineralizing system.

### *ANN/SUE (104G-23), PAYDIRT (104G-108)*

The Ann/Sue and Paydirt showings are located north of Split Creek, a tributary of the Porcupine River (Figure 26). The Ann/Sue showing is hosted by fine-grained, sparsely porphyritic andesite, diorite and granodiorite. The diorite is a biotite hornblende seriate-textured hypabyssal intrusion. It intrudes fine to medium-grained andesitic tuffs and altered greenstones of such similiar appearance that distinguishing intrusive from extrusive is difficult. A rusty weathering fine-grained homogeneous hornblende biotite granodiorite of Eocene age cuts the volcanic and subvolcanic strata. Propylitic alteration has extensively modified both the intrusive rocks and the host volcanics. Relict hornblende and plagioclase phenocrysts are replaced hy chiorite; the matrix by fine-grained chlorite, calcite and epidote. Strong chlorite and sericite alteration accompany disseminated pyrite and lesser chalcopyrite mineralization. Disseminated pyrite is ubiquitous and chalcopyrite is sparsely distributed. Diamond-drill intersections returned assays between trace and 0.32% copper, with average values between 0.10% and 0.20% copper (Jeffery, 1966).

The Paydirt prospect is located on a large malachite-stained pyritic gossan 2 kilometres northeast of the Ann/Sue showing. It was recognized by Teck Corporation during an early 1980s regional reconnaisance for gold throughout the area. Drill indicated reserves are 185 000 tonnes averaging 4.11 grams per tonne gold (Holtby, 1985). Longreach Resources Ltd. began an exploratory adit to intersect the mineralized zone in 1987 but stopped short of the projected target.

The prospect is hosted by a section of massive andesitic tuffs, flows and crystal-lapilli tuffs with subordinate sediments. Eocene monzonite to granodiorite crops out in Split Creek and up-slope from the main showing. The main gold zone on Discovery Creek is a silicified, sericitic and pyritic altered zone in Upper Triassic andesitic tuffs. It strikes north and dips steeply to the east; its surface strike length is less than 100 metres and its maximum thickness 25 metres. An unaltered andesite dike follows the footwall of the mineralized zone. Gold mineralization is best developed in intensely silicified and pyritized zones rather than in sericitic zones.

Table 8 presents the analyses determined in this study for the samples located on Figure 26. Samples from two quartz-carbonate veins and two argillic alteration zones in volcanic rocks all returned low base and precious metal values, however a grab sample from the quartz-sericite alteration zone on the Paydirt prospect returned 15.4 grams per tonne gold.

Panteleyev (1975) reported a K-Ar date of 48.5±1.7 Ma from biotites associated with pyrite mineralization on the Ann/Sue showing (Table 2). A K-Ar age on biotite from granodiorite exposed above the main Paydirt showing gave 48.2±1.7 Ma (Table 2). However, the copper-gold mineralization of these showings is atypical of Eocene mineralization. The biotite hornfels dated by Panteleyev may represent a younger metamorphic aureole overprinting older mineralization. On the other hand, the identical ages of samples from the Ann/Sue and Paydirt showings argue against partial resetting of older dates. Despite this, in our view, the

TABLE 7
SELECTED GEOCHEMICAL ANALYSES AND ASSAYS
FROM THE COPPER CANYON DEPOSIT

| Map No. | Grab Sample Description | Au (ppb) | Ag (ppm) | Cu (ppm) | Pb (ppm) | Zn (ppm) | As (ppm) | Sb (ppm) |
|---|---|---|---|---|---|---|---|---|
| 43 | Oxidized syenite, 1-3 % pyrite | 41 | <0.5 | 227 | 13 | 71 | 72 | 1 |
| 44 | Cu Canyon syenite, 2 % py & cpy | 139 | <0.5 | 0.27% | 16 | 51 | 17 | 1 |
| 45 | Altered syenite, 3-5 % py | 861 | 10 | 3.32% | 18 | 790 | 21 | 2 |
| 45 | Oxidized syenite, 5 % cpy & py | 1820 | 16 | 6.97% | 39 | 93 | 140 | 4 |
| 46 | K-altered volcanic, 3-5 % cpy & py | 1880 | 8 | 2.33% | 28 | 57 | 44 | <0.5 |
| 46 | K-metamorphism, 2-5% py | 25 | <0.5 | 32 | 77 | 48 | 45 | 2 |
| 47 | Hematized fault zone in limestone | 1 | 1 | 5 | 33 | 148 | - | 2 |

TABLE 8
SELECTED GEOCHEMICAL ANALYSES AND ASSAYS FROM THE ANN/SUE AND PAYDIRT SHOWINGS

| Map No. | Grab Sample Description | Au (ppb) | Ag (ppm) | Cu (ppm) | Pb (ppm) | Zn (ppm) | As (ppm) | Sb (ppm) |
|---|---|---|---|---|---|---|---|---|
| 19 | Qtz vein, pyrite to 5 % | 590 | 1 | 76 | 13 | 28 | 13 | 2 |
| 22 | Qtz-chlorite vein 3 % pyrite | 20 | 0.7 | 880 | 8 | 62 | 17 | <0.5 |
| 23 | Qtz carbonate vein, trace pyrite | 21 | <0.5 | 175 | 21 | 71 | 5 | <0.5 |
| 24 | Silicic-pyritic fault zone | 49 | 1 | 53 | 11 | 14 | 4 | <0.5 |
| 25 | Oxidized argillic altered zone | 20 | 2 | 135 | 18 | 18 | 6 | 1 |
| 25 | Sericitic altered volcanic 3 % pyrit | 15410 | 2 | 232 | 11 | 31 | 11 | <0.5 |
| 25 | Massive pyrite, grab from portal | 750 | 7 | 0.88% | 35 | 45 | 124 | 4 |
| 26 | Oxidized pyritic andesite | 29 | <0.5 | 67 | 13 | 54 | 13 | 1 |

mineralization is older. It is comparable with the gold-silver-copper mineralization of typical Triassic-Jurassic age.

## *JW (104G 021); RIDGE (104G 124); SADDLE MOUNTAIN (104G 125); JW6 (104G 126)*

The JW claims are located on the north tributary of Jack Wilson Creek and extend south to Saddle Ridge (Figure 27). In the early 1960s, Kennco Explorations, (Western) Limited discovered a narrow quartz-pyrite vein containing 102.6 grams per tonne gold, in the north tributary of Jack Wilson Creek, while following up regional stream sediment geochemical anomolies. It explored the area between 1963 and 1965 and conducted geological mapping, soil geochemistry, trenching and an induced polarization survey. Southwest and above Jack Wilson Creek on Saddle Ridge, trenching and drilling (212 metres) in 1966 and 1967 by Anuk River Mines Ltd. returned mixed results which were not followed up.

In 1988, Bellex Mining Corporation optioned the JW claims and began an exploration program consisting of line cutting, prospecting, geological mapping, and stream and soil geochemical sampling. The 1988 work delineated a large copper-gold soil anamoly; the 1989 program tested the Central zone (1960 discovery zone) with trenches and sampling. Exploration in 1990 included line cutting, soil sampling, trenching, induced polarization, VLF-EM and magnetometer surveys, geological mapping and sampling. The program culminated with 1392 metres of diamond drilling.

The claims are underlain by a fine-grained, green, massive subvolcanic diorite which intrudes Upper Triassic amygdaloidal volcanics of andesitic to basaltic composition. The diorite is strongly magnetic and carries widespread pyrite as disseminations and fracture fillings. Sulphide mineralization follows prominent northerly trending chloritic shear zones and vein systems marked by well developed gossan zones.

A 2.5 square kilometre, north-trending propylitic alteration zone is centred on the north fork tributary of Jack Wilson Creek. Two north-trending zones of disseminated pyrite surround the central propylitic zone. A north-north-west-trending magnetite zone occupies the eastern half of the alteration zone. Drilling has located zones of quartz-anhydrite-potassium feldspar alteration beneath the propylitic zone. The alteration is consistent with the upper level of a synvolcanic porphyry copper-gold system.

The Central, Boundary and Clag Creek mineralized zones (Figure 27) coincide with north to north-northeast trending areas of intensely sheared and altered volcanic and subvolcanic rocks. The 1990 drilling on the Central zone intersected a chalcopyrite-pyrite-pyrrhotite quartz vein (hole 90JW-1) within a zone of quartz and potassium feldspar alteration. The width of the vein is unknown. It was intersected between 210 and 270 metres in hole 90JW-1, but it has been suggested that the vein was drilled down dip. Step-out drilling to the south (hole 90JW-2) and north (hole 90JW-3) also intersected the vein but here it is less than a metre wide. A mineralized magnetite breccia was intersected in hole 90JW-3 (17 metres averaging 0.17% copper and 0.37 gram per tonne gold). Drilling indicates that the copper-gold mineralization is localized in a series of lenticular zones with long axes trending northerly and widths which rarely exceed 30 to 50 metres (Blann and Vulimiri, 1990).

A strong quartz-sericite-pyrite alteration zone, easily visible from the air, extends down the north-facing flank of Saddle Ridge to Jack Wilson Creek. Discontinuous mineralized shears and narrow sigmoidal chalcopyrite-pyrite-quartz veins containing 100 plus grams per tonne gold and high copper values are exposed at upper elevations of the Saddle Ridge area (Blann and Vulimiri, 1990). The Spire zone (Figure 27) is an east-trending zone of propylitic alteration and disseminated chalcopyrite cropping out at 1065 to 1370 metres elevation on Saddle Horn Ridge. In the creek valley, gold values are associated with sericitized, pyritized and silicified zones in andesites.

Lithogeochemical sampling sites in altered and mineralized zones north and south of Jack Wilson Creek are located on Figure 27, results are tabulated in Table 9. A sample from the north tributary of Jack Wilson Creek returned anomalous gold and copper values. It coincides with the Central zone of Blann and Vulimiri (1990). Other samples from gossans and narrow quartz veins south of Jack Wilson

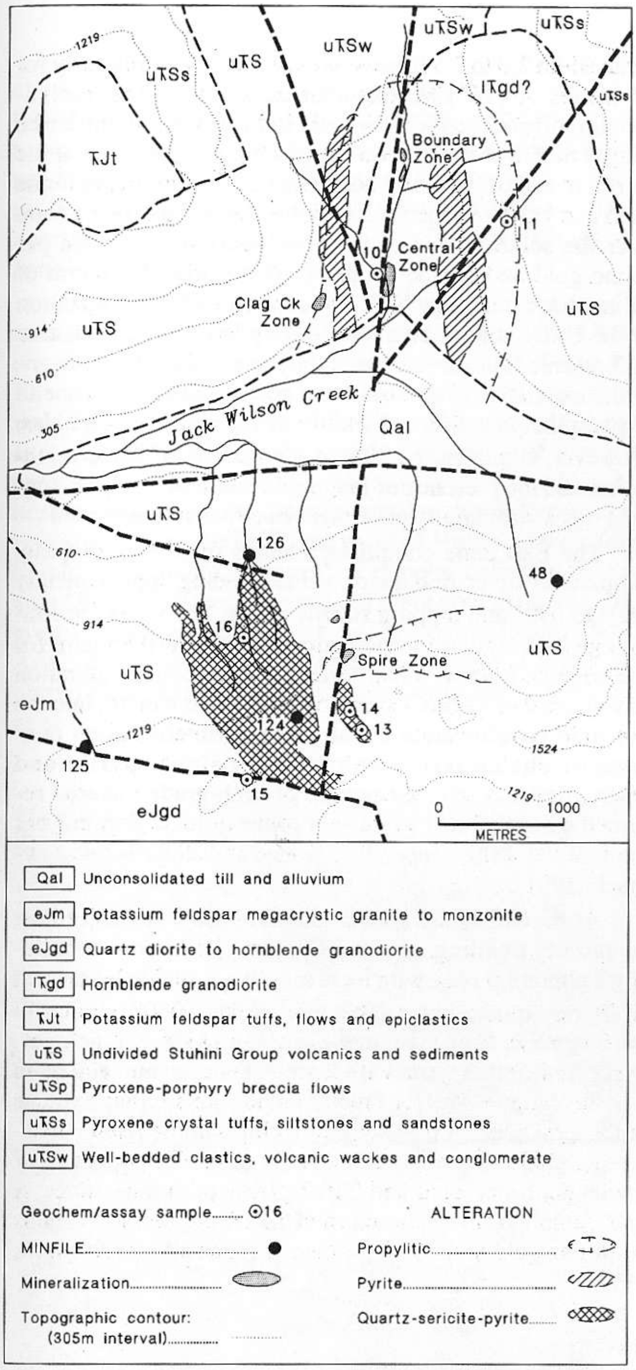


Figure 27. Geological sketch map of the Jack Wilson Creek area, showing the distribution of mineralization and alteration zones and the locations of the JW, Ridge, Saddle Mountain and JW6 occurrences.

Creek on the Ridge, Saddle Mountain and JW6 showings all returned low base and precious metal values.

## *SPHAL 17 and SPHAL 27 (104G 022, 104G 029)*

The Sphal 17 and Sphal 27 showings are located approximately 10 kilometres southeast of the Galore Creek deposit on the north and south sides of Sphaler Creek, respectively (Figure 28). Kennco Explorations, (Western) Limited first explored the property for its porphyry copper potential in 1955. Geological mapping, trenching and stream sediment geochemistry identified six mineralized zones, all associated with monzonitic intrusions (Rayner and Ney, 1964). Diamond drilling totalling 488 metres in seven holes was completed in 1970. No results are available. Consolidated Silver Standard Mines Limited acquired the ground thereafter. Exploration by Teck Corporation in 1980 and 1981 outlined a strong gold geochemical anomaly in soils and associated with northeast-trending faults. In 1988, Equity Engineering Ltd. completed geological mapping, prospecting, geochemistry and geophysical surveys. Follow up in 1989 and 1990 included trenching and detailed mapping, in anticipation of diamond drilling, but the program was discontinued.

The area is underlain by Upper Triassic Stuhini Group pyroxene porphyry flows, andesitic breccias and crystal tuffs. These are intruded by subvolcanic, comagmatic pyroxene-porphyritic diorite plugs and dikes. Volcanic conglomerate, wacke and siltstone crop out west and east of Trek Creek (Figure 28). Prominant north-northeast-trending faults have localized intrusions of Eocene monzonite and felsite, and associated mineralization. Sulphides comprise massive to disseminated pyrite and pyrrhotite, chalcopyrite, galena and sphalerite, with lesser magnetite and precious metals, in sheared and propylitically altered fracture zones in north and northeast-trending fault structures.

Sites of geochemical sampling of alteration and mineralized zones are shown on Figure 28. Analyses returned generally low values (Table 10). Sampling near the Heel and Toe zones (Trek claims) yielded slightly elevated base metal values and sporadic high gold and silver values. This area coincides with a major northeast-trending fault and an Eocene felsic intrusion.

Equity Engineering outlined the Gully, Heel, Toe, and East mineralized zones during its 1988 work (Figure 28). The Gully zone is a steep-dipping body of massive pyrrhotite and chalcopyrite with lesser pyrite and magnetite, striking 030° (Awmack and Yamamura, 1988). The zone

TABLE 9
SELECTED GEOCHEMICAL ANALYSES AND ASSAYS
FROM THE JACK WILSON PROPERTY

| Map No. | Sample Description | Au (ppb) | Ag (ppm) | Cu (ppm) | Pb (ppm) | Zn (ppm) | As (ppm) | Sb (ppm) |
|---|---|---|---|---|---|---|---|---|
| 10 | Andesite, 2 % diss. py & cpy | 1260 | 7 | 1.72% | 10 | 44 | 9 | <0.5 |
| 11 | Oxidized monzonite, 5 % diss. py | 9 | 0.7 | 500 | 10 | 30 | 16 | <0.5 |
| 13 | Oxidized qtz carbonate breccia | 1 | <0.5 | 10 | 11 | 136 | 5 | <0.5 |
| 14 | Oxidized andesite, 1 % pyrite | 10 | 1 | 35 | 15 | 156 | 9 | 1 |
| 14 | Oxidized pyritic andesite | 8 | <0.5 | 46 | 14 | 148 | 4 | 0.8 |
| 15 | Qtz vein, diss. pyrite in fractures | 1 | <0.5 | 99 | 5 | 7 | 1 | 0.6 |
| 16 | Oxidized pyritic volcanic | 1 | <0.5 | 28 | 14 | 46 | | 0.8 |

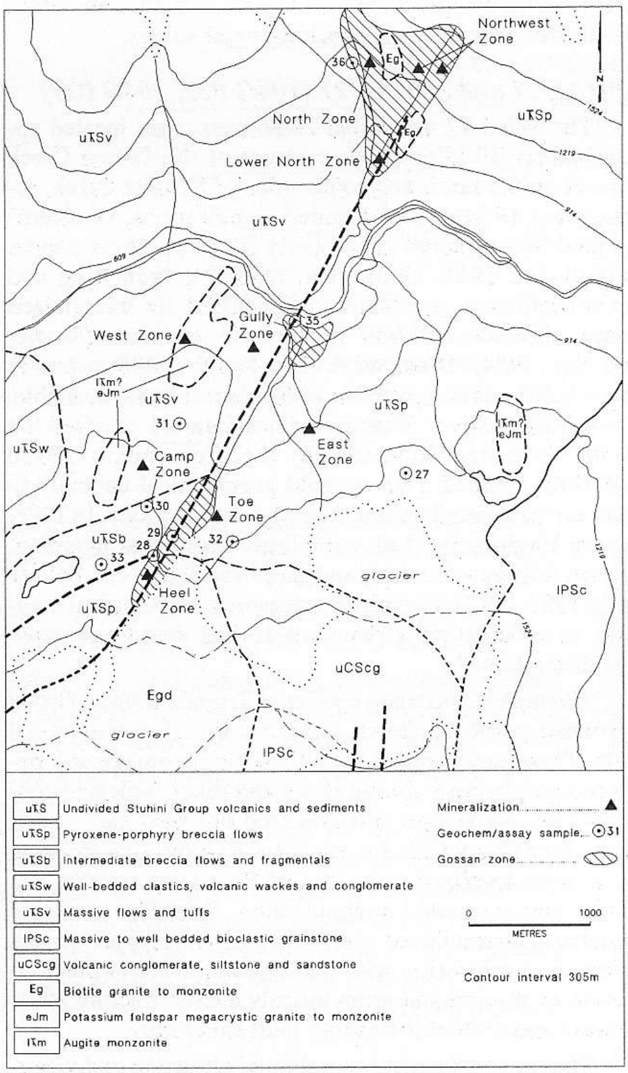


Figure 28. Geological sketch map of the Sphaler Creek area, showing the distribution of mineral showings at the Sphal 17 and Sphal 27 prospects and surrounding Trek claims.

(true width 2.0 to 2.5 metres) is exposed discontinuously for 55 metres. A VLF-EM conductor and a gold-copper-molybdenum soil geochemical anomaly indicate a minimum strike length of 375 metres. A 1.3-metre chip sample taken at the northern end of the Gully zone assayed 0.33 gram per tonne gold and 1.04% copper. A 3.6-metre chip sample taken from near the southern end of the zone assayed 8.77 gram per tonne gold and 5.31% copper (this included 1.0 metre of mineralized hangingwall). The copper-gold mineralization at the Gully zone is characterized by low silver, lead, zinc and arsenic, but elevated molybdenum values. A volcanogenic exhalative origin has been postulated for the zone to explain the presence and texture of the massive sulphides. However, alignment parallel to the main 030° shear orientation and the presence of magnetite and molybdenum suggest it is a structurally controlled massive sulphide vein .

The East zone comprises a series of steeply dipping, subparallel silver-rich quartz veins trending approximately 060° to 090° and dipping steeply north. The veins are continuous and regular in orientation and width (0.8 metre for the widest). Intense silica, sericite and carbonate alteration envelopes these veins, extending as much as a metre into the volcanic conglomerate country rock. Mineralization consists of chalcopyrite, sphalerite, galena, pyrite and arsenopyrite. A selected sample of high-grade material returned assays of 1.51 grams per tonne gold, 809 grams per tonne silver, 1.0% copper, 9.15% lead and 20.50% zinc (Awmack, 1991).

At the Toe zone, gossanous hornfelsed volcanics host an easterly trending, structurally controlled pyrite-sericite-silica alteration zone with local massive sulphide lenses and silver-rich quartz veins. The zone strikes 060°, similar to the East zone. Both contain the same sulphide assemblages: pyrite and chalcopyrite with lesser sphalerite and galena in a barite gangue. Precious metal values are similiar to those in the East zone. A 67-centimetre chip sample from a massive sulphide lens returned an assay of 4.76% copper, 1.17 grams per tonne gold and 246.2 grams per tonne silver. A grab sample from a vein returned 5.22% copper, 1.23 grams per tonne gold and 267.8 grams per tonne silver (Awmack, 1991).

TABLE 10
SELECTED GEOCHEMICAL ANALYSES AND ASSAYS FROM THE TREK AND SPHAL PROPERTIES

| Map No. | Grab Sample Description | Au (ppb) | Ag (ppm) | Cu (ppm) | Pb (ppm) | Zn (ppm) | As (ppm) | Sb (ppm) |
|---|---|---|---|---|---|---|---|---|
| 28 | Pyritic altered intrusive | 109 | 2 | 750 | 42 | 49 | - | 0.8 |
| 29 | Andesite, 1-2% pyrite along fractur | 51 | 2 | 0.11% | 13 | 77 | - | 0.7 |
| 30 | Altered andesite, 3% pyrite | 49 | 2 | 460 | 36 | 70 | - | 3 |
| 31 | Hornfelsed volcanic, 5% py and po | 18 | 1 | 540 | 14 | 26 | - | 3 |
| 32 | Altered andesite, 1-2% diss pyrite | 12 | <0.5 | 170 | 30 | 450 | - | 25 |
| 32 | Pyritic fault zone | 6 | 125 | 450 | 0.65% | 112 | - | 5 |
| 33 | Oxidized shear zone, trace malachit | 3 | <0.5 | 182 | 14 | 75 | - | 0.9 |
| 35 | Limonitic, pyritized andesite | 29 | 0.8 | 74 | 43 | 102 | - | 2 |
| 36 | Oxidized qtz-carb vein | 4 | <0.5 | 46 | 6 | 77 | - | 2 |
| 36 | Oxidized qtz-carb vein | 48 | 0.8 | 30 | 10 | 36 | - | 0.9 |
| 36 | Oxidized pyritic andesite | 7 | 7.5 | 82 | 10 | 83 | 3 | 2 |

At the Heel zone, porphyry-style disseminated pyrite and chalcopyrite occur in metavolcanics and biotite hornfelsed subvolcanic diorite. A number of grab samples returned an assay of 7.61 grams per tonne gold, 117.2 grams per tonne silver and 1.12% copper (Awmack and Yamamura, 1988). Characteristically narrow, gold and silver-bearing quartz-chalcopyrite-pyrite fracture fillings are peripheral to the porphyry mineralization.

North of Sphaler Creek, on the Sphal 17 prospect, disseminated copper mineralization occurs in altered and brecciated zones in volcanics and felsite intrusives (Plate 19). Three mineralized zones have been described; the North zone, the Northeast zone and the Lower North zone (Rayner and Ney, 1964). The main showing is a zone of intrusive breccia measuring 50 by 18 metres at surface. Faulting has broken the breccia into discontinuous sections. Pyrite, chalcopyrite and magnetite fill the matrix between breccia fragments. "Arithmetic averages" of samples collected over an area 18 by 20 metres assayed 0.24 gram gold per tonne, 10.6 grams silver per tonne and 2.45% copper (Folk, 1981). Analyses of samples from quartz-carbonate veins and propylitized, pyritic volcanic rocks peripheral to the North zone are shown in Table 10.

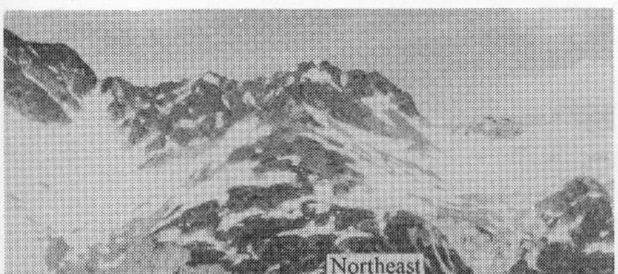


Plate 19. Mineralized cliffs on the North zone of the Sphal 17, viewed northeast across Sphaler Creek from the Trek claims. Also shown are Northeast and Lower North zones.

## BRECCIAS

Hydrothermal breccias are associated with high-level intrusive-related diatremes. Similiar tourmaline and magnetite breccias are associated with porphyry copper deposits in Chile, southern U.S.A. and elsewhere in British Columbia.

The Trophy property covers a large area, centred on the South Scud River. It extends west as far as Galore Creek and an equal distance to the east. The property was originally staked and explored in the early 1960s by the BIK Syndicate (Silver Standard Mines Limited, McIntyre Porcupine Mines Limited, Kerr Addison Mines Ltd.) following discovery of the large porphyry copper-gold deposit at Galore Creek in 1955 by Hudson Bay Mining and Smelting Company. United Minerals Services Limited restaked the Trophy claims in 1987 and later transferred them to Continental Gold Corporation, which initiated an extensive exploration program of geological mapping (1:10 000 regional program; 1:2500 Trophy claims), sampling and drilling (2834 metres in 16 holes) during the 1988 field season. During 1989, Gigi Resources Ltd. (now Rocket Resources Ltd.) carried out geological mapping, prospecting and sampling (stream sediment, contour soil and rock chip). Exploration in 1990 comprised ground follow-up of a 1989-1990 airborne geophysical survey and diamond drilling at the Ptarmigan (1055 metres in six holes) and the N110 grid (830 metres in four holes).

The Ptarmigan zone is a roughly elliptical, heterolithic breccia measuring 400 by 200 metres (Koyanagi *et al.*, 1989; Figure 29). It crosscuts a structurally complicated succession comprising from west to east: Permian limestones, paraconformably overlain by Middle Triassic cherty siltstones and shale, in turn overlain by pervasively altered, massive andesite flows and flow breccia of the Stuhini Group. These are infolded along southeasterly plunging axes and overturned to the east. The layered rocks are faulted against monzonite to monzodiorite of the Hickman batholith along a northwest-trending, southwest-dipping fault. The breccia is centred on this fault, possibly at the intersection of subordinate northeasterly trending faults.

The heterolithic breccia weathers bright yellow and orange, and typically contains angular fragments of Upper Triassic augite porphyry, Late Triassic monzodiorite and monzodiorite breccia, Middle Triassic chert and Late Triassic feldspar porphyry. The breccia matrix is replaced by iron carbonate, chalcedonic quartz and calcite with disseminated sulphides. A monolithic shatter breccia consisting of large angular fragments of the Hickman monzodiorite crops out at the southeast end of the heterolithic breccia. Brecciated and weakly altered intermediate volcanics flank the heterolithic breccia on its northwest side.

The Ptarmigan zone occupies a north-facing cirque and is easily visible from the air as a yellow-orange rusty alteration zone. The intense alteration is structurally controlled along a 140° trend which cuts brecciated monzonite at its southeastern extension. Alteration is characterized by intense sericitization, and moderate silica and carbonate addi-

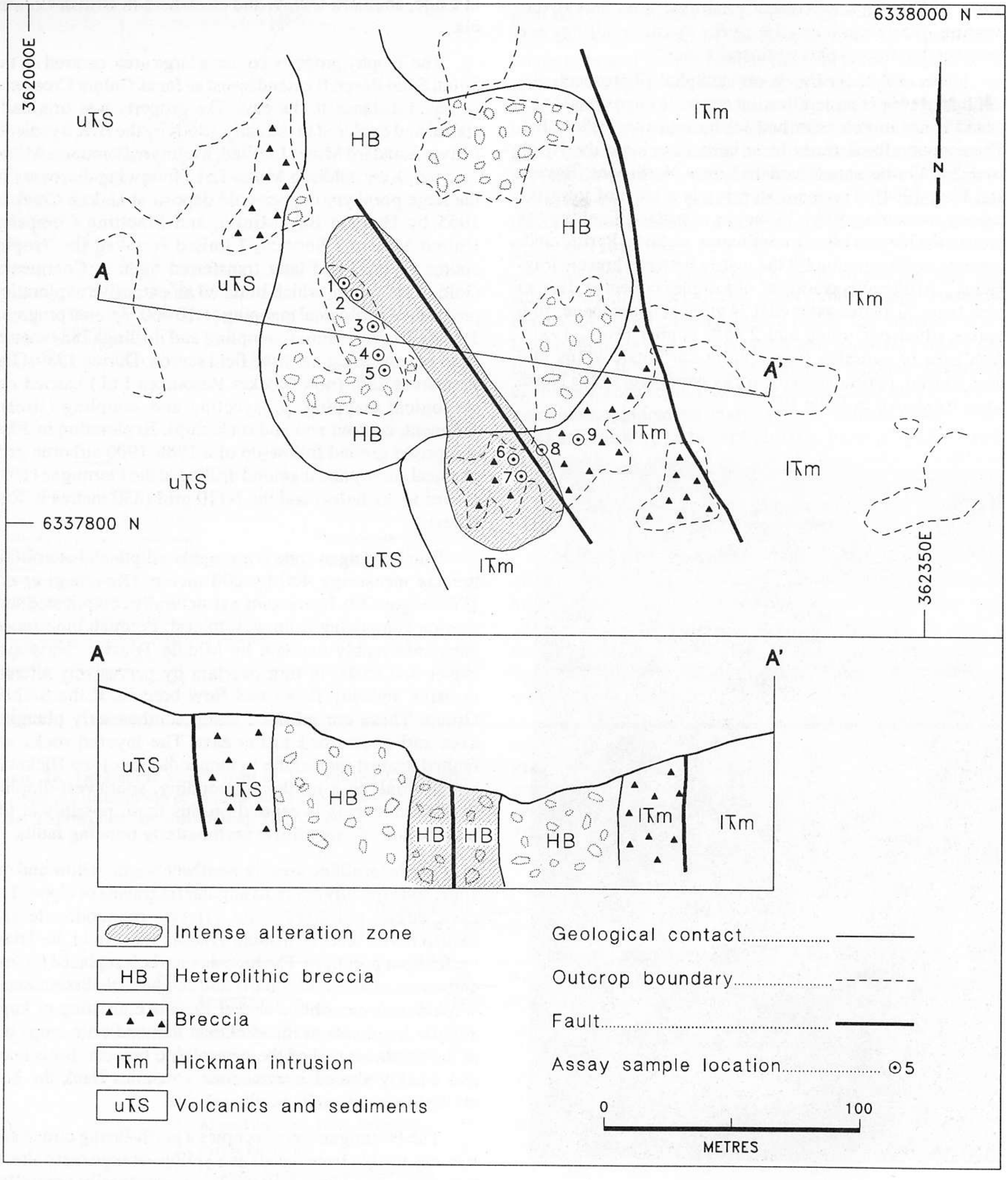


Figure 29. Geological sketch map and schematic longitudinal section of the Ptarmigan zone, Trophy claims.

Plate 20. Mineralized northeast-striking quartz-carbonate veins hosted by heterolithic breccia, Ptarmigan zone. Fragment lithologies include augite porphyry, monzodiorite, chert, feldspar porphyry and fragments of monzodiorite breccia. Altered Upper Triassic volcanics form cliffs in background.

tion. Alteration minerals include quartz, sericite, calcite, ankerite, chlorite, kaolinite, jarosite, goethite and scoradite.

Northeast-striking faults and shear zones appear to crosscut northwest-trending structures. Both structures are mineralized; the younger are sulphide rich. Precious metal mineralization is essentially confined to the zone of intense sericite alteration, however, narrow, widely spaced fractures, veinlets, and stockworks which crosscut the pyritic alteration zone are also mineralized (Plate 20) . These northeast-trending veins are dilational features related to the northwest-trending Ptarmigan fault. Veins are typically 0.5 to 1.0 centimetre wide and contain massive and disseminated pyrite, sphalerite, galena and pyrrhotite, with lesser amounts of chalcopyrite, arsenopyrite, tetrahedrite and electrum in a quartz-carbonate gangue. Mineralization is silver-rich with Ag/Au ratios averaging 80:1.

Lithogeochemical sampling results are tabulated (Table 11), and sample locations plotted on Figure 29. Samples from a fault zone striking 140° and dipping 60° southwest, which cuts the intrusive breccia marginal to the heterolithic breccia, returned gold values up to 11.05 grams per tonne. A grab sample from a mineralized vein within the heterolithic breccia returned 5.55 grams per tonne gold. Quartz-carbonate stockwork within the breccia assayed up to 8.70 grams per tonne gold. Pyritic heterolithic breccia (containing disseminated pyrite, but no vein material) returned values of 1.74 grams per tonne gold.

The heterolithic breccia cuts and therefore postdates the northwest-trending faulted contact between Upper Triassic Stuhini volcanics and the comagmatic Hickman batholith. Quartz-eye rhyolite and Eocene(?) monzonite fragments are contained within the breccia, suggesting an Eocene age. In addition, galena lead from the Ptarmigan zone has isotope ratios similar to Tertiary model ages (Godwin *et al.,* 1991).

## VEINS

Due to the silica undersaturated nature of alkaline magmatism, quartz does not occur as a gangue mineral in the fractures and veins related to these porphyry systems. Mineralization hosted in quartz and quartz-carbonate veins, which is related to other more silicic systems, is an obvious additional classification. However, this may be an over simplification as quartz guange is abundant at Red-Chris, Groat Creek and Rose; all considered to be alkalic porphyry systems (Newell and Peatfield, in preparation).

TABLE 11
SELECTED GEOCHEMICAL ANALYSES AND ASSAYS FROM THE PTARMIGAN ZONE, TROPHY PROPERTY

| Map No. | Figure No. | Grab Sample Description | Au (ppb) | Ag (ppm) | Cu (ppm) | Pb (ppm) | Zn (ppm) | As (ppm) | Sb (ppm) |
|---|---|---|---|---|---|---|---|---|---|
| 73 | 1 | Silicifed, pyritic wall rock | 1740 | 139 | 182 | 0.37% | 0.44% | 0.41% | 230 |
| 73 | 2 | Quartz-carbonate vein (4 cm), diss gn, sp, aspy, tt | 5550 | 775 | 690 | 1.20% | 1.51% | 1.73% | 830 |
| 73 | 3 | Silicifed sericite altered breccia, diss py, sp,gn,tt | 4300 | 205 | 296 | 1.18% | 0.33% | 6.00% | 230 |
| 73 | 4 | Silicifed sericite altered breccia, diss py, sp,gn,tt | 8700 | 390 | 193 | 0.31% | 280 | 0.13% | 230 |
| 73 | 5 | Silicifed sericite altered breccia, diss py, sp,gn,tt | 4240 | 310 | 340 | 0.51% | 2.12% | 0.18% | 268 |
| 73 | 6 | Quartz-carbonate-sericite vein, diss gn, sp, aspy, py | 3170 | 510 | 680 | 4.05% | 11.10% | 0.12% | 255 |
| 73 | 7 | Sericite-ankerite gouge zone, diss sp, gn, py, tt | 11050 | 210 | 470 | 1.23% | 0.33% | 0.58% | 390 |
| 73 | 8 | Brecciated monzodiorite, quartz-carbonate stockwork | 116 | 12 | 213 | 0.18% | 510 | 270 | 6 |
| 73 | 9 | Monzodiorite breccia, quartz-carbonate stockwork | 360 | 6 | 156 | 138 | 137 | 0.22% | 3 |

### BASE METAL VEINS

The Jay showing (104G 46) consists of magnetite-chalcopyrite veins hosted by granodiorite of the Hickman pluton. The veins occupy northerly and northwesterly trending, steep eastward-dipping fractures, joints and breccia zones. Potassic altered wallrock surrounds these zones. The alteration intensity decreases outwards into a weak propylitic alteration several tens of centimetres from the veins. Widths vary from 0.5 metre up to 10.5 metres and these zones are reported to be traceable for over 50 metres (Heinrich *et al.*, 1989). Assays of chip samples returned values up to 2.7 grams per tonne gold, 24.1 grams per tonne silver and 8.9% copper over 1.2 metres (Heinrich *et al.*, 1989).

### BASE METAL QUARTZ VEINS

Quartz veins, made conspicuous by the rusty oxidation of iron carbonate alteration envelopes which surround them, occupy north, northeast, northwest and west-striking structures. Alteration minerals include chlorite, pyrite, ankerite and calcite. Sulphide mineralogy includes pyrite, sphalerite, chalcopyrite and arsenopyrite in concentrations up to 25% of the quartz vein. An east-striking vein at the headwaters of Hickman Creek, the Glacier showing (104G 123) is typical of these veins. The 30-centimetre quartz vein is surrounded by an alteration envelope of bleaching, quartz carbonate veinlets and pyritization which extends 40 centimetres into the wallrock. The vein and its alteration envelopes were sampled for geochemical analysis (Table 12). The vein returned up to 0.1 gram per tonne gold, 3.0 grams per tonne silver, low base metals and noticeably elevated arsenic values. Elevated base and precious metal values are restricted to the vein, with possibly minor copper enrichment extending into the wallrock.

### BASE METAL QUARTZ-CARBONATE VEINS

A prominant northwest-trending zone of limonitic and brecciated rock, up to 50 metres wide, bisects the Scud pluton, south of the confluence of the Scud and South Scud rivers. This structure contains numerous, narrow mineralized shears, quartz and quartz-carbonate veins. At Trench Lake, veins are hosted by Upper Triassic foliated tuff and andesite and Middle Triassic chert and fine-grained sediments. Mineralized veins were not seen in the granodiorite. All the quartz and quartz-carbonate veins trend 120°, have variable widths up to a metre and contain disseminated base metal sulphides, in particular chalcopyrite. Three veins were sampled at Trench Lake (Table 12; Map Nos. 60, 61, 62). This area was sampled extensively in 1988 (Heinrich *et al.*, 1989) and again in 1989 (Caulfield and Archambault, 1990). Assay results are similiar to those presented in Table 12 and include high copper, variable silver values and one anomalous gold value (1.42 grams per tonne; Heinrich *et al.*, 1989).

Narrow quartz and quartz-carbonate veins occur in two northwest-striking fault zones in the valley of the Scud River. These are on strike with the Trench Lake occurrences and are probably localized by the same shear structure. The fault zones are pyritic, up to 40 metres wide and host parallel quartz veins containing massive pyrite and traces of chalcopyrite.

Quartz-carbonate veins which occupy northeasterly trending structures, for example, at Trophy and Trek-Toe properties (described earlier) are particularly silver rich and contain high lead and zinc values.

Foliation-parallel quartz-carbonate veins, sigmoidal quartz-filled tension gashes and folded quartz veins are common in the Devonian metasedimentary and metavolcanic rocks, particularly the sericite and chlorite schist, phyllite and graphitic shale units. Widths rarely exceed 0.3 metre and mineralogy is simple: bull quartz and often euhedral cubic pyrite. Assay results from three quartz veins returned negligible base and precious metal values (Table 12; Map Nos. 76, 77, 78).

## SKARNS

The Hummingbird skarn is located 300 metres northwest of the Ptarmigan zone. Intrusion and contact metamorphism by Eocene(?) hornblende biotite granodiorite has produced exoskarns in Lower Permian and Middle Triassic limestones. Numerous dikes of intermediate to felsic composition crosscut the skarn zone. In the Middle Triassic limestones (Hummingbird zone), skarn mineral assemblages with weak associated sulphide mineralization developed adjacent to the northwest-trending Hummingbird fault. Skarn minerals are brown garnets (andradite?), epidote, diopside and sparse tremolite and/or wollastonite. Sulphides include pyrite, chalcopyrite and pyrrhotite. South of the Hummingbird zone a narrow zone of skarned Lower Permian limestone (skarn C and D) is developed along the granodiorite contact. The skarn is a mottled, green and

TABLE 12
SELECTED GEOCHEMICAL ANALYSES AND ASSAYS FROM BASE METAL QUARTZ-CARBONATE VEINS

| Map No. | Sample Description | Au (ppb) | Ag (ppm) | Cu (ppm) | Pb (ppm) | Zn (ppm) | As (ppm) | Sb (ppm) |
|---|---|---|---|---|---|---|---|---|
| 60 | Carbonate vein, diss. py, & malachite | 1 | 5 | 0.47% | 20 | 360 | 60 | 1 |
| 61 | Stockwork veins, diss. pyrite | 1 | 1 | 620 | 10 | 50 | - | <0.5 |
| 62 | Qty vein, diss. py, cpy, malachite | 6 | 54 | 4.67% | 10 | 50 | - | <0.5 |
| 76 | Breccia qtz vein, no visible sulphides | 1 | <0.5 | 6 | 5 | 22 | - | <0.5 |
| 77 | Qtz-sericite-carb vein, diss. pyrite | 1 | 0.6 | 99 | 7 | 18 | - | 20 |
| 78 | Oxidized qtz-sericite vein, diss. py | 1 | <0.5 | 10 | 2 | 9 | - | <0.5 |
| 82 | Qtz carbonate vein, py, aspy, cpy & sp | 112 | 3 | 390 | 116 | 310 | 2.60% | 97 |
| 82 | Apophysis of vein sample 17-1-1 | 70 | 9 | 0.14% | 220 | 0.15% | 0.11% | 27 |
| 82 | Basalt, pyritic wallrock of vein 17-1-1 | 2 | <0.5 | 107 | 8 | 56 | 48 | 3 |

brown massive intergrowth of garnet, diopside, chlorite, epidote, quartz and magnetite. Sulphides include pyrrhotite and minor chalcopyrite and sphalerite. The sulphides in both skarns occur as podiform massive bodies at the contact between skarned limestones and silicified volcanics. Precious metals are associated with the massive sulphide lenses. Diamond drilling in 1988 tested the Hummingbird zone to a depth of 64 metres before drilling conditions forced abandonment of the hole. Skarn alteration was intersected to a depth of 19.7 metres. No significant base or precious metals were found in the skarn (Caulfield and Archambault, 1990).

## MASSIVE SULPHIDES

Massive concentrations of pyrite, pyrrhotite and lesser chalcopyrite are present in Middle Triassic sediments on both sides of the South Scud River. They form irregular masses up to 20 by 30 metres in size. Mineralization is both conformable and crosscutting. A lens of massive pyrite, pyrrhotite, chalcopyrite and arsenopyrite on the Trophy claims assayed 2.0 grams gold per tonne over 4.0 metres (Forster, 1988). Most of these occurrences are massive iron sulphides with trace amounts of copper and are possibly products of the metasomatic alteration related to skarn development previously discussed.

The potential for volcanogenic massive sulphide deposits is high in Paleozoic rocks. Pyroclastic sulphide fragments and small stratiform lenses of massive sulphides in Paleozoic felsic fragmental rocks exposed to the east at Mess Creek have been reported by Holbek (1988) and massive sulphide deposits are known in correlative stratigraphy in the Tulsequah River area (Nelson and Payne, 1984). Metamorphosed volcanogenic massive sulphide bodies containing pyrite, sphalerite, marcasite, galena and chalcopyrite are known from Paleozoic metavolcanic rocks south of Prince Rupert on the west side of the Coast Belt (Gareau, 1991).

## AGES OF MINERALIZATION

Possible mid-Triassic, latest Triassic to earliest Jurassic and Eocene mineralizing events are postulated for deposits in the Galore Creek area. Middle Triassic sediments host conformable massive polymetallic sulphide occurrences. Adjacent to Hickman intrusions, these are crosscutting, suggesting they are probably younger epigenetic sulphide mineralization.

The age of porphyry copper-gold mineralization at Galore Creek is well constrained stratigraphically and isotopically. The deposits are hosted by alkaline volcanic rocks and syenite intrusions high in the Upper Triassic stratigraphic succession. Intercalated epiclastics contain syenite intrusive clasts and distal siltstones contain the upper Norian bivalve *Monotis subcircularis* Gabb.

Early isotopic dating at Galore Creek utilized coarse hydrothermal biotite from the Central zone. This biotite is intimately associated with the mineralization, but was also subjected to retrograde alteration. The K-Ar results attest to the low blocking temperature and nonrefractory characteristics of biotite. Four K-Ar dates (recalculated to new decay constants) for hydrothermal biotite from the Central zone, range from 177 to 201 Ma - Early to Middle Jurassic (White *et al.*, 1968; Table 2). This age span may reflect argon loss from leaky biotites. An Ar-Ar date from an unaltered biotite crystal lithic tuff above Copper Canyon has a plateau age of 212 Ma. This unit is believed to be an eruptive equivalent of one of the syenites and, as such,would infer an age of mineralization near the Triassic-Jurassic boundary.

Mesothermal vein deposits are peripheral to the volcanic-intrusive centres. Potassium-argon isotope dating of chrome-bearing muscovite from a carbonate-sulphide vein in the Mess Creek area gave an Early Jurassic, 194±6 Ma, age for the mineralization (Holbek, 1988).

High base metal values, associated with silver and molybdenum enrichment, characterize the Tertiary event elsewhere in northwestern British Columbia and these same mineral assemblages are spatially associated with felsic Eocene plugs on the Trek property and in the Trophy-Ptarmagin/Hummingbird zones. Distinctive galena-lead isotope ratio clusters distinguish Jurassic from Tertiary deposits in the Stewart-Iskut area (Godwin *et al.*, 1991). Galena lead from the Ptarmigan zone has isotopic ratios similar to Tertiary model ages.

# REFERENCES


Alaska Geographic Society (1979): The Stikine River; Volume 6, Number 4, 94 pages.

Allen, D.G. (1966): Mineralogy of Stikine Copper's Galore Creek Deposits; unpublished M.Sc. thesis, *The University of British Columbia*, 38 pages.

Allen, D.G. (1971): The Origin of Sheet Fractures in the Galore Creek Copper Deposits, British Columbia; *Canadian Journal of Earth Sciences*, Volume 8, pages 704-711.

Allen, D.G., Panteleyev, A. and Armstrong, A.T. (1976): Galore Creek; *in* Porphyry Deposits of the Canadian Cordillera, Sutherland Brown, A., Editor, *Canadian Institute of Mining and Metallurgy*, Special Volume 15, pages 402-414.

Alldrick, D.J. (1989): Volcanic Centres in the Stewart Complex (103P and 104A,B); *in* Geological Fieldwork 1988, *B.C. Ministry of Energy, Mines and Petroleum Resources*, Paper 1989-1, pages 233-240.

Alldrick, D.J., Gabites, J.E. and Godwin, C.I. (1987): Lead Isotope Data from the Stewart Mining Camp; *in* Geological Fieldwork 1986, *B.C. Ministry of Energy, Mines and Petroleum Resources*, Paper 1987-1, pages 93-102.

Anderson, R.G. (1983): Geology of the Hotailuh Batholith and Surrounding Volcanic and Sedimentary Rocks, North-Central British Columbia; unpublished Ph.D. thesis, *Carleton University*, 669 pages.

Anderson, R.G. (1984): Late Triassic and Jurassic Magmatism along the Stikine Arch and the Geology of the Stikine Batholith, North-central British Columbia; *in* Current Research, Part A, *Geological Survey of Canada*, Paper 84-1A, pages 67-73.

Anderson, R.G. (1989): A Stratigraphic, Plutonic, and Structural Framework for the Iskut River Map Area, Northwestern British Columbia; *in* Current Research, Part E; *Geological Survey of Canada*, Paper 89-1E, pages 143-151.

Anderson, R.G. and Bevier, M.L. (1990): A Note on Mesozoic and Tertiary K-Ar Geochronometry of Plutonic Suites, Iskut River Map Area, Northwestern British Columbia; *in* Current Research, Part E, *Geological Survey of Canada*, Paper 90-1E, pages 141-147.

Anderson, R.G. and Thorkelson, D.J. (1990): Mesozoic Stratigraphy and Setting for some Mineral Deposits in Iskut River Map Area, Northwestern British Columbia; *in* Current Research, Part E, *Geological Survey of Canada*, Paper 90-1E, pages 131-139.

Armstrong, R.L. (1988): Mesozoic and Early Cenozoic Magmatic Evolution of the Canadian Cordillera; *in* Rodgers Symposium Volume, *Geological Society of America*, Special Paper 218, pages 55-91.

Asano, S. (1965): Geological Report on the Joan and M.B. Groups; *B.C. Ministry of Energy, Mines and Petroleum Resources*, Assessment Report 685.

Awmack, H.J. (1991): 1990 Geological, Geochemical and Geophysical Report on the Trek 1-6 Claims; *B.C. Ministry of Energy, Mines and Petroleum Resources*, Assessment Report 20 956.

Awmack, H.J. and Yamamura B.K. (1988): 1988 Summary Report on the Trek 1-6 Claims; *B.C. Ministry of Energy, Mines and Petroleum Resources*, Assessment Report 18 115.

Bamber, E.W. (1988): Report on 17 Collections from the Telegraph Creek Area, Northwestern British Columbia; *Geological Survey of Canada*, Report No. C3-EWB-1988, 7 pages.

Bamber, E.W. (1991): Report on 9 Collections from the Telegraph Creek and Iskut River Map Areas, Northwestern British Columbia, *Geological Survey of Canada*, Report No. C1-EWB-1991, 5 pages.

Barr, D.A. (1966): The Galore Creek Copper Deposit; *Canadian Institute Mining and Metallurgy*, Transactions, Volume 69, pages 251-263.

Barr, D.A., Fox, P.E., Northcote, K.E. and Preto, V.A. (1976): The Alkaline Suite Porphyry Deposits: A Summary; *in* Porphyry Deposits of the Canadian Cordillera, Sutherland Brown, A., Editor, *Canadian Institute of Mining and Metallurgy*, Special Volume 15, pages 359-367.

Bevier, M.L. and Anderson, R.G. (1991): Jurassic Geochronometry in NW Stikinia (56-57°), British Columbia; *Geological Society of America*, Abstracts with Programs, A191.

Blann, D.E. and Vulimiri, M.R. (1990): Summary Report on the Jack Wilson Property - 1990 Exploration Program, Liard Mining Division; *B.C. Ministry of Energy, Mines and Petroleum Resources*, Assessment Report 20 843.

Bloomer, S.H., Stern, R.J., Fisk, E. and Gerschwind, C.H. (1989): Shoshonitic Volcanism in the Northern Mariana Arc 1. Mineralogic and Major and Trace Element Characteristics; *Journal of Geophysical Research*, Volume 94, Number B4, pages 4469-4496.

Bradford, J.A. and Brown, D.A. (1993): Geology of Bearskin Lake and Southern Tatsamenie Lake Map Areas, Northwestern British Columbia; *in* Geological Fieldwork 1992, Grant, B. and Newell, J.M, Editors, *B.C. Ministry of Energy, Mines and Petroleum Resources*, Paper 1993-1, pages 159-176.

Britten, R.M. and Alldrick, D.J. (1990): Gold Deposits in the Iskut-Stikine, Northwestern B.C.; *Geological Association of Canada/Mineralogical Association of Canada, Vancouver '90*, Program with Abstracts, page A15.

Brown, D.A. and Gunning, M.H. (1989a): Geology of the Scud River Area, Northwestern British Columbia (104G/5,6); *in* Geological Fieldwork 1988, *B.C. Ministry of Energy, Mines and Petroleum Resources*, Paper 1989-1, pages 251-267.

Brown, D.A. and Gunning, M.H. (1989b): Geology and Geochemistry of the Scud River Area, Northwestern British Columbia (104G/5,6); *B.C. Ministry of Energy, Mines and Petroleum Resources*, Open File 1989-7.

Brown, D.A. and Greig, C.J. (1990): Geology of the Stikine River - Yehiniko Lake Area, Northwestern British Columbia (104G/11W,12E); *in* Geological Fieldwork 1989, *B.C. Ministry of Energy, Mines and Petroleum Resources*, Paper 1990-1, pages 141-151.

Brown, D.A., Gunning, M.H. and Greig, C.J. (in preparation): Geology of Western Telegraph Creek Map Area, Northwestern

British Columbia; *B.C. Ministry of Energy, Mines and Petroleum Resources*, Bulletin.

Brown, D.A., Logan, J.M., Gunning, M.H., Orchard, M.J. and Bamber, E.W. (1991): Stratigraphic Evolution of the Paleozoic Stikine Assemblage in the Stikine Iskut Rivers Area, Northwestern British Columbia (NTS 104G and 104B); *in* Contributions to the Geology and Geophysics of Northwestern British Columbia and Southeastern Alaska, Anderson, R.G.,Editor, *Canadian Journal of Earth Sciences*, Volume 28, pages 958-972.

Caulfield, D.A. and Archambault M. (1990): Geological, Geochemical Report on the Trophy Gold Project; *B.C. Ministry of Energy, Mines and Petroleum Resources*, Assessment Report 19 783.

Davies, J.F., Grant, R.W.E., and Whitehead, R.E.S. (1979): Immobile Trace Elements and Archean Volcanic Stratigraphy in the Timmins Mining Area, Ontario; *Canadian Journal of Earth Sciences*, Volume 16, pages 305-311.

Dawson, G.M. (1898): Report on an Exploration in Yukon District, N.W.T., and Adjacent Northern Portion of British Columbia; *Geological Survey of Canada*, Annual Report 1887-1888, New Series, Volume III, Part 1 and Publication No. 629.

de Rosen-Spence, A. (1985): Shoshonites and Associated Rocks of Central British Columbia; *in* Geological Fieldwork 1984, *B.C. Ministry of Energy, Mines and Petroleum Resources*, Paper 1985-1, pages 426-442.

Drobe, J.R., Logan, J.M. and McClelland, W.C. (1992): Early Carboniferous Plutonism in Stikinia, Stikine and Iskut Rivers Area, Northwestern British Columbia; *Lithoprobe*, Report No.24, page 85.

Elsby, D.C. (1992): Structure, Ductile Thrusting and Mineralization within the Stikine Assemblage, South Forrest Kerr Area, Northwestern British Columbia (104B/10, 15); *in* Geological Fieldwork 1991, Grant, B. and Newell, J.M., Editors, *B.C. Ministry of Energy, Mines and Petroleum Resources*, Paper 1992-1, pages 197-205.

Evenchick, C.A. (1991): Geometry, Evolution, and Tectonic Framework of the Skeena Fold Belt, North-central British Columbia; *Tectonics*, Volume 10, pages 527-546.

Falconer, R. (1964): Geophysical Report on Mineral Claims BIK 1-86 and BIK 221-226 (Inclusive); *B.C. Ministry of Energy, Mines and Petroleum Resources*, Assessment Report 593.

Folk, P.G. (1981): Report on Rock Chip Sampling of the Sphal 7-12, 19-33, Kim 1-10, 38, 40, 42, Sphal Fraction Claims; *B.C. Ministry of Energy, Mines and Petroleum Resources*, Assessment Report 9614.

Folk, P.G. (1982): Report on the Geological, Geochemical, Geophysical Surveys and Diamond Drilling conducted on the Paydirt Claim Group; *B.C. Ministry of Energy, Mines and Petroleum Resources*, Assessment Report 9999.

Folk, P.G. (1987): Prospecting Report on the Jack Mineral Claim; *B.C. Ministry of Energy, Mines and Petroleum Resources*, Assessment Report 16 531.

Folk, P.G. and Spilsbury W. (1980): Report on Geological Mapping, Magnetometer and Soil Sampling Surveys of Sphal 7-12, 19-33, Kim 1-10, 38, 40, 42, Sphal Fraction; *B.C. Ministry of Energy, Mines and Petroleum Resources*, Assessment Report 8424.

Forster, D.A. (1988): Trophy Gold Project - Geological and Geochemical Report; *United Mineral Services Limited*, private company report, 63 pages.

Fox, P.E. (1989): Alkaline Cu-Au Porphyries - Schizophrenic Cousins of Real Porphyry Coppers; *Mineral Deposits Division, Geological Association of Canada*, Copper-Gold Porphyry Workshop, Vancouver, April, 1989.

Gabrielse, H. (1967): Tectonic Evolution of the Northern Canadian Cordillera; *Canadian Journal of Earth Sciences*, Volume 4, pages 271-298.

Gabrielse, H. (1980): Dease Lake Map Area; *Geological Survey of Canada*, Open File 707.

Gabrielse, H., Monger, J.W.H., Wheeler, J.O. and Yorath, C.J. (1991): Part A: Morphogeological Belts, Tectonic Assemblages, and Terranes; Chapter 2 *in* Geology of the Cordilleran Orogen in Canada, Gabrielse, H. and Yorath, C.J., Editors, Geological Survey of Canada, Geology of Canada, No. 4, pages 15-28 (also *Geological Society of America*, The Geology of North America, Volume G-2).

Gale, R.E. (1964): Geological Report on Mineral Claims BIK 137 to BIK 160 Inclusive; *B.C. Ministry of Energy, Mines and Petroleum Resources*, Assessment Report 592.

Gareau, S.A. (1991): The Scotia-Quaal Metamorphic Belt: A Distinct Assemblage with Pre-early Late Cretaceous Deformational and Metamorphic History, Coast Plutonic Complex, British Columbia; *in* Contributions to the Geology and Geophysics of Northwestern British Columbia and Southeastern Alaska, Anderson, R.G., Editor, *Canadian Journal of Earth Sciences*, Volume 28, pages 870-880.

Gehrels, G.E., McClelland, W.C., Sampson, S.D., Patchett, P.J. and Jackson, J.L. (1990): Ancient Continental Margin Assemblage in the Northern Coast Mountains, Southeast Alaska and Northwest Canada; *Geology*, Volume 18, pages 208-211.

Geological Survey of Canada (1957): Operation Stikine; Map 9-1957.

Gill, J. and Whelan, P. (1989): Early Rifting of an Oceanic Island Arc (Fiji) Produced Shoshonitic to Tholeiitic Basalts; *Journal of Geophysical Research*, Volume 94, Number B4, pages 4561-4578.

Godwin, C.I., Pickering, A.D.R., Gabites, J.E. and Alldrick, D.J (1991): Interpretation of Galena Lead Isotopes from the Stewart-Iskut Area; *in* Geological Fieldwork 1990, *B.C. Ministry of Energy, Mines and Petroleum Resources*, Paper 1991-1, 235-243.

Gordey, S.P., Abbott, J.G., Templelman-Kluit, D.J. and Gabrielse, H. (1987): "Antler" Clastics in the Canadian Cordillera; *Geology*, Volume 15, pages 103-107.

Grant, G.W. (1964): Final Geological Report CW Group - Stikine Area; *B.C. Ministry of Energy, Mines and Petroleum Resources*, Assessment Report 621.

Gunning, M.H. (1990): Stratigraphy of the Stikine Assemblage, Scud River Area, Northwest British Columbia; *in* Geological Fieldwork 1989, *B.C. Ministry of Energy, Mines and Petroleum Resources*, Paper 1990-1, pages 153-161.

Gunning, M.H. (1992): Carboniferous Limestone, Iskut River Region, Northwest British Columbia; *in* Current Research, Part A, *Geological Survey of Canada*, Paper 92-1A, pages 315-322.

Harland, W.B., Armstrong, R.L., Cox, A.V., Craig, L.E., Smith, A.G. and Smith, D.G. (1989): A Geological Time Scale 1989; *Cambridge University Press.*

Heinrich, S.M., Dawson, G.J. and Augsten, B.E.K. (1989): Trophy Gold Project: Geological, Geochemical, and Diamond Drilling Report; *B.C. Ministry of Energy, Mines and Petroleum Resources*, Assessment Report 18 555.

Henderson, J.R., Kirkham, R.V., Henderson, M.N., Payne, J.G., Wright, T.O. and Wright, R.L. (1992): Stratigraphy and Structure of the Sulphurets Area, British Columbia; *in* Current Research, Part A; *Geological Survey of Canada*, Paper 92-1A, pages 323-332.

Hill, H.L. (1965): Report on the "Lot" Mineral Claims, Nos. 34-75; *B.C. Ministry of Energy, Mines and Petroleum Resources*, Assessment Report 717.

Holbek, P.M. (1988): Geology and Mineralization of the Stikine Assemblage, Mess Creek Area, Northwestern British Columbia; Unpublished M.Sc. thesis, *The University of British Columbia*, 174 pages.

Holtby, M.H. (1985): A Geological, Soil Geochemical, Trenching and Diamond Drilling Programme on the Paydirt Claim Group; *B.C. Ministry of Energy, Mines and Petroleum Resources*, Assessment Report 14 980.

Irvine, T.N. and Baragar, W.R.A. (1971): A Guide to the Chemical Classification of the Common Volcanic Rocks; *Canadian Journal of Earth Sciences*, Volume 8, pages 523-548.

James, D.H. (1965): Geological Report on the SIL Group; *B.C. Ministry of Energy, Mines and Petroleum Resources*, Assessment Report 643.

Jeffery, W.G. (1966): Galore Creek (Stikine Copper Limited); B.C. Minister of Mines Annual Report 1965, *B.C. Ministry of Energy, Mines and Petroleum Resources*, pages 19-29.

Jones, B.K. and Leveille, R.A. (1989): Application of Metal Zoning Relationships and Metal Ratios to Gold Exploration in Porhyry Systems; Abstract, *Northwest Mining Association*, Spokane, USA, Dec. 1989.

Kerr, F.A. (1948a): Lower Stikine and Iskut River Areas, British Columbia; *Geological Survey of Canada*, Memoir 246, 94 pages.

Kerr, F.A. (1948b): Taku River Map Area, British Columbia; *Geological Survey of Canada*, Memoir 248, 84 pages.

Koyanagi, V.M., Heinrich, S.M. and Logan, J.M. (1989): Trophy: (Ptarmigan Zone); *in* Exploration in British Columbia 1988, *B.C. Ministry of Energy, Mines and Petroleum Resources*, pages B153-155.

Leary, G. (1990): Report on 1990 Phase i Mapping and Drilling on the Copper Canyon Property, Northwestern British Columbia; *B.C. Ministry of Energy, Mines and Petroleum Resources*, Assessment Report 21062.

LeMaitre, R.W. (1989): Classification of Igneous Rocks and Glossary of Terms; LeMaitre, R.W., Editor, *Oxford: Blackwell Scientific Publications*, 193 pages.

Logan, J.M. and Drobe, J.R. (1993): Geology and Mineral Occurrences of the Mess Lake Area (104G/7W); *in* Geological Fieldwork 1992, Grant, B. and Newell, J.M., Editors, *B.C. Ministry of Energy, Mines and Petroleum Resources*, Paper 1993-1, pages 135-148.

Logan, J.M. and Drobe, J.R. (in preparation): Geology along the Forrest Kerr and Mess Creek Faults, Iskut River Area, Northwestern British Columbia; *B.C. Ministry of Energy, Mines and Petroleum Resources*, Bulletin.

Logan, J.M. and Koyanagi, V.M. (1989): Preliminary Geology and Mineral Deposits of the Galore Creek Area, Northwestern British Columbia (104G/3&4); *in* Geological Fieldwork 1988, *B.C. Ministry of Energy, Mines and Petroleum Resources*, Paper 1989-1, pages 269-284.

Logan, J.M., Drobe, J.R. and Elsby, D.C. (1992): Geology of the More Creek Area, Northwestern British Columbia (104G/2); *in* Geological Fieldwork 1991, Grant, B. and Newell, J.M., Editors, *B.C. Ministry of Energy, Mines and Petroleum Resources*, Paper 1992-1, pages 161-178.

Logan, J.M., Koyanagi, V.M. and Drobe, J.R. (1990a): Geology of the Forrest Kerr Creek Area, Northwestern British Columbia (104B/15); *in* Geological Fieldwork 1989, *B.C. Ministry of Energy, Mines and Petroleum Resources*, Paper 1990-1, pages 127-140.

Logan, J.M., Koyanagi, V.M. and Drobe, J.R. (1990b): Geology and Mineral Occurrences of the Forrest Kerr - Iskut River Area (104B/15); *B.C. Ministry of Energy, Mines and Petroleum Resources*, Open File 1990-2.

Logan, J.M. and Koyanagi, V.M. and Rhys, D.A. (1989): Geology and Mineral Occurences of the Galore Creek Area (104G/3&4); *B.C. Ministry of Energy, Mines and Petroleum Resources*, Open File 1989-8.

Logan, J.M., Drobe, J.R., McClelland, W.C. and Anderson, R.G. (1993): Devonian Intraoceanic Plutonism in Stikinia; *Geological Association of Canada/Mineralogical Association of Canada*, Edmonton '93, Program with Abstracts, page A60.

Macdonald, J.A., van der Heyden, P., Lefebure, D.V. and Alldrick, D.J. (1992): Geochronometry of the Iskut River Area - An Update (104A and B); *in* Geological Fieldwork 1991, *B.C. Ministry of Energy, Mines and Petroleum Resources*, Paper 1992-1, pages 495-501.

Mamet, B.L. (1991a): Report on 5 Collections from the Telegraph Creek and Iskut River Map Areas, Northwestern British Columbia; *Geological Survey of Canada*, Report No. 07-BLM-1991, 3 pages.

Mamet, B.L. (1991b): Report on 4 Collections from the Telegraph Creek Map Area, Northwestern British Columbia; *Geological Survey of Canada*, Report No. 06-BLM-1991, 1 page.

Mathews, W.H. (1991): Physiographic Evolution of the Canadian Cordillera; Chapter 11 *in* Geology of the Cordilleran Orogen in Canada, Gabrielse, H. and Yorath, C.J., Editors, Geological Survey of Canada, Geology of Canada, No. 4, pages 403-418 (also *Geological Society of America*, The Geology of North America, Volume G-2).

McClelland, W.C. (1992): Permian and Older Rocks of the Southwest Iskut River Map Area, Northwestern British Columbia; *in* Current Research, Part A, *Geological Survey of Canada*, Paper 92-1A, pages 303-307.

McClelland, W.C. and Mattinson, J.M. (1991): U-Pb (Zircon) Constraints on the Age of the Yukon-Tanana Terrane in the Coast Mountains, Central Southeast Alaska and British Columbia (abstract); *Geological Society of America*, Abstracts with Programs, Volume 23, page A434.

McMillan, W.J. (1991): Porphyry Deposits in the Canadian Cordillera; *in* Ore Deposits, Tectonics and Metallogeny in the Canadian Cordillera, *B.C. Ministry of Energy, Mines and Petroleum Resource*, Paper 1991-4, pages 253-276.

Monger, J.W.H. (1970): Upper Paleozoic Rocks of the Stikine Arch, British Columbia; *Geological Survey of Canada*, Paper 70-1, Part A, 41-43.

Monger, J.W.H. (1977a): Upper Paleozoic Rocks of Northwestern British Columbia; *in* Current Research, Part A, *Geological Survey of Canada*, Paper 77-1A, pages 255-262.

Monger, J.W.H. (1977b): Upper Paleozoic Rocks of the Western Canadian Cordillera and their Bearing on Cordillera Evolution; *Canadian Journal of Earth Sciences*, Volume 14, pages 1832-1859.

Monger, J.W.H. (1977c): The Triassic Takla Group in McConnell Creek Map-area, North-central British Columbia; *Geological Survey of Canada*, Paper 76-29, 45 pages.

Monger, J.W.H. (1980): Upper Triassic Stratigraphy, Dease Lake and Tulsequah Map Areas, Northwestern British Columbia; *in* Current Research, Part B, *Geological Survey of Canada*, Paper 80-1B, pages 1-9.

Monger, J.W.H. and Thorstad, L.(1978): Lower Mesozoic Stratigraphy, Cry Lake (104I0 and Spatsizi (104H) Map-areas, British Columbia; *in* Current Research, Part A, *Geological Survey of Canada*, Paper 78-1A, pages 21-24.

Mortimer, N. (1986): Late Triassic, Arc-related, Potassic Igneous Rocks in the North American Cordillera; *Geology*, Volume 14, pages 1035-1078.

Mutschler, F.E., Griffin, M.E., Stevens, D.S., Shannon, S.S. (1985): Precious Metal Deposits Related to Alkaline Rocks in the North American Cordillera - An Interpretive Review; *Transactions of the Geological Society South Africa*, Volume 88, pages 355-377.

Mutschler, F.E. and Mooney, T.C. and Johnson, D.C. (1990): Precious Metal Deposits Related to Alkaline Igneous Rocks - A Space-Time Trip through the Cordillera; *in* Proceedings of the Fourth Western Regional Conference on Precious Metals and the Environment, *Society for Mining, Metallurgy, and Exploration, American Institute of Mining Engineers*, pages 43-59.

Nelson, J. (1991): The Tectonic Setting of Alkaline Porphyry Suite Copper-Gold Deposits in the Canadian Cordillera; Abstract, *Canadian Institute of Mining, Metallurgy and Petroleum*, 93rd Annual General Meeting, Vancouver, April, 1991, page 57.

Nelson, J. and Mihalynuk, M.G. (1993): Cache Creek Ocean: Closure or Enclosure?; *Geology*, Volume 21, pages 173-176.

Nelson, J. and Payne J.G. (1984): Paleozoic Volcanic Assemblages and Volcanogenic Massive Sulphide Deposits near Tulsequah, British Columbia; *Canadian Journal of Earth Sciences*, Volume 21, pages 379-381.

Newell, J.M. and Peatfield, R.G. (in preparation): The Red-Chris Porphyry Copper-Gold Deposit in Porphyry Deposits of the Northwestern Cordillera of North Amerieca, Schroeter, T.G., Editor, *Canadian Institute of Mining Metallurgy and Petrleum*, Special Volume 46.

Nixon, G.T. and Ash, C.H. (1989): Alaskan-type Ultramafic Rocks in British Columbia: The Hickman, Gnat Lakes, and Menard Mafic-Ultramafic Complexes; *i n* Geological Fieldwork 1988, *B.C. Ministry of Energy, Mines and Petroleum Resources*, Paper 1989-1, pages 429-442.

Ohmoto, H. and Rye, R.O. (1979): Isotopes of Sulfur and Carbon; Chapter 10 *in* Geochemistry of Hydrothermal Fluids, Barnes, H.L., Editor, *Wiley-Interscience*, New York.

Oliver, J.L. and Gabites, J.E. (1993): Geochronology of Rocks and Polyphase Deformation, Bearskin (Muddy) and Tatsamenie Lakes District, Northwestern British Columbia; *in* Geological Fieldwork 1992, Grant, B. and Newell, J.M., Editors, *B.C. Ministry of Energy, Mines and Petroleum Resources*, Paper 1993-1, pages 177-184.

Orchard, M.J. (1990): Report on Microfossils from the Telegraph Creek Map Area, Northwestern British Columbia; *Geological Survey of Canada*, Conodont Data File, Report No. 01-MJO-1990.

Orchard, M.J. (1991a): Dating Otherwise Undatable Rocks I: Conodonts Put Teeth into Cordilleran Geological Mapping; GEOS, *Energy, Mines and Resources Canada*, Volume 20, No. 3, pages 28-34.

Orchard, M.J. (1991b): Report on Conodonts and other Microfossils from the Telegraph Creek - Iskut River, Northwestern British Columbia; *Geological Survey of Canada*, Conodont Data File, Report No. OF-1991-13.

Orchard, M.J. (1993): Report on Conodonts and other Microfossils from Telegraph Creek (104G/7); *Geological Survey of Canada*, Conodont Data File, Report No. OF-1993-40.

Orchard, M.J. (1994): Report on Conodonts and other Microfossils from Iskut River (104B) and Telegraph Creek (104G); *Geological Survey of Canada*, Conodont Data File, Report No. MJO-1994-18.

Pearce, J.A. and Cann, J.R. (1973): Tectonic Setting of Basic Volcanic Rocks Determined Using Trace Element Analyses; *Earth and Planetary Science Letters*, Volume 19, pages 290-300.

Pearce, J.A., Harris, N.B.W. and Tindle, A.G. (1984): Trace Element Discrimination Diagrams for the Tectonic Interpretation of Granitic Rocks; *Journal of Petrology*, Volume 25, Part 4, pages 956-983.

Panteleyev, A. (1973): GC, HAB, BUY (Stikine Copper); *in* Geology in British Columbia 1972, *B.C. Ministry of Energy, Mines and Petroleum Resources*, pages 520-526.

Pantaleyev, A. (1974): GC, HAB, BUY (Stikine Copper); *in* Geology in British Columbia 1973, *B.C. Ministry of Energy, Mines and Petroleum Resources*, pages 501-504.

Pantaleyev, A. (1975): Galore Creek Map Area; *in* Geological Fieldwork 1974, *B.C. Ministry of Energy, Mines and Petroleum Resources*, Paper 1975-1, pages 59-62.

Pantaleyev, A. (1976): Galore Creek Map Area; *in* Geological Fieldwork 1975, *B.C. Ministry of Energy, Mines and Petroleum Resources*, Paper 1976-1, pages 79-81.

Pantaleyev, A. (1983): GC, HAB, BUY (Stikine Copper); *in* Geology in British Columbia 1976, *B.C. Ministry of Energy, Mines and Petroleum Resources*, pages 122-125.

Pitcher, M.G. (1960): Fusulinids of the Cache Creek Group, Stikine River Area, Cassiar District, B.C.; unpublished M.Sc. thesis, Brigham Young University, 64 pages.

Preto, V.A., (1989): Iron Mask Batholith and Associated Fe-Cu-Au Deposits; *Mineral Deposits Division*, Geological Association of Canada, Copper-Gold Porphyry Workshop, Vancouver, April, 1989.

Rayner, G.H. and Ney, C.S. (1964): Report on Geological and Geochemical Surveys, Sphaler Creek Examination; *B.C. Ministry of Energy, Mines and Petroleum Resources*, Assessment Report 565.

Read, P.B. (1983): Geology, Classy Creek (10J/2E) and Stikine Canyon (104J/1W), British Columbia; *Geological Survey of Canada*, Open File 940.

Read, P.B. (1984): Geology Klastline River (104G/16E), Ealue Lake (104H/13W), Cake Hill (104I/4W), and Stikine Canyon (104J/1E), British Columbia; *Geological Survey of Canada*, Open File 1080.

Read, P.B. (1988): Report on the Trophy Property of Continental Gold Corporation, Liard Mining District, Northwestern British Columbia; private report for *Continental Gold Corporation.*

Read, P.B., Brown, R.L., Psutka, J.F., Moore, J.M., Journeay, M., Lane, L.S. and Orchard,M.J. (1989): Geology, More and Forrest Kerr Creeks (parts of 104B/10, 15, 16 & 104G/1, 2), Northwestern British Columbia; *Geological Survey of Canada,* Open File 2094.

Read, P.B., Psutka, J.F., Brown, R.L. and Orchard, M.J. (1983): "Tahltanian" Orogeny and Younger Deformations, Grand Canyon of the Stikine, British Columbia, *Geological Association of Canada*, Program with Abstracts, Volume 8, page A57.

Ricketts, B.D., Evenchick, C.A., Anderson, R.G. and Murphy, D.C. (1992): Bowser Basin, Northern British Columbia: Constraints on the Timing of Initial Subsidence and Stikinia-North America Terrane Interactions; *Geology,* Volume 20, pages 1119-1122.

Rubin, C.M. and Saleeby, J.B. (1991): Tectonic Framework of the Upper Paleozoic and Lower Mesozoic Alava Sequence: A Revised View of the Polygenetic Taku Terrane in Southeast Alaska; *in* Contributions to the Geology and Geophysics of Northwestern British Columbia and Southeastern Alaska, Anderson, R.G., Editor, *Canadian Journal of Earth Sciences,* Volume 28, pages 881-893.

Rui Lin (1991): Report on 13 Collections from the Telegraph Creek Area and Forrest Kerr/Iskut River Map Area, Northwestern British Columbia; *Geological Survey of Canada,* Report No. 2-RUI-1991, 5 pages.

Samson, S.D., McClelland, W.C., Patchett, P.J., Gehrels, G.E. and Anderson, R.G. (1989): Nd Isotopes and Phanerozoic Crustal Genesis in the Canadian Cordillera; *Nature,* Volume 337, pages 705-709.

Sillitoe, R.H. (1989a): Gold Deposits in Western Pacific Island Arcs: the Magmatic Connection; *in* The Geology of Gold Deposits: the Perspective in 1988, *Economic Geology,* Monograph 6, pages 274-291.

Sillitoe, R.H. (1989b): Gold and Silver Deposits in Porphyry Systems; *in* Bulk Mineable Precious Metal Deposits of Western United States, Symposium Proceedings, Schafer, R.W., Cooper, J.J. and Vikre, P.G., Editors, *Geological Society of Nevada,* pages 233-257.

Sinclair, A.J., Drummond, A.D., Carter, N.C. and Dawson, K.M. (1982): A Preliminary Analysis of Gold and Silver Grades of Porphyry-type Deposits in Western Canada; *in* Precious Metals in the Cordillera, Special Publication No. 10, *The Association of Exploration Geochemists,* pages 157-172.

Smith, M.T., Dickinson, W.R., and Geherels, G.E. (1993): Contractional Nature of Devonian-Mississippian Antler Tectonism along the North American Continental Margin; *Geology,* Volume 21, pages 21-24.

Souther, J.G. (1959): Chutine Map Area; *Geological Survey of Canada,* Preliminary Map 7-1959.

Souther, J.G. (1971): Geology and Mineral Deposits of Tulsequah Map Area; *Geological Survey of Canada,* Memoir 362, 76 pages.

Souther, J.G. (1972): Telegraph Creek Map Area, British Columbia; *Geological Survey of Canada,* Paper 71-44, 38 pages.

Souther, J.G. (1988): Geology, Mount Edziza Volcanic Complex, British Columbia; *Geological Survey of Canada,* Map 1623A.

Souther, J.G. (1992): The Late Cenozoic, Mount Edziza Volcanic Complex, British Columbia; *Geological Survey of Canada,* Memoir 420, 320 pages.

Souther, J.G. and Armstrong, J.E. (1966): North-central Belt of the Cordillera of British Columbia; *Canadian Institute of Mining and Metallurgy,* Special Volume 8, Tectonic History and Mineral Deposits of the Western Cordillera, pages 171-184.

Souther, J.G. and Symons, D.T.A. (1974): Stratigraphy and Paleomagnetism of Mount Edziza Volcanic Complex, Northwestern British Columbia; *Geological Survey of Canada,* Paper 73-32, 25 pages.

Spencer, B. and Dobell, J.P. (1958): Revised Surface Geology, Ore Blocks and Proposed Exploration; unpublished 1:2400 scale map for *American Metal Climax Inc.*

Steiger, R.H. and Jäger, E. (1977): Subcommission on Geochronology - Convention on the Use of Decay Constants in Geo- and Cosmochronology; *Earth and Planetary Science Letters,* Volume 36, pages 359-362.

Streckeisen, A. (1976): To Each Plutonic Rock Its Proper Name; *Earth-Sciences Review,* Volume 12, pages 1-33.

Sutherland Brown, A. (1976): Morphology and Classification; *in* Porphyry Deposits of the Canadian Cordillera, Sutherland Brown, A., Editor, *Canadian Institute of Mining and Metallurgy,* Special Volume 15, pages 44-51.

Sylvester, A.G. (1988): Stike-slip Faults; *Geological Society of America,* Bulletin, Volume 100, pages 1666-1703.

Taylor, K.J. (1989): Report on Soil, Silt and Rock Geochemical Sampling, Trenching and VLF-EM Surveying on the Galore Creek Group I, II, III Claims, Liard Mining Division; *B.C. Ministry of Energy, Mines and Petroleum Resources,* Assessment Report 19 397.

Thorstad, L.E., Gabrielse, H. (1986): The Upper Triassic Kutcho Formation, Cassiar Mountains, North-central British Columbia; *Geological Survey of Canada,* Paper 86-16, 53 pages.

Tozer, E.T. (1988): Report on Triassic Fossils from Telegraph Creek Map Area, British Columbia; *Geological Survey of Canada,* Report No. Tr-1-ETT 1988, 3 pages.

Watkins, R. (1985): Volcaniclastic and Carbonate Sedimentation in Late Paleozoic Island-arc Deposits, Eastern Klamath Mountains, California; *Geology,* Volume 3, pages 709-713.

Watson, J.L. (1969): Garnets of Stikine Copper's Galore Creek Property; unpublished B.Sc. thesis, *The University of British Columbia,* 27 pages.

Wernicke, B. and Klepacki, D.W. (1988): Escape Hypothesis for the Stikine Block; *Geology,* Volume 16, pages 461-464.

Wheeler, J.O. (1967): Tectonics; Chapter 2 *in* Canadian Upper Mantle Report, *Geological Survey of Canada,* Paper 67-41, pages 3-59.

Wheeler, J.O. and McFeely P. (1987): Tectonic Assemblage Map of the Canadian Cordillera and Adjacent Parts of the United States of America; *Geological Survey of Canada,* Open File 1565.

Wilson, J.L. (1982): Wolfcampian Rugose and Tabulate Corals (Coelenterata, Arthozoa) from the Lower Permian McCloud Limestone of Northern California; *Natural History Museum of Los Angeles County, Contributions in Science,* No. 337.

White, W.H., Harakal, J.E. and Carter, N.C. (1968): Potassium-Argon Ages of some Ore Deposits in British Columbia; *Canadian Institute of Mining and Metallurgy,* Bulletin, Volume 61, pages 1326-1334.

Wilcox, R.E., Harding, T.P. and Seely, D.R. (1973): Basic Wrench Tectonics; *American Association of Petroleum Geologists Bulletin,* Volume 57, pages 74-96.

Winchester, J.A. and Floyd, P.A. (1977): Geochemical Discrimination of Different Magma Series and their Differentiation Products Using Immobile Elements; *Chemical Geology*, Volume 20, pages 325-343.

Woodsworth, G.J., Anderson, R.G. and Armstrong, R.L. (1991): Plutonic Regimes; Chapter 15 *in* Geology of the Cordilleran Orogen in Canada, Gabrielse, H. and Yorath, C.J., Editors, Geological Survey of Canada, Geology of Canada, No. 4, pages 491-531 (also *Geological Society of America*, the Geology of North America, Volume G-2).

Yarrow, E. and Taylor, K.J. (1990): Report on Soil, Rock Geochemical Sampling, VLF-EM, Magnetometer and Diamond Drill Surveys on the Galore Creek Group I, II, III Claims, Liard Mining Division; *B.C. Ministry of Energy, Mines and Petroleum Resources*, Assessment Report 20 558.

# APPENDICES

## APPENDIX A-1
## MACROFOSSIL LOCATIONS, IDENTIFICATIONS AND AGES

| GSC Number | Sample Number | NTS MAP | UTM East | Zn 09 North | Strat Unit | Fauna-Description | Age | Ref. |
|---|---|---|---|---|---|---|---|---|
| ——— | 88JLO18-14 | 104G/03 | 378760 | 6340850 | lJHs | *Pityophyllum* sp. (conifer) | Middle Jurassic to Early Cretaceous | 3 |
| C154458 | 88JLO4-13 | 104G/03 | 358800 | 6333400 | mTs | *Daonella* sp. cf *degeeri* Boehm | Middle Triassic, Ladinian | 1A |
| C154459 | 88JLO5-12 | 104G/03 | 361000 | 6339050 | mTs | *Daonella* sp. cf *degeeri* Boehm | Middle Triassic, Ladinian | 1A |
| C154460 | 88JLO12-15 | 104G/04 | 345750 | 6343325 | uTSs | *Monotis* sp. | Late Triassic, upper Norian, Cordilleranus zone | 1A |
| C154461 | 88VKO5-9 | 104G/03 | 358225 | 6336500 | mTs | *Daonella* sp. cf *degeeri* Boehm | Middle Triassic, Ladinian | 1A |
| C154486 | 88JLO25-5 | 104G/03 | 356325 | 6337250 | uTSs | Spongiomorph, indet. | Prob Late Triassic | 1A |
| C154487 | 88JLO25-9 | 104G/03 | 356550 | 6337350 | uTSs | *Monotis subcircularis* Gabb | Late Triassic, late Norian, Cordilleranus zone | 1A |
| C154488 | 88JLO23-8 | 104G/03 | 365445 | 6328200 | lPSc | *Fomichevella* sp. | Late Carboniferous or Early Permian | 2A |
| C154489 | 88JLO25-3.2 | 104G/03 | 356255 | 6337200 | uTSs | *Monotis subcircularis* Gabb | Late Triassic, late Norian, Cordilleranus zone | 1A |
| C154490 | 88JLO25-6.3 | 104G/03 | 356425 | 6337250 | uTSs | *Monotis salinaria* Gabb | Late Triassic, late Norian, Cordilleranus zone | 1A |
| C154491 | 88JLO23-8.2 | 104G/03 | 365445 | 6328200 | lPSc | Clisiophyllid coral, indet., fusulinacean foraminifers | Late Carboniferous or Permian | 2A |
| C154492 | 88JLO14-16 | 104G/04 | 350825 | 6343590 | lPSc | Bryozoans, unidentifiable | Indeterminate | 2A |
| C154493 | 88VKO19-2 | 104G/03 | 359925 | 6331550 | lPSc | Productoid brachiopods, indet., schwagerinid fusulinacean foraminifers | Permian, Artinskian or younger | 2A |
| C154494 | 88DRH26-5 | 104G/03 | 360675 | 6333025 | lPSc | Productoid and spiriferid brachiopods, schwagerinid fusulinacean foraminifers | Permian | 2A |
| C154496 | 88DRH26-5D | 104G/03 | 361000 | 6333050 | lPSc | *Protolonsdaleiastraea* sp., ?*Bothrophyllum* sp.,fusulinacean foraminifers; *Petalaxis* sp., *Spiriferella* sp., gastropod indet. | Early Permian, Asselian or Sakmarian | 2A |
| C159064 | 88DRH30-14 | 104G/03 | 373540 | 6329350 | lCSc | *Solenodendron* sp. cf. S. furcatum (Smith) | Visean, probably late | 2A |
| C159065 | 88DRH30-10 | 104G/03 | 374050 | 6329390 | lCSc | Possibly bothrophyllid coral | Carboniferous or Permian | 2A |
| C159066 | 88DRH31-12 | 104G/03 | 368750 | 6323400 | lPSc | Unidentifiable productoid?, brachiopods, bryozoans and echinoderm fragments, schwagerinid fusulinacean foraminifers | Permian | 2A |
| C159067 | 88DRH31-1 | 104G/03 | 369050 | 6321300 | lPSc | Clisiophyllid coral, incomplete, fusulinacean and other foraminifers | Late Carboniferous or Early Permian Moscovian or younger | 2A |
| C159068 | 88DRH31-7 | 104G/03 | 369220 | 6322150 | lPSc | Bothrophyllid coral, indet. | Late Carboniferous or Permian | 2A |
| C159069 | 88JLO30-11 | 104G/03 | 372500 | 6327770 | lCSc | ?*Heritschioides* sp., fusulinacean foraminifers | Probably Early Permian | 2A |
| C159071 | 88DRH31-5.2 | 104G/03 | 369160 | 6321600 | lPSc | ?*Multithecopra* sp. (coral) | Carboniferous or Permian, probably no older than Late Carboniferous | 2A |
| C159072 | 88JLO31-8 | 104G/03 | 375300 | 6337400 | lJHs | *Weyla*? sp., terebratulid , and rhynchonellid brachiopods | Prob Early Jurassic | 1A |
| C159073 | 88JLO30-4 | 104G/03 | 373300 | 6327120 | lCSc | ?*Heritschioides* sp. | Late Carboniferous or Permian, probably Permian | 2A |
| C159074 | 88JLO30-8.4 | 104G/03 | 372880 | 6327625 | lCSc | Fasciculate colonial coral, poss. *Fomichevella* sp. | Prob Late Carboniferous or Permian | 2A |
| C159075 | 88VKO28-2 | 104G/03 | 375250 | 6332550 | uTSs | Pectenid bivalve, *Lima* (*Plagistoma*) sp. | Triassic or Jurassic | 1A |
| C159076 | 88JLO31-12.2 | 104G/03 | 376015 | 6336630 | uTSs | *Monotis subcircularis* Gabb | Late Triassic, late Norian, Cordilleranus zone | 1A |
| C159077 | 88DRH33-3 | 104G/03 | 366220 | 6326500 | lPSc | ?*Bothrophyllum* sp., rhynchonellid brachiopods, indet | Late Carboniferous or Permian | 2A |
| C159095 | 88VKO14-6 | 104G/04 | 348650 | 6347200 | uTSs | Belemnoid | Late Triassic | 4 |
| C167832 | 75APA-5A | 104G/04 | 345300 | 6343250 | uTSs | *Halobia* sp. | Carnian | 1B |
| C167834 | 75APA-20 | 104G/03 | 350000 | 6339150 | uTSs | *Halobia* sp. | Carnian | 1B |
| C189352 | 90JLO4-12 | 104G/03 | 359100 | 6333600 | mTs | *Halobia* sp. | Carnian | 1B |
| C189353 | 90JLO4-10 | 104G/03 | 358950 | 6333750 | lPSc | Echinoderm ossicles, *Spirifella* sp. | Permian, prob. Early | 2B |
| C189354 | 90JLO4-18 | 104G/03 | 359600 | 6333250 | lPSc | *Lytvophyllum* sp. | Early Permian | 2B |
| C189355 | 90JLO5-9.2 | 104G/03 | 371100 | 6320250 | lPSc | *Neospirifer* sp., ? *Spiriferella* sp., large productoid brachiopod, hexaphyllid coral? - in pebble, | Prob. Early Permian, mid Carboniferous clasts | 2B |
| C189356 | 90JLO5-17 | 104G/03 | 369750 | 6320000 | lPSc | *Heritschiodes* sp., tabulate coral indet. | Early Permian | 2B |
| C189371 | 90JLO10-9 | 104G/03 | 374035 | 6329270 | lCSc | ?*Fomichevella* sp. | Late Carboniferous or Permian | 2C |
| C189373 | 90JLO10-11 | 104G/03 | 373975 | 6329355 | lCSc | *Acrocyathus* sp. | Carboniferous, late Visean to Moscovian | 2C |

**REFERENCES:**

1. E.T. Tozer: A = Report TR-1-ETT-1988; B = personal communication.
2. E.W. Bamber: A = Report C3-EWB-1988; B = Report C1-EWB-1991; C = personal communication.
3. G.E. Rouse, Geological Sciences, U.B.C., Vancouver, B.C., personal communication.
4. H.W. Tipper, Geological Survey of Canada, Vancouver, B.C., personal communication.

## APPENDIX A-2
## CONODONT LOCATIONS, IDENTIFICATIONS, AGES AND COLOUR ALTERATION INDICES

| GSC Loc. Number | Sample Number | NTS Map | UTM East | Zone 9 North | Strat Unit | Fauna Description | Age | CAI Value | Source |
|---|---|---|---|---|---|---|---|---|---|
| C154455 | 88DRH6-4 | 104G/03 | 355075 | 6347050 | lPSc | *Hindeodus* sp., ramiform elements | Carboniferous - Early Triassic | 6.0-7.0 | 3 |
| C154456 | 88DRH6-5 | 104G/03 | 355125 | 6346500 | lPSc | *Hindeodus* sp., *Neogondolella* sp., *Neostreptognathodus* sp., ramiform elements | Early Permian, Artinskian | 6.0-7.0 | 3 |
| C154457 | 88DRH10-7 | 104G/03 | 353175 | 6345500 | lPSc | *Neostreptognathodus*? sp., ramiform elements | Prob Early Permian | 5 | 3 |
| C154462 | 88JLO13-2 | 104G/04 | 341550 | 6346200 | lPSc | *Neostreptognathodus*? sp., gnathodids, ramiform elements | Carboniferous - Early Permian | 5.6-7.0 | 3 |
| C154463 | 88JLO14-5 | 104G/03 | 349350 | 6343250 | mTs | *Neogondolella* ex gr. *regale* Mosher, ramiform elements | Middle Triassic, ?Anisian | 5 | 3 |
| C154465 | 88DRH12-4 | 104G/04 | 348150 | 6345600 | lPSc | *Neogondolella* sp. cf. N. *interedia* (Igo 1981), *Neostreptognathodus* sp. cf. N. *clarki* (Kozur 1976), ramiform elements | Early Permian, Artinskian | 5.5 | 3 |
| C154470 | 88VKO19-2 | 104G/03 | 359950 | 6331550 | lPSc | *Ellisonia* sp., *Neogondolella* sp., *Neostreptognathodus* spp., ramiform elements | Early Permian, Artinskian | 4.5-5.5 | 3 |
| C154471 | 88VKO20-9 | 104G/03 | 356680 | 6341950 | mTs | *Neogondolella* sp., ramiform elements | ?Triassic | 5 | 3 |
| C154474 | 88DRH24-3 | 104G/03 | 362900 | 6326550 | lPSc | *Neostreptognathodus* sp., ramiform elements | Early Permian, Artinskian | 6.0 | 3 |
| C154476 | 88JLO12-5 | 104G/04 | 344900 | 6343325 | uTSb | *Metapolygnathus* sp. | Late Triassic, Carnian | 5 | 3 |
| C154480 | 88DRH26-5 | 104G/03 | 360675 | 6333025 | lPSc | *Neostreptognathodus?* sp., ramiform elements | ?Early Permian, Artinskian | 5.0 | 3 |
| C154481 | 88DRH26-5B | 104G/03 | 360675 | 6333025 | lPSc | *Ellisonia*? sp., *Hindeodus* sp., *Neogondolella* sp., *Neostreptognathodus*? sp., ramiform elements | Early Permian | 4.5-5.5 | 3 |
| C154483 | 88DRH26-6 | 104G/03 | 361178 | 6333020 | lPSc | *Ellisonia* sp., *Hindeodus* sp., *Neogondolella* sp. cf. N. *idahoensis* (Youngquist, Miller & Hawley, 1951), *Neostreptognathodus* sp., ramiform elements | Early Permian, Artinskian | 4.0-6.5 | 3 |
| C154484 | 88DRH26-7 | 104G/03 | 361425 | 6333100 | lPSc | *Ellisonia* sp., *Hindeodus* sp., *Neogondolella* sp., *Neostreptognathodus* sp. cf. N. *rhuzhencevi* (Kozur 1976), ramiform elements | Early Permian | 5.5 | 3 |
| C154497 | 88JLO28-5 | 104G/03 | 350950 | 6343650 | lPSc | *Neogondolella* sp., *Neostreptognathodus* sp. | Early Permian, Artinskian | 7.0 | 3 |
| C154498 | 88JLO30-4.2 | 104G/03 | 373350 | 6327200 | lCSc | *Gnathodus*? sp. | Carboniferous | 7.0 | 3 |
| C154499 | 88JLO30-6 | 104G/03 | 373150 | 6327225 | lCSc | ramiform elements | Indeterminate | 5.5 | 3 |
| C159053 | 88JLO30-13 | 104G/03 | 372025 | 6327550 | lCSc | *Gnathodus*? sp., ramiform elements | Carboniferous | 5 | 3 |
| C159056 | 88VKO28-3.2 | 104G/03 | 375075 | 6332200 | uTSs | *Epigondolella mosheri* (Kuzor & Mostler 1971) | Triassic, late Middle-late Norian | 3.5 | 3 |
| C159058 | 88DRH30-7 | 104G/03 | 374275 | 6329000 | lCSc | *Cavusgnathus* sp., *Polygnathus?* sp., Lochriea? sp., ramiform elements | Early Carboniferous | 5.5-7.0 | 3 |
| C159063 | 88DRH31-13 | 104G/03 | 368700 | 6323650 | lPSc | cavusgnathoid indet., ramiform elements | Carboniferous - Early Permian | 5 | 3 |
| C159078 | 88VKO29-5 | 104G/03 | 372235 | 6326290 | lCSc | *Gnathodus* spp., ramiform elements | Early Carboniferous | 5.5-6.0 | 3 |
| C159080 | 88VKO29-8 | 104G/03 | 371720 | 6326945 | lCSc | ramiform elements | Silurian - Permian | 5 | 3 |
| C159086 | 88DRH34-4.1 | 104G/03 | 356200 | 6346640 | lPSc | *Hindeodus* sp., *Neogondolella* sp., *Neostreptognathodus*? sp. | Early Permian, ?Artinskian | 5.5-7.0 | 3 |
| C159090 | 88JLO34-3 | 104G/04 | 347700 | 6341100 | uTSs | *Epigondolella* sp., ramiform elements | Late Triassic, Norian | 5 | 3 |
| C159096 | 88DRH30-2-2 | 104G/03 | 375130 | 6329150 | lCSc | *Gnathodus?* sp., ramiform elements | Early? Carboniferous | 5.5 | 3 |
| C159098 | 90JLO-10-4 | 104G/03 | 374225 | 6329080 | lCSc | *Declinognathodus* sp. cf. D. *noduliferous* (Ellison & Graves 1941) | Late Carboniferous, late Namurian - Bashkirian | ~5 | 1 |
| C159953 | 88OF-PBR-3F | 104G/03 | 361370 | 6338550 | mTs | *Budurovignathus* ex gr. *mungoensis* (Diebel), *Neogondolella inclinota* Kovacs, ramiform elements | Middle Triassic | 5 | 2 |
| C159955 | 88OF-PBR-5F | 104G/03 | 361285 | 6338820 | lPSc | *Neostreptognathodus pequopensis* Behnken, *Hindeodus*? sp., ramiform elements | Early Permian, Artinskian | 5 | 2 |
| C159956 | 88OF-PBR-6F | 104G/03 | 356925 | 6342006 | mTs | *Neogondolella excelsa* (Mosher), ramiform elements | Middle Triassic | 5 | 2 |
| C167829 | 90VKO4-24 | 104G/03 | 373563 | 6329823 | lCSc | gnathodid indet. | Carboniferous - Early Permian | 5.0-6.0 | 1 |
| C167929 | 90DBR90-15 | 104G/04 | 347806 | 6346734 | lPSc | gnathodid indet. | Carboniferous - Early Permian | ~5 | 1 |
| C189382 | 90JLO3-10 | 104G/03 | 350386 | 6342793 | lPSc | *Neogondolella* sp. indet., ramiform elements | probably Permian | 6.0-7.0 | 1 |
| C189384 | 90JLO4-13 | 104G/03 | 359200 | 6333539 | lPSc | *Hindeodus* sp., *Neogondolella intermedia* Igo 1981, *Neostreptognathodus pequopensis* Behnken 1975, *Ellisonia* sp., ramiform elements | Early Permian, Artinskian | 4.5 | 1 |
| C189386 | 90JLO5-1 | 104G/03 | 369258 | 6329477 | lCSc | ramiform element | Ordivician-Triassic | | 1 |
| C189388 | 90JLO5-21 | 104G/03 | 358961 | 6332556 | lPSc | *Neogondolella* sp., ramiform elements | Permian | ~4 | 1 |
| C189389 | 90JLO5-22 | 104G/03 | 359162 | 6332556 | mTs | *Ellisonia* sp(p)., *Neospathodus* ex gr. *conservtivus* (Muller 1956), *Neospathodus discreta* (Muller 1956), ramiform elements | Early Triassic, Smithian | 4.5 | 1 |
| C189391 | 90JLO6-9 | 104G/03 | 370425 | 6323444 | uCScg | ichthyolith, limestone clasts | Phanerozoic | | 1 |
| C189393 | 90JLO7-16 | 104G/04 | 347500 | 6346650 | lPSc | *Streptognathodus* sp. cf. *S. elegantulus* Stauffer & Plummer 1932, *Streptognathodus* sp. indet. | Late Carboniferous-Early Permian probably Gzhelian-Asselian | 5 | 1 |
| C189395 | 90JLO2-9 | 104G/03 | 346407 | 6345028 | lPSc | *Hindeodus*? sp. indet., *Neogondolella* sp. indet., *Neostreptognathodus*? sp. indet., ramiform elements | probably Early Permian, Artinskian | 6.0-7.0 | 1 |

*Source of fauna description, age and CAI:
1 = Orchard (1991b).
2 = Orchard (1993).
3 = Orchard (1994).

## BARREN SAMPLES

| | | | | | |
|---|---|---|---|---|---|
| C154466 | 88DRH-12-8 | 104G/04 | 348707 | 6345160 | lPSc |
| C154467 | 88DRH-14-4-2 | 104G/03 | 355199 | 6342609 | uTSb |
| C154475 | 88DRH-24-8-1 | 104G/03 | 363705 | 6326079 | lPSc |
| C154479 | 88DRH-26-3 | 104G/03 | 360298 | 6333003 | lPSc |
| C154482 | 88DRH-28-5-2 | 104G/03 | 361990 | 6322751 | uTSs |
| C159059 | 88DRH-30-10- | 104G/03 | 373956 | 6329349 | lCSc |
| C159060 | 88DRH-30-11- | 104G/03 | 373918 | 6329475 | lCSc |
| C159061 | 88DRH-30-13- | 104G/03 | 373598 | 6329453 | lPSmv |
| C159062 | 88DRH-30-14- | 104G/03 | 373512 | 6329338 | lPSmv |
| C159057 | 88DRH-30-5-1 | 104G/03 | 374527 | 6329201 | lCSc |
| C154454 | 88JLO-12-10- | 104G/03 | 345078 | 6343183 | uTSb |
| C154464 | 88JLO-15-9-2 | 104G/04 | 341303 | 6344369 | lPSmv |
| C154468 | 88JLO-18-8 | 104G/03 | 378838 | 6340503 | lJHs |
| C154472 | 88JLO-23-2 | 104G/03 | 364349 | 6327156 | lPSmv |
| C154473 | 88JLO23-13 | 104G/03 | 364320 | 6328180 | lPSc |
| C154477 | 88JLO-25-4-1 | 104G/03 | 356286 | 6337286 | uTSs |
| C154500 | 88JLO-30-8-2 | 104G/03 | 372899 | 6327640 | lCSc |
| C159051 | 88JLO-30-9 | 104G/03 | 372680 | 6327693 | lCSc |
| C159052 | 88JLO-30-12 | 104G/03 | 372257 | 6327773 | lCSc |
| C159083 | 88JLO-32-3 | 104G/03 | 367448 | 6329055 | lPSc |
| C159084 | 88JLO-32-7 | 104G/03 | 368033 | 6328873 | lPSc |
| C159085 | 88JLO-32-9 | 104G/03 | 368019 | 6328787 | lPSmv |
| C154453 | 88JLO-5-10-1 | 104G/03 | 361365 | 6338711 | mTs |
| C154457 | 88VKO-10-7 | 104G/03 | 360175 | 6340657 | lPSc |
| C154469 | 88VKO-19-1 | 104G/03 | 360030 | 6331092 | lPSc |
| C159054 | 88VKO-26-1 | 104G/03 | 372626 | 6330034 | lJHs |
| C159055 | 88VKO-26-10 | 104G/03 | 372100 | 6330002 | lJHs |
| C159079 | 88VKO-29-10 | 104G/03 | 371448 | 6327370 | lCSc |
| C159081 | 88VKO-29-12 | 104G/03 | 370752 | 6327221 | lCSc |
| C159082 | 88VKO-30-1 | 104G/03 | 359582 | 6347337 | lPSc |
| C159087 | 88VKO-31-6 | 104G/04 | 363316 | 6324264 | lPSc |
| C159089 | 88VKO-33-13 | 104G/04 | 348829 | 6346949 | lPSc |

## APPENDIX A-3
## FUSULINACEAN (PROTOZOA) LOCATIONS, IDENTIFICATIONS AND AGES

| GSC Loc. Number | Sample Number | UTM East | Zone 09 North | Fauna-Description | Age | Ref. |
|---|---|---|---|---|---|---|
| C154491 | 88JLO23-8.2 | 365445 | 6328200 | *Schwagerina mankomenensis* Petocz, *Parafusulina* sp. indet.<br>*Pseudofusulinella* sp. *cf. P. spicata* Skinner & Wilde<br>*Pseudofusulinella* sp. | Early Leonardian (Artinskian) | 2 |
| C154488 | 88JLO23-8 | 365445 | 6328200 | Endothyridae ghosts, *Globivalvulina* ghost | Middle Bashkirian, probably mid-Carboniferous | 5 |
| --------- | 88DRH31-8 | 368925 | 6322475 | Fusulinacean foraminifers | Early Permian | 1 |
| C154493 | 88VKO19-2 | 359925 | 6331550 | *Parafusulina* (*Skinnerella*) sp. cf. *P.* (*S.*) *megagrandis* Ross<br>*Schwagerina* sp. *cf. S guembeli* Dunbar & Skinner | Early Leonardian (Artinskian) | 2 |
| C154494 | 88DRH26-5 | 360675 | 6333025 | *Parafusulina* sp. cf. P. *gruperaensis* (Thompson & Miller) | Early Leonardian (Artinskian) | 2 |
| C154495 | 88DRH26-4 | 360575 | 6333000 | *Schwagerina* sp. cf. *S. jenkinsi* Thorsteinsson<br>*Pseudofusulinella* sp. cf. *P. danneri* Skinner & Wilde | Early Leonardian (Artinskian) | 2 |
| C154496 | 88DRH26-5D | 361000 | 6333050 | ?*Paraschwagerina* sp. indet., *Pseudofusulinella* sp. | Late Wolfcampian (Sakmarian) | 2 |
| C159066 | 88DRH31-12 | 368750 | 6323400 | *Schwagerina* sp. cf. *S. mccloudensis* Skinner & Wilde<br>*Pseudofusulinella* sp. indet. | Late Wolfcampian (Sakmarian) | 2 |
| C159065 | 88DRH30-10 | 374050 | 6329390 | Endothyridae ghosts | Insufficient for zonation | 5 |
| C159067 | 88DRH31-1 | 369050 | 6321300 | *Schubertella* spp. | Late Wolfcampian (Sakmarian) | 2 |
| C159069 | 88JLO30-11 | 372500 | 6327770 | Fusulinacean foraminifers | Prob. Early Permian | 3 |
| C159073 | 88JLO30-4 | 373300 | 6327120 | Disolved Apterrinellids, silicified Archaediscidau<br>*Stacheoides meandriformis* Mamet and Rudloff, *Ungdarella* sp. | Prob. mid-Carboniferous | 5 |
| C159074 | 88JLO30-8.4 | 372880 | 6327625 | Stacheinae | Insufficient for zonation | 5 |
| C159077 | 88DRH33-3 | 366220 | 6326500 | *Pseudofusulinella* sp. , *Schubertella* spp. | ?Late Wolfcampian (Sakmarian) | 2 |
| --------- | 88DRH31-13 | 368700 | 6323660 | Fusulinacean foraminifers | Early Permian | 1 |
| C189354 | 90JLO4-18 | 359600 | 6333250 | *Globivalvulina* sp., *Syzrania* sp., small fusulinaceans, indet. | Early Permian | 4 |
| C189355 | 90JLO5-9.2 | 371100 | 6320250 | **Carbonate clasts are mixture of late Mississippian-Peratrovich facies and Middle Carboniferous - red algae facies** | | |
| | | | | A) *Climcammina* sp., *Globivalvulina* sp., *Stacheoides*? sp., silic. Velebitellinae | Mid-Carboniferous | 6 |
| | | | | B) *Asteroarchaediseus* sp., *Climacammina* sp., *Endothyra* sp., *Stacheoides* sp. | Mid-Carboniferous | 6 |
| | | | | C) *Biseriella* sp., *Globivalvulina* sp., *Komia abundans* Korde | Mid-Carboniferous, middle Bashkirian | 6 |
| | | | | D) *Archaediscus* sp., *Calcisphaera* sp., *Climacammina* sp., *Earlandia* sp.,*Endothyra* sp., *Insolentitheca* sp., *Janichewskina*? sp., *Koskinobigenerina* sp., *Mediocris* sp., *Pseudoendothyra* sp., *Tetrataxis* sp. | Typical Peratrovich assemblage<br>Mid-Carboniferous, Serpukhovian | 6 |
| | | | | E) *Asteroarchaediscus* sp., *Climacammina* sp., *Fourstonella*? sp., *Priscella* sp.,*Earlandia vulgaris* (Rauzer-Chernoussova and Reitlinger), *Hexaphyllia* sp. | Typical Peratrovich assemblage<br>Mid-Carboniferous, Serpukhovian | 6<br>6 |
| | | | | F) *Komia abundans* Korde Typical Peratrovich assemblage | Mid-Carboniferous, middle Bashkirian | 6 |
| | | | | G) *Berestovia*, *Ungdarella peratrovichensis* Mamet and Rudloff | | |
| C189356 | 90JLO5-17 | 369900 | 6320000 | *Pseudovidalina* sp., *Climacammina* sp. | Early Permian | 4 |


REFERENCES

1 = D. Rhys and W.R. Danner (1989, personal communication).

2 = Lin Rui (1991).

3 = E.W. Bamber (1988).

4 = S. Pinard *in* E.W. Bamber (1991).

5 = B.L. Mamet (1991a).

6 = B.L. Mamet (1991b).


## APPENDIX A-4
## BIOSTRATIGRAPHY OF THE CARBONIFEROUS CARBONATE AT ROUND LAKE

| GSC Loc. Number | Sample Number | UTM East | Zn 09 North | Fauna-Description | Age | Ref. |
|---|---|---|---|---|---|---|
| C189363 | 90JLO10-1 | 374350 | 6329000 | Slightly stressed, silicified, former echinoderm wackestone. | | 1 |
| C189364 | 90JLO10-2 | 374305 | 6329025 | Strongly deformed, fluidal, former echinid wackestone. | | 1 |
| C189365 | 90JLO10-3 | 374265 | 6329050 | Coarse breccia fragments in bioclastic grainstone. Crinoids, bryozoans, brachiopods. Radiaxal cement. Part of material is reworked from a waulsortian mud-mound. Apterinellids, *Biseriella* sp., cf. *Beresella*? sp., *Bradyina* sp., *Climacammina* sp., *Deckerella*? sp., *Endothyra* sp., *Globivalvulina* sp (coarse diaphanotheca)., *Komia* sp., Ozawainellidae, *Palaeotextularia* sp., *Pseudoendothyra* sp., *Pseudoglomospira* sp., *Pseudostaffella* sp., *Tetrataxis* sp. | Mid-Carboniferous [Zone 21 (middle Bashkirian) or younger]. | 1 |
| C189366 | 90JLO10-4 | 374225 | 6329080 | Apterinellids, *Bradyina* sp., *Climacammina* sp., *Pseudoendothyra* sp., *Tetrataxis* sp. | Same as C-189365 middle Bashkirian | 1 |
| C189366 | 90JLO10-4 | 374225 | 6329080 | *Declinognathodus* sp. cf. *D. noduliferous* (Ellison & Graves 1941). | Late Early Carboniferous, Late Namurian -Bashkirian | 2 |
| C189367 | 90JLO10-5 | 374175 | 6329150 | Fine-grained, laminated mudstone, crinoidal grainstone stringers. | | 1 |
| C189368 | 90JLO10-6 | 374120 | 6329200 | Crinoidal wackestone. Some stress. | | 1 |
| C189369 | 90JLO10-7 | 374100 | 6329220 | Tectonically reoriented, stressed, fluidal echinoderm packstone. Sheared *Komia* strands, vague foraminiferal ghosts, palaeotextulariidae ghosts. | | 1 |
| C189370 | 90JLO10-8 | 374070 | 6329250 | Sponge boundstone/crinoidal packstone. Pressure solution. Brachiopod spines. Abundant spicules(in situ). *Earlandia* sp., *Endothyra* sp. | | 1 |
| C189371 | 90JLO10-9 | 374035 | 6329270 | Corals in crinoidal wackestone. | | 1 |
| C189371 | 90JLO10-9 | 374035 | 6329270 | ?*Fomichevella* sp. | Late Carboniferous or Permian | 3 |
| C189372 | 90JLO10-10 | 374010 | 6329325 | Stressed laminated mudstone/siltstone/crinoidal wackestone. Sponge spicules. | | 1 |
| C189373 | 90JLO10-11 | 373975 | 6329355 | Tectonically stressed, fluidal, echinid wackestone. | | 1 |
| C189373 | 90JLO10-11 | 373975 | 6329355 | *Acrocyathus* sp. | Carboniferous, late Visean to Moscovian | 3 |
| C189374 | 90JLO10-12 | 373945 | 6329395 | Laminated, stressed, sheared former crinoidal wackestone/mudstone. | | 1 |
| C189375 | 90JLO10-13 | 373905 | 6329430 | Tectonically stressed, former echinid wackestone. | | 1 |
| C189376 | 90JLO10-14 | 373875 | 6329470 | Stressed echinoderm-sponge lump-pellet packestone. Foraminiferal ghosts strongly deformed. Apterinellids, *Calcitornella* sp., *Calcivertella* sp., *Climacammina* sp., *Eostaffella* sp., cf. *Pseudopalaeospiroplectammina*?sp. | Mid-Carboniferous | 1 |
| C189377 | 90JLO10-15 | 373830 | 6329490 | Tectonically deformed, echinoderm-lump-pellet packestone/grainstone. Forams are deformed. *Deckerella* sp., *Eostaffella* sp., *Komia* sp., Ozawainellidae, *Palaeotextularia* sp., *Pseudoendothyra* sp. | Mid-Carboniferous | 1 |
| C189378 | 90JLO10-16 | 373820 | 6329500 | Recrystallized crinoidal wackestone, matrix as microspar,spicules and forams dissolved and silicified. *Ammovertella*?sp., *Anthracoporellopsis* sp., *Pseudoendothyra* sp., *Pseudostaffella* sp., *Volvotextularia* sp. | Mid-Carboniferous | 1 |


REFERENCES

1 = B.L. Mamet (1991).

2 = M.J. Orchard (1991b).

3 = E.W. Bamber (1988).


Note:
For sample locations *see* plate A-1 which identifies the locations in sequence using the last digits of the sample number given in Appendix A-4.

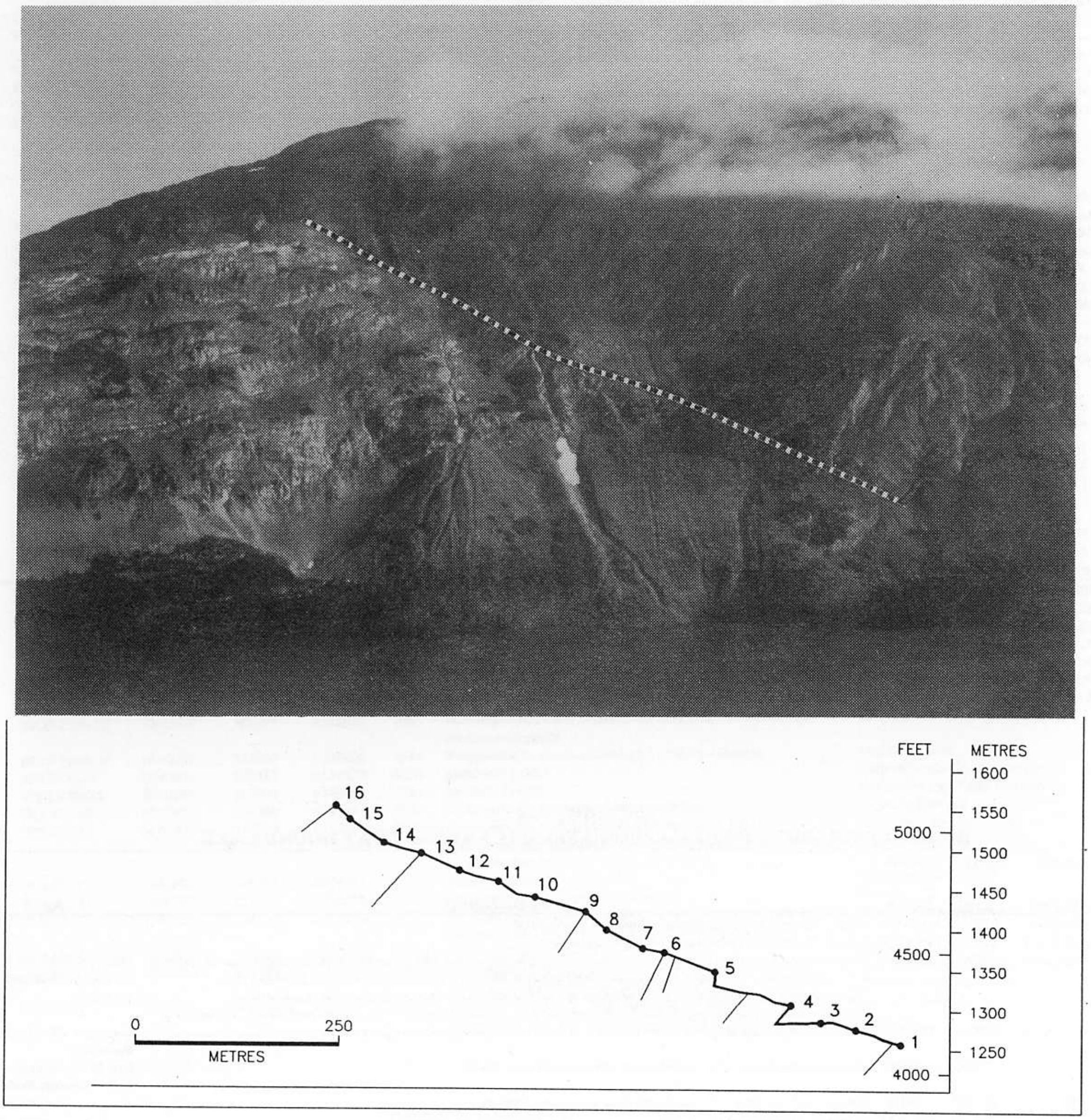


Plate A-1. Carboniferous carbonate section at Round Lake, viewed northward. Dotted line shows sampling traverse which corresponds with line diagram. Fossil data are presented in Appendix A-4.

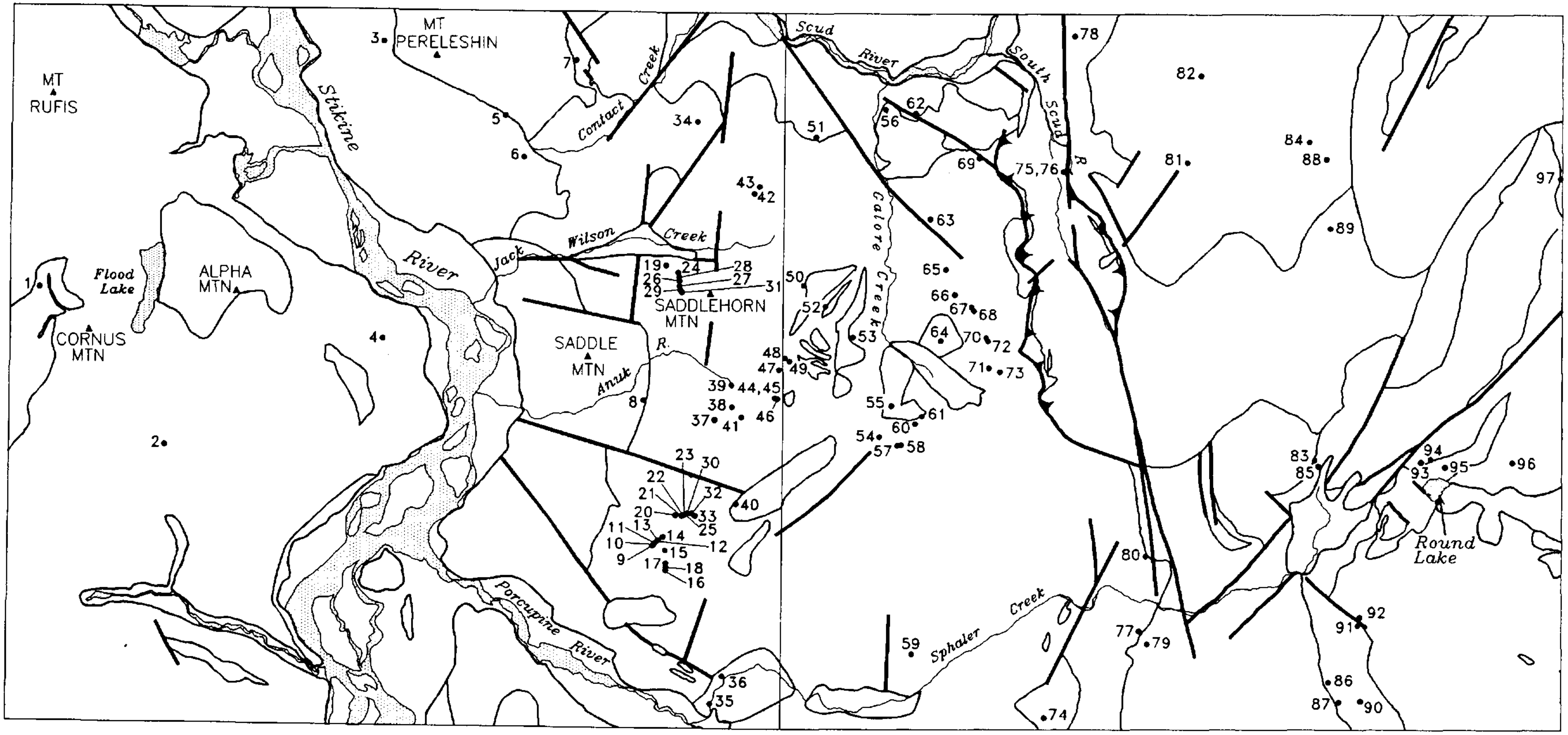


Figure B-1. Sample locations for whole-rock chemical analyses of volcanic and plutonic rocks.

## APPENDIX B
## WHOLE-ROCK AND TRACE ELEMENT CHEMICAL ANALYSES OF VOLCANIC AND PLUTONIC ROCKS

| MAP NO. | 38 | 57 | 58 | 54 | 49 | 48 | 66 | 67 | 45 | 44 | 47 | 41 | 60 | 61 | 55 |
|---|---|---|---|---|---|---|---|---|---|---|---|---|---|---|---|
| SAMPLE | 74APA-114-1 | 75APA-125-1 | 75APA-126-1 | 75APA-139-1 | 75APA-146-1 | 75APA-147-1 | 75APA-159-1 | 88DRH-19-6-2 | 90JLO8-8 | 90JLO8-9 | 90VKO3-19 | 74APA-116-1 | 75APA-128-1 | 75APA-129-1 | 75APA-156-1 |
| NTS | 104G/04 | 104G/03 | 104G/03 | 104G/04 | 104G/03 | 104G/03 | 104G/03 | 104G/03 | 104G04 | 104G04 | 104G04 | 104G/04 | 104G/03 | 104G/03 | 104G/03 |
| UTM EAST | 346664 | 353080 | 358228 | 352350 | 348947 | 348778 | 355510 | 356166 | 348335 | 348335 | 348528 | 347017 | 353786 | 354053 | 352872 |
| UTM NORTH | 6332394 | 6330715 | 6330727 | 6331150 | 6334116 | 6334257 | 6336573 | 6336021 | 6332693 | 6332695 | 6333792 | 6331990 | 6331555 | 6331837 | 6332266 |
| STRAT GROUP | TJt | TJt | TJt | TJt | TJt | TJt | TJt | TJt | TJt | TJt | TJt | TJv | TJv | TJv | TJv |
| ROCK TYPE * | XSTF | LPTF | LPTF | LPTF | CLTF | CLTF | TUFF | TUFF | XSTF | XSTF | XSTF | XSTF | FLOW | FLOW | TUFF |
| SiO2 | 47.73 | 51.81 | 52.06 | 50.55 | 52.22 | 49.14 | 43.28 | 44.83 | 50.90 | 50.51 | 48.28 | 49.87 | 57.27 | 46.89 | 51.61 |
| TiO2 | 0.49 | 0.83 | 0.93 | 0.70 | 0.34 | 0.78 | 0.60 | 0.58 | 0.44 | 0.43 | 0.65 | 0.58 | 0.56 | 0.72 | 0.76 |
| Al2O3 | 13.09 | 15.94 | 17.10 | 16.62 | 15.71 | 13.25 | 11.35 | 12.06 | 15.75 | 15.26 | 13.69 | 16.68 | 16.25 | 13.41 | 17.60 |
| Fe2O3 | 7.44 | 7.78 | 8.97 | 9.66 | 6.07 | 10.17 | 8.88 | 8.36 | 7.70 | 6.91 | 9.37 | 8.35 | 5.39 | 7.06 | 8.09 |
| MnO | 0.19 | 0.18 | 0.21 | 0.28 | 0.16 | 0.16 | 0.41 | 0.15 | 0.17 | 0.17 | 0.15 | 0.18 | 0.17 | 0.16 | 0.22 |
| MgO | 2.75 | 1.96 | 3.17 | 3.27 | 3.30 | 5.13 | 4.75 | 4.61 | 3.87 | 3.59 | 5.17 | 4.60 | 2.19 | 1.42 | 3.26 |
| CaO | 11.39 | 5.61 | 2.23 | 3.86 | 5.75 | 7.56 | 9.07 | 10.50 | 5.26 | 6.33 | 8.57 | 7.49 | 4.69 | 10.55 | 5.39 |
| Na2O | 2.50 | 1.25 | 4.42 | 5.10 | 3.26 | 3.57 | 0.31 | 1.45 | 3.34 | 3.77 | 4.37 | 3.30 | 3.44 | 2.26 | 3.67 |
| K2O | 6.39 | 7.19 | 4.98 | 3.92 | 6.43 | 3.77 | 6.05 | 6.24 | 5.84 | 5.54 | 2.42 | 5.74 | 3.65 | 5.93 | 4.35 |
| P2O5 | 0.39 | 0.57 | 0.57 | 0.48 | 0.25 | 0.37 | 0.28 | 0.46 | 0.41 | 0.40 | 0.48 | 0.48 | 0.37 | 0.48 | 0.53 |
| TOTAL | 92.36 | 93.32 | 94.64 | 94.44 | 93.49 | 93.90 | 84.98 | 89.24 | 93.68 | 92.91 | 93.15 | 97.27 | 93.98 | 88.88 | 95.48 |
| CO2 | 6.60 | 1.32 | 3.12 | 2.50 | 4.00 | 2.95 | 11.40 | 7.58 | 3.48 | 4.52 | 4.50 | 1.58 | 3.52 | 8.69 | 1.72 |
| S | 0.14 | 0.00 | 0.00 | 0.22 | 0.04 | 0.00 | 0.02 | 0.01 | 0.03 | 0.03 | 0.01 | 0.18 | 0.02 | 0.00 | 0.00 |
| LOI | - | - | - | - | - | - | - | 10.33 | 5.22 | 5.97 | 6.45 | - | - | - | - |
| H2OM | 0.09 | 0.22 | 0.22 | 0.40 | 0.30 | 1.94 | 2.53 | - | - | - | - | 0.10 | 0.20 | 0.15 | 0.19 |
| H20P | 0.79 | 5.29 | 0.21 | 1.21 | 1.75 | 0.00 | 0.00 | - | - | - | - | 0.81 | 2.71 | 1.41 | 2.51 |
| H2O | - | - | - | - | - | - | - | - | - | - | - | - | - | - | - |
| c Fe2O3 | 3.76 | 7.08 | 7.93 | 5.42 | 2.05 | 4.22 | 4.93 | 5.36 | - | - | - | 3.08 | 2.34 | 5.99 | 3.44 |
| c FeO | 3.31 | 0.63 | 0.94 | 3.81 | 3.62 | 5.35 | 3.55 | 2.70 | 5.17 | 4.72 | 5.20 | 4.74 | 2.75 | 0.96 | 4.18 |
| Ni | - | - | - | - | - | - | 50 | 46 | - | - | - | - | - | - | - |
| Mo | - | - | - | - | - | - | - | - | - | - | - | - | - | - | - |
| Cr | - | - | - | - | - | - | 82 | 76 | - | - | - | - | - | - | - |
| Ba | - | - | - | - | - | - | 739 | 1200 | - | - | - | - | - | - | - |
| Rb | - | - | - | - | - | - | 96 | 140 | 97 | 96 | 31 | - | - | - | - |
| Sr | - | - | - | - | - | - | 9200 | 540 | - | - | - | - | - | - | - |
| Nb | - | - | - | - | - | - | 5.0 | 20.0 | 13 | 12 | 8 | - | - | - | - |
| Y | - | - | - | - | - | - | 10 | 8 | 20 | 22 | 19 | - | - | - | - |
| Zr | - | - | - | - | - | - | 27 | 69 | 81 | 81 | 57 | - | - | - | - |
| Yb | - | - | - | - | - | - | - | 5 | - | - | - | - | - | - | - |
| Ta | - | - | - | - | - | - | - | 1.00 | - | - | - | - | - | - | - |
| La | - | - | - | - | - | - | - | 7.00 | 28.00 | 26.00 | 20.00 | - | - | - | - |
| V | - | - | - | - | - | - | 166 | - | 259 | 243 | 303 | - | - | - | - |
| K2O/Na2O | 2.56 | 5.75 | 1.13 | 0.77 | 1.97 | 1.06 | 19.52 | 4.30 | 1.75 | 1.47 | 0.55 | 1.74 | 1.06 | 2.62 | 1.19 |
| K2O + Na2O | 8.89 | 8.44 | 9.4 | 9.02 | 9.69 | 7.34 | 6.36 | 7.69 | 9.18 | 9.31 | 6.79 | 9.04 | 7.09 | 8.19 | 8.02 |
| Al2O3/ CaO+Na2O+K2O | 0.41 | 0.78 | 1.02 | 0.84 | 0.69 | 0.56 | 0.48 | 0.43 | 0.74 | 0.64 | 0.54 | 0.66 | 0.89 | 0.46 | 0.86 |

# APPENDIX B
## WHOLE-ROCK AND TRACE ELEMENT CHEMICAL ANALYSES OF VOLCANIC AND PLUTONIC ROCKS

| MAP NO. | 65 | 68 | 70 | 46 | 28 | 27 | 33 | 17 | 15 | 9 | 10 | 12 | 80 | 42 | 43 |
|---|---|---|---|---|---|---|---|---|---|---|---|---|---|---|---|
| SAMPLE | 75APA-161-1 | 88DRH-19-4 | 90JLO4-2 | 90JLO7-15 | 74APA-139-1 | 74APA-142-1 | 74APA-33-1 | 74APA-38-1 | 74APA-41-1 | 74APA-43-1 | 74APA-44-1 | 74APA-46-1 | 74APA-86-1 | 88JLO 34-10 | 88JLO 34-8 |
| NTS | 104G/03 | 104G/03 | 104G03 | 104G04 | 104G/04 | 104G/04 | 104G/04 | 104G/04 | 104G/04 | 104G/04 | 104G/04 | 104G/04 | 104G/03 | 104G/04 | 104G/04 |
| UTM EAST | 355177 | 356234 | 356635 | 348450 | 344783 | 344778 | 345112 | 343915 | 343901 | 343416 | 343480 | 343592 | 362597 | 347796 | 348011 |
| UTM NORTH | 6337520 | 6335883 | 6334824 | 6332661 | 6337544 | 6337204 | 6328234 | 6326421 | 6326932 | 6327136 | 6327179 | 6327304 | 6326130 | 6340746 | 6340970 |
| STRAT GROUP | TJv | TJv | TJv | TJv | uTSb | uTSb | uTSb | uTSb | uTSb | uTSb | uTSb | uTSb | uTSb | uTSd | uTSd |
| ROCK TYPE * | TUFF | BSLT | FLOW | FLOW | FLBR | FLBR | FLBR | FLBR | FLBR | FLBR | FLBR | FLBR | FLBR | TRCT | TRCT |
| SiO2 | 52.36 | 45.12 | 42.67 | 50.35 | 50.40 | 48.37 | 59.44 | 51.01 | 56.81 | 50.74 | 51.33 | 51.60 | 45.47 | 56.16 | 49.77 |
| TiO2 | 0.53 | 0.64 | 0.59 | 0.51 | 0.91 | 0.84 | 0.70 | 0.90 | 0.86 | 0.73 | 0.82 | 0.94 | 1.17 | 0.62 | 1.07 |
| Al2O3 | 18.50 | 12.65 | 12.12 | 14.17 | 15.07 | 14.69 | 17.47 | 16.47 | 15.60 | 14.58 | 14.64 | 14.37 | 17.81 | 19.22 | 15.38 |
| Fe2O3 | 4.24 | 8.92 | 7.59 | 9.11 | 9.68 | 8.21 | 6.53 | 8.72 | 7.42 | 9.36 | 10.35 | 9.92 | 11.14 | 5.00 | 10.97 |
| MnO | 0.14 | 0.18 | 0.14 | 0.16 | 0.16 | 0.19 | 0.24 | 0.21 | 0.14 | 0.15 | 0.19 | 0.19 | 0.22 | 0.21 | 0.20 |
| MgO | 0.85 | 3.72 | 8.84 | 4.40 | 4.26 | 3.40 | 3.31 | 3.46 | 2.43 | 4.11 | 4.87 | 4.09 | 5.42 | 1.05 | 5.11 |
| CaO | 5.08 | 10.72 | 10.22 | 9.53 | 8.42 | 11.45 | 2.30 | 9.71 | 6.14 | 5.93 | 8.62 | 8.24 | 7.02 | 6.22 | 10.31 |
| Na2O | 2.96 | 1.86 | 0.77 | 4.70 | 4.81 | 4.26 | 2.68 | 2.31 | 2.92 | 2.17 | 2.17 | 1.14 | 4.13 | 4.81 | 2.31 |
| K2O | 8.93 | 5.18 | 2.07 | 2.69 | 2.88 | 2.78 | 3.93 | 4.46 | 4.25 | 5.48 | 4.53 | 3.33 | 1.21 | 3.74 | 1.28 |
| P2O5 | 0.15 | 0.46 | 0.15 | 0.58 | 0.41 | 0.44 | 0.25 | 0.46 | 0.44 | 0.53 | 0.61 | 0.73 | 0.22 | 0.18 | 0.26 |
| TOTAL | 93.74 | 89.45 | 85.16 | 96.20 | 97.00 | 94.63 | 96.85 | 97.71 | 97.01 | 93.78 | 98.13 | 94.55 | 93.81 | 97.21 | 96.66 |
| CO2 | 4.18 | 8.00 | 9.42 | 2.37 | 3.30 | 3.99 | 0.62 | 1.98 | 1.17 | 3.92 | 0.70 | 2.97 | 1.25 | 1.29 | 0.79 |
| S | 0.00 | 0.01 | 0.01 | 0.02 | 0.01 | 0.03 | 0.03 | 0.01 | 0.02 | 0.02 | 0.02 | 0.03 | 0.04 | 0.10 | 0.08 |
| LOI | - | 10.38 | 13.54 | 3.37 | - | - | - | - | - | - | - | - | - | 2.47 | 2.82 |
| H2OM | 1.60 | - | - | - | 0.16 | 0.14 | 0.25 | 0.18 | 0.17 | 0.22 | 0.17 | 0.23 | 0.31 | - | - |
| H20P | 0.00 | - | - | - | 0.80 | 0.94 | 2.59 | 1.42 | 0.89 | 1.46 | 1.05 | 2.77 | 3.42 | - | - |
| H2O | - | - | - | - | - | - | - | - | - | - | - | - | - | - | - |
| c Fe2O3 | 2.74 | 4.65 | - | - | 7.04 | 4.46 | 3.17 | 4.92 | 3.98 | 3.77 | 5.25 | 3.00 | 3.83 | 1.20 | 1.62 |
| c FeO | 1.35 | 3.84 | 5.29 | 3.64 | 2.37 | 3.37 | 3.02 | 3.42 | 3.10 | 5.03 | 4.59 | 6.23 | 6.57 | 3.42 | 8.41 |
| Ni | - | 27 | - | - | 33 | 22 | 27 | 22 | 22 | 40 | 22 | 38 | - | 2 | 21 |
| Mo | - | - | - | - | - | - | 23 | 32 | 25 | 33 | - | - | - | - | - |
| Cr | - | 50 | - | - | - | - | - | - | - | - | - | - | - | 50 | 90 |
| Ba | - | 1200 | - | - | - | - | - | - | - | - | - | - | - | 1300 | 580 |
| Rb | - | 130 | 52 | 66 | - | - | - | - | - | - | - | - | - | 91 | 48 |
| Sr | - | 530 | - | - | - | - | - | - | - | - | - | - | - | 1200 | 470 |
| Nb | - | 23.0 | 5 | 7 | - | - | - | - | - | - | - | - | - | 32.0 | 13.0 |
| Y | - | 21 | 17 | 20 | - | - | - | - | - | - | - | - | - | 11 | 25 |
| Zr | - | 63 | 44 | 65 | - | - | - | - | - | - | - | - | - | 86 | 100 |
| Yb | - | 5 | - | - | - | - | - | - | - | - | - | - | - | 5 | 5 |
| Ta | - | 1.00 | - | - | - | - | - | - | - | - | - | - | - | 2.30 | 1.00 |
| La | - | 11.00 | 15.00 | 26.00 | - | - | - | - | - | - | - | - | - | 41.00 | 11.00 |
| V | - | - | 224 | 314 | - | - | - | - | - | - | - | - | - | - | - |
| K2O/Na2O | 3.02 | 2.78 | 2.69 | 0.57 | 0.60 | 0.65 | 1.47 | 1.93 | 1.46 | 2.53 | 2.09 | 2.92 | 0.29 | 0.78 | 0.55 |
| K2O + Na2O | 11.89 | 7.04 | 2.84 | 7.39 | 7.69 | 7.04 | 6.61 | 6.77 | 7.17 | 7.65 | 6.7 | 4.47 | 5.34 | 8.55 | 3.59 |
| Al2O3/ CaO+Na2O+K2O | 0.78 | 0.45 | 0.55 | 0.51 | 0.57 | 0.48 | 1.36 | 0.63 | 0.76 | 0.72 | 0.61 | 0.70 | 0.85 | 0.82 | 0.64 |

## APPENDIX B
## WHOLE-ROCK AND TRACE ELEMENT CHEMICAL ANALYSES OF VOLCANIC AND PLUTONIC ROCKS

| MAP NO. | 73 | 34 | 69 | 29 | 22 | 11 | 13 | 37 | 21 | 32 | 72 | 39 | 24 | 19 | 26 |
|---|---|---|---|---|---|---|---|---|---|---|---|---|---|---|---|
| SAMPLE | 75APA-99a-2 | 90JLO2-2 | 90JLO3-12 | 74APA-143-1 | 74APA-26-1 | 74APA-45-1 | 74APA-47-1 | 74APA-111-1 | 74APA-25-1 | 74APA-32-1 | 75APA-100-1 | 74APA-104-1 | 74APA-136-1 | 74APA-138-1 | 74APA-140-1 |
| NTS | 104G/03 | 104G04 | 104G03 | 104G/04 | 104G/04 | 104G/04 | 104G/04 | 104G/04 | 104G/04 | 104G/04 | 104G/03 | 104G/04 | 104G/04 | 104G/04 | 104G/04 |
| UTM EAST | 357164 | 345690 | 356596 | 344803 | 344654 | 343510 | 343655 | 345977 | 344581 | 344990 | 356739 | 346670 | 344747 | 344283 | 344776 |
| UTM NORTH | 6333448 | 6343598 | 6341834 | 6337043 | 6328281 | 6327237 | 6327357 | 6331924 | 6328259 | 6328340 | 6334692 | 6333256 | 6337733 | 6338016 | 6337388 |
| STRAT GROUP | uTSp | uTSp | uTSp | uTSs | uTSs | uTSs | uTSs | uTSt | uTSt | uTSt | uTSt | uTSv | uTSv | uTSv | uTSv |
| ROCK TYPE * | FLBR | FLBR | DORT | TUFF | ASTF | ASTF | SNDS | ASTF | XSTF | XSTF | ASTF | FLOW | FLOW | DIBS | FLOW |
| SiO2 | 54.23 | 48.78 | 57.13 | 52.38 | 54.29 | 44.79 | 48.89 | 50.06 | 50.40 | 55.84 | 46.89 | 49.91 | 46.51 | 45.96 | 46.37 |
| TiO2 | 0.61 | 0.77 | 0.77 | 0.52 | 0.91 | 0.93 | 0.68 | 0.74 | 0.90 | 0.60 | 0.62 | 0.62 | 1.25 | 1.07 | 0.71 |
| Al2O3 | 18.20 | 12.95 | 18.35 | 17.00 | 16.81 | 11.54 | 16.13 | 17.24 | 16.66 | 17.34 | 13.40 | 15.61 | 17.61 | 17.16 | 14.48 |
| Fe2O3 | 5.58 | 8.13 | 6.60 | 7.00 | 7.97 | 12.36 | 10.27 | 9.28 | 9.00 | 7.48 | 8.10 | 8.64 | 11.75 | 10.53 | 7.98 |
| MnO | 0.07 | 0.13 | 0.16 | 0.13 | 0.19 | 0.20 | 0.25 | 0.19 | 0.17 | 0.23 | 0.13 | 0.21 | 0.20 | 0.21 | 0.18 |
| MgO | 0.76 | 10.39 | 2.20 | 3.56 | 4.67 | 5.70 | 3.80 | 3.80 | 4.71 | 4.27 | 1.94 | 3.90 | 5.25 | 4.74 | 3.87 |
| CaO | 2.37 | 9.09 | 6.91 | 9.31 | 6.15 | 9.67 | 12.70 | 7.67 | 8.37 | 3.86 | 9.99 | 8.57 | 7.62 | 11.93 | 12.38 |
| Na2O | 0.49 | 1.88 | 4.87 | 3.60 | 2.96 | 1.46 | 0.94 | 2.04 | 2.54 | 3.41 | 3.18 | 3.66 | 2.45 | 2.04 | 4.67 |
| K2O | 13.62 | 2.64 | 0.93 | 2.03 | 1.34 | 4.11 | 0.84 | 3.73 | 1.30 | 2.17 | 5.75 | 4.91 | 3.03 | 0.49 | 1.27 |
| P2O5 | 0.15 | 0.45 | 0.25 | 0.23 | 0.41 | 0.34 | 0.50 | 0.60 | 0.39 | 0.32 | 0.21 | 0.53 | 0.18 | 0.21 | 0.37 |
| TOTAL | 96.08 | 95.21 | 98.17 | 95.76 | 95.70 | 91.10 | 95.00 | 95.35 | 94.64 | 95.52 | 90.21 | 96.56 | 95.85 | 94.34 | 92.28 |
| CO2 | 1.74 | 1.00 | 0.29 | 1.94 | 0.89 | 6.18 | 2.09 | 1.14 | 1.25 | 2.02 | 7.27 | 1.80 | 0.95 | 2.29 | 4.84 |
| S | 0.02 | 0.05 | 0.01 | 0.06 | 0.18 | 0.04 | 0.03 | 0.08 | 0.02 | 0.03 | 0.00 | 0.04 | 0.06 | 0.02 | 1.44 |
| LOI | - | 3.31 | 1.20 | - | - | - | - | - | - | - | - | - | - | - | - |
| H2OM | 1.48 | - | - | 0.24 | 0.16 | 0.25 | 0.21 | 0.14 | 0.27 | 0.25 | 1.66 | 0.11 | 0.46 | 0.20 | 0.18 |
| H20P | 0.00 | - | - | 1.88 | 3.09 | 2.05 | 2.51 | 2.63 | 2.90 | 3.26 | 0.00 | 1.20 | 3.00 | 3.10 | 1.28 |
| H2O | - | - | - | - | - | - | - | - | - | - | - | - | - | - | - |
| c Fe2O3 | 4.98 | - | - | 3.87 | 2.34 | 3.92 | 4.14 | 3.83 | 3.28 | 2.10 | 6.74 | 1.58 | 4.49 | 5.20 | 4.48 |
| c FeO | 0.54 | 5.22 | 4.79 | 2.82 | 5.06 | 7.60 | 5.51 | 4.90 | 5.14 | 4.84 | 1.22 | 6.34 | 6.54 | 4.80 | 3.15 |
| Ni | 7 | - | - | 27 | 27 | 32 | 47 | - | 32 | 41 | - | - | 24 | 27 | 38 |
| Mo | - | - | - | - | 26 | - | - | - | 38 | 24 | - | - | - | - | - |
| Cr | 5 | - | - | - | - | - | - | - | - | - | - | - | - | - | - |
| Ba | 2865 | - | - | - | - | - | - | - | - | - | - | - | - | - | - |
| Rb | 230 | 67 | 13 | - | - | - | - | - | - | - | - | - | - | - | - |
| Sr | 1588 | - | - | - | - | - | - | - | - | - | - | - | - | - | - |
| Nb | 9.0 | 5 | 7 | - | - | - | - | - | - | - | - | - | - | - | - |
| Y | 17 | 15 | 31 | - | - | - | - | - | - | - | - | - | - | - | - |
| Zr | 87 | 48 | 84 | - | - | - | - | - | - | - | - | - | - | - | - |
| Yb | - | - | - | - | - | - | - | - | - | - | - | - | - | - | - |
| Ta | - | - | - | - | - | - | - | - | - | - | - | - | - | - | - |
| La | - | 15.00 | 15.00 | - | - | - | - | - | - | - | - | - | - | - | - |
| V | 247 | 226 | 128 | - | - | - | - | - | - | - | - | - | - | - | - |
| K2O/Na2O | 27.80 | 1.40 | 0.19 | 0.56 | 0.45 | 2.82 | 0.89 | 1.83 | 0.51 | 0.64 | 1.81 | 1.34 | 1.24 | 0.24 | 0.27 |
| K2O + Na2O | 14.11 | 4.52 | 5.8 | 5.63 | 4.3 | 5.57 | 1.78 | 5.77 | 3.84 | 5.58 | 8.93 | 8.57 | 5.48 | 2.53 | 5.94 |
| Al2O3/ CaO+Na2O+K2O | 0.91 | 0.58 | 0.85 | 0.68 | 0.96 | 0.47 | 0.63 | 0.81 | 0.81 | 1.16 | 0.45 | 0.58 | 0.83 | 0.67 | 0.46 |

## APPENDIX B
## WHOLE-ROCK AND TRACE ELEMENT CHEMICAL ANALYSES OF VOLCANIC AND PLUTONIC ROCKS

| MAP NO. | 31 | 20 | 23 | 25 | 30 | 16 | 18 | 14 | 59 | 63 | 71 | 7 | 79 | 79 | 77 |
|---|---|---|---|---|---|---|---|---|---|---|---|---|---|---|---|
| SAMPLE | 74APA-144-1 | 74APA-24-1 | 74APA-28-1 | 74APA-29-1 | 74APA-30-1 | 74APA-36-1 | 74APA-37-1 | 74APA-48-1 | 74APA-94-1 | 75APA--120-1 | 75APA-99-1 | 90JLO1-18 | 90JLO6-2 | 90JLO6-2DUP | 90VKO1-2 |
| NTS | 104G/04 | 104G/04 | 104G/04 | 104G/04 | 104G/04 | 104G/04 | 104G/04 | 104G/04 | 104G/03 | 104G/03 | 104G/03 | 104G04 | 104G03 | 104G03 | 104G03 |
| UTM EAST | 344857 | 344341 | 344699 | 344756 | 344807 | 343907 | 343919 | 343844 | 353381 | 354614 | 356731 | 341286 | 362558 | 362558 | 362250 |
| UTM NORTH | 6336959 | 6328289 | 6328298 | 6328315 | 6328346 | 6326168 | 6326279 | 6327471 | 6322595 | 6339532 | 6333637 | 6346257 | 6322706 | 6322706 | 6323550 |
| STRAT GROUP | uTSv | uTSv | uTSv | uTSv | uTSv | uTSv | uTSv | uTSv | uTSv | uTSv | uTSv | uTSv | uTSv | uTSv | uTSv |
| ROCK TYPE * | FL;OW | FLOW | FLOW | FLOW | SILL | FLOW | FLOW | FLOW | ANDT | ANDT | TUFF | DORT | DORT | DORT | FLOW |
| SiO2 | 48.71 | 52.70 | 58.11 | 59.43 | 53.50 | 56.68 | 60.36 | 58.94 | 51.09 | 47.58 | 51.65 | 48.98 | 49.60 | 49.69 | 47.13 |
| TiO2 | 0.69 | 0.64 | 0.60 | 0.59 | 1.05 | 0.84 | 0.85 | 0.98 | 1.14 | 0.88 | 0.78 | 1.06 | 0.89 | 0.89 | 1.00 |
| Al2O3 | 17.14 | 13.54 | 17.10 | 17.46 | 17.76 | 16.40 | 16.37 | 17.30 | 14.93 | 13.55 | 15.41 | 17.18 | 12.94 | 12.86 | 15.57 |
| Fe2O3 | 9.47 | 8.84 | 5.95 | 6.36 | 8.53 | 7.92 | 6.79 | 7.17 | 10.77 | 11.67 | 5.80 | 9.95 | 9.45 | 9.43 | 11.21 |
| MnO | 0.16 | 0.15 | 0.11 | 0.12 | 0.18 | 0.15 | 0.09 | 0.17 | 0.18 | 0.18 | 0.14 | 0.21 | 0.18 | 0.18 | 0.20 |
| MgO | 5.33 | 4.34 | 3.28 | 3.36 | 3.23 | 3.43 | 1.97 | 2.47 | 4.37 | 9.53 | 0.96 | 4.24 | 9.17 | 9.37 | 6.63 |
| CaO | 10.61 | 8.02 | 3.83 | 2.91 | 6.81 | 7.14 | 4.05 | 4.90 | 7.11 | 7.70 | 6.93 | 9.85 | 8.04 | 8.03 | 7.01 |
| Na2O | 2.68 | 1.90 | 3.96 | 3.56 | 3.42 | 2.15 | 4.66 | 3.53 | 2.87 | 2.87 | 1.83 | 1.98 | 3.21 | 3.23 | 2.56 |
| K2O | 1.48 | 5.57 | 2.59 | 2.51 | 1.25 | 2.42 | 3.04 | 2.02 | 2.96 | 3.17 | 7.44 | 3.30 | 0.29 | 0.30 | 2.98 |
| P2O5 | 0.19 | 0.39 | 0.28 | 0.28 | 0.21 | 0.39 | 0.34 | 0.37 | 0.60 | 0.15 | 0.20 | 0.40 | 0.38 | 0.38 | 0.29 |
| TOTAL | 96.46 | 96.09 | 95.81 | 96.58 | 95.94 | 97.52 | 98.52 | 97.85 | 96.02 | 97.28 | 91.14 | 97.15 | 94.15 | 94.36 | 94.58 |
| CO2 | 1.06 | 1.80 | 1.54 | 0.81 | 1.65 | 0.58 | 0.30 | 0.70 | 0.72 | 0.68 | 5.20 | 0.18 | 1.54 | 1.54 | 1.06 |
| S | 0.04 | 0.16 | 0.05 | 0.06 | 0.01 | 0.22 | 0.02 | 0.02 | 0.04 | 0.05 | 0.02 | 0.01 | 0.01 | 0.01 | 0.01 |
| LOI | - | - | - | - | - | - | - | - | - | - | - | 1.67 | 4.60 | - | 4.32 |
| H2OM | 0.18 | 0.28 | 0.20 | 0.20 | 0.16 | 0.18 | 0.18 | 0.32 | 0.18 | 0.16 | 2.02 | - | - | - | - |
| H20P | 2.38 | 0.97 | 2.58 | 2.82 | 2.78 | 1.76 | 1.19 | 2.18 | 2.38 | 2.46 | 0.00 | - | - | - | - |
| H2O | - | - | - | - | - | - | - | - | - | - | - | - | - | - | - |
| c Fe2O3 | 2.94 | 3.84 | 1.22 | 1.35 | 2.28 | 3.78 | 3.37 | 1.69 | 4.83 | 3.93 | 4.31 | - | - | - | - |
| c FeO | 5.87 | 4.50 | 4.26 | 4.51 | 5.63 | 3.72 | 3.07 | 4.93 | 5.34 | 6.97 | 1.34 | 7.93 | 6.84 | 6.94 | 7.74 |
| Ni | 41 | 25 | 25 | 34 | 25 | 37 | 18 | 41 | - | - | 3 | - | - | - | - |
| Mo | - | 24 | 23 | 21 | 27 | 31 | 18 | - | - | - | - | - | - | - | - |
| Cr | - | - | - | - | - | - | - | - | - | - | 5 | - | - | - | - |
| Ba | - | - | - | - | - | - | - | - | - | - | 2750 | - | - | - | - |
| Rb | - | - | - | - | - | - | - | - | - | - | 149 | 55 | 10 | 10 | 72 |
| Sr | - | - | - | - | - | - | - | - | - | - | 1434 | - | - | - | - |
| Nb | - | - | - | - | - | - | - | - | - | - | 12.0 | 5 | 6 | 5 | 5 |
| Y | - | - | - | - | - | - | - | - | - | - | 21 | 24 | 21 | 20 | 15 |
| Zr | - | - | - | - | - | - | - | - | - | - | 87 | 81 | 77 | 72 | 41 |
| Yb | - | - | - | - | - | - | - | - | - | - | - | - | - | - | - |
| Ta | - | - | - | - | - | - | - | - | - | - | - | - | - | - | - |
| La | - | - | - | - | - | - | - | - | - | - | - | 17.00 | 15.00 | 15.00 | 15.00 |
| V | - | - | - | - | - | - | - | - | - | - | 247 | 338 | 231 | 227 | 304 |
| K2O/Na2O | 0.55 | 2.93 | 0.65 | 0.71 | 0.37 | 1.13 | 0.65 | 0.57 | 1.03 | 1.10 | 4.07 | 1.67 | 0.09 | 0.09 | 1.16 |
| K2O + Na2O | 4.16 | 7.47 | 6.55 | 6.07 | 4.67 | 4.57 | 7.7 | 5.55 | 5.83 | 6.04 | 9.27 | 5.28 | 3.5 | 3.53 | 5.54 |
| Al2O3/ CaO+Na2O+K2O | 0.68 | 0.57 | 1.05 | 1.26 | 0.92 | 0.86 | 0.89 | 1.02 | 0.71 | 0.61 | 0.65 | 0.69 | 0.64 | 0.63 | 0.77 |

## APPENDIX B
## WHOLE-ROCK AND TRACE ELEMENT CHEMICAL ANALYSES OF VOLCANIC AND PLUTONIC ROCKS

| MAP NO. | 83 | 83 | 85 | 90 | 87 | 94 | 95 | 93 | 91 | 92 | 94 | 86 | 2 | 1 | 4 |
|---|---|---|---|---|---|---|---|---|---|---|---|---|---|---|---|
| SAMPLE | 90JLO5-1 | 90JLO5-2 | 90JLO5-7 | 90JLO5-12 | 90JLO5-17.2 | 90JLO10-17 | 90JLO10-5 | 90JLO10-22 | 90JLO6-6 | 90VKO1-3 | 90JLO10-17F | 90JLO5-19 | 88DRH23-3 | 88VK024-1 | 88VK024-2 |
| NTS | 104G03 | 104G03 | 104G03 | 104G03 | 104G03 | 104G03 | 104G03 | 104G03 | 104G03 | 104G03 | 104G03 | 104G03 | 104G/04 | 104G/04 | 104G/04 |
| UTM EAST | 369258 | 369258 | 369396 | 370600 | 369605 | 373744 | 374308 | 373379 | 370807 | 370842 | 373744 | 369426 | 324454 | 319774. | 333128 |
| UTM NORTH | 6329677 | 6329677 | 6329403 | 6320074 | 6320293 | 6329543 | 6329200 | 6329437 | 6323252 | 6323480 | 6329543 | 6320837 | 6331609 | 6337895 | 6335520 |
| STRAT GROUP | PSmv | PSmv | PSmv | PSv | PSv | lCScg | lCSt | uCScg | uCSt | uCSt | uCSv | uCSv | Eg | Eg | Eg |
| ROCK TYPE * | LPTF | LPTF | DACT | TUFF | ANDT | TUFF | TUFF | TUFF | TUFF | FLOW | TUFF | FLOW | GRNT | GRNT | BGRN |
| SiO2 | 48.30 | 44.70 | 64.04 | 52.62 | 56.59 | 49.79 | 47.64 | 49.03 | 55.49 | 53.56 | 62.41 | 49.56 | 69.46 | 75.89 | 69.98 |
| TiO2 | 2.64 | 4.64 | 0.74 | 0.77 | 1.06 | 0.86 | 1.06 | 0.80 | 0.75 | 0.79 | 0.53 | 0.82 | 0.36 | 0.05 | 0.36 |
| Al2O3 | 15.98 | 16.49 | 15.37 | 19.10 | 19.00 | 16.42 | 18.33 | 16.43 | 17.89 | 17.33 | 16.31 | 15.65 | 15.44 | 14.20 | 15.49 |
| Fe2O3 | 12.15 | 13.85 | 7.32 | 8.21 | 6.96 | 9.19 | 11.01 | 10.13 | 7.37 | 9.10 | 5.71 | 10.20 | 3.27 | 0.55 | 2.64 |
| MnO | 0.38 | 0.17 | 0.09 | 0.12 | 0.05 | 0.16 | 0.19 | 0.20 | 0.16 | 0.19 | 0.14 | 0.19 | 0.09 | 0.13 | 0.07 |
| MgO | 5.72 | 4.54 | 1.03 | 4.06 | 1.01 | 4.57 | 5.24 | 6.65 | 2.83 | 3.48 | 2.22 | 4.12 | 0.73 | 0.05 | 0.75 |
| CaO | 3.50 | 3.34 | 0.70 | 4.94 | 6.38 | 8.71 | 7.49 | 5.71 | 6.00 | 6.69 | 3.75 | 8.10 | 2.76 | 0.78 | 2.97 |
| Na2O | 3.10 | 4.66 | 8.10 | 4.65 | 3.24 | 3.88 | 2.68 | 5.20 | 4.02 | 3.28 | 3.58 | 2.47 | 3.63 | 4.13 | 3.63 |
| K2O | 1.72 | 0.88 | 0.06 | 0.87 | 1.71 | 0.54 | 0.74 | 0.14 | 1.18 | 1.14 | 2.12 | 0.60 | 3.56 | 4.31 | 3.30 |
| P2O5 | 0.90 | 0.73 | 0.09 | 0.17 | 0.33 | 0.16 | 0.19 | 0.14 | 0.23 | 0.22 | 0.19 | 0.20 | 0.12 | 0.01 | 0.11 |
| TOTAL | 94.39 | 93.90 | 97.54 | 95.51 | 96.33 | 94.28 | 94.57 | 94.43 | 95.92 | 95.78 | 96.96 | 91.91 | 99.42 | 100.10 | 99.30 |
| CO2 | 0.22 | 1.69 | 0.65 | 0.50 | 1.15 | 1.65 | 0.21 | 0.79 | 0.14 | 0.14 | 0.14 | 4.02 | 0.15 | 0.15 | 0.15 |
| S | 0.01 | 0.01 | 0.01 | 0.06 | 0.01 | 0.09 | 0.01 | 0.01 | 0.01 | 0.01 | 0.01 | 0.01 | 0.01 | 0.01 | 0.01 |
| LOI | 4.53 | 5.04 | 1.38 | 3.70 | 3.09 | 4.79 | 4.76 | 4.49 | 3.10 | 3.41 | 2.60 | 7.47 | 0.39 | 0.23 | 0.37 |
| H2OM | - | - | - | - | - | - | - | - | - | - | - | - | - | - | - |
| H20P | - | - | - | - | - | - | - | - | - | - | - | - | - | - | - |
| H2O | - | - | - | - | - | - | - | - | - | - | - | - | - | - | - |
| c Fe2O3 | - | - | - | - | - | - | - | - | - | - | - | - | 1.54 | 0.16 | 1.22 |
| c FeO | 8.57 | 7.29 | 2.24 | 5.86 | 1.00 | 6.62 | 8.40 | 2.07 | 3.29 | 4.21 | 2.60 | 3.74 | 1.56 | 0.35 | 1.28 |
| Ni | - | - | - | - | - | - | - | - | - | - | - | - | 10 | 2 | 2 |
| Mo | - | - | - | - | - | - | - | - | - | - | - | - | 6 | - | - |
| Cr | - | - | - | - | - | - | - | - | - | - | - | - | 50 | 5 | 5 |
| Ba | - | - | - | - | - | - | - | - | - | - | - | - | 1900 | 22 | 1913 |
| Rb | 25 | 10 | 10 | 14 | 30 | 10 | 10 | 10 | 16 | 16 | 41 | 13 | 98 | 138 | 64 |
| Sr | - | - | - | - | - | - | - | - | - | - | - | - | 595 | - | - |
| Nb | 72 | 53 | 82 | 5 | 5 | 5 | 5 | 5 | 5 | 5 | 5 | 5 | 14.0 | 18.0 | 7.0 |
| Y | 46 | 32 | 55 | 20 | 26 | 15 | 18 | 20 | 22 | 22 | 17 | 17 | 5 | 17 | 11 |
| Zr | 419 | 314 | 528 | 62 | 160 | 47 | 51 | 44 | 85 | 73 | 84 | 52 | 110 | 36 | 127 |
| Yb | - | - | - | - | - | - | - | - | - | - | - | - | - | - | - |
| Ta | - | - | - | - | - | - | - | - | - | - | - | - | - | - | - |
| La | 48.00 | 39.00 | 70.00 | 15.00 | - | 15.00 | 17.00 | 15.00 | 15.00 | 15.00 | 15.00 | 15.00 | - | - | - |
| V | 41 | 355 | 5 | 200 | 148 | 238 | 299 | 267 | 147 | 196 | 115 | 251 | 39 | 5 | 42 |
| K2O/Na2O | 0.55 | 0.19 | 0.01 | 0.19 | 0.53 | 0.14 | 0.28 | 0.03 | 0.29 | 0.35 | 0.59 | 0.24 | 0.98 | 1.04 | 0.91 |
| K2O + Na2O | 4.82 | 5.44 | 8.16 | 5.52 | 4.95 | 4.42 | 3.42 | 5.34 | 5.2 | 4.42 | 5.7 | 3.07 | 7.19 | 8.44 | 6.93 |
| Al2O3/ CaO+Na2O+K2O | 1.20 | 1.13 | 1.05 | 1.09 | 1.01 | 0.72 | 0.97 | 0.86 | 0.95 | 0.92 | 1.09 | 0.80 | 1.04 | 1.10 | 1.04 |

# APPENDIX B
## WHOLE-ROCK AND TRACE ELEMENT CHEMICAL ANALYSES OF VOLCANIC AND PLUTONIC ROCKS

| MAP NO. | 3 | 35 | 36 | 74 | 40 | 52 | 56 | 62 | 53 | 53 | 53 | 53 | 53 | 50 | 53 |
|---|---|---|---|---|---|---|---|---|---|---|---|---|---|---|---|
| SAMPLE | 88VKO31-1 | 73APA-73-1 | 88JLO28-1 | 88VKO22-3 | 88VKO31-11 | 75APA-142-1 | 88DRH-29-5 | 88JLO28-4 | 74APA205 | 74APA206 | 74APA207 | 74APA208 | 74APA209 | 75APA-143-2 | APA1* |
| NTS | 104G/04 | 104G/04 | 104G/04 | 104G/03 | 104G/04 | 104G/03 | 104G/03 | 104G/03 | 104G/03 | 104G/03 | 104G/03 | 104G/03 | 104G/03 | 104G/03 | 104G/03 |
| UTM EAST | 332200 | 345750 | 345871 | 358518 | 346708 | 350421 | 353012 | 354178 | 351500 | 351500 | 351500 | 351500 | 351500 | 349600 | 351500 |
| UTM NORTH | 6346175 | 6320100 | 6321948 | 6321537 | 6328640 | 6336207 | 6343821 | 6343646 | 6335000 | 6335000 | 6335000 | 6335000 | 6335000 | 6337095 | 6335000 |
| STRAT GROUP | Egd | Em | Em | Em | Em | eJm | eJm | eJm | TJs | TJs | TJs | TJs | TJs | TJs | TJs |
| ROCK TYPE * | GRDR | QZMN | INTR | GRDR | GRDR | DORT | INTR | INTR | SYNT | SYNT | SYNT | SYNT | SYNT | SYNT | SYNT |
| SiO2 | 66.03 | 66.03 | 74.92 | 68.79 | 56.95 | 51.88 | 65.76 | 57.58 | 51.50 | 50.40 | 58.26 | 55.30 | 55.80 | 56.29 | 53.00 |
| TiO2 | 0.45 | 0.49 | 0.14 | 0.39 | 0.75 | 0.87 | 0.46 | 0.72 | 0.46 | 0.44 | 0.49 | 0.37 | 0.35 | 0.45 | 0.42 |
| Al2O3 | 15.35 | 16.60 | 13.83 | 15.13 | 15.06 | 16.96 | 15.79 | 17.40 | 19.60 | 17.90 | 18.07 | 18.40 | 18.50 | 20.64 | 19.30 |
| Fe2O3 | 4.01 | 4.56 | 1.23 | 3.57 | 8.19 | 8.26 | 4.87 | 7.98 | 3.39 | 4.10 | 4.09 | 5.55 | 2.64 | 3.27 | 6.81 |
| MnO | 0.09 | 0.12 | 0.04 | 0.07 | 0.12 | 0.18 | 0.12 | 0.18 | 0.31 | 0.21 | 0.12 | 0.15 | 0.13 | 0.10 | 0.21 |
| MgO | 1.18 | 1.07 | 0.17 | 1.09 | 3.48 | 3.62 | 1.46 | 2.71 | 0.94 | 1.07 | 1.27 | 1.63 | 0.47 | 0.57 | 2.12 |
| CaO | 3.54 | 3.89 | 1.16 | 3.22 | 6.83 | 8.36 | 4.41 | 6.89 | 3.82 | 4.94 | 3.32 | 4.65 | 2.66 | 1.74 | 1.68 |
| Na2O | 3.04 | 3.89 | 3.73 | 3.45 | 2.57 | 2.24 | 3.01 | 3.03 | 0.58 | 1.92 | 4.50 | 2.86 | 1.77 | 0.28 | 0.77 |
| K2O | 3.44 | 2.79 | 4.13 | 3.13 | 4.19 | 6.63 | 3.21 | 2.31 | 12.20 | 10.42 | 7.26 | 9.00 | 11.62 | 13.72 | 12.75 |
| P2O5 | 0.13 | 0.27 | 0.05 | 0.11 | 0.40 | 0.48 | 0.12 | 0.23 | 0.15 | 0.21 | 0.15 | 0.20 | 0.15 | 0.10 | 0.15 |
| TOTAL | 97.26 | 99.71 | 99.40 | 98.95 | 98.54 | 98.48 | 99.21 | 99.03 | 92.95 | 91.61 | 97.53 | 98.11 | 94.09 | 97.16 | 97.21 |
| CO2 | 1.07 | 0.29 | 0.15 | 0.15 | 0.15 | 0.21 | 0.15 | 0.15 | 0.51 | 0.51 | 0.22 | - | 1.98 | 1.20 | - |
| S | 0.01 | 0.01 | 0.01 | 0.02 | 0.01 | 0.00 | 0.01 | 0.01 | - | - | - | - | - | 0.06 | - |
| LOI | 2.38 | | 0.47 | 0.75 | 1.23 | - | 0.82 | 0.97 | - | - | - | - | - | - | - |
| H2OM | - | 0.07 | - | - | - | 0.14 | - | - | - | - | - | - | - | 0.14 | - |
| H20P | - | 0.80 | - | - | - | 1.12 | - | - | - | - | - | - | - | 1.12 | - |
| H2O | - | - | - | - | - | - | - | - | 2.08 | 2.15 | 1.76 | - | 1.26 | - | - |
| c Fe2O3 | 1.98 | 1.52 | 0.44 | 1.75 | 4.56 | 4.57 | 1.87 | -0.89 | 1.72 | 0.98 | 2.50 | 2.85 | 1.42 | 2.83 | 1.56 |
| c FeO | 1.83 | 2.73 | 0.71 | 1.64 | 3.27 | 3.32 | 2.70 | 7.98 | 1.50 | 2.81 | 1.43 | 2.43 | 1.10 | 0.39 | 4.72 |
| Ni | 2 | - | - | 2 | 13 | - | 2 | 2 | - | - | - | - | - | - | - |
| Mo | 6 | - | - | - | 6 | - | - | - | - | - | - | - | - | - | - |
| Cr | 50 | - | - | 5 | 50 | - | 5 | 5 | - | - | - | - | - | - | - |
| Ba | 2800 | - | - | 1718 | 2700 | - | 1271 | 1284 | - | - | - | - | - | - | - |
| Rb | 78 | - | - | 72 | 100 | - | 82 | 46 | - | - | - | - | - | - | - |
| Sr | 505 | - | - | 506 | 730 | - | 383 | 566 | - | - | - | - | - | - | - |
| Nb | 25.0 | - | - | 8.0 | 18.0 | - | 5.0 | 7.0 | - | - | - | - | - | - | - |
| Y | 19 | - | - | 14 | 5 | - | 18 | 22 | - | - | - | - | - | - | - |
| Zr | 105 | - | - | 111 | 76 | - | 116 | 133 | - | - | - | - | - | - | - |
| Yb | - | - | - | - | - | - | - | - | - | - | - | - | - | - | - |
| Ta | - | - | - | - | - | - | - | - | - | - | - | - | - | - | - |
| La | - | - | - | - | - | - | - | - | - | - | - | - | - | - | - |
| V | 78 | - | - | 56 | 282 | - | 84 | 174 | - | - | - | - | - | - | - |
| K2O/Na2O | 1.13 | 0.72 | 1.11 | 0.91 | 1.63 | 2.96 | 1.07 | 0.76 | 21.03 | 5.43 | 1.61 | 3.15 | 6.56 | 49.00 | 16.56 |
| K2O + Na2O | 6.48 | 6.68 | 7.86 | 6.58 | 6.76 | 8.87 | 6.22 | 5.34 | 12.78 | 12.34 | 11.76 | 11.86 | 13.39 | 14 | 13.52 |
| Al2O3/ CaO+Na2O+K2O | 1.01 | 1.01 | 1.09 | 1.01 | 0.71 | 0.61 | 0.96 | 0.87 | 0.93 | 0.76 | 0.85 | 0.80 | 0.91 | 1.11 | 1.06 |

# APPENDIX B
## WHOLE-ROCK AND TRACE ELEMENT CHEMICAL ANALYSES OF VOLCANIC AND PLUTONIC ROCKS

| MAP NO. | 53 | 53 | 64 | 53 | 53 | 53 | 53 | 6' | 6 | 5 | 89 | 75 | 75 | 97 | 51 |
|---|---|---|---|---|---|---|---|---|---|---|---|---|---|---|---|
| SAMPLE | APA11**** | APA12**** | APA13***** | APA3* | APA5** | APA6*** | APA9**** | 73APA-75-1 | 73APA-80-1 | 88VKO33-12 | 88JLO16-11 | 90JLO4-21 | 90JLO4-21-2 | 88JLO18-5 | 90JLO3-7 |
| NTS | 104G/03 | 104G/03 | 104G/03 | 104G/03 | 104G/03 | 104G/03 | 104G/03 | 104G/04 | 104G/04 | 104G/04 | 104G/03 | 104G03 | 104G03 | 104G/03 | 104G03 |
| UTM EAST | 351500 | 351600 | N110 Creek | 351500 | 351500 | 351500 | 351500 | 343250 | 338923 | 338181 | 370066 | 359992 | 359992 | 378929 | 350247 |
| UTM NORTH | 6335000 | 6335000 | | 6335000 | 6335000 | 6335000 | 6335000 | 6332800 | 6342440 | 6344046 | 6338685 | 6341211 | 6341211 | 6340418 | 6342835 |
| STRAT GROUP | TJs | TJs | TJs | TJs | TJs | TJs | TJs | mJd | mJd | mJd | mJm | p | p | qp | lTd |
| ROCK TYPE * | SYNT | SYNT | SYNT | SYNT | SYNT | SYNT | SYNT | DORT | DORT | DORT | SYNT | PRXN | PRXN | DYKE | DYKE |
| SiO2 | 55.10 | 57.00 | 54.20 | 54.00 | 56.00 | 53.24 | 55.40 | 60.39 | 48.75 | 55.90 | 63.77 | 39.31 | 38.67 | 52.30 | 40.72 |
| TiO2 | 0.39 | 0.68 | 0.43 | 0.12 | 0.24 | 0.38 | 0.33 | 0.78 | 0.93 | 0.84 | 0.63 | 0.24 | 0.26 | 0.65 | 2.06 |
| Al2O3 | 18.40 | 17.60 | 19.10 | 19.00 | 17.60 | 18.20 | 18.50 | 16.88 | 13.93 | 16.43 | 15.31 | 3.36 | 3.46 | 17.09 | 11.56 |
| Fe2O3 | 4.13 | 4.40 | 5.53 | 2.40 | 2.79 | 7.55 | 5.42 | 6.64 | 9.69 | 8.18 | 4.74 | 10.18 | 10.32 | 8.18 | 7.41 |
| MnO | 0.15 | 0.11 | 0.15 | 0.19 | 0.11 | 0.23 | 0.16 | 0.16 | 0.18 | 0.16 | 0.07 | 0.16 | 0.16 | 0.19 | 0.11 |
| MgO | 1.17 | 1.40 | 0.70 | 1.40 | 0.50 | 1.23 | 1.60 | 1.73 | 10.16 | 3.45 | 2.45 | 31.27 | 31.31 | 2.08 | 3.10 |
| CaO | 5.09 | 4.20 | 4.78 | 2.00 | 2.40 | 4.40 | 5.10 | 6.00 | 9.87 | 7.39 | 3.25 | 4.93 | 4.21 | 5.14 | 15.48 |
| Na2O | 3.15 | 5.10 | 2.47 | 0.45 | 1.42 | 3.02 | 2.72 | 3.26 | 1.82 | 2.69 | 4.12 | 0.07 | 0.06 | 5.87 | 2.54 |
| K2O | 8.56 | 4.45 | 9.40 | 12.40 | 12.20 | 11.45 | 9.70 | 2.07 | 1.77 | 2.90 | 3.31 | 0.02 | 0.02 | 0.80 | 1.31 |
| P2O5 | 0.15 | 0.26 | 0.20 | 0.07 | 0.07 | 0.22 | 0.21 | 0.23 | 0.14 | 0.32 | 0.17 | 0.06 | 0.06 | 0.36 | 0.39 |
| TOTAL | 96.29 | 95.18 | 96.96 | 92.03 | 93.33 | 99.92 | 99.14 | 98.14 | 97.24 | 98.26 | 97.82 | 89.60 | 88.53 | 92.66 | 84.68 |
| CO2 | 0.07 | - | - | - | - | - | - | 0.44 | 0.07 | 0.15 | 0.15 | 0.14 | 0.25 | 4.75 | 12.40 |
| S | - | - | - | - | - | - | - | 0.01 | 0.02 | 0.01 | 0.01 | 0.03 | 0.03 | 0.02 | 0.01 |
| LOI | - | - | - | - | - | - | - | - | - | 1.62 | 1.88 | 9.39 | 10.48 | 7.19 | 14.35 |
| H2OM | - | - | - | - | - | - | - | 0.05 | 0.06 | - | - | - | - | - | - |
| H20P | - | - | - | - | - | - | - | 1.19 | 1.14 | - | - | - | - | - | - |
| H2O | 1.80 | 2.80 | - | 4.90 | 0.41 | - | - | - | - | - | - | - | - | - | - |
| c Fe2O3 | 2.59 | 2.96 | 3.11 | 1.16 | 1.87 | 2.67 | 2.85 | 1.92 | 2.95 | 5.01 | 0.63 | - | - | 4.38 | - |
| c FeO | 1.39 | 1.30 | 2.18 | 1.12 | 0.83 | 4.39 | 2.31 | 4.24 | 6.06 | 2.85 | 3.70 | 2.93 | 3.06 | 3.42 | 8.12 |
| Ni | - | - | - | - | - | - | - | - | - | 13 | - | - | - | - | - |
| Mo | - | - | - | - | - | - | - | - | - | 6 | - | - | - | - | - |
| Cr | - | - | - | - | - | - | - | - | - | 50 | 63 | - | - | - | - |
| Ba | - | - | - | - | - | - | - | - | - | 1700 | 1730 | - | - | - | - |
| Rb | - | - | - | - | - | - | - | - | - | 120 | 73 | 10 | 10 | - | 29 |
| Sr | - | - | - | - | - | - | - | - | - | 670 | 594 | | | - | |
| Nb | - | - | - | - | - | - | - | - | - | 24.0 | 6.0 | 5 | 5 | - | 35 |
| Y | - | - | - | - | - | - | - | - | - | 15 | 14 | 10 | 10 | - | 19 |
| Zr | - | - | - | - | - | - | - | - | - | 87 | 140 | 20 | 20 | - | 141 |
| Yb | - | - | - | - | - | - | - | - | - | - | - | - | - | - | - |
| Ta | - | - | - | - | - | - | - | - | - | - | - | - | - | - | - |
| La | - | - | - | - | - | - | - | - | - | - | - | 15.00 | 15.00 | - | 27.00 |
| V | - | - | - | - | - | - | - | - | - | 222 | 92 | 108 | 105 | - | 180 |
| K2O/Na2O | 2.72 | 0.87 | 3.81 | 27.56 | 8.59 | 3.79 | 3.57 | 0.63 | 0.97 | 1.08 | 0.80 | 0.29 | 0.33 | 0.14 | 0.52 |
| K2O + Na2O | 11.71 | 9.55 | 11.87 | 12.85 | 13.62 | 14.47 | 12.42 | 5.33 | 3.59 | 5.59 | 7.43 | 0.09 | 0.08 | 6.67 | 3.85 |
| Al2O3/ CaO+Na2O+K2O | 0.78 | 0.84 | 0.83 | 1.07 | 0.88 | 0.72 | 0.76 | 0.91 | 0.61 | 0.78 | 0.94 | 0.37 | 0.44 | 0.86 | 0.34 |

Rock type abbreviations: ANDT=andesite, ASTF=ash tuff, BGRN=biotite granite, BSLT=basalt, CLTF=chlo
FLBR=flow breccia, GRDR=granodiorite, GRNT=granite, INTR=intrusive, LPTF=lapilli tuff, PRXN=pyroxeni

## APPENDIX B
## WHOLE-ROCK AND TRACE ELEMENT CHEMICAL ANALYSES OF VOLCANIC AND PLUTONIC ROCKS

| MAP NO. | 78 | 82 | 84 | 88 | 88 | 81 | 96 |
|---|---|---|---|---|---|---|---|
| SAMPLE | 90JLO7-18 | 88VKO-30-3 | 88VKO-30-6 | 88VKO-30-7-1 | 88VKO-30-7-2 | 88VKO-30-8 | 88JLO29-15 |
| NTS | 104B10 | 104G/03 | 104G/03 | 104G/03 | 104G/03 | 104G/03 | 104G/03 |
| UTM EAST | 392850 | 365255 | 369360 | 370000 | 370000 | 364629 | 376917 |
| UTM NORTH | 628820 | 6344803 | 6342084 | 6341376 | 6341375 | 6341412 | 6329329 |
| STRAT GROUP | lTd | lTm | lTm | lTm | lTm | lTm | d |
| ROCK TYPE * | DORT | DORT | DORT | DORT | DORT | DORT | DORT |
| SiO2 | 48.25 | 63.29 | 65.82 | 48.15 | 48.22 | 64.96 | 45.88 |
| TiO2 | 0.98 | 0.53 | 0.39 | 0.90 | 0.87 | 0.45 | 2.81 |
| Al2O3 | 16.57 | 15.89 | 16.26 | 19.68 | 19.57 | 16.34 | 17.83 |
| Fe2O3 | 10.97 | 5.13 | 3.76 | 9.77 | 9.84 | 4.36 | 10.68 |
| MnO | 0.21 | 0.09 | 0.07 | 0.14 | 0.15 | 0.09 | 0.16 |
| MgO | 5.87 | 2.43 | 1.30 | 3.69 | 3.90 | 1.72 | 3.30 |
| CaO | 9.14 | 3.97 | 2.87 | 10.42 | 10.09 | 3.37 | 6.32 |
| Na2O | 3.10 | 4.15 | 4.63 | 2.94 | 2.93 | 4.31 | 4.53 |
| K2O | 1.25 | 3.02 | 3.43 | 1.82 | 1.87 | 3.22 | 1.86 |
| P2O5 | 0.24 | 0.20 | 0.13 | 0.04 | 0.04 | 0.16 | 0.71 |
| TOTAL | 96.58 | 98.70 | 98.66 | 97.55 | 97.48 | 98.98 | 94.08 |
| | | | | | | | |
| CO2 | 0.50 | 0.15 | 0.15 | 0.15 | 0.15 | 0.15 | 2.24 |
| S | 0.01 | 0.01 | 0.01 | 0.01 | 0.01 | 0.01 | 0.01 |
| LOI | 2.25 | 1.05 | 1.08 | 2.53 | 2.52 | 0.86 | 5.40 |
| | | | | | | | |
| H2OM | - | - | - | - | - | - | - |
| H20P | - | - | - | - | - | - | - |
| H2O | - | - | - | - | - | - | - |
| | | | | | | | |
| c Fe2O3 | - | 1.96 | 2.03 | 5.02 | 4.77 | 2.17 | 1.81 |
| c FeO | 8.64 | 2.85 | 1.56 | 4.27 | 4.56 | 1.97 | 7.98 |
| | | | | | | | |
| Ni | - | 20 | 4 | 24 | 25 | 9 | 2 |
| Mo | - | - | - | - | - | - | - |
| Cr | - | 44 | 10 | 28 | 25 | 24 | 5 |
| Ba | - | 1065 | 1236 | 434 | 469 | 1216 | 1624 |
| Rb | 10 | 71 | 74 | 72 | 75 | 82 | 29 |
| Sr | | 774 | 833 | 684 | 695 | 802 | 540 |
| Nb | 5 | 5.0 | 5.0 | 5.0 | 5.0 | 5.0 | 79.0 |
| Y | 19 | 17 | 18 | 13 | 14 | 15 | 26 |
| Zr | 71 | 162 | 122 | 52 | 52 | 156 | 234 |
| Yb | - | - | - | - | - | - | - |
| Ta | - | - | - | - | - | - | - |
| La | - | - | - | - | - | - | - |
| V | 284 | 111 | 74 | 311 | 308 | 87 | 182 |
| | | | | | | | |
| K2O/Na2O | 0.40 | 0.73 | 0.74 | 0.62 | 0.64 | 0.75 | 0.41 |
| K2O + Na2O | 4.35 | 7.17 | 8.06 | 4.76 | 4.8 | 7.53 | 6.39 |
| Al2O3/ CaO+Na2O+K2O | 0.72 | 0.92 | 0.98 | 0.76 | 0.78 | 0.98 | 0.85 |

ritic tuff, DACT=dacite, DIBS=diabase, DIKE=dike, DORT=diorite, FLOW=flow,
ite, QZMN=quartz monzonite, SYNT=syenite, TRCT=trachyte, TUFF=tuff, XSTF=crystal tuff.

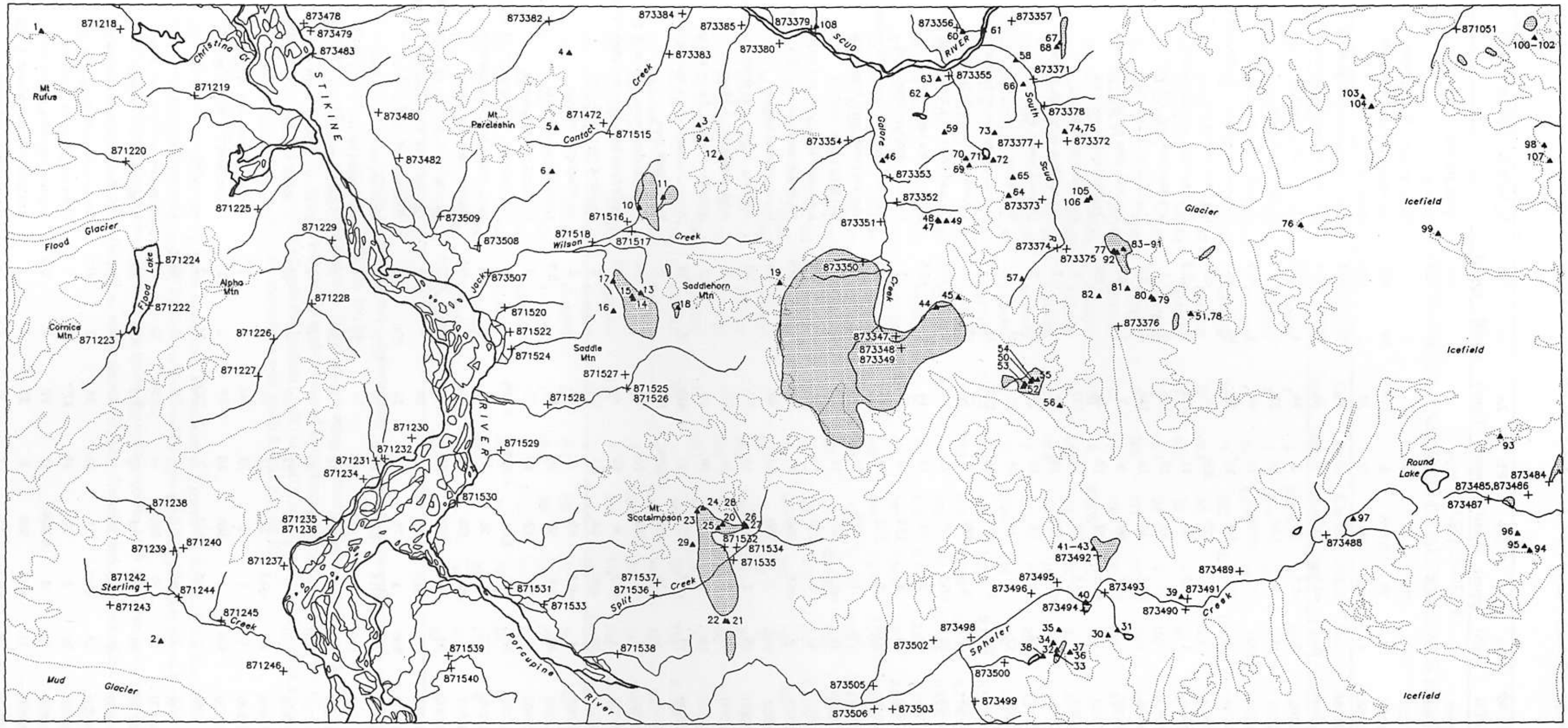


Figure C-1. Sample locations for geochemical and assay analyses of altered and mineralized rocks.

# APPENDIX C
## GEOCHEMICAL ANALYSES OF ALTERED AND MINERALIZED ROCKS

| Map No. | Sample Number | UTM EAST | ZONE 09 NORTH | Au (ppb) | Ag (ppm) | Cu (ppm) | Pb (ppm) | Zn (ppm) | As (ppm) | Sb (ppm) | SAMPLE DESCRIPTION |
|---|---|---|---|---|---|---|---|---|---|---|---|
| 1 | 88JLO20-11-2 | 320350 | 6347850 | 20 | 3 | 100 | 279 | 98 | | 0.8 | Pyritic qtz vein |
| 2 | 88VKO21-7 | 324100 | 6324000 | 1 | <0.5 | 3 | 2 | 2 | | <0.5 | Qtz vein |
| 3 | 88JLO12-20 | 345800 | 6343259 | 41 | 0.8 | 39 | 36 | 68 | 1 | 2 | Trachyte dike, 3 % diss. pyrite |
| 4 | 88JLO13-13 | 340900 | 6346250 | 33 | 99 | 0.11% | 8 | 174 | 20 | 620 | Qtz veinlet 1 % diss. tetrahedrite |
| 5 | 88JLO13-4 | 340300 | 6343350 | 4 | <0.5 | 46 | 11 | 39 | 1 | <0.5 | Pyritic tuff |
| 6 | 88VKO13-10 | 340060 | 6341670 | 2 | <0.5 | 131 | 16 | 45 | 3 | <0.5 | Silicic sediments, minor py & cpy |
| 7 | 88VKO13-13 | 398500 | 6342000 | 58 | <0.5 | 2 | 3 | 4 | 2 | <0.5 | Qtz vein, no visible sulphides |
| 8 | 88VKO13-14 | 398000 | 6342100 | 2 | <0.5 | 10 | 5 | 34 | 1 | <0.5 | Qtz vein and wallrock |
| 9 | 88VKO15-1-1 | 346120 | 6342700 | 45 | 3 | 540 | 14 | 28 | 47 | 1 | Oxidized pyritic dacite |
| 10 | 88DRH15-1 | 343400 | 6340150 | 1260 | 7 | 1.72% | 10 | 44 | 9 | <0.5 | Andesite, 2 % diss. py & cpy |
| 11 | 88DRH15-8 | 344350 | 6340500 | 9 | 0.7 | 500 | 10 | 30 | 16 | <0.5 | Oxidized monzonite, 5 % diss. pyrite |
| 12 | 88DRH35-1 | 346650 | 6341975 | 1 | 1 | 129 | 224 | 4 | | <0.5 | Qtz vein , diss. pyrite |
| 13 | 88VKO18-2 | 343350 | 6336800 | 1 | <0.5 | 10 | 11 | 136 | 5 | <0.5 | Oxidized qtz carbonate breccia |
| 14 | 88VKO18-3-1 | 343050 | 6336600 | 10 | 1 | 35 | 15 | 156 | 9 | 1 | Oxidized andesite, 1 % pyrite |
| 15 | 88VKO18-3-2 | 343000 | 6336700 | 8 | <0.5 | 46 | 14 | 148 | 4 | 0.8 | Oxidized pyritic andesite |
| 16 | 88VKO18-4-3 | 342250 | 6336150 | 1 | <0.5 | 99 | 5 | 7 | 1 | 0.6 | Qtz vein, diss. pyrite in fractures |
| 17 | 88VKO31-4 | 342280 | 6337300 | 1 | <0.5 | 28 | 14 | 46 | | 0.8 | Oxidized pyritic volcanic |
| 18 | 88VKO33-10 | 344770 | 6336200 | 7 | <0.5 | 52 | 13 | 173 | | 1 | Oxidized pyritic gossan |
| 19 | 88VKO33-11 | 348775 | 6337000 | 1 | <0.5 | 82 | 14 | 81 | | 7 | Qtz veinlets, no visible sulphides |
| 20 | 88DRH8-7 | 346200 | 6327760 | 590 | 1 | 76 | 13 | 28 | 13 | 2 | Qtz vein, pyrite to 5 % |
| 21 | 88JLO8-3 | 346240 | 6323990 | 57 | 2 | 75 | 95 | 224 | 25 | 2 | Fault zone |
| 22 | 88JLO8-4 | 346170 | 6324000 | 286 | 0.8 | 121 | 36 | 270 | 32 | 3 | Sericite-pyrite-altered fault zone |
| 23 | 88JLO9-3 | 345240 | 6328300 | 20 | 0.7 | 880 | 8 | 62 | 17 | <0.5 | Qtz-chlorite vein 3 % pyrite |
| 24 | 88JLO9-4 | 345470 | 6328400 | 21 | <0.5 | 175 | 21 | 71 | 5 | <0.5 | Qtz-carbonate vein, trace pyrite |
| 25 | 88JLO9-5 | 346020 | 6327630 | 49 | 1 | 53 | 11 | 14 | 4 | <0.5 | Silicic-pyritic fault zone |
| 26 | 88JLO9-6 | 347050 | 6327750 | 20 | 2 | 135 | 18 | 18 | 6 | 1 | Oxidized argillic-altered zone |
| 27 | 88JLO9-7 | 347120 | 6327650 | 15410 | 2 | 232 | 11 | 31 | 11 | <0.5 | Sericitic-altered volcanic 3 % pyrite |
| 28 | 88JLO9-8 | 347030 | 6327630 | 750 | 7 | 0.88% | 35 | 45 | 124 | 4 | Massive pyrite, grab from portal |
| 29 | 88VKO9-2 | 345000 | 6327000 | 29 | <0.5 | 67 | 13 | 54 | 13 | 1 | Oxidized pyritic andesite |
| 30 | 88DRH28-1-1 | 361020 | 6322925 | 6 | 1 | 270 | 14 | 64 | | 0.7 | Limestone with pyrite and malachite |
| 31 | 88DRH28-1-2 | 362050 | 6322875 | 3 | <0.5 | 144 | 25 | 48 | | <0.5 | Epidote-altered volcanic, diss. pyrite |
| 32 | 88JLO27-10 | 359050 | 6322425 | 109 | 2 | 750 | 42 | 49 | | 0.8 | Pyritic, altered intrusive |
| 33 | 88JLO27-11 | 359020 | 6322250 | 51 | 2 | 0.11% | 13 | 77 | | 0.7 | Andesite, 1-2% pyrite along fractures |
| 34 | 88JLO27-13 | 358925 | 6322700 | 49 | 2 | 460 | 36 | 70 | | 3 | Altered andesite, 3-5% pyrite |
| 35 | 88JLO27-17 | 359150 | 6323200 | 18 | 1 | 540 | 14 | 26 | | 3 | Silicified volcanic, 5% py and po |
| 36 | 88JLO27-8 | 359550 | 6322300 | 12 | <0.5 | 170 | 30 | 450 | 3 | 25 | Altered andesite, 1-2% diss. pyrite |
| 37 | 88JLO27-8-2 | 359545 | 6322320 | 6 | 125 | 450 | 0.65% | 112 | | 5 | Pyritic fault zone |
| 38 | 88VKO22-7 | 358500 | 6322200 | 3 | <0.5 | 182 | 14 | 75 | | 0.9 | Oxidized shear zone, trace ml & py |
| 39 | 88VKO31-5 | 363900 | 6324300 | 1 | <0.5 | 4 | 12 | 4 | | <0.5 | Tuffa from hotsprings on Sphaler Creek |
| 40 | 88VKO31-7 | 360200 | 6324220 | 29 | 0.8 | 74 | 43 | 102 | | 2 | Oxidized pyritic volcanic |
| 41 | 88VKO32-1 | 360575 | 6326300 | 4 | <0.5 | 46 | 6 | 77 | | 2 | Oxidized qtz-carb vein |
| 42 | 88VKO32-2 | 360575 | 6326300 | 48 | 0.8 | 30 | 10 | 36 | | 0.9 | Oxidized qtz-carb vein |
| 43 | 88VKO32-3 | 360575 | 6326300 | 7 | 7.5 | 82 | 10 | 83 | | 2 | Oxidized pyritic andesite |
| 44 | 88DRH19-15 | 354820 | 6335850 | 320 | 109 | 8.04% | 0.65% | 3.30% | | 7 | Qtz-carb vein, 10 % (py, cpy, gl, sph) |
| 45 | 88DRH19-9 | 355700 | 6336200 | 72 | 6 | 56 | 217 | 95 | 137 | 4 | Fault gouge, no visible sulphides |
| 46 | 88DRH29-1 | 352950 | 6341625 | 1 | <0.5 | 120 | 10 | 27 | | <0.5 | Diorite, trace diss. pyrite |
| 47 | 88VKO25-10 | 355050 | 6339200 | 62 | 32 | 1.75% | 57 | 0.15% | 0.60% | 0.28% | Qtz-carb vein, py, cpy, ml & tetrahedrite |
| 48 | 88VKO25-11 | 355000 | 6339250 | 7 | <0.5 | 31 | 13 | 84 | | 2 | Qtz-carb vein, trace malachite & pyrite |
| 49 | 88VKO25-8 | 355350 | 6339200 | 700 | 3 | 75 | 23 | 24 | 270 | 2 | Oxidized carb. breccia zone |
| 50 | 88DRH4-1 | 358450 | 6332780 | 41 | <0.5 | 227 | 13 | 71 | 72 | 1 | Oxidized syenite, 1-3 % pyrite |
| 51 | 88DRH4-4 | 364680 | 6335250 | 139 | <0.5 | 0.27% | 16 | 51 | 17 | 1 | Cu Canyon syenite, 2 % py & cpy |
| 52 | 88JLO4-2 | 358120 | 6332650 | 861 | 10 | 3.32% | 18 | 790 | 21 | 2 | Altered syenite, 3-5 % py |
| 53 | 88JLO4-3 | 358180 | 6332750 | 1820 | 16 | 6.97% | 39 | 93 | 140 | 4 | Oxidized syenite, 5 % cpy & py |
| 54 | 88JLO4-7 | 358520 | 6332850 | 1880 | 8 | 2.33% | 28 | 57 | 44 | <0.5 | K-altered volcanic, 3-5 % cpy & py |
| 55 | 88JLO4-9 | 358680 | 6332890 | 25 | <0.5 | 32 | 77 | 48 | 45 | 2 | K-metasomatism, 2-5% py |
| 56 | 88VKO19-5 | 359500 | 6331870 | 1 | 1 | 5 | 33 | 148 | | 2 | Hematized shear zone in limestone |
| 57 | 88VKO5-12 | 358220 | 6336820 | 390 | 2 | 500 | 10 | 53 | 2 | 0.7 | Qtz veinlets, 2-3 % po & py |
| 58 | 88DRH13-1-2 | 358270 | 6345350 | 8 | <0.5 | 162 | 7 | 120 | 11 | 2 | Laminated tuff, trace pyrite |
| 59 | 88DRH14-2 | 355400 | 6342650 | 6 | <0.5 | 67 | 7 | 38 | 4 | <0.5 | Laminated tuff, trace pyrite |
| 60 | 88DRH34-1 | 356200 | 6346630 | 35 | 10 | 760 | 19 | 0.63% | 80 | 60 | Limestone, oxidized fault zone |
| 61 | 88DRH34-1-2 | 357085 | 6346550 | 61 | 3 | 50 | 65 | 223 | 471 | 0.8 | Monzonite, 2 % diss. pyrite |
| 62 | 88JLO1-12 | 354760 | 6344070 | 20 | <0.5 | 25 | 11 | 25 | 2 | <0.5 | Silicified pyritic metasediment |
| 63 | 88JLO1-8 | 355230 | 6344720 | 25 | <0.5 | 51 | 16 | 38 | 2 | <0.5 | Pyritic diabase dike |
| 64 | 88JLO11-4 | 357800 | 6340100 | 20 | 2 | 72 | 19 | 177 | 10 | 5 | Chert conglomerate, 3 % pyrite |
| 65 | 88JLO11-9 | 358000 | 6340800 | 20 | 4 | 0.30% | 11 | 98 | 8 | <0.5 | Massive sulphides, py, po, cpy |
| 66 | 88JLO2-6 | 358530 | 6344400 | 33 | <0.5 | 360 | 8 | 37 | 4 | 2 | Oxidized, foliated andesite, 1 % py |
| 67 | 88JLO3-4 | 359980 | 6345960 | 20 | <0.5 | 35 | 7 | 34 | 1 | 2 | Carbonatized fault gouge |
| 68 | 88JLO3-6 | 359850 | 6345800 | 33 | 2 | 32 | 3 | 26 | 11 | 1 | Carbonatized mafic volcanic |

# APPENDIX C
# GEOCHEMICAL ANALYSES OF ALTERED AND MINERALIZED ROCKS

| Map No. | Sample Number | UTM EAST | ZONE 09 NORTH | Au (ppb) | Ag (ppm) | Cu (ppm) | Pb (ppm) | Zn (ppm) | As (ppm) | Sb (ppm) | SAMPLE DESCRIPTION |
|---|---|---|---|---|---|---|---|---|---|---|---|
| 69 | 88VKO20-5 | 356320 | 6341330 | 1 | 5 | 0.47% | 20 | 360 | 60 | 1 | Carbonate vein, diss. py, & malachite |
| 70 | 88VKO20-6 | 356200 | 6341600 | 1 | 1 | 620 | 10 | 50 | | <0.5 | Stockwork veins, diss. pyrite |
| 71 | 88VKO20-8 | 356950 | 6341600 | 6 | 54 | 4.67% | 10 | 50 | | <0.5 | Qty vein, diss. py, cpy, malachite |
| 72 | 88VKO3-14 | 357260 | 6341500 | 360 | 9 | 302 | 1.17% | 0.39% | 240 | 3 | Mineralized contact zone, lmst & andt |
| 73 | 88VKO3-5 | 357350 | 6342550 | 20 | <0.5 | 65 | 8 | 268 | 19 | 1 | Oxidized pyritic porphyritc andesite |
| 74 | 88JLO10-15 | 360050 | 6342500 | 20 | <0.5 | 20 | 7 | 87 | 8 | 3 | Cherty pyritic siltstone |
| 75 | 88JLO10-16 | 360050 | 6342500 | 20 | <0.5 | 24 | 7 | 100 | 46 | 2 | Cherty pyritic siltstone |
| 76 | 88JLO16-4 | 369070 | 6338550 | 3 | 0.8 | 217 | 31 | 126 | 120 | 10 | Oxidized pyritic volcanic |
| 77 | 88JLO5-3 | 361770 | 6337800 | 110 | 2 | 360 | 22 | 126 | 17 | 1 | Altered syenite, 3-5 % pyrite |
| 78 | 88JLO6-4 | 364680 | 6335250 | 1490 | 4 | 0.51% | 10 | 50 | 6 | <0.5 | Oxidized pyritic volcanic, cpy, malachite |
| 79 | 88VKO11-1 | 363250 | 6335850 | 25 | <0.5 | 43 | 10 | 35 | 10 | 2 | Andesite, diss. pyrite |
| 80 | 88VKO11-2 | 363150 | 6335950 | 1250 | <0.5 | 54 | 10 | 39 | 13 | 1 | Andesite, diss. pyrite |
| 81 | 88VKO11-4 | 362250 | 6336300 | 32 | 2 | 490 | 11 | 42 | 14 | 0.9 | Andesite, diss. pyrite |
| 82 | 88VKO11-5 | 361150 | 6336050 | 73 | 13 | 0.19% | 30 | 720 | 140 | 32 | Oxidized fault zone in limestone, py & cpy |
| 83 | 88VKO23-1 | 362150 | 6337850 | 11050 | 210 | 470 | 1.23% | 0.33% | 0.58% | 390 | Gouge zone, diss. sp, gl, py, tetrahedrite |
| 84 | 88VKO23-2 | 362150 | 6337850 | 3170 | 510 | 680 | 4.05% | 11.10% | 0.12% | 255 | Gouge zone, qtz-carb vein, gl, sp, py |
| 85 | 88VKO23-3 | 362150 | 6337850 | 4240 | 310 | 340 | 0.51% | 2.12% | 0.18% | 268 | Stockwork/breccia, diss. py |
| 86 | 88VKO23-4 | 362150 | 6337850 | 8700 | 390 | 193 | 0.31% | 280 | 0.13% | 230 | Stockwork/breccia, diss. to massive py |
| 87 | 88VKO23-5 | 362150 | 6337850 | 4300 | 205 | 296 | 1.18% | 0.33% | 6.00% | 230 | Massive & diss. pyrite, minor sp & tetrahedri |
| 88 | 88VKO23-6 | 362150 | 6337850 | 5550 | 775 | 690 | 1.20% | 1.51% | 1.73% | 830 | Stockwork veins, diss. gl, sp, py, tetrahedrite |
| 89 | 88VKO23-7 | 362150 | 6337850 | 1740 | 139 | 182 | 0.37% | 0.44% | 0.41% | 230 | Pyritic wall rock |
| 90 | 88VKO23-8 | 362150 | 6337850 | 116 | 12 | 213 | 0.18% | 510 | 270 | 6 | Gouge zone, diss. pyrite |
| 91 | 88VKO23-9 | 362150 | 6337850 | 360 | 6 | 156 | 138 | 137 | 0.22% | 3 | Syenite breccia, pyritized matrix |
| 92 | 88JLO5-2 | 361920 | 6337730 | 77 | 11 | 346 | 117 | 440 | 260 | 131 | Fault zone, oxidized gouge |
| 93 | 88JLO29-7 | 376500 | 6330075 | 1 | <0.5 | 11 | 22 | 86 | | <0.5 | Carb-talc alteration, 3 % diss. pyrite |
| 94 | 88VKO27-10 | 377500 | 6325625 | 1 | <0.5 | 6 | 5 | 22 | | <0.5 | Breccia qtz vein, no visible sulphides |
| 95 | 88VKO27-11 | 377300 | 6325800 | 1 | 0.6 | 99 | 7 | 18 | | 20 | Qtz-sericite-carb vein, diss. pyrite |
| 96 | 88VKO27-13 | 377050 | 6326300 | 1 | <0.5 | 10 | 2 | 9 | | <0.5 | Oxidized qtz-sericite vein, diss. py |
| 97 | 88VKO29-12 | 370710 | 6327100 | 390 | 9 | 44 | 64 | 510 | 0.13% | 122 | Oxidized gossan, geothite, limonite, pyrite |
| 98 | 88JLO18-17 | 378600 | 6341300 | 6 | 1 | 0.35% | 44 | 42 | 148 | 56 | Qtz vein, diss. pyrite & cpy |
| 99 | 88JLO31-2 | 374350 | 6338020 | 63 | 6 | 0.63% | 23 | 34 | 0.19% | 3 | Fault zone, trace malachite |
| 100 | 88DRH17-1-1 | 378350 | 6345500 | 112 | 3 | 390 | 116 | 310 | 2.60% | 97 | Qtz-carbonate vein, py, cpy & sp to < 2 % |
| 101 | 88DRH17-1-2 | 378350 | 6345500 | 70 | 9 | 0.14% | 220 | 0.15% | 0.11% | 27 | Apophysis of vein sample 17-1-1 |
| 102 | 88DRH17-1-3 | 378350 | 6345500 | 2 | <0.5 | 107 | 8 | 56 | 48 | 3 | Basalt, pyritic wallrock of vein 17-1-1) |
| 103 | 88VKO16-1-1 | 371650 | 6343450 | 1 | <0.5 | 30 | 11 | 102 | 3 | <0.5 | Pyritic qtz-carb vein |
| 104 | 88VKO16-4 | 371950 | 6343050 | 3 | 2 | 2.06% | 26 | 51 | 23 | 7 | Qtz-carb vein, trace malachite |
| 105 | 88VKO10-5 | 360950 | 6339900 | 20 | 0.8 | 35 | 18 | 24 | 64 | 7 | Shear zone, pyritic volcanic |
| 106 | 88VKO10-4 | 360800 | 6339800 | 21 | <0.5 | 9 | 21 | 25 | 6 | 6 | Qtz vein, diss. pyrite |
| 107 | 88JLO18-6 | 378800 | 6340700 | 3 | <0.5 | 40 | 5 | 36 | | 3 | Qtz-carb vein |
| 108 | 88DRH10-1 | 350550 | 6346950 | 20 | <0.5 | 15 | 3 | 30 | 1 | <0.5 | Qtz-carb vein, diss. py & po |

ANALYTICAL PROCEDURES

Sample Preparation: samples are pulverized to approximately -200 mesh using tungsten carbide equipment.

Trace Element Analysis: Ag, Cu, Pb, Zn, As, Sb

Samples (usually 0.5 gram) are digested in Teflon beakers using a mixed acid attack which includes HF. A dilute acid dissolution of the residue is then diluted to a specific volume and the elements measured using atomic absorption spectroscopy. As and Sb were determined by atomic adsorption using a hydride evolution method wherein the hydride ($AsH_3$ or $SbH_3$) is evolved, passed through a heated quartz tube in the light of an atomic adsorption spectrometer. Background corrections were made for Pb, As and Sb.

Trace Element Analysis: Au

Gold analyses were performed by Acme Analytical Laboratories of Vancouver, British Columbia. A 20-gram sample is concentrated into a silver bead by the classical fire assay method. The bead is dissolved by aqua regia and gold determined by graphite furnace assay.

Abbreviations: qtz= quartz, carb= carbonate, py= pyrite, cpy= chalcopyrite, sph= sphalerite, po= pyrrhotite, mgnt= magnetite, ml= malachite, az= azurite, aspy= arsenopyrite, gl= galena, stwk= stockwork, alt= alteration, brcc= breccia, dort= diorite, bsl= basalt, andt= andesite, lmst= limestone, diss.= disseminated.

BC Ministry of Energy, Mines and Petroleum Resources

Geological Survey Branch

# FIGURE 30

# GEOLOGY AND MINERAL OCCURRENCES OF THE GALORE CREEK AREA

NTS 104G/03-04

Geology by James M. Logan, Victor M. Koyanagi and David Rhys

Scale 1:100 000

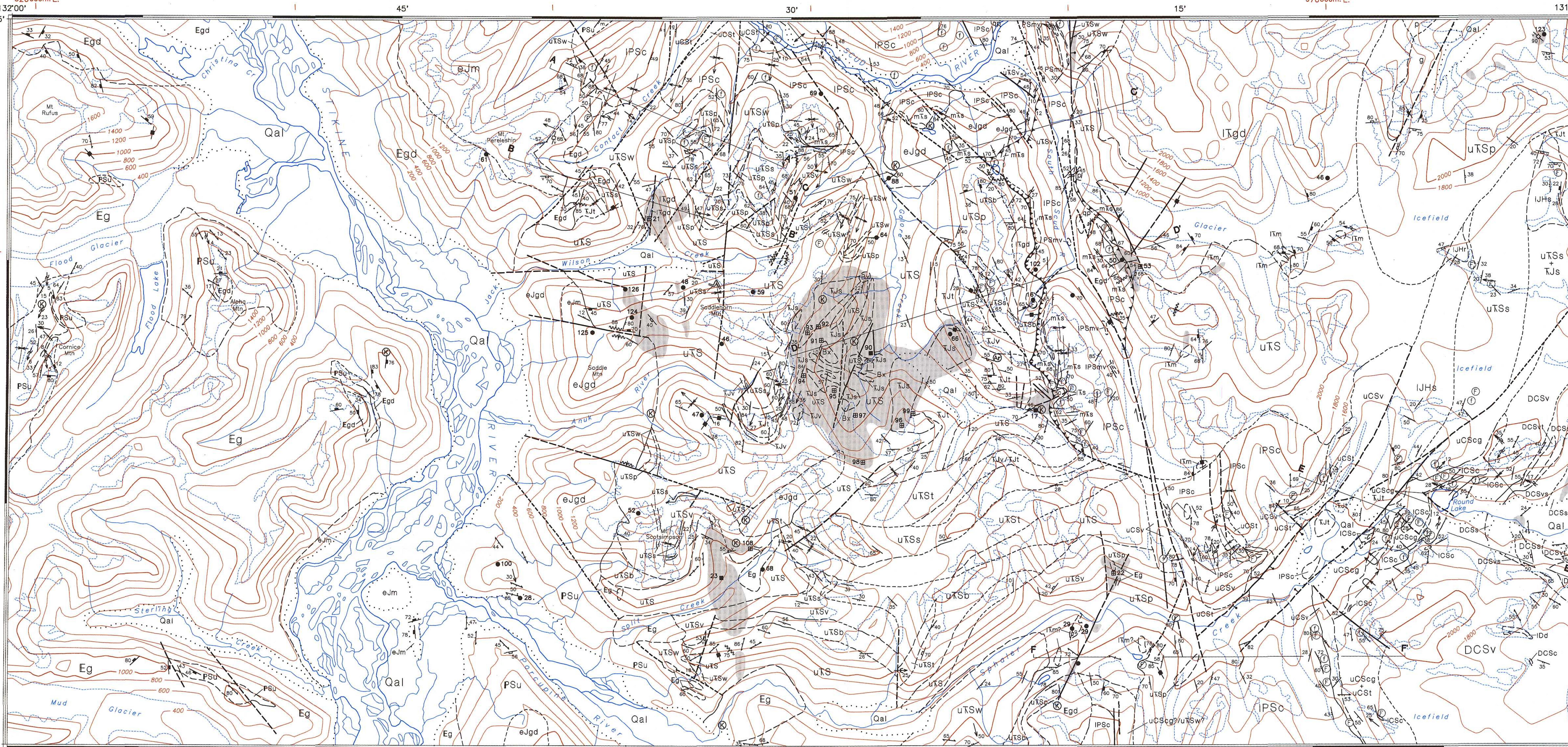


## SCHEMATIC CROSS-SECTIONS

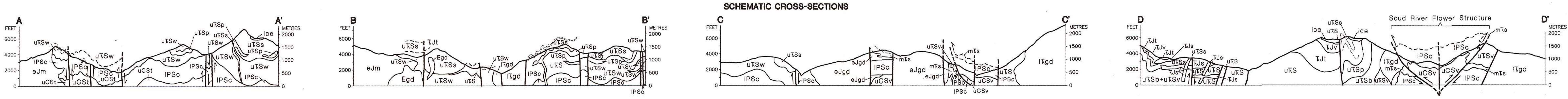


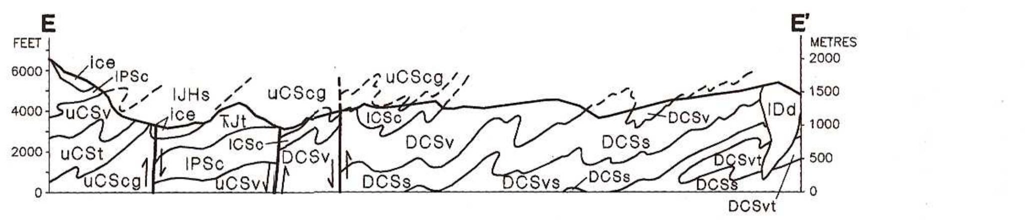


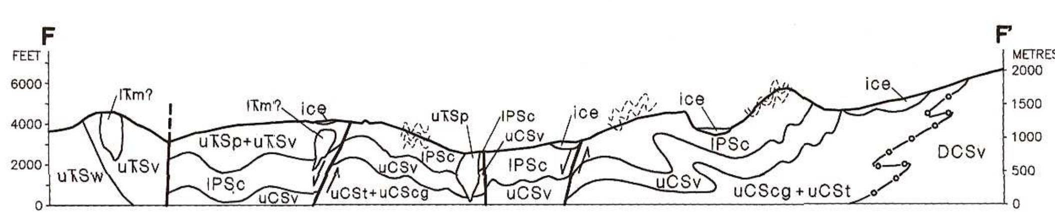


## LEGEND

### INTRUSIVE ROCKS

| | |
|---|---|
| Bx | Intrusive or tectonic breccia |
| **EOCENE** | |
| Eg | Pink, medium to coarse-grained and potassium feldspar megacrystic biotite granite and eguigranular biotite quartz monzonite |
| Egd | Grey, medium-grained hornblende biotite granodiorite |
| **EARLY JURASSIC OR YOUNGER** | |
| qp | Plagioclase-quartz porphyritic diorite, pyritic (age unknown) |
| **EARLY JURASSIC** | |
| eJm | Medium-grained, potassium feldspar megacrystic hornblende granite to biotite quartz monzonite |
| eJgd | Medium-grained quartz diorite, biotite hornblende granodiorite |
| **LATE TRIASSIC-EARLY JURASSIC** GALORE CREEK INTRUSIONS | |
| TJs | Syenite, biotite orthoclase porphyritic monzonite |
| **MIDDLE-LATE TRIASSIC** HICKMAN BATHOLITH | |
| lTgd | Coarse to medium-grained, biotite hornblende granodiorite, augite monzonite (lTm), coarse-grained plagioclase megacrystic diorite (lTd) |
| ULTRAMAFIC ROCKS | |
| g | Coarse to medium-grained, clinopyroxene gabbro |
| p | Pyroxenite |
| **LATE DEVONIAN** | |
| lDd | Hornblende diorite |

### LAYERED ROCKS

| | |
|---|---|
| **QUATERNARY** | |
| Qal | Unconsolidated glacial till and poorly sorted alluvium |
| **LOWER JURASSIC** | |
| lJHr | Felsic tuffite |
| lJHs | Polymictic, maroon volcanic conglomerate, limy siltstone, shale and airfall tuff, contains coaly material |

| VOLCANIC FACIES | | SEDIMENTARY FACIES | |
|---|---|---|---|
| **UPPER TRIASSIC-LOWER JURASSIC** | | | |
| TJv | Potassium feldspar and pseudoleucite-bearing fragmentals and alkaline basalt flows | TJt | Well-bedded maroon potassium feldspar crystal tuff, epiclastics and volcanic conglomerate |
| **UPPER TRIASSIC** STUHINI GROUP | | | |
| uTS | Undivided volcanics and sediments | | |
| uTSp | Maroon pyroxene porphyry breccia flows and fragmentals | | |
| uTSs | Fine-grained black clastics, bedded tuff and volcanic conglomerate | uTSs | Well-bedded siltstone, sandstone and pyroxene crystal tuffs, flows and minor limestone contains *Monotis* |
| uTSt | Aphyric andesite lapilli tuffs | | |
| uTSb | Breccia flows, lahar and intermediate fragmentals | uTSp | Green pyroxene-porphyry breccia flows |
| uTSv | Massive basaltic-andesite, plagioclase and hornblende porphyry flows and tuffs | uTSw | Well-bedded silicic clastics and volcanic wackes, minor andesite flows and basal polymictic conglomerate contains *Halobia* |

| | |
|---|---|
| **MIDDLE TRIASSIC** | |
| mTs | Carbonaceous silty shale with elliptical concretions, siliceous and limy siltstone contains *Daonella* |
| **LOWER TRIASSIC** | |
| lTs | Siliceous and limy siltstone, minor limestone |

### STIKINE ASSEMBLAGE

| | |
|---|---|
| PSu | Undivided Paleozoic metavolcanics and metasediments |
| **LOWER PERMIAN** | |
| lPSc | Upper: light grey or buff massive to thickly bedded, bioclastic grainstone, foliated maroon and green epiclastics and tuff (lPSmv) Lower: dark grey to buff thinly bedded, bioclastic limestone, chert interbeds, argillaceous near base |
| **UPPER CARBONIFEROUS TO LOWER PERMIAN** | |
| uCSv | Maroon and green intermediate volcaniclastics |
| uCSt | Green and buff siliceous siltstones and felsic dust tuffs |
| uCScg | Thick-bedded, boulder to pebble conglomerate, clasts are augite phyric, plagioclase phyric, andesite, basalt, and limestone; thin bedded siltstone and sandstone |
| **LOWER CARBONIFEROUS** | |
| lCSc | Upper: dark grey, massive to thinly bedded grainstone, chert interbeds Lower: pale grey coarse-grained echinoderm packstone, interbedded maroon tuffs and epiclastics |
| **DEVONIAN TO LOWER CARBONIFEROUS** | |
| DCSv | Upper: mafic and felsic flows Lower: intermediate flows; purple ash tuff (DCSvt), chlorite and sericite schist (DCSvs) |
| DCSc | Deformed grey and buff thin-bedded coralline limestone |
| DCSs | Quartz sericite schist, slate and carbonaceous argillite |

## SYMBOLS

Geological boundaries: defined, approximate, assumed

Unconformity: defined, assumed

Bedding (tops unknown): inclined, vertical

Bedding (tops known): inclined, vertical, overturned

Bedding (tops unknown, estimated dip): gentle, moderate, steep

Foliation (ages indicated by number of ticks): inclined, vertical

Joint: inclined, vertical

Dike: inclined, vertical

Vein: inclined, vertical

Antiform, synform (arrow indicates plunge)

Overturned antiform and synform (arrow indicates plunge)

Anticline, syncline (arrow indicates plunge)

Fold axis of minor fold with M, S, and Z symmetry: double arrow = second phase; arrow indicates plunge; numbers for phase greater than 2

Crenulation lineation (inclined): $S_0/S_1$, $S_1/S_2$

Fault or shear zone attitude: inclined, vertical

High-angle fault (solid circle indicates downthrow side; arrows indicate relative movement): defined, approximate, assumed

Thrust fault (teeth in direction of upper plate): Defined, approximate, assumed

Cross-section line — A A'

Fossil location: conodont, macrofossil, foram

Fossil location age indeterminate/barren

Isotopic age locality (potassium-argon, argon-argon)

Mineral occurrence: MINFILE number, developed prospect, prospect, showing — 68

Adit

Zone of alteration

Icefield or glacier

Topographic contour (200m interval) — 600

## REFERENCES

Allen, D.G., Panteleyev, A. and Armstrong, A.T. (1976): Galore Creek *in* Porphyry Deposits of the Canadian Cordillera, *Canadian Institute of Mining and Metallurgy*, Special Volume 15, pages 402-414.

Kerr, F.A. (1948): Lower Stikine and Western Iskut River Areas, British Columbia; *Geological Survey of Canada*, Memoir 246, 95 pages.

Souther, J.G. (1972): Telegraph Creek Map Area, British Columbia; *Geological Survey of Canada*, Paper 71-44, 38 pages.

Plus unpublished material from A. Panteleyev.

Macro and microfossil identifications provided by E.W. Bamber, M.J. Orchard, Lin Rui and E.T. Tozer of the Geological Survey of Canada and B.L. Mamet of the University of Montreal.

## LOCATION MAP

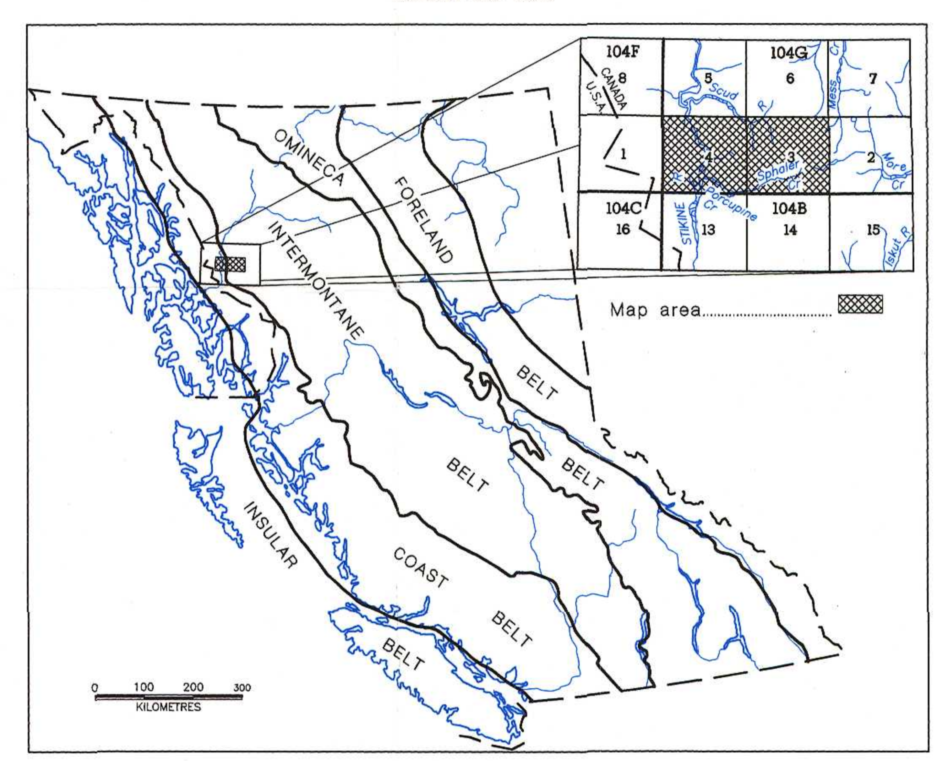


Cartography by P. Chicorelli